Nuclear charge-exchange excitations in a self-consistent covariant approach

H. Liang

THESE

Présentée

Pour obtenir

Le GRADE de DOCTEUR EN SCIENCES
de L'UNIVERSITE PARIS XI ORSAY

PAR

Haozhao LIANG

Subjet:

Nuclear charge-exchange excitations in a self-consistent covariant approach

Soutenue le 10 Juin 2010 devant la Commission d'examen

M. Jie MENG

M. NGUYEN Van Giai

M. Peter SCHUCK

M. Hiroshi TOKI

M. Furong XU

M. Shan-Gui ZHOU

Abstract

Nowadays, charge-exchange excitations in nuclei become one of the central topics in nuclear physics and astrophysics. Basically, a systematic pattern of the energy and collectivity of these excitations could provide direct information on the spin and isospin properties of the in-medium nuclear interaction, and the equation of state of asymmetric nuclear matter. Furthermore, a basic and critical quantity in nuclear structure, neutron skin thickness, can be determined indirectly by the sum rule of spin-dipole resonances (SDR) or the excitation energy spacing between the isobaric analog states (IAS) and Gamow-Teller resonances (GTR). More generally, charge-exchange excitations allow one to attack other kinds of problems outside the realm of nuclear structure, like the description of neutron star and supernova evolutions, the β-decay of nuclei which lie on the r-process path of stellar nucleosynthesis, and the neutrino-nucleus cross sections. They also play an essential role in extracting the value of the Cabibbo-Kobayashi-Maskawa (CKM) matrix element V_{ud} via the nuclear $0^+ \to 0^+$ superallowed Fermi β decays. For all these reasons, it is important to develop the microscopic theories of charge-exchange excitations and it is the main motivation of the present work.

In this work, a fully self-consistent charge-exchange relativistic random phase approximation (RPA) based on the relativistic Hartree-Fock (RHF) approach is established. Its self-consistency is verified by the so-called IAS check. This approach is then applied to investigate the nuclear spin-isospin resonances, isospin symmetry-breaking corrections for the superallowed β decays, and the charged-current neutrino-nucleus cross sections.

For two important spin-isospin resonances, GTR and SDR, it is shown that a very satisfactory agreement with the experimental data can be obtained without any readjustment of the energy functional. Furthermore, the isoscalar mesons are found to play an essential role in spin-isospin resonances via the exchange terms, which leads to a profound effect in the nuclear isovector properties, e.g., the density dependence of the symmetry energy in nuclear matter.

In the investigation of the isospin symmetry-breaking corrections for the superallowed β decays, it is found that the corrections δ_c are sensitive to the proper treatments of the Coulomb mean field, but not so much to specific effective interactions. With these corrections δ_c, the nucleus-independent $\mathcal{F}t$ values are obtained in combination with the experimental ft values in the most recent survey and the improved radiative corrections. The values of Cabibbo-Kobayashi-Maskawa matrix element $|V_{ud}|$ thus obtained well agree with those obtained in neutron decay, pion decay, and nuclear mirror transitions, while the sum of squared top-row elements somehow deviates from

the unitarity condition.

Expressing the weak lepton-hadron interaction in the standard current-current form, the relevant transitions from the nuclear ground state to the excited states are calculated with RHF+RPA approach. In this way, the semileptonic weak interaction processes, e.g., neutrino reactions, charged-lepton capture, β-decays, can be investigated microscopically and self-consistently. First illustrative calculations of the inclusive neutrino-nucleus cross section are performed for the ^{16}O(ν_e,e^-)^{16}F reaction, and a good agreement with the previous theoretical studies is obtained. The main effort is dedicated to discussing the substantial influence of different recipes for the axial vector coupling strength and the theoretical low-lying excited states of the daughter nucleus.

Résumé de la thèse de M. Haozhao Liang:

Excitations d'échange de charge dans les noyaux atomiques: une approche covariante et self-consistante

Les excitations d'échange de charge dans les noyaux constituent l'un des sujets importants et actuels en physique nucléaire et en astrophysique. En principe, une connaissance systématique de l'évolution du comportement de ces excitations à travers la table des éléments fournirait des informations directes sur les propriétés en spin et isospin de l'interaction entre nucléons dans le milieu nucléaire, et sur l'équation d'état de la matière nucléaire. Par ailleurs, une quantité d'importance essentielle pour la structure des noyaux, l'épaisseur de la peau de neutrons, peut être déterminée par la règle de somme de la résonance spin-dipolaire (RSD) ou par la séparation en énergie entre l'état isobarique analogue (EIA) et la résonance de Gamow-Teller (RGT). Plus généralement, les excitations d'échange de charge permettent d'aborder des problèmes d'intérêt général tels que l'étude de l'évolution des étoiles à neutrons et des supernovae, la décroissance β des noyaux le long du processus r dans la nucléosynthèse stellaire, ou les interactions neutrino-noyau. Elles jouent aussi un rôle essentiel pour extraire la valeur de l'élément V_{ud} de la matrice de Cabibbo-Kobayashi-Maskawa par le biais de la réaction de décroissance β super-permise $0^+ \to 0^+$ dans les noyaux. Pour toutes ces raisons, il est important de développer des théories microscopiques des excitations d'échange de charge, et ceci constitue la principale motivation de notre recherche.

Dans ce travail, nous établissons le formalisme et les méthodes numériques pour décrire les excitations d'échange de charge dans le cadre de la Random Phase Approximation (RPA) self-consistante construite sur l'approximation de Hartree-Fock relativiste (RHF). Un test important de précision numérique est réalisé sur l'état isobarique analogue. La méthode est ensuite utilisée pour mener des applications numériques réalistes sur un certain nombre de questions physiques: les résonances de spin-isospin dans les noyaux proches des noyaux magiques, les corrections dûes aux mélanges d'isospin dans les transitions β super-permises, les interactions neutrino-noyau dans les voies de courants chargés.

Pour les deux modes importants de spin-isospin que sont la RGT et la RSD nous trouvons qu'un excellent accord avec l'expérience est obtenu sans aucun réajustement des paramètres du modèle. De plus, les termes d'échange de l'interaction induite par les mésons isoscalaires jouent un rôle essentiel dans les excitations de spin-isospin, à la différence de la RPA construite sur l'approximation de Hartree relativiste.

En ce qui concerne notre étude des transitions β $0^+ \to 0^+$ super-permises l'une des conclusions est que les corrections δ_c dûes aux violations de la symétrie d'isospin dépendent sensiblement du champ moyen d'échange produit par les interactions coulombiennes, mais ne changent pas sensiblement avec le modèle de Lagrangien utilisé. Nous utilisons ces valeurs de δ_c pour déduire des plus récentes valeurs expérimentales de ft dans les noyaux $T = 1$, et en tenant compte des corrections radiatives, les valeurs de $\mathcal{F}t$ "indépendantes de noyaux". Nous obtenons ainsi des

valeurs de l'élément de matrice $|V_{ud}|$ de Cabbibo-Kobayashi-Maskawa en bon accord avec les valeurs déduites des décroissances neutronique et pionique, et les transitions dans les noyaux miroirs, tandis que la somme des carrés des éléments de la première ligne dévie légèrement de la condition d'unitarité.

Nous avons également utilisé nos fonctions d'onde RPA pour évaluer les amplitudes de transition correspondant à l'interaction faible lepton-hadron sous la forme standard courant-courant. Ainsi, les processus faibles semi-leptoniques tels que les réactions neutrino-noyau, capture leptonique chargée, désintégration β, peuvent être étudiés. Nos premières applications concernent la réaction $^{16}O(\nu_e, e^-)^{16}F$ pour laquelle nous comparons nos prédictions avec celles d'autres auteurs. Dans la discussion des résultats nous nous efforçons en particulier de clarifier l'influence appréciable des différentes prescriptions que l'on peut adopter pour le choix de la constante de couplage vecteur axiale et l'inclusion ou non des états excités de basse énergie dans le noyau final.

Contents

List of Figures

List of Tables

Chapter 1

Introduction

The nuclear charge-exchange excitations correspond to the transitions from the ground-state of the nucleus (N,Z) to the final states in the neighbouring nuclei ($N \mp 1, Z \pm 1$) in the isospin lowering T_- and raising T_+ channels, respectively. These excitations can take place spontaneously, like in the well-known case of β decays, or be induced by external fields, like the charge-exchange reactions, e.g., (p, n), (^{3}He, t), and so on. These excitations are categorized into different modes according to the nucleons with spin up and spin down oscillating either in phase, the non-spin-flip modes with $S = 0$, or out of phase, the spin-flip modes with $S = 1$. The important modes which have attracted an extensive attention experimentally and theoretically include the isobaric analog state (IAS) with $S = 0$, $\Delta J^\pi = 0^+$, Gamow-Teller resonance (GTR) with $S = 1$, $\Delta J^\pi = 1^+$, and spin-dipole resonance (SDR) with $S = 1$, $\Delta J^\pi = 0^-, 1^-, 2^-$ (Osterfeld, 1992; Ichimura *et al.*, 2006; Krasznahorkay *et al.*, 1999; Yako *et al.*, 2006).

At present, the charge-exchange excitations in nuclei become one of the central topics in nuclear physics, because a systematic pattern of the excitation energy and collectivity of these resonances could provide direct information on the spin and isospin properties of the in-medium nuclear interaction, and the symmetry term of the nuclear equation of state (EOS). Furthermore, a basic and critical quantity in nuclear structure, the neutron skin thickness, can be determined indirectly by the SD non-energy weighted sum rule (Krasznahorkay *et al.*, 1999; Yako *et al.*, 2006) or the excitation energy spacing between the IAS and GTR (Vretenar *et al.*, 2003). The neutron skin thickness in heavy nuclei has been shown to be a unique measure of the density dependence of the neutron EOS (Alex Brown, 2000; Centelles *et al.*, 2009), which, as a step forward, have a strong impact on the properties of neutron stars (Horowitz and Piekarewicz, 2001a,b, 2002). More generally, the charge-exchange excitations allow us to attack other kinds of problems outside the realm of nuclear structure. For example, these excitations are important for the charged current weak interaction processes in nuclear astrophysics and neutrino physics, e.g., the description of neutron star and supernova evolutions, the β decays of nuclei which lie on the r-process path of stellar nucleosynthesis (Engel *et al.*, 1999; Borzov, 2006), and the neutrino-nucleus cross sections (Kolbe *et al.*, 2003; Vogel, 2006). They also play an essential role in extracting the value of the Cabibbo-Kobayashi-Maskawa (CKM) matrix (Cabibbo, 1963; Kobayashi and Maskawa, 1973) ele-

ment V_{ud} via the nuclear $0^+ \to 0^+$ superallowed Fermi β decays (Hardy and Towner, 2009). For all these reasons, it is important to develop the microscopic theories of charge-exchange excitations and it is the main motivation of the present work.

For the theoretical description of charge-exchange excitations in nuclei, the two main approaches are the shell model calculations and the linear response in density functional theory (DFT), i.e., the random phase approximation (RPA) based on the self-consistent mean field. In a recent review (Caurier *et al.*, 2005), it is shown that the experimental data on the charge-exchange excitations and the related β decay rates in light and medium-mass nuclei can be well reproduced by the shell model calculations. The development of the shell model Monte Carlo and large-scale shell-model techniques allows nowadays the calculations of the GT strength distributions in the complete pf shell with the mass number $A \sim 60$ (Radha *et al.*, 1997; Caurier *et al.*, 1999). However, as the number of valence nucleons increases, the dimension of shell-model configuration space becomes too large to perform practical applications.

Meanwhile, the RPA calculations based on the self-consistent mean field can be, in principle, implemented for the whole nuclear chart, except for a small amount of very light nuclei. Furthermore, the relatively large particle-hole (p-h) configuration space allows for the description of the high-lying excitations up to ~ 100 MeV, which is essential for the charge-exchange monopole resonances, and other high-J excitations. In the RPA framework, the model self-consistency requires that the same density functional is used for describing both the nuclear ground-state and the excited states. Its importance has been extensively discussed, e.g., in Refs. (Engelbrecht and Lemmer, 1970; Ring and Schuck, 1980). It is crucial for restoring the symmetries which are broken by the mean field approximation, and for separating the spurious states from the physical states. It is also an important requirement for extrapolating the theoretical analysis towards the nucleon drip lines.

On the non-relativistic side, the charge-exchange RPA, also known as proton-neutron RPA in some literature, was first established on the self-consistent Skyrme Hartree-Fock (SHF) scheme about 30 years ago (Auerbach *et al.*, 1981). This approach was then used to explore various non-spin-flip and spin-flip excitations (Auerbach and Klein, 1983, 1984), and also extended to investigate the escape and spreading properties of the giant resonances (Colò *et al.*, 1994), the GT β decays of the so-call waiting-point nuclei in r-process path (Engel *et al.*, 1999), and the effects of the spin-isospin channel of the Skyrme energy functional on predictions for GT distributions and superdeformed rotational bands (Bender *et al.*, 2002). Very recently, a fully self-consistent charge-exchange quasiparticle RPA (QRPA) beyond the SHF mean field with Bardeen-Cooper-Schrieffer (BCS) pairing correlations has been developed (Fracasso and Colò, 2005).

On the relativistic side, even though limited to the Hartree approximation, the relativistic mean field (RMF) theory (Walecka, 1974) has received wide attention due to its successful description of a large variety of nuclear phenomena during the past 25 years (Serot and Walecka, 1986; Reinhard, 1989; Ring, 1996; Vretenar *et al.*, 2005; Meng *et al.*, 2006). In this thesis, we refer to it as the relativistic Hartree (RH) theory in order to distinguish it from the relativistic Hartree-Fock (RHF) theory. In this covariant density functional framework, the nucleons are described as Dirac

spinors interacting via the exchange of mesons and photons. Comparing with the non-relativistic approaches, the combination of the scalar and vector fields, which are of the order of a few hundred MeV, provide a natural and more efficient description of both the nuclear mean field central and spin-orbit potentials. Other successful features include the nuclear saturation properties in nuclear matter (Brockmann and Machleidt, 1990; Brockmann and Toki, 1992), binding energies and densities of nuclei throughout the nuclear chart (Ring, 1996), the isotopic shifts in the Pb isotopes (Sharma *et al.*, 1993), halos and giant halos in exotic nuclei (Meng and Ring, 1996, 1998), possible explanation of pseudospin symmetry in single-particle spectra (Ginocchio, 2005), spin symmetry in anti-nucleon spectrum (Zhou *et al.*, 2003), and so on.

The RPA approach based on the RH theory (RH+RPA) was firstly extended to charge-exchange channel in Ref. (De Conti *et al.*, 1998). Then, the relation between the zero-range counter-term and the ρ-nucleon (ρ-N) tensor coupling was investigated (De Conti *et al.*, 2000). Based on the relativistic description, a new kind of Gamow-Teller quenching mechanism due to the effects of the Dirac sea states was pointed out (Kurasawa *et al.*, 2003). Later, relativistic QRPA was formulated in the canonical basis of relativistic Hartree-Bogoliubov (RHB) model (Paar *et al.*, 2003) and applied to analyze IAS and GTR of ^{48}Ca, ^{90}Zr, ^{208}Pb and Sn isotopes (Paar *et al.*, 2004), to suggest a new method for extracting the neutron-skin thickness with the energy spacings between GTR and IAS (Vretenar *et al.*, 2003), to calculate the β decay half-lives of neutron-rich nuclei (Nikšić *et al.*, 2005), the muon capture rates (Marketin *et al.*, 2009), and the inclusive neutrino-nucleus cross sections (Paar *et al.*, 2008).

However, the self-consistency of this charge-exchange RH+RPA approach is not completely fulfilled for the following reason. First, the isovector pion plays an important role in the relativistic description of spin-isospin resonances. Because of the parity conservation this degree of freedom is absent in the ground-state description under the Hartree approximation. Thus, the pion is out of control in this best-fitting effective field theory. Second, to cancel the contact interaction coming from the pseudovector pion-nucleon (π-N) coupling, a zero-range counter-term is needed with the strength $g' = 1/3$ exactly (Bouyssy *et al.*, 1987). However, in order to reproduce the excitation energies of the GTR, g' must be treated as an adjustable parameter in the RH+RPA model with the value $g' \approx 0.6$ (De Conti *et al.*, 1998; Paar *et al.*, 2004). In other words, additional parameters are needed for the description of the nuclear charge-exchange excitations within the RH+RPA framework.

One of the possibilities for curing the above defect is to extend the relativistic framework to the Hartree-Fock level. Indeed, within the newly developed density-dependent RHF theory (Long, 2005; Long *et al.*, 2006), the importance of the Fock terms has been evidenced by the improvement on the description of the nuclear shell structures (Long *et al.*, 2007) and their evolution (Long *et al.*, 2008; Tarpanov *et al.*, 2008) due to the π-N and ρ-N tensor interactions, and the influence on isovector properties of nuclear matter and neutron stars at high densities (Sun *et al.*, 2008). We will show in this thesis that, contrary to the RH+RPA approach, the RHF+RPA does not need to readjust the value of $g' = 1/3$ and that full self-consistency is insured. At this point, we must mention that RHF

with form factors for meson-nucleon couplings can also be envisaged (Hu *et al.*, 2010a,b), in which case the question of contact interaction and its zero-range counter-term is eliminated. However, such a theory has still to be developed for finite nuclei. It also can be seen that the proper inclusion of the Coulomb exchange terms is essential for specific issues, e.g., the isospin symmetry-breaking corrections for superallowed β decays (Liang *et al.*, 2009).

Within the charge-exchange RHF+RPA framework, it is expected that 1) the p-h residual interaction induced by the pion can be derived self-consistently, since the π-N interaction contributes to the total energy of the system via the exchange (Fock) terms; 2) the isoscalar σ- and ω-mesons can contribute to the nuclear isovector properties of both ground-state and excited state also via the exchange terms. These two points might lead to a profound effect in the theoretical description of nuclear charge-exchange excitations.

In this thesis, a fully self-consistent relativistic RPA based on the RHF approach is established. The general formalism is shown in **Chapter 2**. In **Chapter 3**, the numerical details are explained, and the numerical checks for restoring the translational and isospin symmetries are presented. The formalism will then be applied to investigate the nuclear spin-isospin resonances, the isospin symmetry-breaking corrections for the superallowed β decays, and the charged-current neutrino-nucleus cross sections. In **Chapter 4**, the properties of the IAS, GTR, SDR, and spin-quadrupole resonances (SQR) in doubly magic nuclei ^{48}Ca, ^{90}Zr, ^{208}Pb, and the effects of the Dirac sea in their non-energy weighted sum rules are investigated. In **Chapter 5**, in combination with the isospin symmetry-breaking corrections, the radiative corrections and the experimental data on superallowed β decays, we finally extract the value of the matrix element V_{ud} and discuss the unitarity of the CKM matrix. In **Chapter 6**, the illustrative calculations are performed for the $^{16}\mathrm{O}(\nu_e,e^-)^{16}\mathrm{F}$ reaction, especially, the different recipes for the axial vector coupling strength and the theoretical low-lying excited states of the daughter nucleus are discussed. In the end, the summary and perspectives are given in **Chapter 7**.

Chapter 2

General Theory of Covariant Hartree-Fock and Random Phase Approximation

In this chapter, we briefly recall the theoretical framework of the relativistic Hartree-Fock (RHF) approach in **Section 2.1**, and the general formalism of the random phase approximation (RPA) in **Section 2.2**. The most challenging work is to establish the fullly self-consistent RPA based on the RHF approach. The density-dependent meson-nucleon couplings in the Lagrangians used in this thesis, in particular, lead to complicated rearrangement terms. The main ideas for the derivation and the key formulas will be shown in **Section 2.3**, while all the details are given in **Appendix A**.

2.1 Relativistic Hartree-Fock theory

The basic starting point of the RHF theory is a Lagrangian density $\mathcal{L}$, in which nucleons are described as Dirac spinors that interact each other via the exchanges of σ-, ω-, ρ-, π-mesons and photons. The effective Hamiltonian $\hat{H}$ is then obtained with the general Legendre transformation. In the Hartree-Fock approximation, the total energy E of the system is the expectation value of the Hamiltonian $\hat{H}$ on the trial ground-state (Slater determinant), where both direct (Hartree) and exchange (Fock) terms are kept. Finally, the Dirac equations, i.e., the equations of motion of nucleons, can be obtained via the variation of the total energy E with respect to the single-particle wave functions, or equivalently to the densities and currents. Details can be found in W. H. Long's Ph.D. thesis (Long, 2005).

2.1.1 Effective Lagrangian and Hamiltonian

The starting point of the RHF approach is an effective Lagrangian density (Bouyssy *et al.*, 1987; Long, 2005; Long *et al.*, 2006),

$$\begin{aligned}\mathcal{L} &= \bar{\psi}\left[i\gamma^\mu\partial_\mu - M - g_\sigma\sigma - g_\omega\gamma^\mu\omega_\mu - g_\rho\gamma^\mu\vec{\tau}\cdot\vec{\rho}_\mu - \frac{f_\pi}{m_\pi}\gamma_5\gamma^\mu\partial_\mu\vec{\pi}\cdot\vec{\tau} - e\gamma^\mu\frac{1-\tau_3}{2}A_\mu\right]\psi \\ &+\frac{1}{2}\partial^\mu\sigma\partial_\mu\sigma - \frac{1}{2}m_\sigma^2\sigma^2 - \frac{1}{4}\Omega^{\mu\nu}\Omega_{\mu\nu} + \frac{1}{2}m_\omega^2\omega^\mu\omega_\mu - \frac{1}{4}\vec{R}^{\mu\nu}\cdot\vec{R}_{\mu\nu} + \frac{1}{2}m_\rho^2\vec{\rho}^\mu\cdot\vec{\rho}_\mu \\ &+\frac{1}{2}\partial_\mu\vec{\pi}\cdot\partial^\mu\vec{\pi} - \frac{1}{2}m_\pi^2\vec{\pi}\cdot\vec{\pi} - \frac{1}{4}F^{\mu\nu}F_{\mu\nu},\end{aligned} \tag{2.1}$$

where the tensor quantities for the vector fields are defined as follows,

$$\Omega^{\mu\nu} \equiv \partial^\mu\omega^\nu - \partial^\nu\omega^\mu, \tag{2.2a}$$

$$\vec{R}^{\mu\nu} \equiv \partial^\mu\vec{\rho}^\nu - \partial^\nu\vec{\rho}^\mu, \tag{2.2b}$$

$$F^{\mu\nu} \equiv \partial^\mu A^\nu - \partial^\nu A^\mu. \tag{2.2c}$$

In this thesis, we use arrows to denote the isospin vectors and bold type for the space vectors. It is well known that the π-N pseudo-scalar coupling is not suitable for the HF approximation (Bouyssy *et al.*, 1987), thus we adopt its pseudo-vector coupling in this work. Furthermore, the ρ-N tensor interaction is not included in all parametrizations used in the present work.

The Hamiltonian density can be formally obtained via the general Legendre transformation,

$$\mathcal{H} = \mathcal{T}^{00} = \frac{\partial\mathcal{L}}{\partial\dot{\phi}_i}\dot{\phi}_i - \mathcal{L}, \tag{2.3}$$

where ϕ_i represent the nucleon, meson and photon field operators. With the compact notations for the interaction matrix,

$$\Gamma_\sigma(1,2) \equiv -g_\sigma(1)g_\sigma(2), \tag{2.4a}$$

$$\Gamma_\omega(1,2) \equiv g_\omega(1)\gamma_\mu(1)g_\omega(2)\gamma^\mu(2), \tag{2.4b}$$

$$\Gamma_\rho(1,2) \equiv g_\rho(1)\gamma_\mu(1)\vec{\tau}(1)\cdot g_\rho(2)\gamma^\mu(2)\vec{\tau}(2), \tag{2.4c}$$

$$\Gamma_\pi(1,2) \equiv -\left[\frac{f_\pi}{m_\pi}\vec{\tau}\gamma_5\gamma_\mu\partial^\mu\right]_1\cdot\left[\frac{f_\pi}{m_\pi}\vec{\tau}\gamma_5\gamma_\nu\partial^\nu\right]_2, \tag{2.4d}$$

$$\Gamma_A(1,2) \equiv \frac{e^2}{4}[\gamma_\mu(1-\tau_3)]_1[\gamma^\mu(1-\tau_3)]_2, \tag{2.4e}$$

the Hamiltonian in the nucleon space can be expressed as

$$\hat{H} = \int d^3x\,[\bar{\psi}[-i\boldsymbol{\gamma}\cdot\boldsymbol{\nabla} + M]\psi] + \frac{1}{2}\int d^3x d^4y \sum_{i=\sigma,\omega,\rho,\pi,A}\bar{\psi}(x)\bar{\psi}(y)\Gamma_i(x,y)D_i(x,y)\psi(y)\psi(x), \tag{2.5}$$

where $D_i(x,y)$ is the retarded Green function of the Klein-Gordon equation for each meson. Neglecting the retardation effects, the meson propagator has the usual Yukawa form,

$$D_i(\boldsymbol{x},\boldsymbol{y}) = \frac{1}{4\pi}\frac{e^{-m_i|\boldsymbol{x}-\boldsymbol{y}|}}{|\boldsymbol{x}-\boldsymbol{y}|}. \tag{2.6}$$

2.1.2 Hartree-Fock approximation

To quantize the Hamiltonian $\hat{H}$ in Eq. (2.5), the nucleon field operators ψ and $\psi^\dagger$ are expanded on the set of creation and annihilation operators defined by the stationary solutions of the Dirac equation (Bouyssy *et al.*, 1987),

$$\psi(x) = \sum_i \left(f_i(\boldsymbol{x}) e^{-i\varepsilon_i t} c_i + g_i(\boldsymbol{x}) e^{i\varepsilon'_i t} d_i^\dagger \right), \tag{2.7a}$$

$$\psi^\dagger(x) = \sum_i \left(f_i^\dagger(\boldsymbol{x}) e^{i\varepsilon_i t} c_i^\dagger + g_i^\dagger(\boldsymbol{x}) e^{-i\varepsilon'_i t} d_i \right). \tag{2.7b}$$

Here, $f_i(\boldsymbol{x})$ and $g_i(\boldsymbol{x})$ are Dirac spinors, c_i and $c_i^\dagger$ represent annihilation and creation operators for nucleons in a positive energy state i, while d_i and $d_i^\dagger$ are the corresponding operators for negative energy states. Within the so-called no-sea approximation, the summation of the densities and currents is restricted to positive energy states, i.e., the d_i and $d_i^\dagger$ terms are omitted in the above expansions. The related vacuum polarization effects are supposed to be effectively contained in the parameters of the model.

Thus, the Hamiltonian $\hat{H}$ is composed of the one-body and two-body interactions,

$$\hat{H} = \hat{T} + \sum_i \hat{V}_i \tag{2.8}$$

with

$$\hat{T} = \int d\boldsymbol{x} \sum_{\alpha\beta} \bar{f}_\alpha (i\boldsymbol{\gamma}\cdot\boldsymbol{\nabla} + M) f_\beta c_\alpha^\dagger c_\beta, \tag{2.9a}$$

$$\hat{V}_i = \frac{1}{2} \int d\boldsymbol{x}_1 d\boldsymbol{x}_2 \sum_{\alpha\beta;\alpha'\beta'} c_\alpha^\dagger c_\beta^\dagger c_{\beta'} c_{\alpha'} \bar{f}_\alpha(1) \bar{f}_\beta(2) \Gamma_i(1,2) D_i(1,2) f_{\beta'}(2) f_{\alpha'}(1). \tag{2.9b}$$

In the Hartree-Fock approximation, the trial ground-state is chosen as a Slater determinant, i.e.,

$$|\Phi_0\rangle = \prod_a c_a^\dagger |0\rangle \tag{2.10}$$

with the physical vacuum $|0\rangle$. The total energy can thus be written as

$$\begin{aligned} E &= \langle\Phi_0|\hat{H}|\Phi_0\rangle = \langle\Phi_0|\hat{T}|\Phi_0\rangle + \sum_i \langle\Phi_0|\hat{V}_i|\Phi_0\rangle \\ &= \sum_a \langle a| -i\boldsymbol{\alpha}\cdot\boldsymbol{\nabla} + \beta M |a\rangle + \frac{1}{2}\sum_{ab} \langle ab| V(1,2) |ba\rangle - \frac{1}{2}\sum_{ab} \langle ab| V(1,2) |ab\rangle , \end{aligned} \tag{2.11}$$

where the first term is the kinetic energy, the second and the last terms are the direct (Hartree) and exchange (Fock) energies, respectively.

The equations of motion of nucleons are derived by requiring that the total energy of the system E is stationary with respect to norm-conserving variations of the Dirac spinors f_a,

$$\delta \left[E - \sum_a E_a \int f_a^\dagger f_a d\boldsymbol{r} \right] = 0 \tag{2.12}$$

with Lagrange multipliers E_a. It turns out that E_a are the single-particle energies including the nucleon mass.

2.1.3 Density-dependent meson-nucleon couplings

In this work, the relativistic Hartree-Fock approach with density-dependent meson-nucleon couplings (DDRHF) will be applied to the investigations. In these effective interactions, the meson-nucleon coupling strengths g_σ, g_ω, g_ρ, f_π are functions of the baryonic density ρ_b. Therefore, in the variational procedure in Eq. (2.12), the density-dependence in meson-nucleon couplings will lead to an additional term Σ_R^μ, the so-called rearrangement term, in the self-energy Σ,

$$\Sigma = \Sigma' + \gamma_\mu \Sigma_R^\mu. \tag{2.13}$$

It has been shown that the rearrangement terms are necessary for the energy-momentum conservation (Fuchs *et al.*, 1995). In **Section 2.3**, we will see the profound effects of these rearrangement terms on the RPA matrix elements.

2.1.4 DDRHF approach for spherical nuclei

Within spherical symmetry, the single-particle state with energy E_a is specified by the set of quantum numbers $a = (q_a, n_a, l_a, j_a, m_a)$, with $q_a = 1$ for neutron and $q_a = -1$ for proton. $\kappa_a = (l_a - j_a)(2j_a + 1)$ is another convenient good quantum number. The single-particle wave function is explicitly expressed as

$$f_a(\boldsymbol{r}) = \frac{1}{r} \begin{Bmatrix} iG_a(r) \\ F_a(r)\hat{\boldsymbol{\sigma}} \cdot \hat{\boldsymbol{r}} \end{Bmatrix} \mathscr{Y}_a(\hat{\boldsymbol{r}}) \chi_{\frac{1}{2}}(q_a), \tag{2.14}$$

where $\chi_{\frac{1}{2}}(q_a)$ is an isospinor, and $\mathscr{Y}_a$ is a spherical spinor defined as

$$\mathscr{Y}_a = \sum_{\mu_a, s_a} C^{j_a m_a}_{l_a \mu_a \frac{1}{2} s_a} Y_{l_a \mu_a}(\hat{\boldsymbol{r}}) \chi_{\frac{1}{2}}(s_a), \tag{2.15}$$

where $Y_{l_a \mu_a}(\hat{\boldsymbol{r}})$ are spherical harmonics. In the following, a short-hand notation

$$\mathscr{Y}_{a'}(\hat{\boldsymbol{r}}) = -\hat{\boldsymbol{\sigma}} \cdot \hat{\boldsymbol{r}} \mathscr{Y}_a(\hat{\boldsymbol{r}}) \tag{2.16}$$

will be used for the angular part of the lower component, where $a = (q_a, n_a, l_a, j_a)$ and $a' = (q_a, n_a, l'_a, j_a)$ with $l'_a = 2j_a - l_a$. The corresponding normalization of the Dirac spinor reads

$$\int f_a^\dagger(\boldsymbol{r}) f_a(\boldsymbol{r}) d\boldsymbol{r} = \int \left[G_a^2(r) + F_a^2(r) \right] dr = 1. \tag{2.17}$$

The densities can then be expressed as,

$$\rho_s^{(\text{n or p})} \equiv \frac{1}{4\pi r^2} \sum_a^{\text{n or p}} \hat{j}_a^2 \left[G_a^2(r) - F_a^2(r) \right], \quad \rho_s \equiv \rho_s^{(n)} + \rho_s^{(p)}, \quad \rho_s^{(3)} \equiv \rho_s^{(n)} - \rho_s^{(p)}, \tag{2.18a}$$

$$\rho_b^{(\text{n or p})} \equiv \frac{1}{4\pi r^2} \sum_a^{\text{n or p}} \hat{j}_a^2 \left[G_a^2(r) + F_a^2(r) \right], \quad \rho_b \equiv \rho_b^{(n)} + \rho_b^{(p)}, \quad \rho_b^{(3)} \equiv \rho_b^{(n)} - \rho_b^{(p)}, \tag{2.18b}$$

$$\rho_T^{(\text{n or p})} \equiv \frac{1}{4\pi r^2} \sum_a^{\text{n or p}} \hat{j}_a^2 \left[2G_a(r) F_a(r) \right], \quad \rho_T \equiv \rho_T^{(n)} + \rho_T^{(p)}, \quad \rho_T^{(3)} \equiv \rho_T^{(n)} - \rho_T^{(p)}, \tag{2.18c}$$

where $\hat{j}_a^2 = 2j_a + 1$ represents the degeneracy of state (q_a, n_a, l_a, j_a).

In the spherical case, the Yukawa-type meson propagators in Eq. (2.6) can be also expanded in terms of Bessel functions and spherical harmonics,

$$D_i(\boldsymbol{r_1}, \boldsymbol{r_2}) = \sum_{L=0}^{\infty} R_{LL}(m_i; r_1, r_2) \boldsymbol{Y}_L(\hat{\boldsymbol{r}}_1) \cdot \boldsymbol{Y}_L(\hat{\boldsymbol{r}}_2). \tag{2.19}$$

The definition of $R_{LL}(m_i; r_1, r_2)$ and the gradients of $D_i(\boldsymbol{r_1}, \boldsymbol{r_2})$ with respect to $\boldsymbol{r}_1$ and $\boldsymbol{r}_2$ can be found in **Remark 10**.

The total energy of the system in Eq. (2.11) is the sum of the kinetic energy and the direct and exchange contributions from mesons and photon,

$$E = E_k + E_\sigma^D + E_\sigma^E + E_\omega^D + E_\omega^E + E_\rho^D + E_\rho^E + E_\pi^E + E_A^D + E_A^E, \tag{2.20}$$

where the direct term of pion vanishes because of the parity conservation. For spherical nuclei, each term can be expressed as one- or two-dimensional radial integrals over the products of the radial wave functions $G(r)$ and $F(r)$, and the radial multipoles of the Yukawa propagator $R_{LL}(m_i; r_1, r_2)$. These integrals are carried out numerically, whereas the angular integrals can be calculated analytically using the angular momentum algebra. The explicit expressions are listed in **Section A.1**.

The variational procedure (Eq. (2.12)) with respect to the single-particle wave functions $G(r)$ and $F(r)$ leads to the radial integro-differential Dirac equations,

$$E_a \begin{pmatrix} G_a(r) \\ F_a(r) \end{pmatrix} = \begin{pmatrix} M + \Sigma_s(r) + \Sigma_0(r) & -\frac{d}{dr} + \frac{\kappa_a}{r} \\ \frac{d}{dr} + \frac{\kappa_a}{r} & -M - \Sigma_s(r) + \Sigma_0(r) \end{pmatrix} \begin{pmatrix} G_a(r) \\ F_a(r) \end{pmatrix} + \begin{pmatrix} Y_a(r) \\ X_a(r) \end{pmatrix}. \tag{2.21}$$

In these equations, Σ_S and Σ_0 represent the contributions from the direct terms and the rearrangement term. They can be expressed in terms of the mean fields,

$$\Sigma_S = g_\sigma \sigma, \qquad \Sigma_0 = g_\omega \omega + g_\rho \rho \tau_3 + eA\frac{1 - \tau_3}{2} + \Sigma_R. \tag{2.22}$$

While, the X and Y functions, which contain the non-local exchange contributions, are defined as

$$X_a \equiv \frac{1}{2\hat{j}_a^2} \frac{\delta}{\delta F_a} E, \qquad Y_a \equiv \frac{1}{2\hat{j}_a^2} \frac{\delta}{\delta G_a} E. \tag{2.23}$$

They are in fact integrals involving the unknown functions $\{G_a(r), F_a(r)\}$. This is the reason why the RHF equations are integro-differential equations.

For the case of density-dependent meson-nucleon couplings, there is a so-called rearrangement term contributing to the self-energies. In the effective interactions used in this work, the density-dependence is chosen with respect to the baryonic density ρ_b. Then, the rearrangement term in Eq. (2.13) has only a time component Σ_R. It can be obtained by taking the variation of the energy functional with respect to ρ_b. Taking the σ-meson as an example, the rearrangement self-energy is expressed as

$$\Sigma_R^{(\sigma)}(r) = \frac{\partial g_\sigma}{\partial \rho_v} \frac{1}{g_\sigma} \left[\rho_s(r)\sigma(r) + \sum_a \hat{j}_a^2 \left(G_a(r) Y_a^{(\sigma)}(r) + F_a(r) X_a^{(\sigma)}(r) \right) / r^2 \right]. \tag{2.24}$$

The contributions of other mesons to Σ_R can be obtained in an analogous way.

The trick for solving the radial Dirac equations (Eq. (2.21)) should be emphasized before ending this subsection. One can formally rewrite the inhomogeneous terms as

$$X_a(r) = \frac{G_a(r)X_a(r)}{G_a^2(r)+F_a^2(r)}G_a(r) + \frac{F_a(r)X_a(r)}{G_a^2(r)+F_a^2(r)}F_a(r) \equiv X_{a,G_a}(r)G_a(r) + X_{a,F_a}(r)F_a(r), \tag{2.25a}$$

$$Y_a(r) = \frac{G_a(r)Y_a(r)}{G_a^2(r)+F_a^2(r)}G_a(r) + \frac{F_a(r)Y_a(r)}{G_a^2(r)+F_a^2(r)}F_a(r) \equiv Y_{a,G_a}(r)G_a(r) + Y_{a,F_a}(r)F_a(r). \tag{2.25b}$$

The radial Dirac equations can then be cast in the form

$$E_a \begin{pmatrix} G_a(r) \\ F_a(r) \end{pmatrix} = \begin{pmatrix} M+\Sigma_s(r)+\Sigma_0(r)+Y_{a,G_a}(r) & -\frac{d}{dr}+\frac{\kappa_a}{r}+Y_{a,F_a}(r) \\ \frac{d}{dr}+\frac{\kappa_a}{r}+X_{a,G_a}(r) & -M-\Sigma_s(r)+\Sigma_0(r)+X_{a,F_a}(r) \end{pmatrix} \begin{pmatrix} G_a(r) \\ F_a(r) \end{pmatrix}. \tag{2.26}$$

The equations (2.26) are formally coupled differential equations which can be solved numerically like in RH by the shooting method, with the auxiliary potential terms X and Y to be determined iteratively until convergency.

2.1.5 Effective interactions in DDRHF approach

According to the spirit of effective field theory (EFT), the masses and the couplings strengths in the effective Lagrangian in Eq. (2.1) must be determined by some best fitting processes.

For the density-dependence of the meson-nucleon couplings, g_σ, g_ω, g_ρ and f_π are taken as functions of the baryonic density ρ_b following the experience and success in the density-dependent RH theory. For σ- and ω-mesons, the density-dependent behaviors of the coupling constants g_σ and g_ω are chosen as

$$g_i(\rho_b) = g_i(\rho_{\text{sat.}})f_i(\xi), \tag{2.27}$$

where

$$f_i(\xi) = a_i\frac{1+b_i(\xi+d_i)^2}{1+c_i(\xi+d_i)^2}, \tag{2.28}$$

is a function of $\xi = \rho_b/\rho_{\text{sat.}}$. For the functions $f_i(\xi)$, five constraint conditions $f_i(1) = 1$, $f_\sigma''(1) = f_\omega''(1)$ and $f_i''(0) = 0$ are introduced. For the coupling strengths g_ρ and f_π of ρ-meson and pion, an exponential density-dependence is adopted

$$g_\rho(\rho_b) = g_\rho(0)e^{-a_\rho\xi}, \qquad f_\pi(\rho_b) = f_\pi(0)e^{-a_\pi\xi}. \tag{2.29}$$

Three sets of effective interactions in DDRHF approach have been developed by fitting the masses of the nuclei ^{16}O, ^{40}Ca, ^{48}Ca, ^{56}Ni, ^{68}Ni, ^{90}Zr, ^{116}Sn, ^{132}Sn, ^{182}Pb, ^{194}Pb, ^{208}Pb and ^{214}Pb, and the values of the baryonic saturation density $\rho_{\text{sat.}}$, the compression modulus K and the symmetry energy J of nuclear matter at the saturation point (Long, 2005).

The results for the parameterizations PKO1 (Long *et al.*, 2006), PKO2 (Long *et al.*, 2008), and PKO3 (Long *et al.*, 2008) are shown in **Table 2.1**. In particular, the pion is excluded in the effective interaction PKO2.

Table 2.1: Effective interactions PKO1, PKO2 and PKO3 for the relativistic Hartree-Fock approach with density-dependent meson-nucleon couplings, with $M = 938.9$ MeV, $m_\omega = 783.0$ MeV, $m_\rho = 769.0$ MeV and $m_\pi = 138.0$ MeV (Long *et al.*, 2006, 2008).

	m_σ (MeV)	g_σ	g_ω	$g_\rho(0)$	$f_\pi(0)$	a_ρ	a_π	$\rho_{\text{sat.}}$ (fm^{-3})
PKO1	525.769084	8.833239	10.729933	2.629000	1.000000	0.076760	1.231976	0.151989
PKO2	534.461766	8.920597	10.550553	4.068299	———	0.631605	———	0.151021
PKO3	525.667686	8.895635	10.802690	3.832480	1.000000	0.635336	0.934122	0.153006
	a_σ	b_σ	c_σ	d_σ	a_ω	b_ω	c_ω	d_ω
PKO1	1.384494	1.513190	2.296615	0.380974	1.403347	2.008719	3.046686	0.330770
PKO2	1.375772	2.064391	3.052417	0.330459	1.451420	3.574373	5.478373	0.246668
PKO3	1.244635	1.566659	2.074581	0.400843	1.245714	1.645754	2.177077	0.391293

2.2 Random Phase Approximation

The derivations of the RPA equations are well explained in many standard textbooks, for example, P. Ring and P. Schuck's *The Nuclear Many-Body Problem* (Ring and Schuck, 1980). In this section, the RPA equations will be derived via the linear response of the time-dependent external field in the small amplitude limit. In contrast to the equation of motion method, the present method can be applied to the effective interaction with density-dependent couplings as well (Ring and Schuck, 1980).

In this thesis, we use the letters $a, b, \cdots$ to denote the occupied (hole) states, capital letters $A, B, \cdots$ to denote the unoccupied (particle) states, Greek letters $\alpha, \beta, \cdots$ to denote the states in the empty Dirac sea (also particle states), and letters $i, j, \cdots$ for general cases.

2.2.1 RPA equations

As shown in the previous section, starting from an effective Hamiltonian $\hat{H}$ (Eq. (2.8)) of the system and the trial ground-state $|\Phi_0\rangle$ (Eq. (2.10)), one can first obtain the total energy E,

$$E = \left\langle \Phi_0 \left| \hat{H} \right| \Phi_0 \right\rangle = \sum_a \langle a|T|a\rangle + \frac{1}{2}\sum_{ab} \left[\langle ab|V(1,2)|ba\rangle - \langle ab|V(1,2)|ab\rangle\right]. \tag{2.30}$$

The static Hartree-Fock equation is derived via the variational principle (Eq. (2.12)), i.e.,

$$(H_0[f] - E_a) f_a = 0, \tag{2.31}$$

where

$$H_0[f] f_a(1) = T f_a(1) + \sum_b \langle b(2)|V(1,2)|b(2)\rangle f_a(1) - \sum_b \langle b(2)|V(1,2)|a(2)\rangle f_b(1). \tag{2.32}$$

$H_0[f]$ is the so-called Hartree-Fock Hamiltonian, which is a one-body Hamiltonian, and a functional with respect to the single-particle wave functions.

Adding a time-dependent external field $\mathcal{W}(t)$

$$\mathcal{W}(t) = W(\boldsymbol{r})e^{-i\omega t} + W^\dagger(\boldsymbol{r})e^{i\omega t}, \tag{2.33}$$

the system Hamiltonian becomes

$$H \to H + \mathcal{W}(t). \tag{2.34}$$

This leads to changes in the single-particle wave functions and in the HF Hamiltonian,

$$f_a \quad \to \quad \varphi_a = f_a + \sum_A \beta_{Aa}(t) f_A + \sum_\alpha \beta_{\alpha a}(t) g_\alpha, \tag{2.35a}$$

$$H_0[f] \quad \to \quad H_0[\varphi] + \mathcal{W}. \tag{2.35b}$$

Thus, the time-dependent Hartree-Fock (TDHF) equation becomes

$$i\frac{\partial}{\partial t}\varphi_a = (H_0[\varphi] + \mathcal{W} - E_a)\varphi_a. \tag{2.36}$$

In the small amplitude limit, only the linear response to the external field is taken into account, i.e., just the the linear terms of $\beta_{Aa}, \beta_{\alpha a}$ are kept.

Supposing that the expansion coefficients β have the same time-dependent behaviors as $\mathcal{W}(t)$, they can be expressed as

$$\beta_{Aa}(t) \quad = \quad X_{Aa}e^{-i\omega t} - Y^*_{Aa}e^{i\omega t}, \tag{2.37a}$$

$$\beta_{\alpha a}(t) \quad = \quad X_{\alpha a}e^{-i\omega t} - Y^*_{\alpha a}e^{i\omega t}. \tag{2.37b}$$

Using $\langle f_A|$ to act on the TDHF equation (2.36), one can obtain that

$$\text{lhs} = \langle f_A | i\frac{\partial}{\partial t}|\varphi_a\rangle = i\dot{\beta}_{Aa} = \omega(X_{Aa}e^{-i\omega t} + Y^*_{Aa}e^{i\omega t}), \tag{2.38}$$

and

$$\text{rhs} = \langle f_A | H_0[\varphi] + \mathcal{W} - E_a | f_a + \sum_{A'} \beta_{A'a}(t) f_{A'} + \sum_\alpha \beta_{\alpha a}(t) g_\alpha \rangle. \tag{2.39}$$

Nine terms appearing in the rhs are shown explicitly in the following. For the first term,

$$\langle f_A | H_0[\varphi] | f_a \rangle = \langle f_A | H_0[f] + \delta H_0 | f_a \rangle. \tag{2.40}$$

Its zeroth-order term $\langle f_A|H_0[f]|f_a\rangle$ vanishes because of the orthogonality of the single-particle wave functions, and its first-order term reads

$$\begin{aligned}\langle f_A|\delta H_0|f_a\rangle \quad = \quad & \sum_{Bb} \{\beta^*_{Bb}\langle AB|V(1,2)|ba-ab\rangle + \beta_{Bb}\langle Ab|V(1,2)|Ba-aB\rangle\} \\ & + \sum_{\beta b} \left\{\beta^*_{\beta b}\langle A\beta|V(1,2)|ba-ab\rangle + \beta_{\beta b}\langle Ab|V(1,2)|\beta a-a\beta\rangle\right\}. \end{aligned} \tag{2.41}$$

The other eight terms are simpler. The non-vanishing terms are

$$\langle f_A|\mathcal{W}|f_a\rangle \quad = \quad \langle f_A|We^{-i\omega t} + W^\dagger e^{i\omega t}|f_a\rangle, \tag{2.42a}$$

$$\langle f_A|H_0[\varphi]|\sum_{A'}\beta_{A'a}f_{A'}\rangle \quad = \quad E_A\beta_{Aa}, \tag{2.42b}$$

$$\langle f_A|-E_a|\sum_{A'}\beta_{A'a}f_{A'}\rangle \quad = \quad -E_a\beta_{Aa}. \tag{2.42c}$$

Separating the coefficients of the non-vanishing $e^{i\omega t}$ and $e^{-i\omega t}$ terms, one has

$$\begin{aligned} -\langle A|W|a\rangle &= [(E_A - E_a) - \omega]X_{Aa} \\ &\quad + \sum_{Bb}[\langle Ab|V|Ba - aB\rangle X_{Bb} - \langle AB|V|ba - ab\rangle Y_{Bb}] \\ &\quad + \sum_{\beta b}[\langle Ab|V|\beta a - a\beta\rangle X_{\beta b} - \langle A\beta|V|ba - ab\rangle Y_{\beta b}], \end{aligned} \tag{2.43a}$$

$$\begin{aligned} -\langle A|W^\dagger|a\rangle^* &= [-(E_A - E_a) - \omega]Y_{Aa} \\ &\quad + \sum_{Bb}[\langle AB|V|ba - ab\rangle X_{Bb} - \langle Ab|V|Ba - aB\rangle Y_{Bb}] \\ &\quad + \sum_{\beta b}[\langle A\beta|V|ba - ab\rangle X_{\beta b} - \langle Ab|V|\beta a - a\beta\rangle Y_{\beta b}]. \end{aligned} \tag{2.43b}$$

Analogously, using $\langle g_\alpha|$ to act on the TDHF equation (2.36), one can obtain

$$\begin{aligned} -\langle \alpha|W|a\rangle &= [(E_\alpha - E_a) - \omega]X_{\alpha a} \\ &\quad + \sum_{Bb}[\langle \alpha b|V|Ba - aB\rangle X_{Bb} - \langle \alpha B|V|ba - ab\rangle Y_{Bb}] \\ &\quad + \sum_{\beta b}[\langle \alpha b|V|\beta a - a\beta\rangle X_{\beta b} - \langle \alpha\beta|V|ba - ab\rangle Y_{\beta b}], \end{aligned} \tag{2.44a}$$

$$\begin{aligned} -\langle \alpha|W^\dagger|a\rangle^* &= [-(E_\alpha - E_a) - \omega]Y_{\alpha a} \\ &\quad + \sum_{Bb}[\langle \alpha B|V|ba - ab\rangle X_{Bb} - \langle \alpha b|V|Ba - aB\rangle Y_{Bb}] \\ &\quad + \sum_{\beta b}[\langle \alpha\beta|V|ba - ab\rangle X_{\beta b} - \langle \alpha b|V|\beta a - a\beta\rangle Y_{\beta b}]. \end{aligned} \tag{2.44b}$$

With the compact notations,

$$\mathcal{A}_{12,34} = (E_1 - E_2)\delta_{12,34} + \langle 14|V|32 - 23\rangle, \tag{2.45a}$$

$$\mathcal{B}_{12,34} = -\langle 13|V|42 - 24\rangle, \tag{2.45b}$$

$$\mathcal{C}_{12,34} = +\langle 14|V|32 - 23\rangle, \tag{2.45c}$$

the RPA equations can be written in the matrix form,

$$\begin{pmatrix} \mathcal{A}_{Aa,Bb} & \mathcal{C}_{Aa,\beta b} & \mathcal{B}_{Aa,Bb} & \mathcal{B}_{Aa,\beta b} \\ \mathcal{C}_{\alpha a,Bb} & \mathcal{A}_{\alpha a,\beta b} & \mathcal{B}_{\alpha a,Bb} & \mathcal{B}_{\alpha a,\beta b} \\ -\mathcal{B}_{Aa,Bb} & -\mathcal{B}_{Aa,\beta b} & -\mathcal{A}_{Aa,Bb} & -\mathcal{C}_{Aa,\beta b} \\ -\mathcal{B}_{\alpha a,Bb} & -\mathcal{B}_{\alpha a,\beta b} & -\mathcal{C}_{\alpha a,Bb} & -\mathcal{A}_{\alpha a,\beta b} \end{pmatrix} \begin{pmatrix} X_{Bb} \\ X_{\beta b} \\ Y_{Bb} \\ Y_{\beta b} \end{pmatrix} - \omega \begin{pmatrix} X_{Aa} \\ X_{\alpha a} \\ Y_{Aa} \\ Y_{\alpha a} \end{pmatrix} = - \begin{pmatrix} \langle A|W|a\rangle \\ \langle \alpha|W|a\rangle \\ \langle A|W^\dagger|a\rangle^* \\ \langle \alpha|W^\dagger|a\rangle^* \end{pmatrix}, \tag{2.46}$$

where the repeated indices B, b, β indicate the summations.

RPA equations in angular momentum coupled form

For the spherical case, the basis vectors are given by $|jm\rangle$ in the representation according to the operators $\hat{J}^2$, $\hat{J}_z$. Then, the angular integrals in the RPA matrix elements $\mathcal{A}$, $\mathcal{B}$, and $\mathcal{C}$ can be calculated independently and analytically by the angular momentum algebra (Brink and Satchler, 1968;

Varshalovich *et al.*, 1987). Therefore, this subsection is dedicated to deriving the RPA equations in angular momentum coupled form.

Supposing that the external field $W(\boldsymbol{r})$ has a specific angular momentum and parity, i.e., $W(\boldsymbol{r}) = W_{J^\pi M}(\boldsymbol{r})$, the expectation values in the rhs of the RPA equations (Eq. (2.46)) read

$$\langle A|W|a\rangle = (-)^{j_A-m_A}\begin{pmatrix} j_A & j_a & J \\ m_A & -m_a & -M \end{pmatrix}\langle A||W_J||a\rangle, \tag{2.47a}$$

$$\langle A|W^\dagger|a\rangle^* = (-)^{j_A-m_A+M}\begin{pmatrix} j_A & j_a & J \\ m_A & -m_a & M \end{pmatrix}\langle A||W_J^\dagger||a\rangle^*, \tag{2.47b}$$

where the Wigner-Eckart theorem is used (see **Remark 13**) and $\langle A||W_J||a\rangle$ is the reduced matrix element.

We define the angular momentum coupled X, Y amplitudes as following,

$$X_{Bm_B,bm_b} = \hat{J}(-)^{j_B-m_B}\begin{pmatrix} j_B & j_b & J \\ m_B & -m_b & -M \end{pmatrix}X^J_{Bb}, \tag{2.48a}$$

$$Y_{Bm_B,bm_b} = \hat{J}(-)^{j_B-m_B+M}\begin{pmatrix} j_B & j_b & J \\ m_B & -m_b & M \end{pmatrix}Y^J_{Bb}, \tag{2.48b}$$

where the minus sign in $-m_b$ is due to state b standing for a hole state here.

The angular momentum coupled RPA equations read

$$\begin{pmatrix} \mathcal{A}^J_{Aa,Bb} & \mathcal{C}^J_{Aa,\beta b} & \mathcal{B}^J_{Aa,Bb} & \mathcal{B}^J_{Aa,\beta b} \\ \mathcal{C}^J_{\alpha a,Bb} & \mathcal{A}^J_{\alpha a,\beta b} & \mathcal{B}^J_{\alpha a,Bb} & \mathcal{B}^J_{\alpha a,\beta b} \\ -\mathcal{B}^J_{Aa,Bb} & -\mathcal{B}^J_{Aa,\beta b} & -\mathcal{A}^J_{Aa,Bb} & -\mathcal{C}^J_{Aa,\beta b} \\ -\mathcal{B}^J_{\alpha a,Bb} & -\mathcal{B}^J_{\alpha a,\beta b} & -\mathcal{C}^J_{\alpha a,Bb} & -\mathcal{A}^J_{\alpha a,\beta b} \end{pmatrix}\begin{pmatrix} X^J_{Bb} \\ X^J_{\beta b} \\ Y^J_{Bb} \\ Y^J_{\beta b} \end{pmatrix} - \omega\begin{pmatrix} X^J_{Aa} \\ X^J_{\alpha a} \\ Y^J_{Aa} \\ Y^J_{\alpha a} \end{pmatrix} = -\begin{pmatrix} \langle A||W_J||a\rangle \\ \langle \alpha||W_J||a\rangle \\ \langle A||W_J^\dagger||a\rangle^* \\ \langle \alpha||W_J^\dagger||a\rangle^* \end{pmatrix}, \tag{2.49}$$

with the definitions

$$\mathcal{A}^J_{Aa,Bb} = \sum_{mM}(-)^{j_A-m_A+j_B-m_B}\begin{pmatrix} j_A & j_a & J \\ m_A & -m_a & -M \end{pmatrix}\begin{pmatrix} j_B & j_b & J \\ m_B & -m_b & -M \end{pmatrix}\mathcal{A}_{Aa,Bb}, \tag{2.50a}$$

$$\mathcal{B}^J_{Aa,Bb} = \sum_{mM}(-)^{j_A-m_A+j_B-m_B+M}\begin{pmatrix} j_A & j_a & J \\ m_A & -m_a & -M \end{pmatrix}\begin{pmatrix} j_B & j_b & J \\ m_B & -m_b & M \end{pmatrix}\mathcal{B}_{Aa,Bb}, \tag{2.50b}$$

$$\mathcal{C}^J_{Aa,\beta b} = \sum_{mM}(-)^{j_A-m_A+j_\beta-m_\beta}\begin{pmatrix} j_A & j_a & J \\ m_A & -m_a & -M \end{pmatrix}\begin{pmatrix} j_\beta & j_b & J \\ m_\beta & -m_b & -M \end{pmatrix}\mathcal{C}_{Aa,\beta b}, \tag{2.50c}$$

where $\sum_m$ means $\sum_{m_A,m_a,m_B,m_b}$. All other $\mathcal{A}^J, \mathcal{B}^J, \mathcal{C}^J$s are defined in a similar way by changing the indices.

RPA equations in charge-exchange channels

In the charge-exchange channels, the p-h configurations are built by taking pairs of proton-neutron. Proton particle-neutron hole and neutron particle-proton hole correspond to the isospin lowering T_- and raising T_+ channels, respectively. Denoting the unoccupied and occupied proton (neutron) states as p and $\bar{p}$ (n and $\bar{n}$), the angular momentum coupled RPA eigenequations (2.49) are written explicitly as

$$\begin{pmatrix} \mathcal{A}^J_{p\bar{n}p'\bar{n}'} & \mathcal{A}^J_{p\bar{n}n'\bar{p}'} & \mathcal{B}^J_{p\bar{n}p'\bar{n}'} & \mathcal{B}^J_{p\bar{n}n'\bar{p}'} \\ \mathcal{A}^J_{n\bar{p}p'\bar{n}'} & \mathcal{A}^J_{n\bar{p}n'\bar{p}'} & \mathcal{B}^J_{n\bar{p}p'\bar{n}'} & \mathcal{B}^J_{n\bar{p}n'\bar{p}'} \\ -\mathcal{B}^J_{p\bar{n}p'\bar{n}'} & -\mathcal{B}^J_{p\bar{n}n'\bar{p}'} & -\mathcal{A}^J_{p\bar{n}p'\bar{n}'} & -\mathcal{A}^J_{p\bar{n}n'\bar{p}'} \\ -\mathcal{B}^J_{n\bar{p}p'\bar{n}'} & -\mathcal{B}^J_{p\bar{n}n'\bar{p}'} & -\mathcal{A}^J_{n\bar{p}p'\bar{n}'} & -\mathcal{A}^J_{n\bar{p}n'\bar{p}'} \end{pmatrix} \begin{pmatrix} X^J_{p'\bar{n}'} \\ X^J_{n'\bar{p}'} \\ Y^J_{p'\bar{n}'} \\ Y^J_{n'\bar{p}'} \end{pmatrix} = \omega \begin{pmatrix} X^J_{p'\bar{n}'} \\ X^J_{n'\bar{p}'} \\ Y^J_{p'\bar{n}'} \\ Y^J_{n'\bar{p}'} \end{pmatrix}. \tag{2.51}$$

Due to the charge conservation, the matrix elements $\mathcal{A}^J_{p\bar{n}n'\bar{p}'}$, $\mathcal{A}^J_{n\bar{p}p'\bar{n}'}$, $\mathcal{B}^J_{p\bar{n}p'\bar{n}'}$, and $\mathcal{B}^J_{p\bar{n}n'\bar{p}'}$ vanish, i.e., the above RPA equations have a form of

$$\begin{pmatrix} \mathcal{A}^J_{p\bar{n}p'\bar{n}'} & 0 & 0 & \mathcal{B}^J_{p\bar{n}n'\bar{p}'} \\ 0 & \mathcal{A}^J_{n\bar{p}n'\bar{p}'} & \mathcal{B}^J_{n\bar{p}p'\bar{n}'} & 0 \\ 0 & -\mathcal{B}^J_{p\bar{n}n'\bar{p}'} & -\mathcal{A}^J_{p\bar{n}p'\bar{n}'} & 0 \\ -\mathcal{B}^J_{n\bar{p}p'\bar{n}'} & 0 & 0 & -\mathcal{A}^J_{n\bar{p}n'\bar{p}'} \end{pmatrix} \begin{pmatrix} X^J_{p'\bar{n}'} \\ X^J_{n'\bar{p}'} \\ Y^J_{p'\bar{n}'} \\ Y^J_{n'\bar{p}'} \end{pmatrix} = \omega \begin{pmatrix} X^J_{p'\bar{n}'} \\ X^J_{n'\bar{p}'} \\ Y^J_{p'\bar{n}'} \\ Y^J_{n'\bar{p}'} \end{pmatrix}. \tag{2.52}$$

Hence, it turns out that one just needs to diagonalize the following matrix,

$$\begin{pmatrix} \mathcal{A}^J_{p\bar{n}p'\bar{n}'} & \mathcal{B}^J_{p\bar{n}n'\bar{p}'} \\ -\mathcal{B}^J_{n\bar{p}p'\bar{n}'} & -\mathcal{A}^J_{n\bar{p}n'\bar{p}'} \end{pmatrix} \begin{pmatrix} U^J_{p'\bar{n}'} \\ V^J_{n'\bar{p}'} \end{pmatrix} = \omega \begin{pmatrix} U^J_{p\bar{n}} \\ V^J_{n\bar{p}} \end{pmatrix}, \tag{2.53}$$

whose dimension is half of that in Eq. (2.51), and the solutions for both T_- and T_+ channels can be obtained at the same time. The eigenvectors of the RPA equations (2.53) are separated according to the following normalization conditions,

$$\begin{cases} \sum_{p\bar{n}} (U^J_{p\bar{n}})^2 - \sum_{n\bar{p}} (V^J_{n\bar{p}})^2 = +1, & \text{for } T_- \text{ channel}, \\ \sum_{p\bar{n}} (U^J_{p\bar{n}})^2 - \sum_{n\bar{p}} (V^J_{n\bar{p}})^2 = -1, & \text{for } T_+ \text{ channel}. \end{cases} \tag{2.54}$$

The excitation energies and X, Y amplitudes in the T_- channel read

$$\Omega = +\omega, \quad X^J_{p\bar{n}} = U^J_{p\bar{n}}, \quad Y^J_{n\bar{p}} = V^J_{n\bar{p}}, \tag{2.55}$$

whereas the excitation energies and X, Y amplitudes in the T_+ channel are

$$\Omega = -\omega, \quad X^J_{n\bar{p}} = V^J_{n\bar{p}}, \quad Y^J_{p\bar{n}} = U^J_{p\bar{n}}. \tag{2.56}$$

2.2.2 Transition densities and probabilities

In this subsection, it will be shown that the transition probabilities between the ground-state and excited states driven by a one-body operator.

Formally, the excited states $|\nu\rangle$, which is an eigenstate of the system Hamiltonian $\hat{H}$, can be constructed via a operator $Q^\dagger$ acting on the ground-state $|\mathrm{GS}\rangle$. In the RPA framework, the operator $Q^\dagger$ can be expressed with the X and Y amplitudes of the RPA equations (Eq. (2.46)),

$$Q^\dagger_\nu = \sum_{pm_phm_h} X^\nu_{ph} c^\dagger_p c_h + \sum_{pm_phm_h} Y^\nu_{ph} c^\dagger_h c_p, \tag{2.57}$$

and the ground-state is the so-called RPA ground-state $|\mathrm{RPA}\rangle$, which satisfies

$$|\nu\rangle = Q^\dagger_\nu |\mathrm{RPA}\rangle, \qquad Q_\nu |\mathrm{RPA}\rangle = 0. \tag{2.58}$$

In principle, $|\mathrm{RPA}\rangle$ is different from the Hartree-Fock ground-state $|\mathrm{HF}\rangle = |\Phi_0\rangle$ shown in Eq. (2.10).

For a one-body operator $\hat{F}$ with specific quantum numbers JM, one has

$$\hat{F}_{JM} = \sum_{ij} \langle i|F_{JM}|j\rangle c^\dagger_i c_j \tag{2.59}$$

in the second-quantized notation. In particular,

$$\begin{aligned}
\langle \nu_{JM}|c^\dagger_i c_j|\mathrm{RPA}\rangle &= \langle \mathrm{RPA}| \left[Q_{JM}, c^\dagger_i c_j\right] |\mathrm{RPA}\rangle \\
&= \sum_{pm_phm_h} \langle \mathrm{RPA}| \left[X^\nu_{ph} c^\dagger_h c_p + Y^\nu_{ph} c^\dagger_p c_h, c^\dagger_i c_j\right] |\mathrm{RPA}\rangle \\
&\approx \sum_{pm_phm_h} \langle \mathrm{HF}| \left[X^\nu_{ph} c^\dagger_h c_p + Y^\nu_{ph} c^\dagger_p c_h, c^\dagger_i c_j\right] |\mathrm{HF}\rangle \\
&= \sum_{pm_phm_h} \left\{X^\nu_{ph}\delta_{ip}\delta_{jh} - Y^\nu_{ph}\delta_{ih}\delta_{jp}\right\}.
\end{aligned} \tag{2.60}$$

It should be emphasized that in the above derivation firstly the property of the RPA ground-state $Q_\nu |\mathrm{RPA}\rangle = 0$ is used to form the commutator, then the so-called quasi-boson approximation, $|\mathrm{RPA}\rangle \approx |\mathrm{HF}\rangle$, is used to calculate the commutator.

With the definitions of angular coupled X^J and Y^J in Eqs. (2.48), and the Wigner-Eckart theorem (see **Remark 13**), the expectation value $\langle \nu_{JM}|\hat{F}_{JM}|\mathrm{RPA}\rangle$ can be written in terms of the (X, Y) solutions of the angular momentum coupled RPA equations (Eq. (2.49)),

$$\langle \nu_{JM}|\hat{F}_{JM}|\mathrm{RPA}\rangle = \hat{J}^{-1} \sum_{ph} \left\{X^{J\nu}_{ph}\langle p||F_J||h\rangle + (-)^{j_p+j_h} Y^{J\nu}_{ph}\langle h||F_J||p\rangle\right\}. \tag{2.61}$$

Finally, the transition probabilities between the ground-state and excited states induced by a one-body operator reads

$$B_\nu = \left|\langle \nu_{JM}|\hat{F}_{JM}|\mathrm{RPA}\rangle\right|^2. \tag{2.62}$$

To obtain a smooth transition strength as a function of the excitation energy, one usually calculates the Lorentzian-averaged strength distribution

$$R(E) = \sum_\nu B_\nu \frac{\Gamma/2\pi}{(E-\Omega_\nu)^2 + \Gamma^2/4} \tag{2.63}$$

with the averaging width Γ.

2.2.3 Non-energy weighted sum rules

In general, the kth energy weighted sum rule related to a one-body operator $\hat{F}$ is given by

$$S_k \equiv \sum_\nu (\Omega_\nu - E_0)^k |\langle \nu|\hat{F}|\mathrm{RPA}\rangle|^2, \tag{2.64}$$

where $|\nu\rangle$ represent the complete set of eigenstates of the exact Hamiltonian H with the energies E_ν. Using the completeness relation, one has

$$S_k = \langle \mathrm{RPA}|\hat{F}^\dagger (H - E_0)^k \hat{F}|\mathrm{RPA}\rangle. \tag{2.65}$$

In some cases, this expression can be calculated by the ground-state properties in a rather simple way.

For the cases of charge-exchange excitations, the IAS, GTR, and SDR operators are

$$\hat{F}^\pm_{\mathrm{IAS}} = \sum_{i=1}^{A} \tau_\pm(i), \tag{2.66a}$$

$$\hat{F}^\pm_{\mathrm{GTR}} = \sum_{i=1}^{A} [1 \otimes \vec{\sigma}(i)]_{J=1} \tau_\pm(i), \tag{2.66b}$$

$$\hat{F}^\pm_{\mathrm{SDR}} = \sum_{i=1}^{A} [r_i Y_1(i) \otimes \vec{\sigma}(i)]_{J=(0,1,2)} \tau_\pm(i). \tag{2.66c}$$

The non-energy weighted sum rule for the IAS reads

$$\begin{aligned}
S^-_{\mathrm{IAS}} - S^+_{\mathrm{IAS}} &= \sum_\nu B^-_\nu - \sum_\nu B^+_\nu \\
&= \sum_\nu \langle \mathrm{RPA}| \sum_{i=1}^{A} \tau_+(i) |\nu\rangle\langle\nu| \sum_{i=1}^{A} \tau_-(i) |\mathrm{RPA}\rangle - \sum_\nu \langle \mathrm{RPA}| \sum_{i=1}^{A} \tau_-(i) |\nu\rangle\langle\nu| \sum_{i=1}^{A} \tau_+(i) |\mathrm{RPA}\rangle \\
&= \langle \mathrm{RPA}| \left[\sum_{i=1}^{A} \tau_+(i), \sum_{i=1}^{A} \tau_-(i) \right] |\mathrm{RPA}\rangle \\
&= \langle \mathrm{RPA}| \sum_{i=1}^{A} \tau_z(i) |\mathrm{RPA}\rangle \\
&= N - Z.
\end{aligned} \tag{2.67}$$

Analogously, the non-energy weighted sum rule for the GTR, the so-called Ikeda sum rule (Ikeda *et al.*, 1963), reads

$$S^-_{\mathrm{GTR}} - S^+_{\mathrm{GTR}} = 3(N - Z). \tag{2.68}$$

Since only the numbers of nucleons are concerned, these sum rules are model-independent. Furthermore, the non-energy weighted sum rule for the SDR reads

$$S^-_{\mathrm{SDR}} - S^+_{\mathrm{SDR}} = \frac{9}{4\pi} (N \langle r^2 \rangle_n - Z \langle r^2 \rangle_p). \tag{2.69}$$

2.3 Self-consistent RPA based on DDRHF theory

In this section, we will first show the main ideas for establishing the fully self-consistent RPA based on the RHF theory with explicit density-dependent meson-nucleon couplings. Then the contributions to the RPA matrix elements $\mathcal{A}^J$, $\mathcal{B}^J$, and $\mathcal{C}^J$ induced by each meson and photon will be summarized. One will see that the present results of the direct contributions are identical to those of Ref. (Nikšić *et al.*, 2002b), where the self-consistent RPA on top of the density-dependent RH theory was developed. The detailed derivations are given in **Appendix A**.

2.3.1 Particle-hole residual interactions with density-dependent couplings

In order to figure out the effects of the explicit density-dependent meson-nucleon couplings, let's again start from the total energy of the system (Eq. (2.11)),

$$E = \sum_a \langle a|T|a\rangle + \frac{1}{2}\sum_{ab}\left[\langle ab|V(1,2)(1-P_{ab})|ba\rangle\right], \tag{2.70}$$

where the operator P_{ab} exchanges all the variables of particles a and b. To separate the density-dependent part from the density-independent part, the two-body interactions are generally expressed as

$$V_i(1,2) = g_i(1)g_i(2)I_i(1,2), \tag{2.71}$$

where i stands for σ-, ω-, ρ-, $\pi-$mesons and photon, and the coupling strengths g_i are the functions of the baryonic density ρ_b. Following the variational procedure (also see Eq. (2.12)),

$$\delta\left[E - \sum_a E_a \langle a|a\rangle\right] = 0, \tag{2.72}$$

it turns out that the lhs of Eq. (2.72) reads

$$\begin{aligned}\text{lhs} &= \left[\langle \delta i|T|i\rangle + \sum_b \langle \delta ib|V(1,2)(1-P_{ib})|bi\rangle - E_i\langle \delta i|i\rangle\right] + c.c. \\ &\quad + \frac{1}{2}\sum_{ab}\langle ab|\delta V(1-P_{ab})|ba\rangle,\end{aligned} \tag{2.73}$$

where the last term is the so-called rearrangement term. Thus, the static HF equation reads

$$(H_0[f] - E_i)f_i(1) = 0, \tag{2.74}$$

with the HF Hamiltonian

$$\begin{aligned}H_0[f]f_i(1) &= Tf_i(1) + \int d\boldsymbol{r}_2\left\{\sum_b f_b^\dagger(2)g(1)g(2)I(1,2)(1-P_{ib})f_b(2)\right\}f_i(1) \\ &\quad + \int d\boldsymbol{r}_2\left\{\sum_{ab} f_a^\dagger(1)f_b^\dagger(2)\left[\frac{\partial g(1)}{\partial\rho_b(1)}g(2)I(1,2)(1-P_{ab})\right]f_b(2)f_a(1)\right\}f_i(1).\end{aligned} \tag{2.75}$$

Following the derivation of the RPA equations in the previous section, it is found that eight terms in the expansion of Eq. (2.39) are the same as those in the case without density-dependent couplings, except the term $\langle f_A|H_0[\varphi]|f_a\rangle$. In the present case,

$$\begin{aligned}\langle f_A|H_0[\varphi]|f_a\rangle &= \sum_{Bb}\{\beta^*_{Bb}\langle AB|\mathcal{V}(1,2)|ba\rangle+\beta_{Bb}\langle Ab|\mathcal{V}(1,2)|Ba\rangle\}\\ &\quad+\sum_{\beta b}\left\{\beta^*_{\beta b}\langle A\beta|\mathcal{V}(1,2)|ba\rangle+\beta_{\beta b}\langle Ab|\mathcal{V}(1,2)|\beta a\rangle\right\}. \end{aligned}\tag{2.76}$$

Here, $\mathcal{V}(1,2)$ denotes the p-h residual interaction in the self-consistent RPA. It contains both the regular term and several complicated rearrangement terms as follows,

$$\begin{aligned}\mathcal{V}(1,2) &= g(1)g(2)I(1,2)(1-P_{ab})\\ &\quad+\int d\boldsymbol{r}_3\sum_d f^\dagger_d(3)\frac{\partial g(1)}{\partial\rho_b(1)}g(3)I(1,3)(1-P_{ad})f_d(3)\delta(\boldsymbol{r}_1-\boldsymbol{r}_2)\\ &\quad+\sum_d f^\dagger_d(2)g(1)\frac{\partial g(2)}{\partial\rho_b(2)}I(1,2)(1-P_{ad})f_d(2)\\ &\quad+\int d\boldsymbol{r}_3\sum_d f^\dagger_d(3)\frac{\partial g(1)}{\partial\rho_b(1)}g(3)I(1,3)(1-P_{bd})f_d(3)\delta(\boldsymbol{r}_1-\boldsymbol{r}_2)\\ &\quad+\sum_d f^\dagger_d(1)\frac{\partial g(1)}{\partial\rho_b(1)}g(2)I(1,2)(1-P_{bd})f_d(1)\\ &\quad+\int d\boldsymbol{r}_3\sum_{cd} f^\dagger_c(1)f^\dagger_d(3)\frac{\partial^2 g(1)}{\partial\rho_b^2(1)}g(3)I(1,3)(1-P_{cd})f_d(3)f_c(1)\delta(\boldsymbol{r}_1-\boldsymbol{r}_2)\\ &\quad+\sum_{cd} f^\dagger_c(1)f^\dagger_d(2)\frac{\partial g(1)}{\partial\rho_b(1)}\frac{\partial g(2)}{\partial\rho_b(2)}I(1,2)(1-P_{cd})f_d(2)f_c(1),\end{aligned}\tag{2.77}$$

where the derivatives of the coupling strength with respect to the baryonic density are evaluated at the ground-state density ρ_b^0.

Therefore, on one hand, the direct contributions to $\langle Ab|\mathcal{V}(1,2)|Ba\rangle$ are composed of 7 terms,

$$\text{Term1}=\int d\boldsymbol{r}_1d\boldsymbol{r}_2f^\dagger_A(1)f^\dagger_b(2)g(1)g(2)I(1,2)f_B(2)f_a(1),\tag{2.78a}$$

$$\text{Term2}=\sum_d\int d\boldsymbol{r}_1d\boldsymbol{r}_2f^\dagger_A(1)f^\dagger_d(2)\frac{\partial g(1)}{\partial\rho_b(1)}f^\dagger_b(1)f_B(1)g(2)I(1,2)f_d(2)f_a(1),\tag{2.78b}$$

$$\text{Term3}=\sum_d\int d\boldsymbol{r}_1d\boldsymbol{r}_2f^\dagger_A(1)f^\dagger_d(2)g(1)\frac{\partial g(2)}{\partial\rho_b(2)}f^\dagger_b(2)f_B(2)I(1,2)f_d(2)f_a(1),\tag{2.78c}$$

$$\text{Term4}=\sum_d\int d\boldsymbol{r}_1d\boldsymbol{r}_2f^\dagger_A(1)f^\dagger_b(1)f^\dagger_d(2)\frac{\partial g(1)}{\partial\rho_b(1)}g(2)I(1,2)f_d(2)f_B(1)f_a(1),\tag{2.78d}$$

$$\text{Term5}=\sum_d\int d\boldsymbol{r}_1d\boldsymbol{r}_2f^\dagger_A(1)f^\dagger_d(1)f^\dagger_b(2)\frac{\partial g(1)}{\partial\rho_b(1)}g(2)I(1,2)f_B(2)f_d(1)f_a(1),\tag{2.78e}$$

$$\text{Term6}=\sum_{cd}\int d\boldsymbol{r}_1d\boldsymbol{r}_2f^\dagger_A(1)f^\dagger_c(1)f^\dagger_d(2)\frac{\partial^2 g(1)}{\partial\rho_b^2(1)}f^\dagger_b(1)f_B(1)g(2)I(1,2)f_d(2)f_c(1)f_a(1),\tag{2.78f}$$

$$\text{Term7}=\sum_{cd}\int d\boldsymbol{r}_1d\boldsymbol{r}_2f^\dagger_A(1)f^\dagger_c(1)f^\dagger_d(2)\frac{\partial g(1)}{\partial\rho_b(1)}\frac{\partial g(2)}{\partial\rho_b(2)}f^\dagger_b(2)f_B(2)I(1,2)f_d(2)f_c(1)f_a(1),\tag{2.78g}$$

where Term1 is the regular term and Term2 to Term7 are the accompanying rearrangement terms. These results are exactly the same as those in Ref. (Nikšić *et al.*, 2002b). On the other hand, the exchange contributions to $\langle Ab|\mathcal{V}(1,2)|Ba\rangle$ are also composed of 7 terms,

$$\text{Term8} = -\int d\boldsymbol{r}_1 d\boldsymbol{r}_2 f_A^\dagger(1) f_b^\dagger(2) g(1) g(2) I(1,2) f_a(2) f_B(1), \tag{2.79a}$$

$$\text{Term9} = -\sum_d \int d\boldsymbol{r}_1 d\boldsymbol{r}_2 f_A^\dagger(1) f_d^\dagger(2) \frac{\partial g(1)}{\partial \rho_b(1)} f_b^\dagger(1) f_B(1) g(2) I(1,2) f_a(2) f_d(1), \tag{2.79b}$$

$$\text{Term10} = -\sum_d \int d\boldsymbol{r}_1 d\boldsymbol{r}_2 f_A^\dagger(1) f_d^\dagger(2) g(1) \frac{\partial g(2)}{\partial \rho_b(2)} f_b^\dagger(2) f_B(2) I(1,2) f_a(2) f_d(1), \tag{2.79c}$$

$$\text{Term11} = -\sum_d \int d\boldsymbol{r}_1 d\boldsymbol{r}_2 f_A^\dagger(1) f_b^\dagger(1) f_d^\dagger(2) \frac{\partial g(1)}{\partial \rho_b(1)} g(2) I(1,2) f_B(2) f_d(1) f_a(1), \tag{2.79d}$$

$$\text{Term12} = -\sum_d \int d\boldsymbol{r}_1 d\boldsymbol{r}_2 f_A^\dagger(1) f_d^\dagger(1) f_b^\dagger(2) \frac{\partial g(1)}{\partial \rho_b(1)} g(2) I(1,2) f_d(2) f_B(1) f_a(1), \tag{2.79e}$$

$$\text{Term13} = -\sum_{cd} \int d\boldsymbol{r}_1 d\boldsymbol{r}_2 f_A^\dagger(1) f_c^\dagger(1) f_d^\dagger(2) \frac{\partial^2 g(1)}{\partial \rho_b^2(1)} f_b^\dagger(1) f_B(1) g(2) I(1,2) f_c(2) f_d(1) f_a(1), \tag{2.79f}$$

$$\text{Term14} = -\sum_{cd} \int d\boldsymbol{r}_1 d\boldsymbol{r}_2 f_A^\dagger(1) f_c^\dagger(1) f_d^\dagger(2) \frac{\partial g(1)}{\partial \rho_b(1)} \frac{\partial g(2)}{\partial \rho_b(2)} f_b^\dagger(2) f_B(2) I(1,2) f_c(2) f_d(1) f_a(1), \tag{2.79g}$$

where Term8 is the regular term and Term9 to Term14 are the accompanying rearrangement terms. It should be emphasized that, since the rearrangement terms are due to the dependence on isoscalar ground-state densities, their contributions vanish in the charge-exchange channels.

2.3.2 Direct and exchange contributions

If we write the A^J of Eq. (2.49) as following

$$\mathcal{A}^J_{Aa,Bb} = (E_A - E_a)\delta_{Aa,Bb} + \sum_{i=1}^{14} H_i^J(AaBb), \tag{2.80}$$

to express the 14 terms of the p-h residual interactions shown in the previous subsection, it is easy to see that the C^J in Eq. (2.49) can be expressed as

$$\mathcal{C}^J_{Aa,\beta b} = \sum_{i=1}^{14} H_i^J(Aa\beta b), \tag{2.81}$$

and it is not difficult to prove that the B^J in Eq. (2.49) can be expressed as

$$\mathcal{B}^J_{Aa,Bb} = (-)^{j_B+j_b} \sum_{i=1}^{14} H_i^J(AabB). \tag{2.82}$$

Furthermore, one can derive the following relations among the 14 terms:

$$H_8^J(1234) = (-)^{j_2+j_3+J+1} \sum_{J'} (-)^{J'} \hat{J'}^2 \begin{Bmatrix} j_2 & j_1 & J \\ j_3 & j_4 & J' \end{Bmatrix} H_1^{J'}(1324), \tag{2.83}$$

where the contraction of 3-j symbols to 6-j symbols is used (see **Remark 7**), and

$$\begin{aligned} H_4^J(1234) &= H_2^J(3412), && (2.84a)\\ H_5^J(1234) &= H_3^J(3412), && (2.84b)\\ H_{10}^J(1234) &= (-)^{j_1+j_2+1}H_9^J(2134), && (2.84c)\\ H_{11}^J(1234) &= (-)^{j_3+j_4+1}H_9^J(4312), && (2.84d)\\ H_{12}^J(1234) &= H_9^J(3412), && (2.84e) \end{aligned}$$

due to the symmetries in the p-h residual interactions.

Therefore, the key and challenging task for deriving the RPA matrix elements is to calculate the quantities

$$\begin{aligned} &H_1^J(1234),\ H_2^J(1234),\ H_3^J(1234),\ H_6^J(1234),\\ &H_7^J(1234),\ H_9^J(1234),\ H_{13}^J(1234),\ H_{14}^J(1234), \end{aligned} \tag{2.85}$$

with the two-body interactions induced by the σ-, ω-, ρ-, π-mesons and the photons.

Particle-hole interaction induced by the σ-meson

For the σ-meson, the two-body interaction reads

$$\begin{aligned} V^\sigma(1,2) &= -g_\sigma(1)\gamma_0(1)g_\sigma(2)\gamma_0(2)D_\sigma(1,2)\\ &= -\sum_{L\nu} g_\sigma(1)\gamma_0(1)g_\sigma(2)\gamma_0(2)R_{LL}(m_\sigma;1,2)(-)^\nu Y_L^\nu(\hat{r}_1)Y_L^{-\nu}(\hat{r}_2). \end{aligned} \tag{2.86}$$

With the detailed derivations given in **Section A.2**, the quantities $H^{J\sigma}(1234)$ in Eq. (2.85) are listed in the following, where the summations over c, d stand for summations over all the occupied states,

$$\begin{aligned} H_1^{J\sigma}(1234) =& -\delta_{q_1q_2}\delta_{q_3q_4}\hat{J}^{-2}\langle 1||Y_J||2\rangle\langle 3||Y_J||4\rangle\\ &\times\int dr_1dr_2R_{JJ}(m_\sigma;r_1,r_2)[g_\sigma(G_1G_2-F_1F_2)]_{r_1}[g_\sigma(G_3G_4-F_3F_4)]_{r_2}, \end{aligned} \tag{2.87a}$$

$$\begin{aligned} H_2^{J\sigma}(1234) =& -\delta_{q_1q_2}\delta_{q_3q_4}\hat{J}^{-2}\langle 1||Y_J||2\rangle\langle 3||Y_J||4\rangle\\ &\times\int dr\frac{1}{r^2}g'_\sigma(r)\sigma(r)(G_1G_2-F_1F_2)(G_3G_4+F_3F_4), \end{aligned} \tag{2.87b}$$

$$\begin{aligned} H_3^{J\sigma}(1234) =& -\delta_{q_1q_2}\delta_{q_3q_4}\hat{J}^{-2}\langle 1||Y_J||2\rangle\langle 3||Y_J||4\rangle\\ &\times\int dr_1dr_2R_{JJ}(m_\sigma;r_1,r_2)[g_\sigma(G_1G_2-F_1F_2)]_{r_1}[g'_\sigma\rho_s(G_3G_4+F_3F_4)]_{r_2}, \end{aligned} \tag{2.87c}$$

$$\begin{aligned} H_6^{J\sigma}(1234) =& -\delta_{q_1q_2}\delta_{q_3q_4}\hat{J}^{-2}\langle 1||Y_J||2\rangle\langle 3||Y_J||4\rangle\\ &\times\int dr\frac{1}{r^2}g''_\sigma(r)\rho_s(r)\sigma(r)(G_1G_2+F_1F_2)(G_3G_4+F_3F_4), \end{aligned} \tag{2.87d}$$

$$H_7^{J\sigma}(1234) = -\delta_{q_1q_2}\delta_{q_3q_4}\hat{J}^{-2}\langle 1||Y_J||2\rangle\langle 3||Y_J||4\rangle \times \int dr_1 dr_2 R_{JJ}(m_\sigma; r_1, r_2)[g'_\sigma\rho_s(G_1G_2 + F_1F_2)]_{r_1}[g'_\sigma\rho_s(G_3G_4 + F_3F_4)]_{r_2}, \quad (2.87e)$$

$$H_9^{J\sigma}(1234) = \delta_{q_1q_2}\delta_{q_3q_4}(-)^{j_1+j_2}\frac{\hat{J}^{-1}}{\sqrt{4\pi}}\sum_{j_dLL'}\delta_{q_dq_2}\hat{L}\hat{L}'\begin{pmatrix} J & L & L' \\ 0 & 0 & 0 \end{pmatrix}\begin{Bmatrix} j_1 & j_2 & J \\ L & L' & j_d \end{Bmatrix} \times \langle 3||Y_J||4\rangle\langle 1||Y_{L'}||d\rangle\langle d||Y_L||2\rangle \times \int dr_1 dr_2 R_{LL}(m_\sigma; r_1, r_2)\left[g'_\sigma\frac{(G_3G_4 + F_3F_4)(G_1G_d - F_1F_d)}{r^2}\right]_{r_1} \times [g_\sigma(G_dG_2 - F_dF_2)]_{r_2}, \quad (2.87f)$$

$$H_{13}^{J\ \sigma}(1234) = \delta_{q_1q_2}\delta_{q_3q_4}\frac{\hat{J}^{-2}}{4\pi}\langle 1||Y_J||2\rangle\langle 3||Y_J||4\rangle\sum_{j_cj_dL}\delta_{q_cq_d}\langle c||Y_L||d\rangle^2 \times \int dr_1 dr_2 R_{LL}(m_\sigma; r_1, r_2)\left[g''_\sigma\frac{(G_1G_2 + F_1F_2)(G_3G_4 + F_3F_4)(G_cG_d - F_cF_d)}{r^4}\right]_{r_1} \times [g_\sigma(G_cG_d - F_cF_d)]_{r_2}, \quad (2.87g)$$

$$H_{14}^{J\ \sigma}(1234) = \delta_{q_1q_2}\delta_{q_3q_4}\frac{\hat{J}^{-2}}{4\pi}\langle 1||Y_J||2\rangle\langle 3||Y_J||4\rangle\sum_{j_cj_dLL'}\delta_{q_cq_d}\hat{L}^2\begin{pmatrix} J & L & L' \\ 0 & 0 & 0 \end{pmatrix}^2\langle c||Y_{L'}||d\rangle^2 \times \int dr_1 dr_2 R_{LL}(m_\sigma; r_1, r_2)\left[g'_\sigma\frac{(G_1G_2 + F_1F_2)(G_cG_d - F_cF_d)}{r^2}\right]_{r_1} \times \left[g'_\sigma\frac{(G_3G_4 + F_3F_4)(G_cG_d - F_cF_d)}{r^2}\right]_{r_2}. \quad (2.87h)$$

In the above expressions, the short-hand notation for the so-called σ-field

$$\sigma(1) = \int dr_2 r_2^2 R_{00}(m_\sigma; 1, 2)\rho_s(2)g_\sigma(2) \quad (2.88)$$

is employed, in which the scalar density is

$$\rho_s(r) = \sum_d \frac{1}{4\pi r^2}[G_d^2(r) - F_d^2(r)]. \quad (2.89)$$

The reduced matrix element of the spherical harmonics (see **Remark 14**) reads

$$\langle a||Y_L||b\rangle = (-)^{j_b - L - \frac{1}{2}}\frac{\hat{j}_a\hat{j}_b\hat{L}}{\sqrt{4\pi}}\begin{pmatrix} j_a & j_b & L \\ \frac{1}{2} & -\frac{1}{2} & 0 \end{pmatrix} \quad (2.90)$$

provided $l_a + l_b + L$ is even, and zero otherwise.

Particle-hole interaction induced by the ω-meson

For the ω-meson, the two-body interaction reads

$$\begin{aligned} V^\omega(1,2) &= g_\omega(1)\gamma_0(1)\gamma^\mu(1)g_\omega(2)\gamma_0(2)\gamma_\mu(2)D_\omega(1,2) \\ &= \sum_{L\nu} g_\omega(1)\gamma_0(1)\gamma^\mu(1)g_\omega(2)\gamma_0(2)\gamma_\mu(2)R_{LL}(m_\omega; 1, 2)(-)^\nu Y_L^\nu(\hat{r}_1)Y_L^{-\nu}(\hat{r}_2). \end{aligned} \quad (2.91)$$

It is convenient to divide the $H^{J\omega}(1234)$ into two parts, where the time component with $\mu = 0$ is denoted as $\bar{H}^{J\omega}(1234)$, and the space component with $\mu = 1, 2, 3$ is denoted as $\bar{\bar{H}}^{J\omega}(1234)$.

For the time component with $\mu = 0$, the $\bar{H}^{J\omega}(1234)$ values in Eq. (2.85) can be derived in analogy with the derivation of the σ-meson. They are listed in the following, where the summations over c, d stand for summations over all the occupied states,

$$\begin{aligned}\bar{H}_1^{J\omega}(1234) =&\delta_{q_1q_2}\delta_{q_3q_4}\hat{J}^{-2}\langle 1||Y_J||2\rangle\langle 3||Y_J||4\rangle \\ &\times\int dr_1dr_2R_{JJ}(m_\omega;r_1,r_2)[g_\omega(G_1G_2+F_1F_2)]_{r_1}[g_\omega(G_3G_4+F_3F_4)]_{r_2},\end{aligned}\tag{2.92a}$$

$$\begin{aligned}\bar{H}_2^{J\omega}(1234) =&\delta_{q_1q_2}\delta_{q_3q_4}\hat{J}^{-2}\langle 1||Y_J||2\rangle\langle 3||Y_J||4\rangle \\ &\times\int dr\frac{1}{r^2}g'_\omega(r)\omega(r)(G_1G_2+F_1F_2)(G_3G_4+F_3F_4),\end{aligned}\tag{2.92b}$$

$$\begin{aligned}\bar{H}_3^{J\omega}(1234) =&\delta_{q_1q_2}\delta_{q_3q_4}\hat{J}^{-2}\langle 1||Y_J||2\rangle\langle 3||Y_J||4\rangle \\ &\times\int dr_1dr_2R_{JJ}(m_\omega;r_1,r_2)[g_\omega(G_1G_2+F_1F_2)]_{r_1}[g'_\omega\rho_b(G_3G_4+F_3F_4)]_{r_2},\end{aligned}\tag{2.92c}$$

$$\begin{aligned}\bar{H}_6^{J\omega}(1234) =&\delta_{q_1q_2}\delta_{q_3q_4}\hat{J}^{-2}\langle 1||Y_J||2\rangle\langle 3||Y_J||4\rangle \\ &\times\int dr\frac{1}{r^2}g''_\omega(r)\rho_b(r)\omega(r)(G_1G_2+F_1F_2)(G_3G_4+F_3F_4),\end{aligned}\tag{2.92d}$$

$$\begin{aligned}\bar{H}_7^{J\omega}(1234) =&\delta_{q_1q_2}\delta_{q_3q_4}\hat{J}^{-2}\langle 1||Y_J||2\rangle\langle 3||Y_J||4\rangle \\ &\times\int dr_1dr_2R_{JJ}(m_\omega;r_1,r_2)[g'_\omega\rho_b(G_1G_2+F_1F_2)]_{r_1}[g'_\omega\rho_b(G_3G_4+F_3F_4)]_{r_2},\end{aligned}\tag{2.92e}$$

$$\begin{aligned}\bar{H}_9^{J\omega}(1234) =&\delta_{q_1q_2}\delta_{q_3q_4}(-)^{j_1+j_2+1}\frac{\hat{J}^{-1}}{\sqrt{4\pi}}\sum_{j_dLL'}\delta_{q_dq_2}\hat{L}\hat{L}'\begin{pmatrix}J&L&L'\\0&0&0\end{pmatrix}\begin{Bmatrix}j_1&j_2&J\\L&L'&j_d\end{Bmatrix} \\ &\times\langle 3||Y_J||4\rangle\langle 1||Y_{L'}||d\rangle\langle d||Y_L||2\rangle \\ &\times\int dr_1dr_2R_{LL}(m_\omega;r_1,r_2)\left[g'_\omega\frac{(G_3G_4+F_3F_4)(G_1G_d+F_1F_d)}{r^2}\right]_{r_1} \\ &\times[g_\omega(G_dG_2+F_dF_2)]_{r_2},\end{aligned}\tag{2.92f}$$

$$\begin{aligned}\bar{H}_{13}^{J\omega}(1234) =&-\delta_{q_1q_2}\delta_{q_3q_4}\frac{\hat{J}^{-2}}{4\pi}\langle 1||Y_J||2\rangle\langle 3||Y_J||4\rangle\sum_{j_cj_dL}\delta_{q_cq_d}\langle c||Y_L||d\rangle^2 \\ &\times\int dr_1dr_2R_{LL}(m_\omega;r_1,r_2)\left[g''_\omega\frac{(G_1G_2+F_1F_2)(G_3G_4+F_3F_4)(G_cG_d+F_cF_d)}{r^4}\right]_{r_1} \\ &\times[g_\omega(G_cG_d+F_cF_d)]_{r_2},\end{aligned}\tag{2.92g}$$

$$\bar{H}_{14}^{J\omega}(1234) = -\delta_{q_1q_2}\delta_{q_3q_4}\frac{\hat{J}^{-2}}{4\pi}\langle 1||Y_J||2\rangle\langle 3||Y_J||4\rangle \sum_{j_cj_dLL'}\delta_{q_cq_d}\hat{L}^2\begin{pmatrix} J & L & L' \\ 0 & 0 & 0 \end{pmatrix}^2\langle c||Y_{L'}||d\rangle^2$$
$$\times\int dr_1dr_2R_{LL}(m_\omega;r_1,r_2)\left[g'_\omega\frac{(G_1G_2+F_1F_2)(G_cG_d+F_cF_d)}{r^2}\right]_{r_1}$$
$$\times\left[g'_\omega\frac{(G_3G_4+F_3F_4)(G_cG_d+F_cF_d)}{r^2}\right]_{r_2}. \tag{2.92h}$$

In the above expressions, the short-hand notation for the so-called ω-field

$$\omega(1) = \int dr_2r_2^2R_{00}(m_\omega;1,2)\rho_b(2)g_\omega(2), \tag{2.93}$$

is employed, in which the baryonic density is

$$\rho_b(r) = \sum_d\frac{1}{4\pi r^2}[G_d^2(r)+F_d^2(r)]. \tag{2.94}$$

For the space component with $\mu = 1,2,3$,

$$\bar{\bar{V}}^\omega(1,2) = -\sum_{L\nu k}(-)^{\nu+k}g_\omega(1)\alpha_k(1)g_\omega(2)\alpha_{-k}(2)R_{LL}(m_\omega;1,2)Y_L^\nu(\hat{r}_1)Y_L^{-\nu}(\hat{r}_2). \tag{2.95}$$

With the detailed derivations given in **Section A.3**, the quantities $\bar{\bar{H}}^{J\omega}(1234)$ in Eq. (2.85) are listed in the following, where the summations over c,d stand for summations over all the occupied states,

$$\bar{\bar{H}}_1^{J\omega}(1234) = -\delta_{q_1q_2}\delta_{q_3q_4}\hat{J}^{-2}$$
$$\times\sum_L\int dr_1dr_2R_{LL}(m_\omega;r_1,r_2)\left[g_\omega\left(G_1F_2\langle 1||\mathscr{T}_{JL}||2'\rangle - F_1G_2\langle 1'||\mathscr{T}_{JL}||2\rangle\right)\right]_{r_1}$$
$$\times\left[g_\omega\left(G_3F_4\langle 3||\mathscr{T}_{JL}||4'\rangle - F_3G_4\langle 3'||\mathscr{T}_{JL}||4\rangle\right)\right]_{r_2}, \tag{2.96a}$$
$$\bar{\bar{H}}_i^{J\omega}(1234) = 0, \qquad \text{for} \quad i = 2,3,\cdots,7, \tag{2.96b}$$

$$\bar{\bar{H}}_9^{J\omega}(1234) = \delta_{q_1q_2}\delta_{q_3q_4}(-)^{j_1+j_2+1}\frac{\hat{J}^{-1}}{\sqrt{4\pi}}\sum_{j_dLL'J'J''}\delta_{q_dq_2}(-)^{J''+L}\hat{L}\hat{L}'\hat{J}'\hat{J}''$$
$$\times\begin{pmatrix} J & L & L' \\ 0 & 0 & 0 \end{pmatrix}\begin{Bmatrix} j_2 & j_1 & J \\ J' & J'' & j_d \end{Bmatrix}\begin{Bmatrix} J' & J'' & J \\ L & L' & 1 \end{Bmatrix}\langle 3||Y_J||4\rangle$$
$$\times\int dr_1dr_2R_{LL}(m_\omega;r_1,r_2)$$
$$\times\left[g'_\omega\frac{(G_3G_4+F_3F_4)}{r^2}\left(G_1F_d\langle 1||\mathscr{T}_{J'L'}||d'\rangle - F_1G_d\langle 1'||\mathscr{T}_{J'L'}||d\rangle\right)\right]_{r_1}$$
$$\times\left[g_\omega\left(G_dF_2\langle d||\mathscr{T}_{J''L}||2'\rangle - F_dG_2\langle d'||\mathscr{T}_{J''L}||2\rangle\right)\right]_{r_2}, \tag{2.96c}$$

$$\bar{\bar{H}}_{13}^{J\omega}(1234) = \delta_{q_1q_2}\delta_{q_3q_4}\frac{\hat{J}^{-2}}{4\pi}\langle 1||Y_J||2\rangle\langle 3||Y_J||4\rangle\sum_{j_cj_dLJ'}\delta_{q_cq_d}\int dr_1dr_2R_{LL}(m_\omega;r_1,r_2)$$
$$\times\left[g''_\omega\frac{(G_1G_2+F_1F_2)(G_3G_4+F_3F_4)}{r^4}\left(G_cF_d\langle c||\mathscr{T}_{J'L}||d'\rangle - F_cG_d\langle c'||\mathscr{T}_{J'L}||d\rangle\right)\right]_{r_1}$$
$$\times\left[g_\omega\left(G_cF_d\langle c||\mathscr{T}_{J'L}||d'\rangle - F_cG_d\langle c'||\mathscr{T}_{J'L}||d\rangle\right)\right]_{r_2}, \tag{2.96d}$$

$$\begin{aligned}\bar{\bar{H}}_{14}^{J\omega}(1234) =&\delta_{q_1q_2}\delta_{q_3q_4}\frac{\hat{J}^{-2}}{4\pi}\langle 1||Y_J||2\rangle\langle 3||Y_J||4\rangle\sum_{j_cj_dLL'J'}\delta_{q_cq_d}\hat{L}^2\begin{pmatrix} J & L & L' \\ 0 & 0 & 0\end{pmatrix}^2\\ &\times\int dr_1dr_2R_{LL}(m_\omega;r_1,r_2)\\ &\quad\times\left[g'_\omega\frac{(G_1G_2+F_1F_2)}{r^2}\left(G_cF_d\langle c||\mathscr{T}_{J'L'}||d'\rangle-F_cG_d\langle c'||\mathscr{T}_{J'L'}||d\rangle\right)\right]_{r_1}\\ &\quad\times\left[g'_\omega\frac{(G_3G_4+F_3F_4)}{r^2}\left(G_cF_d\langle c||\mathscr{T}_{J'L'}||d'\rangle-F_cG_d\langle c'||\mathscr{T}_{J'L'}||d\rangle\right)\right]_{r_2}. \end{aligned}\tag{2.96e}$$

In the above expressions, the vector spherical harmonic $\mathscr{T}^L_{JM}$ is defined as

$$Y_{L\nu}\sigma_k=\sum_{JM}(-)^{L-1+M}\hat{J}\begin{pmatrix} L & 1 & J \\ \nu & k & -M\end{pmatrix}\mathscr{T}^L_{JM}.\tag{2.97}$$

Its reduced matrix element (see **Remark 14**) reads

$$\langle a||\mathscr{T}_{JL}||b\rangle=(-)^{l_a}\frac{\hat{j}_a\hat{j}_b}{\sqrt{4\pi}}Z_{JL}(a,b)\begin{pmatrix} j_a & j_b & J \\ \frac{1}{2} & -\frac{1}{2} & 0\end{pmatrix},\qquad l_a+l_b+L\text{ is even},\tag{2.98}$$

where

$$Z_{JL}(a,b)=\begin{cases}(-)^{j_b+l_b+\frac{1}{2}}\dfrac{(l_a-j_a)\hat{j}_a^2+(l_b-j_b)\hat{j}_b^2+L}{\sqrt{L}}, & \text{for } L=J+1,\\ -\dfrac{1}{2}\dfrac{\hat{J}}{[J(J+1)]^{\frac{1}{2}}}\left[\hat{j}_b^2+(-)^{j_a+j_b+J}\hat{j}_a^2\right], & \text{for } L=J,\\ (-)^{j_b+l_b+\frac{1}{2}}\dfrac{(l_a-j_a)\hat{j}_a^2+(l_b-j_b)\hat{j}_b^2-L-1}{\sqrt{L+1}}, & \text{for } L=J-1.\end{cases}\tag{2.99}$$

Particle-hole interaction induced by the ρ-meson

For the ρ-meson with vector coupling, the two-body interaction reads

$$V^\rho(1,2)=[g_\rho\gamma_0\gamma^\mu\vec{\tau}]_1\cdot[g_\rho\gamma_0\gamma_\mu\vec{\tau}]_2D_\rho(1,2).\tag{2.100}$$

The quantities $H^{J\rho}(1234)$ in Eq. (2.85) can be derived in analogy with the derivations of the $\omega-$meson, with the two following replacements. First, one should replace the mass of the meson and the coupling strength,

$$g_\omega,m_\omega\rightarrow g_\rho,m_\rho.\tag{2.101}$$

Second, one should be careful about the isospin factors at the interaction vertices. For example, in $\bar{H}_1^{J\rho}(1234)$, the following substitution is needed,

$$\delta_{q_1q_2}\delta_{q_4q_3}\rightarrow\langle q_1|\vec{\tau}|q_2\rangle\cdot\langle q_4|\vec{\tau}|q_3\rangle.\tag{2.102}$$

The final results are listed in **Section A.4**.

Particle-hole interaction induced by the pion

For the pion with pseudo-vector coupling, the two-body interaction reads

$$V^{\pi}(1,2) = -[\frac{f_\pi}{m_\pi}\vec{\tau}\gamma_0\gamma_5\gamma^\mu\partial_\mu]_1 \cdot [\frac{f_\pi}{m_\pi}\vec{\tau}\gamma_0\gamma_5\gamma^\nu\partial_\nu]_2 D_\pi(1,2). \tag{2.103}$$

Because the retardation effect is neglected, the meson propagator is time independent. The interaction can be expressed as

$$V^{\pi}(1,2) = -[\frac{f_\pi}{m_\pi}\vec{\tau}\gamma_0\gamma_5\gamma^k\partial_k]_1 \cdot [\frac{f_\pi}{m_\pi}\vec{\tau}\gamma_0\gamma_5\gamma^l\partial_l]_2 D_\pi(1,2). \tag{2.104}$$

With the derivatives of the Yukawa propagator (see **Remark 10**), the two-body interaction can be rewritten as

$$\begin{aligned} V^{\pi}(1,2) &= -\sum_{L\nu}\sum_{L_1L_2}^{L\pm1}(-)^\nu \hat{L}_1\hat{L}_2 \begin{pmatrix} L & 1 & L_1 \\ 0 & 0 & 0 \end{pmatrix}\begin{pmatrix} L & 1 & L_2 \\ 0 & 0 & 0 \end{pmatrix} \\ &\quad \times \left(f_\pi\vec{\tau}\gamma_0\gamma_5\boldsymbol{\gamma}\cdot\boldsymbol{Y}^{L_1}_{L\nu}\right)_{r_1} \mathscr{V}_L^{L_1L_2}(m_\pi;r_1,r_2)\left(f_\pi\vec{\tau}\gamma_0\gamma_5\boldsymbol{\gamma}\cdot\boldsymbol{Y}^{L_2}_{L-\nu}\right)_{r_2}. \end{aligned} \tag{2.105}$$

The detailed derivations are given in **Section A.5**. Here we just list the final results for the quantities $H^{J\pi}(1234)$ in Eq. (2.85), where summations over c,d stand for summations over all the occupied states,

$$\begin{aligned} &H_1^{J\pi}(1234) \\ &= -\langle q_1|\vec{\tau}|q_2\rangle\cdot\langle q_4|\vec{\tau}|q_3\rangle\hat{J}^{-2} \\ &\quad \times \sum_{L_1L_2}^{J\pm1}\hat{L}_1\hat{L}_2\begin{pmatrix} J & 1 & L_1 \\ 0 & 0 & 0 \end{pmatrix}\begin{pmatrix} J & 1 & L_2 \\ 0 & 0 & 0 \end{pmatrix} \\ &\quad \times \int dr_1dr_2\mathscr{V}_J^{L_1L_2}(m_\pi;r_1,r_2)\left[f_\pi\left(G_1G_2\langle 1||\mathscr{T}_{JL_1}||2\rangle + F_1F_2\langle 1'||\mathscr{T}_{JL_1}||2'\rangle\right)\right]_{r_1} \\ &\qquad \times \left[f_\pi\left(G_3G_4\langle 3||\mathscr{T}_{JL_2}||4\rangle + F_3F_4\langle 3'||\mathscr{T}_{JL_2}||4'\rangle\right)\right]_{r_2}, \end{aligned} \tag{2.106a}$$

$$\begin{aligned} &H_9^{J\pi}(1234) \\ &=\delta_{q_1q_2}\delta_{q_3q_4}(-)^{j_1+j_2+1}\frac{\hat{J}^{-1}}{\sqrt{4\pi}}\sum_{j_dLL_1L_2L'J'}(2-\delta_{q_dq_2})\hat{L}\hat{L}_1^2\hat{L}_2\hat{L}'\hat{J}' \\ &\quad \times \begin{pmatrix} L & 1 & L_1 \\ 0 & 0 & 0 \end{pmatrix}\begin{pmatrix} L & 1 & L_2 \\ 0 & 0 & 0 \end{pmatrix}\begin{pmatrix} J & L_1 & L' \\ 0 & 0 & 0 \end{pmatrix}\begin{Bmatrix} J' & J & L \\ L_1 & 1 & L' \end{Bmatrix}\begin{Bmatrix} j_2 & j_1 & J \\ J' & L & j_d \end{Bmatrix}\langle 3||Y_J||4\rangle \\ &\quad \times \int dr_1dr_2\mathscr{V}_L^{L_1L_2}(m_\pi;r_1,r_2)\left[f'_\pi\frac{(G_3G_4+F_3F_4)}{r^2}\left(G_1G_d\langle 1||\mathscr{T}_{J'L'}||d\rangle + F_1F_d\langle 1'||\mathscr{T}_{J'L'}||d'\rangle\right)\right]_{r_1} \\ &\qquad \times \left[f_\pi\left(G_dG_2\langle d||\mathscr{T}_{LL_2}||2\rangle + F_dF_2\langle d'||\mathscr{T}_{LL_2}||2'\rangle\right)\right]_{r_2}, \end{aligned} \tag{2.106b}$$

$$
\begin{aligned}
&H_{13}^{J\pi}(1234)\\
=&\delta_{q_1q_2}\delta_{q_3q_4}\frac{\hat{J}^{-2}}{4\pi}\langle 1||Y_J||2\rangle\langle 3||Y_J||4\rangle\sum_{j_cj_dLL_1L_2}(2-\delta_{q_cq_d})\hat{L}_1\hat{L}_2\begin{pmatrix} L & 1 & L_1\\ 0 & 0 & 0\end{pmatrix}\begin{pmatrix} L & 1 & L_2\\ 0 & 0 & 0\end{pmatrix}\\
&\times\int dr_1dr_2\mathscr{V}_L^{L_1L_2}(m_\pi;r_1,r_2)\\
&\times\left[f_\pi''\frac{(G_1G_2+F_1F_2)(G_3G_4+F_3F_4)}{r^4}\left(G_cG_d\langle c||\mathscr{T}_{LL_1}||d\rangle+F_cF_d\langle c'||\mathscr{T}_{LL_1}||d'\rangle\right)\right]_{r_1}\\
&\times\left[f_\pi\left(G_cG_d\langle c||\mathscr{T}_{LL_2}||d\rangle+F_cF_d\langle c'||\mathscr{T}_{LL_2}||d'\rangle\right)\right]_{r_2},
\end{aligned}
\tag{2.106c}
$$

$$
\begin{aligned}
&H_{14}^{J\pi}(1234)\\
=&\delta_{q_1q_2}\delta_{q_3q_4}\frac{\hat{J}^{-2}}{4\pi}\langle 1||Y_J||2\rangle\langle 3||Y_J||4\rangle\sum_{j_cj_dLL_1L_2L'J'L''}(2-\delta_{q_cq_d})\hat{L}^2\hat{L}_1^2\hat{L}_2^2\hat{L}'\hat{L}''\begin{pmatrix} L & 1 & L_1\\ 0 & 0 & 0\end{pmatrix}\\
&\times\begin{pmatrix} L & 1 & L_2\\ 0 & 0 & 0\end{pmatrix}\begin{pmatrix} J & L_1 & L'\\ 0 & 0 & 0\end{pmatrix}\begin{pmatrix} J & L_2 & L''\\ 0 & 0 & 0\end{pmatrix}\begin{Bmatrix} J' & J & L\\ L_1 & 1 & L'\end{Bmatrix}\begin{Bmatrix} J' & J & L\\ L_2 & 1 & L''\end{Bmatrix}\\
&\times\int dr_1dr_2\mathscr{V}_L^{L_1L_2}(m_\pi;r_1,r_2)\left[f_\pi'\frac{(G_1G_2+F_1F_2)}{r^2}\left(G_cG_d\langle c||\mathscr{T}_{J'L'}||d\rangle+F_cF_d\langle c'||\mathscr{T}_{J'L'}||d'\rangle\right)\right]_{r_1}\\
&\times\left[f_\pi'\frac{(G_3G_4+F_3F_4)}{r^2}\left(G_cG_d\langle c||\mathscr{T}_{J'L''}||d\rangle+F_cF_d\langle c'||\mathscr{T}_{J'L''}||d'\rangle\right)\right]_{r_2}.
\end{aligned}
\tag{2.106d}
$$

In order to cancel the contact interaction coming from the pion pseudo-vector coupling, a pionic zero-range counterterm should be included (Bouyssy *et al.*, 1987), which reads

$$
\begin{aligned}
V^{\pi\delta}(1,2) &= \frac{1}{3}[\frac{f_\pi}{m_\pi}\vec{\tau}\gamma_0\gamma_5\boldsymbol{\gamma}]_1\cdot[\frac{f_\pi}{m_\pi}\vec{\tau}\gamma_0\gamma_5\boldsymbol{\gamma}]_2\delta(\boldsymbol{r}_1-\boldsymbol{r}_2)\\
&= \frac{1}{3}\sum_{Lk\nu}(-)^{k+\nu}[\frac{f_\pi}{m_\pi}\vec{\tau}\gamma_0\gamma_5\gamma^kY_L^\nu]_1\cdot[\frac{f_\pi}{m_\pi}\vec{\tau}\gamma_0\gamma_5\gamma^{-k}Y_L^{-\nu}]_2\frac{\delta(r_1-r_2)}{r_1^2}.
\end{aligned}
\tag{2.107}
$$

It has a form similar to $\bar{\bar{V}}^\omega$, so it is not difficult to obtain that

$$
\begin{aligned}
H_1^{J\pi\delta}(1234)=&\frac{1}{3m_\pi^2}\langle q_1|\vec{\tau}|q_2\rangle\cdot\langle q_4|\vec{\tau}|q_3\rangle\hat{J}^{-2}\\
&\times\sum_L\int dr\frac{f_\pi^2}{r^2}\left[G_1G_2\langle 1||\mathscr{T}_{JL}||2\rangle+F_1F_2\langle 1'||\mathscr{T}_{JL}||2'\rangle\right]\\
&\times\left[G_3G_4\langle 3||\mathscr{T}_{JL}||4\rangle+F_3F_4\langle 3'||\mathscr{T}_{JL}||4'\rangle\right],
\end{aligned}
\tag{2.108a}
$$

$$
\begin{aligned}
H_9^{J\pi\delta}(1234)=&\frac{1}{3m_\pi^2}\delta_{q_1q_2}\delta_{q_3q_4}(-)^{j_1+j_2+1}\frac{\hat{J}^{-1}}{\sqrt{4\pi}}\sum_{j_dLL'J'J''}(2-\delta_{q_dq_2})(-)^{J''+L}\hat{L}\hat{L}'\hat{J}'\hat{J}''\\
&\times\begin{pmatrix} J & L & L'\\ 0 & 0 & 0\end{pmatrix}\begin{Bmatrix} j_2 & j_1 & J\\ J' & J'' & j_d\end{Bmatrix}\begin{Bmatrix} J' & J'' & J\\ L & L' & 1\end{Bmatrix}\langle 3||Y_J||4\rangle\\
&\times\int dr\frac{f_\pi'f_\pi}{r^4}(G_3G_4+F_3F_4)\left(G_1G_d\langle 1||\mathscr{T}_{J'L'}||d\rangle+F_1F_d\langle 1'||\mathscr{T}_{J'L'}||d'\rangle\right)\\
&\times\left(G_dG_2\langle d||\mathscr{T}_{J''L}||2\rangle+F_dF_2\langle d'||\mathscr{T}_{J''L}||2'\rangle\right).
\end{aligned}
\tag{2.108b}
$$

$$
\begin{aligned}
&H_{13}^{J\pi\delta}(1234) \\
&= -\frac{1}{3m_\pi^2}\delta_{q_1q_2}\delta_{q_3q_4}\frac{\hat{J}^{-2}}{4\pi}\langle 1||Y_J||2\rangle\langle 3||Y_J||4\rangle \sum_{j_cj_dLJ'}(2-\delta_{q_cq_d})\int dr\frac{f_\pi'' f_\pi}{r^6} \\
&\quad\times (G_1G_2+F_1F_2)(G_3G_4+F_3F_4)\left[G_cG_d\langle c||\mathscr{T}_{J'L}||d\rangle + F_cF_d\langle c'||\mathscr{T}_{J'L}||d'\rangle\right]^2. \qquad (2.108c)
\end{aligned}
$$

$$
\begin{aligned}
&H_{14}^{J\pi\delta}(1234) \\
&= -\frac{1}{3m_\pi^2}\delta_{q_1q_2}\delta_{q_3q_4}\frac{\hat{J}^{-2}}{4\pi}\langle 1||Y_J||2\rangle\langle 3||Y_J||4\rangle \sum_{j_cj_dLL'J'}(2-\delta_{q_cq_d})\hat{L}^2\begin{pmatrix} J & L & L' \\ 0 & 0 & 0\end{pmatrix}^2\int dr\frac{{f_\pi'}^2}{r^6} \\
&\quad\times (G_1G_2+F_1F_2)(G_3G_4+F_3F_4)\left[G_cG_d\langle c||\mathscr{T}_{J'L'}||d\rangle + F_cF_d\langle c'||\mathscr{T}_{J'L'}||d'\rangle\right]^2. \qquad (2.108d)
\end{aligned}
$$

where summations over c, d stand for summations over all the occupied states.

It should be also pointed out that, because of parity conservation the pion does not contribute to direct rearrangement terms, i.e.,

$$H_i^{J\pi,J\pi\delta}(1234) = 0, \qquad \text{for} \quad i = 2, 3, \cdots, 7. \qquad (2.109)$$

Particle-hole interaction induced by the photon

Finally, the electro-magnetic field,

$$V_A(1,2) = e^2\left[\gamma_0\gamma^\mu\frac{1-\tau_3}{2}\right]_1\left[\gamma_0\gamma_\mu\frac{1-\tau_3}{2}\right]_2 D_A(1,2), \qquad (2.110)$$

has a structure similar to that of the ω-meson, expect the following three properties. First, only protons take part in this interaction, i.e., all the summations are just over protons. Second, since the photon has zero mass, the propagator of the electro-magnetic field is

$$D_A(\boldsymbol{r}_1,\boldsymbol{r}_2) = \frac{1}{4\pi}\frac{1}{|\boldsymbol{r}_1-\boldsymbol{r}_2|}, \qquad (2.111)$$

whose expansion reads

$$D_A(\boldsymbol{r}_1,\boldsymbol{r}_2) = \sum_L R_{LL}(\text{photon};r_1,r_2)\boldsymbol{Y}_L(\hat{\boldsymbol{r}}_1)\cdot\boldsymbol{Y}_L(\hat{\boldsymbol{r}}_2), \qquad (2.112)$$

with

$$R_{LL}(\text{photon};r_1,r_2) = \hat{L}^{-2}\frac{r_<^L}{r_>^{L+1}}. \qquad (2.113)$$

Third, since the Coulomb interaction is not density-dependent, there is no rearrangement term for the Coulomb field.

Therefore, in analogy with the ω-meson, the contributions from the electro-magnetic field read,

$$
\begin{aligned}
\bar{H}_1^{JA}(1234) \;&=\; (\text{proton})e^2\hat{J}^{-2}\langle 1||Y_J||2\rangle\langle 3||Y_J||4\rangle \\
&\quad\times\int dr_1dr_2R_{JJ}(\text{photon};r_1,r_2)(G_1G_2+F_1F_2)_{r_1}(G_3G_4+F_3F_4)_{r_2}, \qquad (2.114)
\end{aligned}
$$

and

$$\begin{aligned}\bar{\bar{H}}_1^{JA}(1234) &= -(\text{proton})e^2\hat{J}^{-2} \\ &\quad\times\sum_L\int dr_1dr_2R_{LL}(\text{photon};r_1,r_2)\left(G_1F_2\langle 1||\mathscr{T}_{JL}||2'\rangle - F_1G_2\langle 1'||\mathscr{T}_{JL}||2\rangle\right)_{r_1} \\ &\quad\times\left(G_3F_4\langle 3||\mathscr{T}_{JL}||4'\rangle - F_3G_4\langle 3'||\mathscr{T}_{JL}||4\rangle\right)_{r_2}. \end{aligned} \tag{2.115}$$

So far, we have all the theoretical ingredients of the fully self-consistent RHF+RPA approach. In the next chapter, the numerical tools for realizing the RHF+RPA calculations will be explained. Then, its applications to the nuclear spin-isospin resonances, the isospin symmetry-breaking corrections for the superallowed β decays, and the charged-current neutrino-nucleus cross sections will be discussed from **Chapter 4** to **Chapter 6**.

Chapter 3

Numerical Tools for RHF+RPA

In this chapter, the numerical tools for realizing the RHF+RPA calculations will be explained. Then, the numerical checks for restoring the translational and isospin symmetries will be presented to demonstrate correctness of the codes.

3.1 Information on the numerical code

We have developed the numerical code for the RHF+RPA calculations in Fortran90 language. In Fig. 3.1, the flow diagram for the RHF+RPA code is illustrated.

The code starts by choosing the effective Lagrangian. The inputs include the single-particle energies and wave functions given by the RHF ground-state calculations, including not only the single-particle states in the Fermi sea, but also those in the Dirac sea. The single-particle spectra are calculated by solving the RHF equations in a spherical volume with box boundary conditions at a chosen radius R, thus, these spectra are entirely discrete. Filling up the single-particle states in the Fermi sea from the bottom to the Fermi surface, the occupied states are labeled as the hole states and the ground-state densities can be calculated. The unoccupied states in the Fermi and Dirac sea inside the single-particle energy truncation $[E_{\min}, E_{\max}]$ are labeled as particle states. The p-h configurations are built by taking those pairs of the particle and hole states which can be coupled to a total angular momentum and parity J^π. Since we are dealing with the density-dependent meson-nucleon couplings, the coupling strengths are calculated at each mesh point in the coordinate space. In order to save time, the radial multipoles of the Yukawa propagators in Eq. (2.19) and the reduced matrix elements in **Remark 14** are calculated just once and stored. In the present code, the most lengthy and time consuming part is to construct the RPA matrix elements according to the $H^J(1234)$ expressions shown in **Section 2.3** and **Appendix A**. To take the benefit of modern computers which have multi processors, this part has been parallelized with OpenMP[1]. The RPA matrix thus obtained is diagonalized with the Linear Algebra PACKage (LAPACK)[2]. Finally, the eigenenergies and transition strengths in Eq. (2.62) and other useful

[1] www.openmp.org

[2] www.netlib.org/lapack

spectroscopic information ,e.g., transition densities, transition amplitudes, can be obtained.

In total, this code has roughly 10,000 lines excluding the standard subroutines, and the typical time for calculating the GTR in ^{208}Pb with the single-particle energy truncation $[-M, M+120$ MeV] is 3 CPU hours.

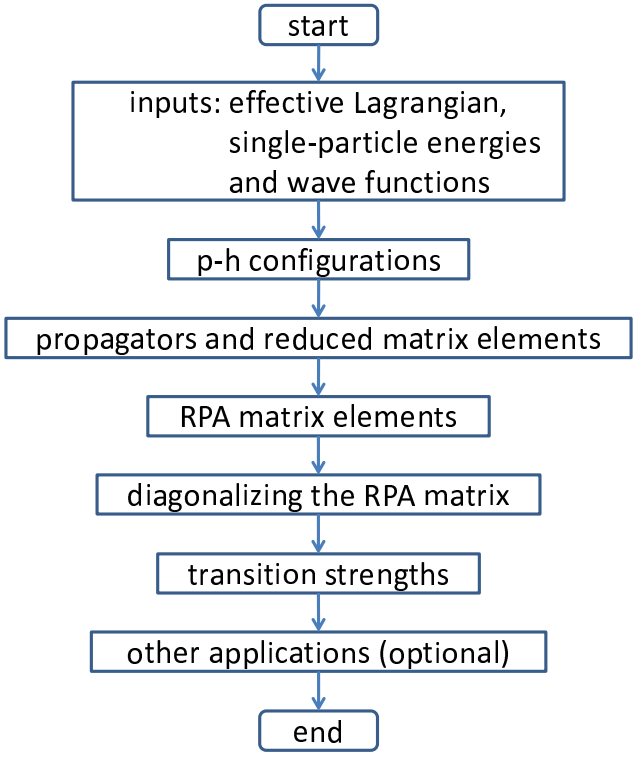

Figure 3.1: Flow diagram for the RHF+RPA code.

3.2 Numerical checks

We have developed two different RPA codes, the first one for non-charge-exchange excitations where the configurations are of the neutron particle-neutron hole and proton particle-proton hole type, and the second one for charge-exchange excitations with neutron particle-proton hole and proton particle-neutron hole configurations. In this thesis we discuss in full detail the applications to charge-exchange excitations, but we would like to comment also briefly here the non-charge-exchange code as far as accuracy checks are concerned.

3.2.1 Restoration of the translational symmetry

A general property of the RPA approach is that, when full self-consistency is preserved, i.e., the HF mean field and the p-h residual interaction of RPA are derived from the same starting Hamiltonian H, then any symmetry of H which is broken by the HF approximation must be restored by the RPA. This restoration is realized by an RPA mode at zero energy, the Goldstone mode. The

first explicit derivation of this result was given by D. J. Thouless (Thouless, 1961) for the case of the translational mode which corresponds to $\Delta J^\pi = 1^-, \Delta T = 0$. This spurious mode is thus decoupled from other $\Delta J^\pi = 1^-, \Delta T = 0$ physical modes which appear at non-zero excitation energies (Ring and Schuck, 1980).

We have numerically check this property by performing the following study. Taking the nucleus ^{16}O as an example, the Dirac equations obtained in the RHF approach are solved in coordinate space by the Runge-Kutta method within a spherical box with a box radius $R = 15$ fm and a mesh size $dr = 0.1$ fm. The single-particle wave functions thus obtained are used to construct the RPA matrix elements $\mathcal{A}^J$, $\mathcal{B}^J$, and $\mathcal{C}^J$ in Eq. (2.49) with the single-particle energy truncation $[-M, M+200$ MeV], i.e., the occupied states are the positive energy states below the Fermi surface, whereas the unoccupied states can be either positive energy states above the Fermi surface or bound negative energy states. With these numerical inputs, we get the lowest dipole state ($J^\pi = 1^-$) at $E = 0.394$ MeV.

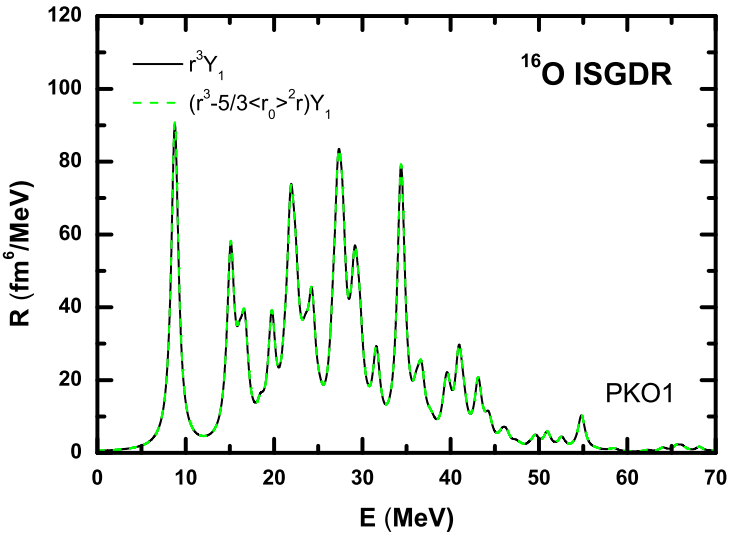

Figure 3.2: Strength distributions of ISGDR in ^{16}O calculated by RHF+RPA with PKO1. The transitions driven by the operators $\hat{F} = \sum_i r_i^3 Y_1(i)$ and $\hat{F} = \sum_i (r_i^3 - 5/3 \langle r_0 \rangle^2 r_i) Y_1(i)$ are shown with solid and dashed lines, respectively. They can be hardly distinguished on the figure.

Enhancing or reducing the strength of the p-h residual interactions with a overall factor $(1+\delta)$, one can obtain the exact zero excitation energy. The order of magnitude of δ shows the numerical accuracy of the code. In the present case, we find $\delta = 0.00066$. This indicates that the numerical code works well.

Furthermore, it is known that the isoscalar giant dipole resonance (ISGDR) operator can be written as (Van Giai and Sagawa, 1981)

$$\hat{F} = \sum_i (r_i^3 - 5/3 \langle r_0 \rangle^2 r_i) Y_1(i), \tag{3.1}$$

where the second term in the bracket is for decoupling the physical RPA excitations from the spurious state. In other words, in the fully self-consistent calculations, the transitions driven by

the operators with and without the term $5/3\,\langle r_0\rangle^2\, r_i$ in Eq. (3.1) should be the same. In Fig. 3.2, the strength distributions of ISGDR in ^{16}O calculated by RHF+RPA with PKO1 are shown. It is found that these two curves are almost on top of each other, which indicates that in the present case the physical RPA excitations are well decoupled from the spurious state.

At this point, there is one remark that must be made. In our models of effective Lagrangians, the meson-nucleon couplings are assumed to depend on the local baryonic density, i.e., the resulting effective Hamiltonians are not necessarily commuting with the translation operator. Thus, there is no strict requirement that the translational invariance should be preserved. Then, the question arises why this invariance seems nevertheless preserved in self-consistent RHF+RPA.

3.2.2 Restoration of the isospin symmetry

It is expected that the IAS defined as $T_-\,|\text{parent}\rangle$ or $T_+\,|\text{parent}\rangle$ would be degenerate with its isobaric multiplet partner $|\text{parent}\rangle$, i.e., $E_{\text{IAS}} = 0$, and it would contain 100% of the model-independent sum rule shown in Eq. (2.67) if the system Hamiltonian commutes with the isospin lowering T_- and raising T_+ operators, which is true when the Coulomb field is switched off in nuclei. Even though this degeneracy is broken by the mean field approximation, since the single-particle Hamiltonian no longer commutes with $T_\pm$, it can be explicitly shown that this isospin symmetry can be restored by the self-consistent RPA approaches (Engelbrecht and Lemmer, 1970).

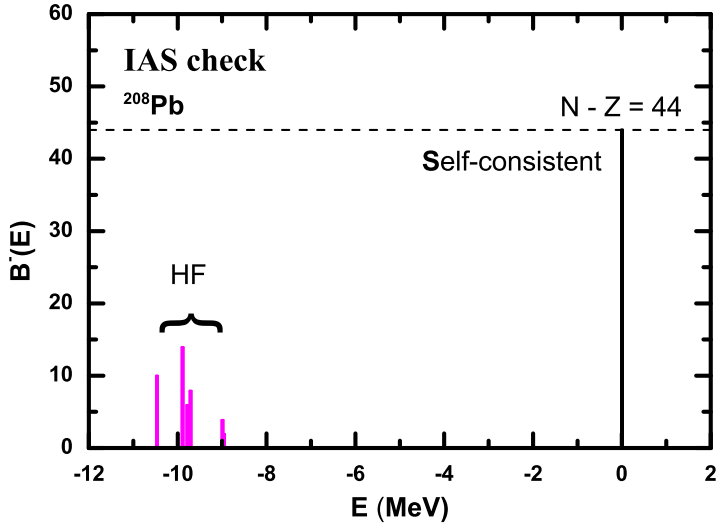

Figure 3.3: IAS transition probabilities of unperturbed excitations (HF) and self-consistent RPA excitations for ^{208}Pb by RHF+RPA with PKO1.

Taking the nucleus ^{208}Pb as an example, the Dirac equations obtained by the RHF approach are solved in coordinate space by the Runge-Kutta method within a spherical box with a box radius $R = 20$ fm and a mesh size $dr = 0.1$ fm. We have used the parametrization PKO1 with the Coulomb interactions switched off. The single-particle wave functions thus obtained are used to construct the RPA matrix elements $\mathcal{A}^J$ and $\mathcal{B}^J$ in Eq. (2.53) with the single-particle energy

truncation $[-M, M + 80$ MeV$]$.

The IAS transition probabilities of unperturbed single-particle excitations (HF) and self-consistent RPA excitations are shown in Fig. 3.3. It is found that the unperturbed excitations are located between -10.46 and -8.96 MeV when the Coulomb interaction is put to zero, thus showing the isospin symmetry breaking within mean field approximation. While the self-consistent RHF+RPA calculation leads to $E_{\rm IAS} = 4$ keV, and the single isobaric analog state contains 99.999% of the model-independent non-energy weighted sum rule $N - Z = 44$. This indicates that the present approach is fully self-consistent and the numerical code works well. This degree of numerical accuracy is certainly well appropriate for specific applications such as the isospin symmetry-breaking corrections in superallowed Fermi transition presented in **Chapter 5**.

Chapter 4

Spin-Isospin Resonances

4.1 Introduction

The charge-exchange experiments using (p, n) reactions have demonstrated the existence of very collective spin-isospin resonances in nuclei (see (Osterfeld, 1992; Ichimura *et al.*, 2006) and references therein). The isobaric analog state (IAS), which was first discovered in the nucleus ^{51}V with a low incident energy proton beam in 1961 (Anderson and Wong, 1961), is the simplest collective charge-exchange mode where the excess neutrons coherently change the direction of their isospins without changing their orbital angular momenta. Since the isospin mixing in nuclei is quite small, this mode is characterized by a single and rather sharp peak in its transition strength distribution, in contrast to the fragmented single-particle excitations. Due to the strong energy dependence of the isospin coupling strength V_τ in the projectile-target interaction, the IAS peak is gradually swamped by another collective charge-exchange mode, the Gamow-Teller resonance (GTR), when the (p, n) reactions are performed at incident energies above 100 MeV.

The collective GTR was predicted by Ikeda, Fujii, and Fujita in 1963 (Ikeda *et al.*, 1963) to explain the absence of spin-isospin strength at low excitation energies and the resulting hindrance of the allowed GT β decays in medium-mass and heavy nuclei. In this resonance, the excess neutrons coherently change the direction of their spins and isospins conserving their orbital angular momenta. The GTR was indeed first detected in the nucleus ^{90}Zr in 1975 (Doering *et al.*, 1975). Later, systematic experiments providing much better energy resolution have been performed. Since the 1980s, one of the central topics is the quenching problem of the model-independent GT non-energy weighted sum rule, known as the Ikeda-Fujii-Fujita sum rule. For various medium-mass and heavy nuclei, only around 60% of the expected GT sum rule value could be detected experimentally in the giant resonance region (Rapaport *et al.*, 1983; Gaarde, 1985). From a theoretical point of view, two physical mechanisms have been proposed for this quenching problem: 1) Due to the couplings between the $\Delta(1232)$ isobar-nucleon hole and the proton particle-neutron hole, the missing GT strength should be found at very high excitation energy ($E \approx 300$ MeV); 2) Due to the mixing with the two particle-two hole (2p-2h) states, the missing GT strength is pushed far beyond the giant resonance region. For these two points, the reader can consult the references quoted in

Ref. (Osterfeld, 1992). However, the experimental status has somehow changed recently. $88\% \pm 6\%$ of the GT sum rule value has been detected in recent experiments performed in both $^{90}\mathrm{Zr}(p,n)$ and $^{90}\mathrm{Zr}(n,p)$ channels with more reliable multipole decomposition analysis of the cross sections (Yako *et al.*, 2005).

Another spin-isospin mode of interest is the spin-dipole resonances (SDR). It has been proposed that the neutron skin thickness could be extracted via the SD non-energy weighted sum rule (Krasznahorkay *et al.*, 1999). Now that experimental data in both $^{90}\mathrm{Zr}(p,n)$ (Wakasa *et al.*, 1997) and $^{90}\mathrm{Zr}(n,p)$ (Yako *et al.*, 2005) channels and the corresponding multipole decomposition analysis of the cross sections are available, the SDR becomes another important tool for understanding nuclear properties. Since the SDR is characterized by the quantum numbers $\Delta L = 1$ and $S = 1$, this resonance contains three components with $\Delta J^\pi = 0^-, 1^-, 2^-$. A promising tool for experimentally resolving these different multipolarities is the charge-exchange reactions with polarized beams. Such experiments have been carried out in $^{12}\mathrm{C}(\boldsymbol{d},^2\mathrm{H})$ reactions (de Huu *et al.*, 2007).

As mentioned in the general introduction, the spin-isospin resonances in nuclei have been extensively investigated based on the shell model calculations as well as the RPA calculations within non-relativistic and relativistic frameworks. In this chapter, the RHF+RPA approach will be applied to describe the IAS, GTR, SDR, and spin-quadrupole resonances (SQR). Comparing the RPA calculations based on the RH and RHF theories, the different physical mechanisms in determining the GTR will be investigated. Then, the theoretical descriptions of SDR and SQR will be presented. In particular, the energy hierarchies of different components in these resonances will be focused on. Finally, the effects of the Dirac Sea in the non-energy weighted sum rules will be examined.

4.2 Results and discussion

4.2.1 Isobaric analog states

The simplest isospin-flip mode is the isobaric analog states (IAS) with the transition operators F^{IAS} shown in Eq. (2.66). As discussed in **Subsection 3.2.2**, when the Coulomb interaction is switched off, the IAS excitation energy would be zero and this state contains 100% of the non-energy weighted sum rule as long as the RPA calculations are self-consistent. It is useful to evaluate the importance of different components of the p-h residual interaction. Switching off these components piece by piece, deviations of the excitation energy from zero indicate the respective importance of the missing mesons.

In Fig. 4.1, the IAS transition probabilities obtained by switching off the $\sigma + \omega$ mesons, ρ meson, pionic zero-range counter-term, and π meson p-h residual interactions are shown. They are compared with the unperturbed single-particle excitations (HF) and the fully self-consistent results. First, the calculation without ρ-meson shows that this isovector meson is important as expected. Second, the calculation without σ- and ω-mesons tells us that the isoscalar mesons can play a role, even an extremely important role via the exchange terms. This is one of the distinct points in RHF+RPA approach. Third, it should be emphasized that the pion also plays its role in

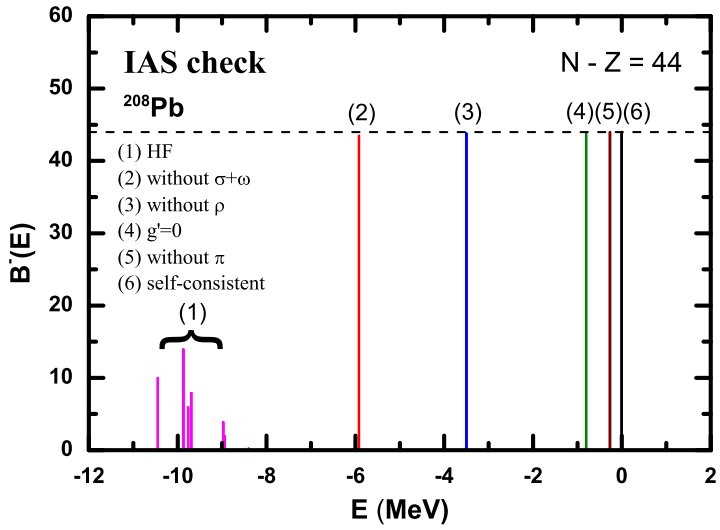

Figure 4.1: IAS energies and transition probabilities in ^{208}Pb by RHF+RPA with PKO1. The unperturbed excitations (HF), and the calculations excluding $\sigma + \omega$ mesons, ρ meson, pionic zero-range counter-term, π meson in the p-h residual interaction, as well as the fully self-consistent result are shown from left to right.

this restoration process. The coefficient g' of the pionic zero-range counter-term must adopt the same value as that in the ground-state description, i.e., $g' = 1/3$. If the value of g' is changed, for example, $g' = 0$ leads to $E_{\rm IAS} = -801$ keV, and the restoration process will be destroyed. Therefore, it is clearly shown that g' is not a free parameter.

Table 4.1: IAS excitation energies in MeV and strength in percentage of the $N - Z$ sum rule within the RHF+RPA framework. Experimental (Anderson *et al.*, 1985; Bainum *et al.*, 1980; Wakasa *et al.*, 1997; Horen *et al.*, 1980; Akimune *et al.*, 1995) and the RH+RPA (Paar *et al.*, 2004) results are given for comparison.

		^{48}Ca		^{90}Zr		^{208}Pb	
		energy	strength	energy	strength	energy	strength
experiment		7.17	~ 100	12.0 ± 0.2	~ 100	18.83 ± 0.02	~ 100
RHF+RPA	PKO1	6.86	99.7	11.41	99.3	18.03	95.8
	PKO2	6.93	99.7	11.52	99.3	18.30	95.3
	PKO3	6.91	99.7	11.49	99.4	18.26	95.8
RH+RPA	DD-ME1	7.08	99.6	11.69	99.2	18.44	95.3

In realistic nuclei, the IAS excitations are pushed into higher energy region due to the Coulomb interaction. In Table 4.1, the IAS excitation energies and their strength in percentage of the $N-Z$ sum rule obtained by RHF+RPA are compared with the experimental data (Anderson *et al.*, 1985; Bainum *et al.*, 1980; Wakasa *et al.*, 1997; Horen *et al.*, 1980; Akimune *et al.*, 1995) and the

RH+RPA (Paar *et al.*, 2004) results. It is found that the calculated IAS excitation energies are slightly lower than the experimental data, and the single collective state contains almost 100% of the sum rule value. Furthermore, it is also found that the IAS excitation energies by RHF+RPA are systematically ~ 200 keV lower than those by RH+RPA, which is due to the different treatments of the Coulomb field, and the lack of the exchange Coulomb mean field in RH+RPA.

4.2.2 Gamow-Teller resonances

Table 4.2: GTR excitation energies in MeV, and strength in percentage of the $3(N-Z)$ sum rule within the RHF+RPA framework. Experimental (Anderson *et al.*, 1985; Bainum *et al.*, 1980; Wakasa *et al.*, 1997; Horen *et al.*, 1980; Akimune *et al.*, 1995) and the RH+RPA (Paar *et al.*, 2004) results are given for comparison.

		^{48}Ca		^{90}Zr		^{208}Pb	
		energy	strength	energy	strength	energy	strength
experiment		~ 10.5		15.6 ± 0.3		19.2 ± 0.2	60-70
RHF+RPA	PKO1	10.72	69.4	15.80	68.1	18.15	65.6
	PKO2	10.83	66.7	15.99	66.3	18.20	60.5
	PKO3	10.42	70.7	15.71	68.9	18.14	67.7
RH+RPA	DD-ME1	10.28	72.5	15.81	71.0	19.19	70.6

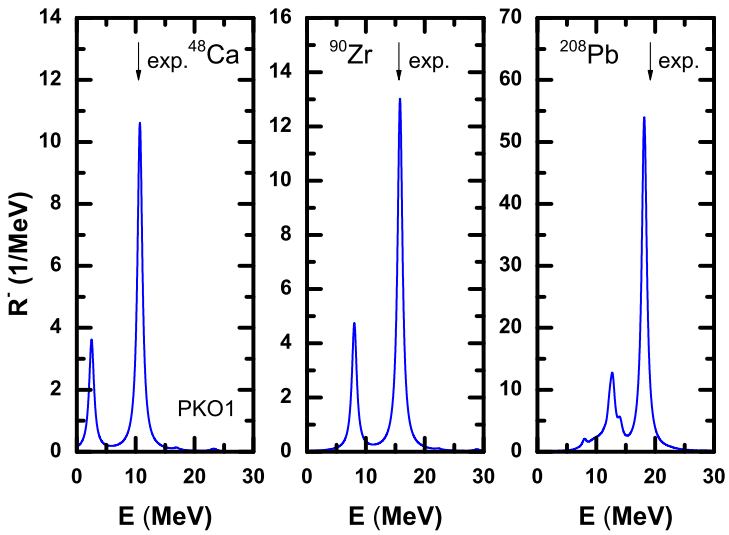

Figure 4.2: Strength distributions of GTR in ^{48}Ca, ^{90}Zr, and ^{208}Pb calculated by RHF+RPA with PKO1, where a Lorentzian smearing parameter $\Gamma = 1$ MeV is used. The experimental excitation energies are denoted with arrows.

Taking the doubly magic nuclei ^{48}Ca, ^{90}Zr and ^{208}Pb as examples, the GTR excitation energies

and strengths calculated with the fully self-consistent RHF+RPA approach using the parametrizations PKO1, PKO2, PKO3 are summarized in Table 4.2. The corresponding Lorentzian-averaged strength distributions are shown in Fig. 4.2, where a Lorentzian smearing parameter $\Gamma = 1$ MeV is used. It is found that a good agreement with empirical energies is obtained without any re-adjusted parameter. All calculated strengths correspond to the main peak, and they contain 60-70% of the Ikeda sum rule (Eq. (2.68)).

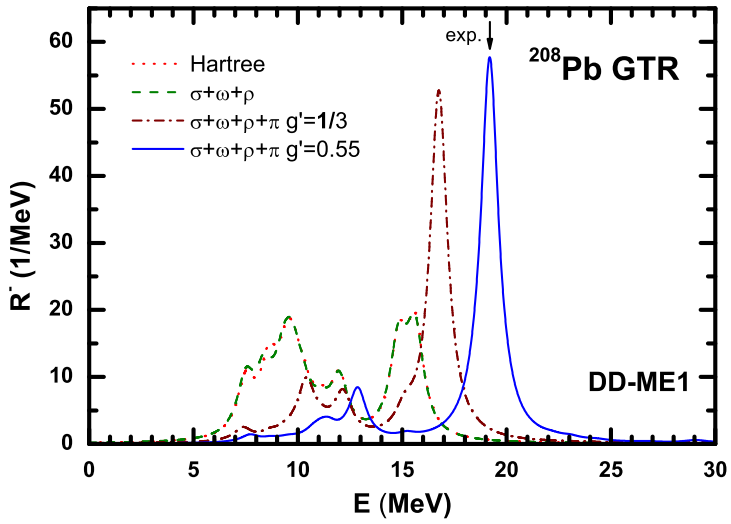

Figure 4.3: Strength distribution of GTR in ^{208}Pb calculated by RH+RPA with DD-ME1 (Nikšić *et al.*, 2002a) (solid line). The unperturbed (Hartree) strength (dotted line), the calculation with only $\sigma + \omega + \rho$ p-h residual interaction (dashed line), and the calculation including pion but $g' = 1/3$ (dash-dotted line) are also shown. A Lorentzian smearing parameter $\Gamma = 1$ MeV is used.

We can understand the different physical mechanisms between the present RHF+RPA and other RH+RPA approaches by the following analysis. On the one hand, the GT strength distribution in ^{208}Pb by RH+RPA with DD-ME1 (Nikšić *et al.*, 2002a) is shown in Fig. 4.3. It is compared with the unperturbed (Hartree) strength, the calculation with only $\sigma + \omega + \rho$ p-h residual interaction, and the calculation including pion but $g' = 1/3$. It is found that the contribution of the p-h residual interaction induced by the isoscalar mesons vanishes due to the isospin conservation in the direct term, and the result with only p-h residual interaction induced by ρ-meson is almost on top of the unperturbed strength. Adding the pion degree of freedom, the peak energy is pushed to high energy, and it is further pushed up to the experimental value when g' is changed from 1/3 to 0.55. Thus, the π-N interaction and its zero-range counter-term are the dominant ingredients in p-h residual interaction, and g' is treated as an adjustable parameter to reproduce the experimental date. On the other hand, in the present RHF+RPA calculations, three parametrizations PKO1, PKO2 and PKO3 lead to similar results for the GTR excitation energies. It should be emphasized that the pion is not included in PKO2, and therefore, there is no g' term when calculating RPA with PKO2. This hints to the fact that the pion interaction is not the only dominant ingredient for

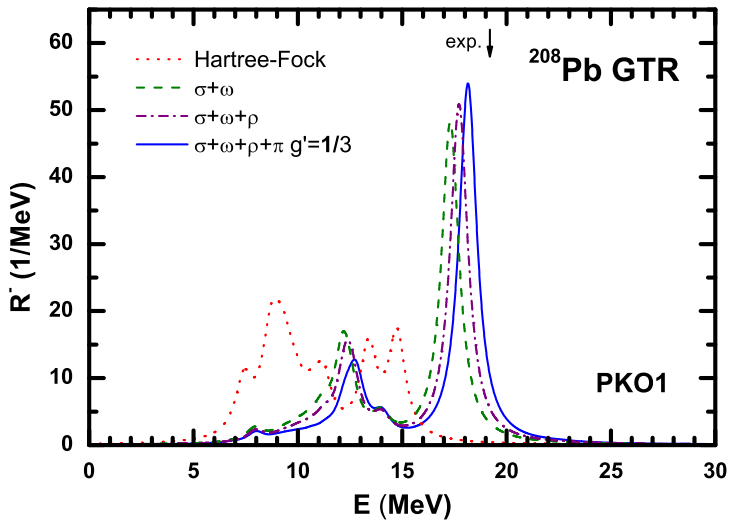

Figure 4.4: Strength distribution of GTR in ^{208}Pb calculated by RHF+RPA with PKO1 (solid line). The unperturbed (Hartree-Fock) strength (dotted line), the calculation with only $\sigma + \omega$ p-h residual interaction (dashed line), and the calculation excluding pion ($f_\pi = 0$) in the p-h residual interaction (dash-dotted line) are also shown. A Lorentzian smearing parameter $\Gamma = 1$ MeV is used.

the GT excitations in this framework. The GT strength distribution in ^{208}Pb by RHF+RPA with PKO1 is shown in Fig. 4.4. It is compared with the calculation in which the pion is excluded in the p-h channel, the calculation including only $\sigma + \omega$ p-h residual interactions, and the unperturbed (Hartree-Fock) case. Comparing these theoretical results, one can conclude that the isoscalar σ- and ω-mesons play an essential role via the exchange terms, whereas the pion just stands on a marginal position in determining the GTR strength distribution. Thus, this is a fundamental difference with RH+RPA where σ and ω play no role in the p-h interaction for the GTR.

4.2.3 Spin-dipole and spin-quadrupole resonances

As discussed in the previous subsection, even though different relativistic RPA approaches lead to similar GTR strength distributions, the physical mechanisms are substantially different, and these different physical mechanisms can be clearly demonstrated in other charge-exchange spin-flip modes.

In Fig. 4.5 and Fig. 4.6, the strength distributions in the T_- and T_+ channels of the SDR in ^{90}Zr calculated by RH+RPA with DD-ME1 and RHF+RPA with PKO3 are shown in left and right panels, respectively. The dash-dotted, dotted, dashed lines show the 0^-, 1^-, 2^- contributions respectively, and the solid line shows their sum. It is found that the experimental dominant resonance structure centered at $E \approx 27$ MeV in the T_- channel (Yako *et al.*, 2006) is well reproduced in the RHF+RPA calculations, while the RH+RPA calculations present a more fragmented structure.

The difference between the RHF+RPA and RH+RPA approaches can be explicitly distinguished by examining the 0^-, 1^-, 2^- components separately. For the results obtained by RHF+RPA

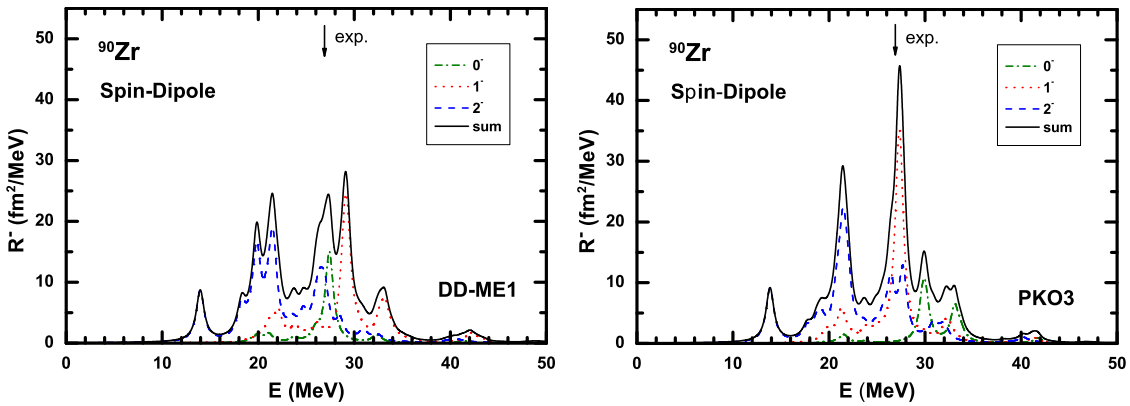

Figure 4.5: Strength distributions in the T_- channel of the SDR in ^{90}Zr calculated by RH+RPA with DD-ME1 (left panel) and RHF+RPA with PKO3 (right panel). The dash-dotted, dotted, dashed lines show the 0^-, 1^-, 2^- contributions respectively, while the solid line shows their sum. The arrows indicate the experimental data.

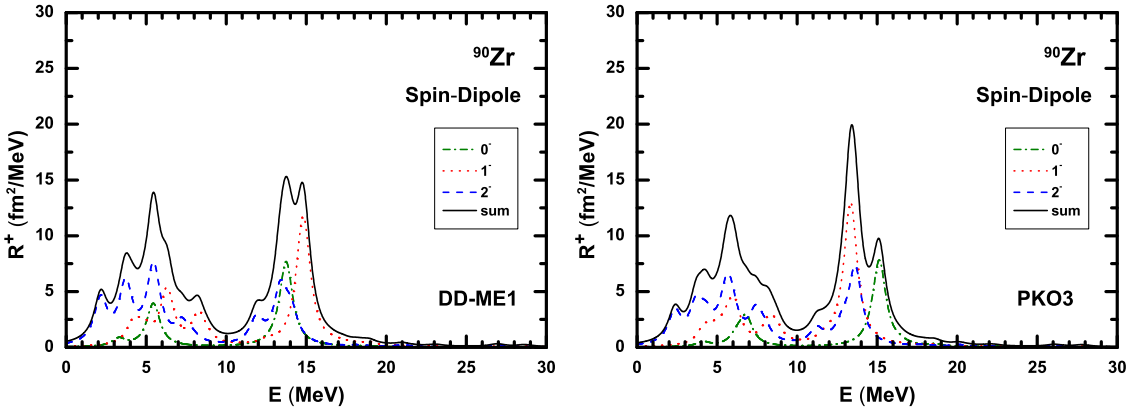

Figure 4.6: Same as Fig. 4.5, but for the T_+ channel.

Table 4.3: Average excitation energies for different components of spin-dipole resonances (SDR) and spin-quadrupole resonances (SQR) in ^{90}Zr calculated by RH+RPA with DD-ME1, RHF+RPA with PKO3, as well as SHF+RPA with SLy5 (Fracasso and Colò, 2007) and SIII (Auerbach and Klein, 1984). All values are expressed in MeV.

		RH+RPA	RHF+RPA	SHF+RPA	
		DD-ME1	PKO3	SLy5	SIII
SDR(T_-)	0^-	27.1	31.0	30.8	31.8
	1^-	29.5	27.1	27.5	28.4
	2^-	22.9	23.5	22.9	23.5
SDR(T_+)	0^-	11.2	13.3		12.5
	1^-	11.8	11.2		10.3
	2^-	8.5	8.9		9.1
SQR(T_-)	1^+	37.0	39.8		40.1
	2^+	36.3	34.5		35.1
	3^+	27.6	29.2		28.5
SQR(T_+)	1^+	23.4	24.7		22.9
	2^+	22.3	21.4		19.8
	3^+	16.6	17.1		14.6

approach, in the T_- channel, both the excitation energies of the dominant peaks shown in Fig. 4.5 and the average excitation energies listed in Table 4.3 follow the energy hierarchy that the 2^- is the lowest and the 0^- the highest. This energy hierarchy is also reported in recent investigations with fully self-consistent SHF+RPA calculations (Fracasso and Colò, 2007), and those with Landau approximation (Auerbach and Klein, 1984). It is also found that in all these three components the dominant p-h residual interactions are those due to isoscalar meson exchanges.

Meanwhile, in RH+RPA calculations, the peak and average energies of 1^- are found to be higher than those of 0^-. Tracing the effects of the p-h residual interactions, it is found that the Hartree contribution of the pseudo-vector π-N p-h residual interaction is always attractive, whereas that of the pionic zero-range counterterm is repulsive, and this balance lead to the correct position of the GTR excitation energy as shown in the previous subsection. However, for the 1^- component of SDR, the contribution of the pseudo-vector π-N interaction vanishes due to the natural parity, and such balance is broken. Thus, the pionic zero-range counterterm alone pushes the 1^- excitation energies even higher than those of 0^-, which is a result provided by adjusting the g'.

In the T_+ channel, it can also be seen that the RHF+RPA and SHF+RPA calculations lead to the same energy hierarchy, as shown in Table 4.3, whereas the 1^- states become the highest component in RH+RPA calculations.

Separating experimentally the 0^-, 1^-, 2^- components from the total SDR transition strength would be helpful to evaluate the predictive power of the above theoretical approaches. So far, such experiment has been carried out in ^{12}C (de Huu *et al.*, 2007). However, the SDR strength distributions in such light nucleus are too fragmented to pin down the energy hierarchy.

As a further step, the theoretical description of SQR have been examined, and the average excitation energies for the 1^+, 2^+, and 3^+ components are listed in the second part of Table 4.3, comparing with those obtained with SHF+RPA calculations. Focusing on the relative position of these three components, the results obtained by RHF+RPA and SHF+RPA approaches are almost the same, while the excitation energies in the 2^+ component with natural parity are substantially pushed towards the high energy region in the RH+RPA results.

4.2.4 Effects of the Dirac Sea in non-energy weighted sum rules

The relativistic RPA is equivalent to the time-dependent relativistic mean field in the small amplitude limit only if the p-h configuration space includes both the pairs formed from the occupied and unoccupied Fermi states and the pairs formed from the empty Dirac states and occupied Fermi states (Ring *et al.*, 2001). Due to the pairs formed from the Dirac states and occupied Fermi states, the RPA equations have negative eigenvalues ($\Omega_\nu < -1.1$ GeV), and the transition probabilities to these negative energy excitations are not always negligible. Based on this idea, a relativistic reduction mechanism of the Gamow-Teller strength due to the effects of the Dirac sea states was pointed out (Kurasawa *et al.*, 2003). This kind of reduction mechanism appears in both nuclear matter (Kurasawa *et al.*, 2003) and finite nuclei (Ma *et al.*, 2004; Paar *et al.*, 2004).

Taking the GTR in the nucleus ^{208}Pb as an example, the transition probabilities in the T_- and

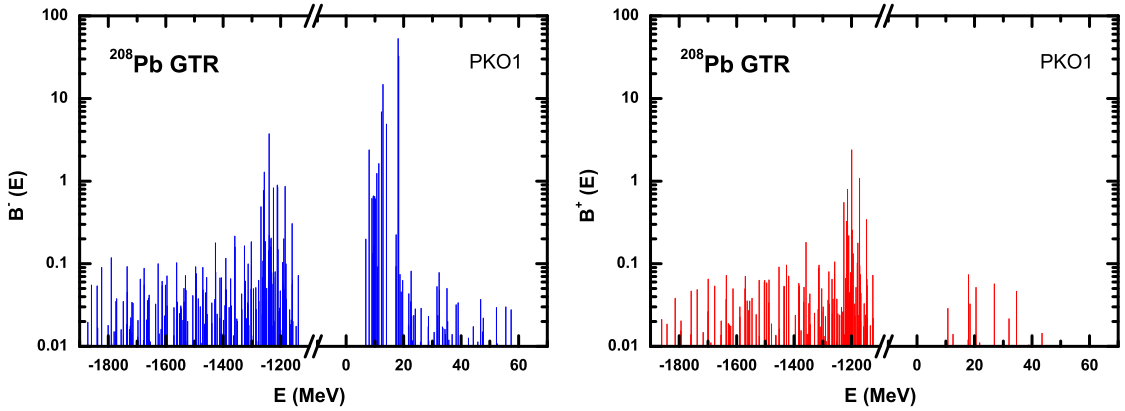

Figure 4.7: Transition probabilities in the T_- (left panel) and T_+ (right panel) channels of the GTR in ^{208}Pb calculated by RHF+RPA with PKO1.

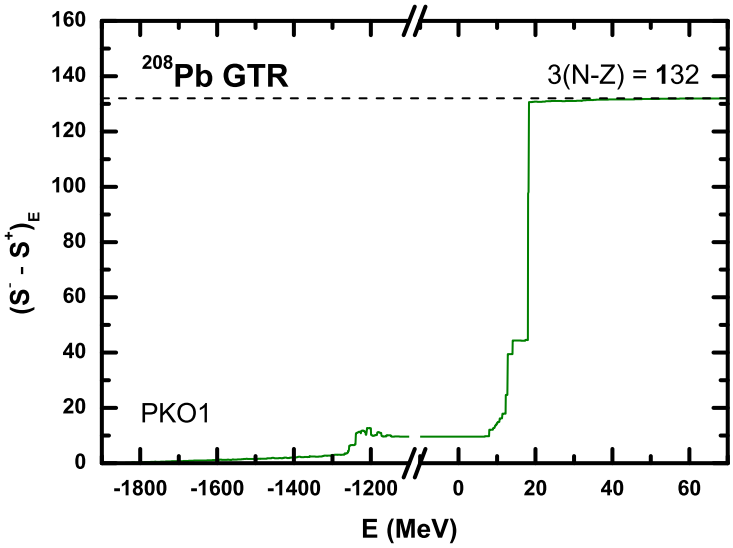

Figure 4.8: Running sum of transition probabilities of the GTR in ^{208}Pb calculated by RHF+RPA with PKO1. The corresponding GT sum rule value is shown as the horizontal dashed line.

Table 4.4: Ikeda sum rule values from Fermi ($S_{\rm F}$) and Dirac ($S_{\rm D}$) sectors calculated by RHF+RPA with PKO1. S^-, S^+ are the sum rule values of the T_- and T_+ channels, respectively. The reduction factor, $1-(S^-_{\rm F}-S^+_{\rm F})/(S^- - S^+)$, is given in the last column.

	$S^-_{\rm F}$	$S^-_{\rm D}$	$S^+_{\rm F}$	$S^+_{\rm D}$	$S^-_{\rm F}-S^+_{\rm F}$	$S^- - S^+$	reduction
^{48}Ca	22.67	4.23	0.10	2.83	22.57	23.97	5.9%
^{90}Zr	28.22	8.08	0.32	5.99	27.91	29.99	7.0%
^{208}Pb	122.94	21.54	0.51	11.98	122.43	131.99	7.2%

T_+ channels obtained by self-consistent RHF+RPA calculations with PKO1 are shown in the left and right panels of Fig. 4.7, respectively. It is found that there are plenty of excitations in the Dirac sector in both channels, and their transition probabilities are one to three orders of magnitude smaller than the dominant resonance in the Fermi sector. In order to examine their contributions to the non-energy weighted sum rule, the running sum of transition probabilities, which is defined by

$$(S^- - S^+)_E = \sum_{\Omega_\nu < E} (B^-_\nu - B^+_\nu), \tag{4.1}$$

are shown in Fig. 4.8, where the corresponding GT sum rule value $3(N-Z) = 132$ is shown as the horizontal dashed line. First of all, the big jumps in the curve correspond to the low-lying and giant resonances shown in Fig. 4.2. It also can be seen that the GT sum rule is fully exhausted when the running sum is calculated up to $E = 50$ MeV. One of the most important points from this figure is that around 7% of the sum rule value is carried by the excitations in the Dirac sector, where the dominant contributions come from the deeply bound single-particle states in the Dirac sea. This indicates that the GT non-energy weighted sum rule can be 100% exhausted only when the strengths of the transition from the occupied positive energy states to the empty negative energy states are included. The reduction factors, $1-(S^{\rm F}_- - S^{\rm F}_+)/(S_- - S_+)$, of GTR in ^{48}Ca, ^{90}Zr, ^{208}Pb, which are summarized in Table 4.4, indicate to which extent the antinucleon degrees of freedom play a role in the present self-consistent approach.

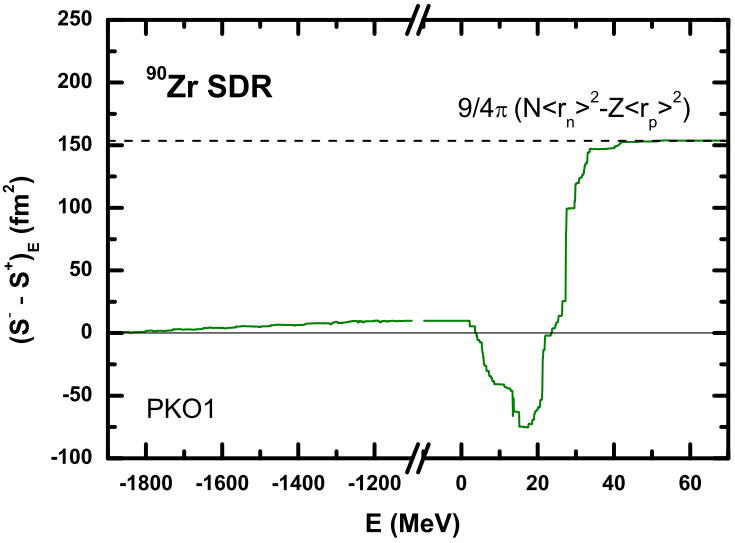

Figure 4.9: Running sum of transition probabilities of the SDR in ^{90}Zr calculated by RHF+RPA with PKO1. The corresponding SD sum rule value is shown as the horizontal dashed line.

For the case of SDR, the running sum of transition probabilities in ^{90}Zr is shown in Fig. 4.9. The curve exhibits a dip in the energy region 5 MeV to 15 MeV due to the fact that the excitation energies of dominant resonances in the T_+ channel are smaller than those in the T_- channel as shown in Fig. 4.5 and Fig. 4.6. While the SD sum rule are fully exhausted when the running sum is calculated up to $E = 50$ MeV, it is found that 6.4% of the sum rule value is carried by the

excitations in the Dirac sector. Furthermore, in contrast to the GTR case, these contributions come from not only the deeply bound but also the weakly bound single-particle states in the Dirac sea.

In general, a substantial reduction of the non-energy weighted sum rule value due to the effects of the Dirac sea is found in spin-flip modes. On the other hand, we find that there is practically no reduction in non-spin-flip modes, for example, IAS, charge-exchange dipole, quadrupole resonances, and so on.

In summary, in this chapter the RHF+RPA approach is applied to describe the nuclear spin-isospin resonances. First of all, in the case of IAS without Coulomb interaction, by switching off the p-h residual interaction piece by piece, it is found that the σ-, ω-, ρ-mesons play important roles in this mode, and the coefficient g' of pionic zero-range counter-term must be maintained as $g' = 1/3$, otherwise the restoration of the isospin symmetry would be destroyed. Furthermore, the experimental data on the IAS and GTR in doubly magic nuclei ^{48}Ca, ^{90}Zr, ^{208}Pb can be well reproduced by the present RHF+RPA approach without any readjustment of the energy functional. In comparison with the RH+RPA description, the physical mechanisms in determining the GTR are investigated by examining the importance of different p-h residual interactions. It is found that in RH+RPA approach the attractive πNN interaction and its repulsive zero-range counter-term are the dominant ingredients in p-h residual interaction for the GT mode, while in RHF+RPA approach the isoscalar σ- and ω-mesons play an essential role via the exchange terms. These different physical mechanisms can be clearly demonstrated in the other charge-exchange spin-flip modes, e.g., SDR and SQR. As an example, the energy hierarchies of different components in these resonances obtained by RHF+RPA approach are the same as those obtained by SHF+RPA calculations. In contrast, since the the attractive πNN p-h residual interaction vanishes in the natural parity 1^- component of SDR and 2^+ component of SDR, the corresponding excitation energies are substantially pushed towards the high energy region in RH+RPA results. If the energy hierarchies of the different J^π components in SDR or SQR could be determined experimentally in the future, this would be helpful to verify the predictive power of various theoretical approaches. Finally, by examining the effects of the Dirac Sea in the non-energy weighted sum rules, a substantial reduction of the sum rule value is found in spin-flip modes, while there is practically no reduction in non-spin-flip modes.

Chapter 5

Isospin Corrections for Superallowed β Decays

5.1 Introduction

The Cabibbo-Kobayashi-Maskawa (CKM) matrix (Cabibbo, 1963; Kobayashi and Maskawa, 1973) relates the quark eigenstates of the weak interaction with the quark mass eigenstates. The unitarity condition of the CKM matrix provides a rigorous test for the Standard Model description of electroweak interactions. Its leading matrix element, V_{ud}, only depends on the first generation quarks and so it is the element that can be determined most precisely. There are three traditional methods to determine $|V_{ud}|$ experimentally: nuclear $0^+ \rightarrow 0^+$ superallowed Fermi β decays (Hardy and Towner, 2005, 2009), neutron decay (Thompson, 1990) and pion β decay (Počanić *et al.*, 2004). Recently, experiments with nuclear mirror transitions provide another independent sensitive source for extracting the value of $|V_{ud}|$ (Naviliat-Cuncic and Severijns, 2009).

Among these methods, the most precise determination of $|V_{ud}|$ comes from the study of nuclear $0^+ \rightarrow 0^+$ superallowed Fermi β decays (Amsler *et al.*, 2008). These pure Fermi transitions between nuclear isobaric analog states (IAS) allow for a direct measurement of the vector coupling constant G_V of semileptonic weak interactions by

$$G_V^2 = \frac{K}{2(1+\Delta_R^V)\mathcal{F}t}. \tag{5.1}$$

Together with the Fermi coupling constant G_F for purely leptonic decays, the up-down element of the CKM matrix can be determined, $V_{ud} = G_V/G_F$. In Eq. (5.1), $K/(\hbar c)^6 = 2\pi^3\hbar \ln 2/(m_e c^2)^5$ and Δ_R^V is the transition-independent part of radiative corrections caused, for example, by the processes where the emitted electron may emit a bremsstrahlung photon that goes undetected in the experiment (Marciano and Sirlin, 2006; Towner and Hardy, 2008). The nucleus-independent $\mathcal{F}t$ value is duduced from the experimental ft values after correcting them by the radiative effects as well as effects due to isospin symmetry breaking by Coulomb and charge-dependent nuclear forces (Hardy and Towner, 2009),

$$\mathcal{F}t = ft(1+\delta_R')(1+\delta_{\rm NS}-\delta_c), \tag{5.2}$$

where f and t represent the statistical rate function and partial half-life, respectively. These experimental values are obtained through measurements of the Q values, branching ratios, and half-lives for the superallowed β decays. The correction terms δ'_R and $\delta_{\rm NS}$ represent the transition-dependent radiative corrections (Marciano and Sirlin, 2006; Towner and Hardy, 2008). The correction term δ_c is the isospin symmetry-breaking correction, accounting for the isospin symmetry breaking in nuclei.

The isospin is not an exact symmetry mainly due to the presence of the Coulomb forces in nuclei. The non-conservation of isospin symmetry induces a slight reduction of the superallowed transition strength $|M_F|^2$ from its ideal value $|M_0|^2$,

$$|M_F|^2 = |\langle f|T_\pm|i\rangle|^2 = |M_0|^2(1-\delta_c), \tag{5.3}$$

where $M_0 = \sqrt{2}$ for $T = 1$ states with the exact isospin symmetry.

Shell model calculations are generally used to determine the isospin symmetry-breaking corrections δ_c. Recently, by including the core orbitals, an improvement on such corrections has been achieved and a good agreement among the nucleus-independent $\mathcal{F}t$ values for the 13 well-measured cases (^{10}C $\rightarrow$ ^{10}B, ^{14}O $\rightarrow$ ^{14}N, ^{22}Mg $\rightarrow$ ^{22}Na, ^{34}Ar $\rightarrow$ ^{34}Cl, ^{26}Al $\rightarrow$ ^{26}Mg, ^{34}Cl $\rightarrow$ ^{34}S, ^{38}K $\rightarrow$ ^{38}Ar, ^{42}Sc $\rightarrow$ ^{42}Ca, ^{46}V $\rightarrow$ ^{46}Ti, ^{50}Mn $\rightarrow$ ^{50}Cr, ^{54}Co $\rightarrow$ ^{54}Fe, ^{62}Ga $\rightarrow$ ^{62}Zn, ^{74}Rb $\rightarrow$ ^{74}Kr) has been obtained (Towner and Hardy, 2008).

Alternatively, self-consistent Random Phase Approximation (RPA) based on microscopic mean field theories is another microscopic approach for the superallowed transition strength M_F. Such calculations have been performed for a few nuclei with the non-relativistic Skyrme Hartree-Fock approach in the 1990s (Sagawa *et al.*, 1996). Since then no further investigations have been done even though significant progress in self-consistent RPA in charge-exchange channels have been made (Engel *et al.*, 1999; Fracasso and Colò, 2005; De Conti *et al.*, 1998; Paar *et al.*, 2004; Liang *et al.*, 2008).

During the last decade, great efforts have been dedicated to developing the charge-exchange (Q)RPA within the relativistic framework. From the early model which only contains a rather small configuration space (De Conti *et al.*, 1998) to the sophisticated model which includes Bogoliubov transformation and proton-neutron pairing (Paar *et al.*, 2004), these approaches are aimed at describing the spin-isospin resonances, β decay rates, neutrino-nucleus cross sections, etc., in a systematical, reliable and predictive way. Recently, based on the success of the newly established density-dependent relativistic Hartree-Fock (RHF) approach, a fully self-consistent charge-exchange RPA has been established and the first applications were performed for spin-isospin resonances like Gamow-Teller and spin-dipole resonances (Liang *et al.*, 2008). A very satisfactory agreement with the experimental data was obtained without any readjustment of the energy functional. Therefore, it is appropriate now to re-investigate the isospin corrections for superallowed Fermi β decays with these relativistic models.

In this chapter, the self-consistent RPA approaches in the relativistic framework will be applied to calculate the isospin symmetry-breaking corrections δ_c. With the corrections thus obtained,

the nucleus-independent $\mathcal{F}t$ values will be deduced in combination with the experimental ft values in the most recent survey (Hardy and Towner, 2009) and the improved radiative corrections (Marciano and Sirlin, 2006; Towner and Hardy, 2008). The element V_{ud} and the unitarity of the CKM matrix will then be discussed.

Before ending this section, it is worthwhile to make the following remark about the self-consistency of the RH+RPA approach when it is applied to the $0^+ \to 0^+$ transitions. Within this approach, it is known that, in order to reproduce the excitation energies of GTR, one has to adjust the π-N p-h residual interaction and that g' cannot be kept equal to 1/3 (De Conti *et al.*, 1998; Paar *et al.*, 2004). However, for the $0^+ \to 0^+$ channel, the direct contributions from the pion vanish. Therefore, in this sense, the self-consistency is also fulfilled in the RH+RPA approach as far as the superallowed Fermi β decays are concerned.

5.2 Results and discussion

For all the calculations in this section, the spherical symmetry is assumed and the filling approximation is applied to the last partially occupied orbital. The Dirac equations are solved in coordinate space within a spherical box with a box radius $R = 15$ fm and a mesh size $dr = 0.1$ fm. The single-particle wave functions thus obtained are used to construct the RPA matrix elements $\mathcal{A}^J$ and $\mathcal{B}^J$ in Eq. (2.53) with the single-particle energy truncation $[-M, M + 120$ MeV$]$. With these numerical inputs, the IAS non-energy weighted sum rule in Eq. (2.67) can be fulfilled up to 10^{-5} accuracy, and the isospin symmetry-breaking corrections δ_c are stable with respect to these numerical inputs at the same level of accuracy.

5.2.1 Isospin symmetry-breaking corrections δ_c

In Table 5.1, the isospin symmetry-breaking corrections δ_c in Eq. (5.3) for the $0^+ \to 0^+$ superallowed transitions are shown. The results are obtained by self-consistent RHF+RPA calculations with PKO1 (Long *et al.*, 2006), PKO2 (Long *et al.*, 2008), PKO3 (Long *et al.*, 2008) effective interactions, as well as by self-consistent RH+RPA calculations with DD-ME1 (Nikšić *et al.*, 2002a), DD-ME2 (Lalazissis *et al.*, 2005), NL3 (Lalazissis *et al.*, 1997), TM1 (Sugahara and Toki, 1994) effective interactions. The results obtained by shell model calculations (T&H) (Towner and Hardy, 2008) are also listed for comparison. The RPA corrections δ_c range from about 0.1% for the lightest nucleus ^{10}C to about 1.2% for the heaviest nucleus ^{74}Rb, which are 2 to 3 times smaller than the T&H results. It is noticed that even smaller values of δ_c compared to the shell model calculations have been recently obtained in Ref. (Auerbach, 2009) using perturbation theory. In addition, in Table 5.2 the excitation energies E_x for the $0^+ \to 0^+$ superallowed transitions corresponding to PKO1 and DD-ME2 are shown as examples. These energies are measured by taking the ground-state of the corresponding even-even nuclei as reference. In the comparison with the experimental values taken from the recent survey (Hardy and Towner, 2009), the corrections due to the proton-neutron mass difference in p-h configurations are included in the calculated results. A good agreement

Table 5.1: Isospin symmetry-breaking corrections δ_c for the $0^+ \rightarrow 0^+$ superallowed transitions obtained by self-consistent RHF+RPA calculations with PKO1 (Long *et al.*, 2006), PKO2 (Long *et al.*, 2008), and PKO3 (Long *et al.*, 2008) as well as self-consistent RH+RPA calculations with DD-ME1 (Nikšić *et al.*, 2002a), DD-ME2 (Lalazissis *et al.*, 2005), NL3 (Lalazissis *et al.*, 1997), and TM1 (Sugahara and Toki, 1994). The column PKO1* presents the results obtained with PKO1 without the Coulomb exchange (Fock) term. The results obtained by shell model calculations (Towner and Hardy, 2008) are listed in the column T&H for comparison. All values are expressed in %.

	PKO1	PKO2	PKO3	PKO1*	DD-ME1	DD-ME2	NL3	TM1	T&H
^{10}C $\rightarrow$ ^{10}B	0.082	0.083	0.088	0.148	0.149	0.150	0.124	0.133	0.175(18)
^{14}O $\rightarrow$ ^{14}N	0.114	0.134	0.110	0.178	0.189	0.197	0.181	0.159	0.330(25)
^{18}Ne $\rightarrow$ ^{18}F	0.270	0.277	0.288	0.357	0.424	0.430	0.344	0.373	0.565(39)
^{26}Si $\rightarrow$ ^{26}Al	0.176	0.176	0.184	0.246	0.252	0.252	0.213	0.226	0.435(27)
^{30}S $\rightarrow$ ^{30}P	0.497	0.550	0.507	0.625	0.612	0.633	0.551	0.648	0.855(28)
^{34}Ar $\rightarrow$ ^{34}Cl	0.268	0.281	0.267	0.359	0.368	0.376	0.438	0.320	0.665(56)
^{38}Ca $\rightarrow$ ^{38}K	0.313	0.330	0.313	0.406	0.431	0.441	0.390	0.572	0.765(71)
^{42}Ti $\rightarrow$ ^{42}Sc	0.384	0.387	0.390	0.460	0.515	0.523	0.436	0.443	0.935(78)
^{26}Al $\rightarrow$ ^{26}Mg	0.139	0.138	0.144	0.193	0.198	0.198	0.172	0.179	0.310(18)
^{34}Cl $\rightarrow$ ^{34}S	0.234	0.242	0.231	0.298	0.302	0.307	0.289	0.267	0.650(46)
^{38}K $\rightarrow$ ^{38}Ar	0.278	0.290	0.276	0.344	0.363	0.371	0.334	0.484	0.655(59)
^{42}Sc $\rightarrow$ ^{42}Ca	0.333	0.334	0.336	0.395	0.442	0.448	0.377	0.383	0.665(56)
^{54}Co $\rightarrow$ ^{54}Fe	0.319	0.317	0.321	0.392	0.395	0.393	0.355	0.368	0.770(67)
^{66}As $\rightarrow$ ^{66}Ge	0.475	0.475	0.469	0.571	0.568	0.572	0.560	0.524	1.56(40)
^{70}Br $\rightarrow$ ^{70}Se	1.140	1.118	1.107	1.234	1.232	1.268	1.230	1.226	1.60(25)
^{74}Rb $\rightarrow$ ^{74}Kr	1.088	1.091	1.071	1.230	1.233	1.258	1.191	1.234	1.63(31)

Table 5.2: Excitation energies E_x for the $0^+ \rightarrow 0^+$ superallowed transitions measured by taking the ground-state of the corresponding even-even nuclei as reference. In the comparison with the experimental values taken from the recent survey (Hardy and Towner, 2009), the corrections due to the proton-neutron mass difference in p-h configurations are included in the calculated results. All units are in MeV.

	expt.	PKO1	PKO1*	DD-ME2
^{10}C $\rightarrow$ ^{10}B	-1.908	-1.698	-2.307	-2.236
^{14}O $\rightarrow$ ^{14}N	-2.831	-2.420	-2.989	-3.081
^{18}Ne $\rightarrow$ ^{18}F	-3.402	-3.195	-3.497	-3.451
^{26}Si $\rightarrow$ ^{26}Al	-4.842	-4.531	-5.139	-5.110
^{30}S $\rightarrow$ ^{30}P	-5.460	-4.845	-5.326	-5.395
^{34}Ar $\rightarrow$ ^{34}Cl	-6.063	-5.559	-6.129	-6.278
^{38}Ca $\rightarrow$ ^{38}K	-6.612	-6.035	-6.611	-6.775
^{42}Ti $\rightarrow$ ^{42}Sc	-7.000	-6.661	-6.970	-6.964
^{26}Al $\rightarrow$ ^{26}Mg	4.233	3.908	4.372	4.350
^{34}Cl $\rightarrow$ ^{34}S	5.492	5.062	5.428	5.561
^{38}K $\rightarrow$ ^{38}Ar	6.044	5.557	5.936	6.083
^{42}Sc $\rightarrow$ ^{42}Ca	6.426	6.118	6.333	6.333
^{54}Co $\rightarrow$ ^{54}Fe	8.244	7.720	8.221	8.240
^{66}As $\rightarrow$ ^{66}Ge	9.579	9.044	9.488	9.677
^{70}Br $\rightarrow$ ^{70}Se	9.970	9.632	9.805	9.852
^{74}Rb $\rightarrow$ ^{74}Kr	10.417	10.005	10.349	10.437

between the data and the calculated ones can be seen in Table 5.2.

In Table 5.1, it is found that the present isospin symmetry-breaking corrections δ_c for each nucleus can be unambiguously divided into two categories, those obtained by RHF+RPA calculations and those obtained by RH+RPA calculations. Comparing these two categories, it is seen that the corrections δ_c of RHF+RPA are systematically smaller than those of RH+RPA. On the other hand, it is also found that within one category the corrections δ_c are not sensitive to specific effective interactions or the structure of the Lagrangian density. For instance, within the RH+RPA framework, both the Lagrangian densities with density-dependent meson-nucleon couplings (DD-ME1, DD-ME2) or with non-linear meson couplings (NL3, TM1) lead to quite similar results.

To understand this systematic discrepancy between RHF+RPA and RH+RPA, it must be kept in mind that in RHF+RPA the exchange (Fock) terms of mesons and photon are kept in both the mean field and RPA levels, whereas they are neglected altogether in RH+RPA. Among all the Fock terms, we expect, in particular, the exchange terms of the Coulomb field to play an important role due to the following reason. The IAS would be degenerate with its isobaric multiplet partner, i.e., $E_x = 0$, and it would contain 100% of the model-independent sum rule (2.67), i.e., $\delta_c = 0$, if the nuclear Hamiltonian commutes with the isospin raising and lowering operators $T_\pm$. This would be the case when the Coulomb field is switched off. While this degeneracy is broken by the mean field approximation, no matter the exchange terms of mesons are included or not, it can be restored by the RPA as long as the RPA calculations are fully self-consistent (Engelbrecht and Lemmer, 1970). Therefore, the Coulomb field is essential for the $0^+ \rightarrow 0^+$ superallowed transitions and the Coulomb exchange (Fock) term should be responsible for the difference in isospin symmetry-breaking corrections δ_c in the RHF+RPA and RH+RPA approaches.

In order to verify the above argument, we have performed the following calculations. Using PKO1, the Hartree-Fock calculations are performed by switching off the exchange contributions of the Coulomb field. From the single-particle spectra thus obtained, self-consistent RPA calculations are then performed. One may notice that in such calculations some nuclear properties including binding energies and rms radii can no longer be reproduced. However, this does not hinder us from discussing the physics we are concerned with. The isospin symmetry-breaking corrections δ_c and the excitation energies E_x thus obtained are listed in the column denoted as PKO1* in Table 5.1 and Table 5.2. It is seen that these results are practically the same as those of RH+RPA calculations with DD-ME1, DD-ME2, NL3, and TM1. Thus, by switching off the exchange contributions of the Coulomb field, E_x and δ_c in the RHF+RPA calculations recover the results in RH+RPA calculations. In other words, although the meson exchange terms can be somehow effectively included by adjusting the parameters in the direct terms, this has not been done for the Coulomb part in the usual RH approximation.

Therefore, one can conclude that the proper treatment of the Coulomb field is very important to extract correctly the isospin symmetry-breaking corrections δ_c.

5.2.2 Nucleus-independent $\mathcal{F}t$ values

Among the $0^+ \to 0^+$ superallowed transitions listed in Table 5.1, some of their measured ft values are summarized in a recent survey (Hardy and Towner, 2009). To obtain the nucleus-independent $\mathcal{F}t$ values from each experimental ft value, apart from the isospin symmetry-breaking corrections δ_c in Table 5.1, one still needs the values of the transition-dependent radiative corrections δ'_R and nuclear-structure-dependent radiative corrections $\delta_{\rm NS}$.

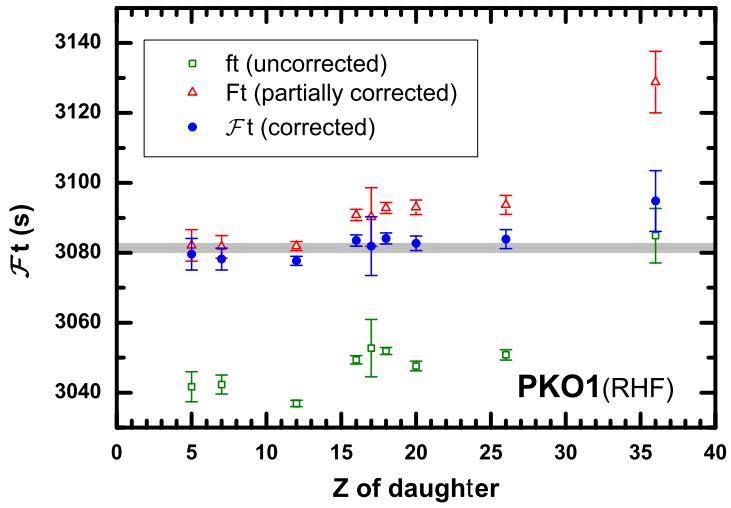

Figure 5.1: Corrected $\mathcal{F}t$ values by RHF+RPA with PKO1 (full circle) as a function of the charge Z for the daughter nucleus. The shaded horizontal band gives one standard deviation around the average $\mathcal{F}t$ value. The uncorrected experimental ft values (Hardy and Towner, 2009) (open square) and partially corrected ($\delta_c = 0$) Ft values (open triangle) are shown for comparison.

Using the δ'_R and $\delta_{\rm NS}$ values from recent calculations (Towner and Hardy, 2008), δ_c in Table 5.1, and measured ft values (Hardy and Towner, 2009), the nucleus-independent $\mathcal{F}t$ values by RHF+RPA with PKO1 for superallowed Fermi β decays are plotted in full circles as a function of the charge Z of the daughter nucleus in Fig. 5.1. The shaded horizontal band gives the standard deviation, which combines the statistical errors and χ^2/ν, around the average $\overline{\mathcal{F}t}$ value. For comparison, the uncorrected experimental ft values (Hardy and Towner, 2009) and the partially corrected Ft values, only including the radiative corrections, are shown as the open squares and triangles, respectively. One can find the importance of the radiative and isospin symmetry-breaking corrections by comparing the three sets of data. It can also be seen that the isospin symmetry-breaking corrections become more important when the charge Z increases.

The $\mathcal{F}t$ values with all effective interactions used are listed in Table 5.3 together with the average $\overline{\mathcal{F}t}$ values and the values of chi-square per degree of freedom χ^2/ν, in which the uncertainty of δ_c is taken as zero. The results of RH+RPA with DD-ME2 are also plotted as a function of the charge Z for the daughter nucleus in the left panel of Fig. 5.2. It is found that the chi-square per degree of freedom χ^2/ν is 1.0 $\sim$ 1.1 s for all effective interactions employed. This indicates that the constancy of the nucleus-independent $\mathcal{F}t$ values is satisfied, even though not as well as in the

Table 5.3: Nucleus-independent $\mathcal{F}t$ values. The average $\overline{\mathcal{F}t}$ value and the normalized χ^2/ν appear at the bottom. All units are in s.

	PKO1	PKO2	PKO3	DD-ME1	DD-ME2	NL3	TM1
$^{10}C \rightarrow {}^{10}B$	3079.6(45)	3079.5(45)	3079.4(45)	3077.5(45)	3077.5(45)	3078.3(45)	3078.0(45)
$^{14}O \rightarrow {}^{14}N$	3078.2(31)	3077.5(31)	3078.3(31)	3075.8(31)	3075.6(31)	3076.1(31)	3076.8(31)
$^{34}Ar \rightarrow {}^{34}Cl$	3081.9(84)	3081.5(84)	3082.0(84)	3078.8(84)	3078.6(84)	3076.7(83)	3080.3(84)
$^{26}Al \rightarrow {}^{26}Mg$	3077.7(13)	3077.7(13)	3077.5(13)	3075.8(13)	3075.8(13)	3076.6(13)	3076.4(13)
$^{34}Cl \rightarrow {}^{34}S$	3083.5(16)	3083.3(16)	3083.6(16)	3081.4(16)	3081.3(16)	3081.8(16)	3082.5(16)
$^{38}K \rightarrow {}^{38}Ar$	3084.1(16)	3083.8(16)	3084.2(16)	3081.5(16)	3081.3(16)	3082.4(16)	3077.8(16)
$^{42}Sc \rightarrow {}^{42}Ca$	3082.7(21)	3082.6(21)	3082.6(21)	3079.3(21)	3079.1(21)	3081.3(21)	3081.1(21)
$^{54}Co \rightarrow {}^{54}Fe$	3083.9(27)	3083.9(27)	3083.8(27)	3081.5(27)	3081.6(27)	3082.7(27)	3082.4(27)
$^{74}Rb \rightarrow {}^{74}Kr$	3094.8(87)	3094.7(87)	3095.3(87)	3090.2(87)	3089.4(87)	3091.5(87)	3090.2(87)
average	3081.4(7)	3081.3(7)	3081.4(7)	3079.1(7)	3079.0(7)	3080.0(7)	3079.1(7)
χ^2/ν	1.1	1.1	1.1	1.0	1.0	1.0	1.0

shell model calculations of Ref. (Hardy and Towner, 2009). It is also found that the $\mathcal{F}t$ values of RHF+RPA are about 2 s larger than those of RH+RPA, which is larger than the difference due to the different effective interactions in either RHF or RH approximations.

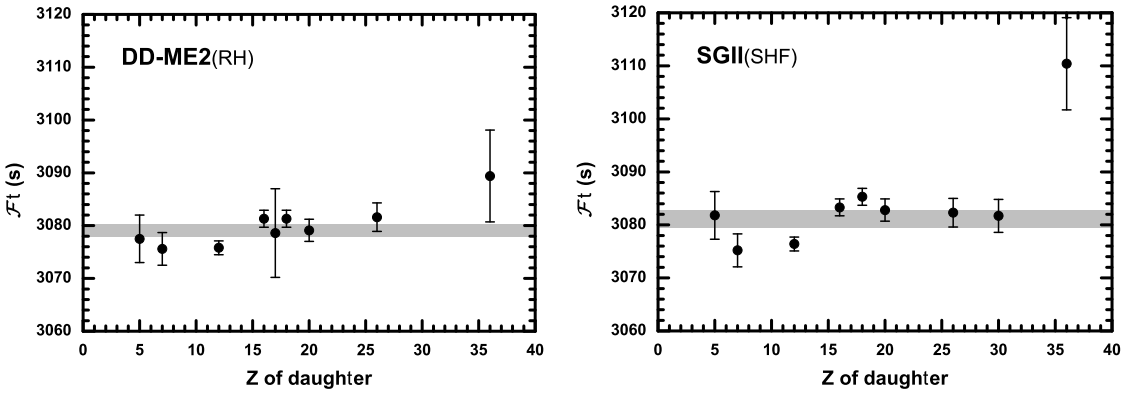

Figure 5.2: Nucleus-independent $\mathcal{F}t$ values as a function of the charge Z for the daughter nucleus. The values of δ_c are respectively obtained by RH+RPA calculations with DD-ME2 (left panel) and by SHF+RPA calculations with SGII (Sagawa *et al.*, 1996) (right panel). The shaded horizontal band gives one standard deviation around the average $\mathcal{F}t$ value.

In order to get a deeper understanding on the treatment of the Coulomb field, the $\mathcal{F}t$ values from RPA calculations using Skyrme Hartree-Fock (SHF) with SGII effective interaction are shown in the right panel of Fig. 5.2, in which the isospin symmetry-breaking corrections δ_c are taken from the Table I in Ref. (Sagawa *et al.*, 1996). It should be emphasized that in these results the exchange contributions to the Coulomb mean field are treated in the Slater approximation. Although this

model leads to a similar average $\mathcal{F}t$ value, $\overline{\mathcal{F}t} = 3081.1(7)$ s, it is found that the chi-square per degree of freedom $\chi^2/\nu = 1.5$, i.e., the constancy of the $\mathcal{F}t$ values in this SHF framework is not as good as that given by the relativistic calculations. In particular, the $\mathcal{F}t$ value deduced from the nucleus ^{74}Rb is somewhat overestimated.

5.2.3 Unitarity of the CKM matrix

With the nucleus-independent $\mathcal{F}t$ value, the element V_{ud} of the CKM matrix can be calculated by (see Eq. (5.1))

$$V_{ud}^2 = \frac{K}{2G_F^2(1+\Delta_R^V)\overline{\mathcal{F}t}}, \tag{5.4}$$

where $K/(\hbar c)^6 = 8120.2787(11)\times10^{-10}$ GeV^{-4}s, $G_F/(\hbar c)^3 = 1.16637(1)\times10^{-5}$ GeV^{-2} (Amsler *et al.*, 2008), and $\Delta_R^V = 2.361(38)\%$ (Towner and Hardy, 2008). Then, in combination with the other two CKM matrix elements $|V_{us}| = 0.2255(19)$ and $|V_{ub}| = 0.00393(36)$ (Amsler *et al.*, 2008), one can test the unitarity of the first line of the matrix.

Table 5.4: The element V_{ud} and the sum of squared top-row elements of the CKM matrix.

	$\lvert V_{ud}\rvert$	$\lvert V_{ud}\rvert^2 + \lvert V_{us}\rvert^2 + \lvert V_{ub}\rvert^2$
PKO1	0.97273(27)	0.9971(10)
PKO2	0.97275(27)	0.9971(10)
PKO3	0.97273(27)	0.9971(10)
PKO1*	0.97303(26)	0.9977(10)
DD-ME1	0.97309(26)	0.9978(10)
DD-ME2	0.97311(26)	0.9978(10)
NL3	0.97295(26)	0.9975(10)
TM1	0.97309(26)	0.9978(10)

The element V_{ud} as well as the sum of squared top-row elements of the CKM matrix are listed in Table 5.4. The uncertainties of the present results are underestimated to some extent as the uncertainty of δ_c is assumed to be zero and the systematic errors are not taken into account. In Fig. 5.3, the sum of squared top row elements of the CKM matrix obtained by RHF+RPA calculations with PKO1 and by RH+RPA calculations with DD-ME2 are shown in comparison with those in shell model (H&T) (Hardy and Towner, 2009) as well as in neutron decay (Amsler *et al.*, 2008), pion β decay (Počanić *et al.*, 2004) and nuclear mirror transitions (Naviliat-Cuncic and Severijns, 2009).

It can be clearly seen in Table 5.4 that the matrix element $|V_{ud}|$ determined by the $0^+ \to 0^+$ superallowed transitions mainly depends on the treatment of the Coulomb field and it is less sensitive to the particular effective interactions. Switching on or off the exchange contributions of the Coulomb field, the discrepancy caused by different effective interactions is much smaller than the statistic deviation. It is interesting to note that the present $|V_{ud}|$ values well agree with those ob-

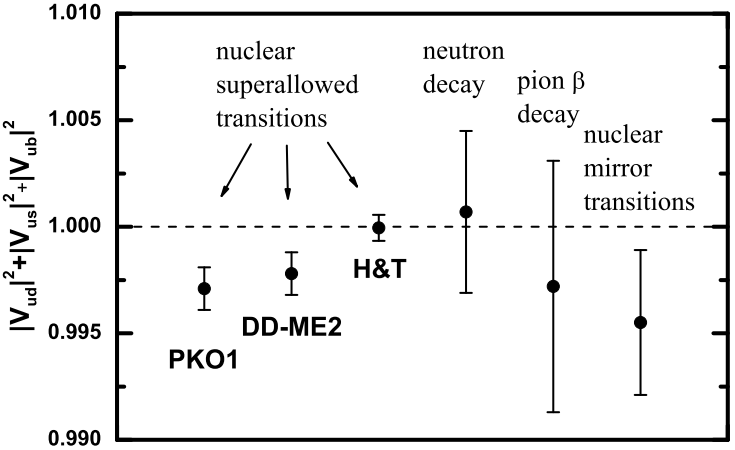

Figure 5.3: The sum of squared top row elements of the CKM matrix obtained by RHF+RPA calculations with PKO1 and by RH+RPA calculations with DD-ME2 in comparison with those in shell model (H&T) (Hardy and Towner, 2009) as well as in neutron decay (Amsler *et al.*, 2008), pion β decay (Počanić *et al.*, 2004) and nuclear mirror transitions (Naviliat-Cuncic and Severijns, 2009).

tained in neutron decay, pion β decay and nuclear mirror transitions. However, the sum of squared top-row elements considerably deviates from the unitarity condition, which is in contradiction with the conclusion of shell model calculations (H&T) (Hardy and Towner, 2009). This calls for more intensive investigations in the future. For example, mean field and RPA calculations including the proper neutron-proton mass difference, isoscalar and isovector pairing, and deformation should be done. It should also be emphasized that apart from the proper treatment of pairing by either BCS or Bogoliubov approaches, the particle number projection must be implemented as well in order to remove the artificial isospin symmetry breaking effects due to the particle number violation. Finally, the errors due to the filling approximation have to be evaluated.

5.2.4 Effects of the neutron-proton mass difference

In this subsection, we examine the effects of the neutron-proton mass difference on the V_{ud} value. We repeat the self-consistent relativistic RPA calculations with effective interactions PKO1 and DD-ME2, but adopting experimental values of neutron and proton masses. The isospin symmetry-breaking corrections δ_c thus obtained are listed in the columns PKO1† and DD-ME2† of Table 5.5. The difference between the results of PKO1† and PKO1, as well as DD-ME2† and DD-ME2 are presented in the columns $\Delta\delta_c$ to show the net effects of the neutron-proton mass difference.

It can be seen that the effects of the neutron-proton mass difference on the corrections δ_c range from about 0.01% to about 0.05%, and roughly speaking, larger δ_c lead to larger $\Delta\delta_c$. With these effects, the V_{ud} value predicted by RHF+RPA with PKO1 is changed from $|V_{ud}| = 0.97273(27)$ to $|V_{ud}| = 0.97280(27)$, and the value predicted by RH+RPA with DD-ME2 is changed from $|V_{ud}| = 0.97311(26)$ to $|V_{ud}| = 0.97321(26)$. This indicates the effects of the neutron-proton mass

Table 5.5: Isospin symmetry-breaking corrections δ_c for the $0^+ \rightarrow 0^+$ superallowed transitions. The columns PKO1† and DD-ME2† present the results obtained with effective interactions PKO1 and DD-ME2 but adopting experimental values of neutron and proton masses. The columns $\Delta\delta_c$ show the difference between the results of PKO1† and PKO1, as well as DD-ME2† and DD-ME2. All values are expressed in %.

	PKO1†	$\Delta\delta_c$	DD-ME2†	$\Delta\delta_c$
^{10}C $\rightarrow$ ^{10}B	0.089	0.007	0.161	0.011
^{14}O $\rightarrow$ ^{14}N	0.127	0.013	0.214	0.017
^{18}Ne $\rightarrow$ ^{18}F	0.288	0.017	0.454	0.024
^{26}Si $\rightarrow$ ^{26}Al	0.188	0.012	0.268	0.016
^{30}S $\rightarrow$ ^{30}P	0.531	0.034	0.672	0.039
^{34}Ar $\rightarrow$ ^{34}Cl	0.287	0.019	0.400	0.024
^{38}Ca $\rightarrow$ ^{38}K	0.334	0.021	0.467	0.026
^{42}Ti $\rightarrow$ ^{42}Sc	0.405	0.020	0.549	0.026
^{26}Al $\rightarrow$ ^{26}Mg	0.150	0.011	0.212	0.014
^{34}Cl $\rightarrow$ ^{34}S	0.252	0.018	0.329	0.022
^{38}K $\rightarrow$ ^{38}Ar	0.299	0.020	0.395	0.024
^{42}Sc $\rightarrow$ ^{42}Ca	0.352	0.019	0.472	0.024
^{54}Co $\rightarrow$ ^{54}Fe	0.336	0.017	0.414	0.020
^{66}As $\rightarrow$ ^{66}Ge	0.500	0.026	0.601	0.028
^{70}Br $\rightarrow$ ^{70}Se	1.188	0.048	1.320	0.051
^{74}Rb $\rightarrow$ ^{74}Kr	1.132	0.044	1.308	0.050

difference are small compared to other kinds of uncertainties, and it is not the main reason why the present results of the sum of squared top row elements of the CKM matrix deviate from the unitarity condition.

In summary, in this chapter self-consistent relativistic RPA approaches are applied to calculate the isospin symmetry-breaking corrections δ_c for the superallowed β transitions. It is found that the proper treatment of the Coulomb field is very important to extract the isospin symmetry-breaking corrections δ_c. By switching off the exchange contributions of the Coulomb field, the corrections δ_c in RHF+RPA calculations recover the results in RH+RPA calculations. In other words, one cannot effectively take care of the Coulomb exchange term by adjusting the parameters in the direct terms of mesons as done in the usual RH approximation. With the isospin symmetry-breaking corrections δ_c calculated by relativistic RPA approaches, the values of $|V_{ud}|$ thus obtained agree well with those obtained in neutron decay, pion β decay and nuclear mirror transitions. However, the sum of squared top-row elements seems to deviate from the unitarity condition. The effects of the neutron-proton mass difference on the isospin symmetry-breaking corrections δ_c have been investigated. It is shown that these effects are small compared to other kinds of uncertainties. The neutron-proton mass difference is not the main reason why the present results of the sum of squared top row elements of the CKM matrix deviate from the unitarity condition. For further studies, more intensive investigations including the proper isoscalar and isovector pairing and deformation should be done.

Chapter 6

Inclusive Charged-Current Neutrino-Nucleus Reactions

6.1 Introduction

Neutrino-nucleus reactions at low energies, $E_\nu < 100$ MeV, are of particular importance for many phenomena in nuclear physics, particle physics, and astrophysics (Hayes, 1999; Vogel, 2006). One of the worldwide focus is the measurements of neutrino masses and their mixing angles, which open a door to explore the physics beyond the Standard Model. Furthermore, around the core-collapse supernova explosion, the neutrino flux is so large that significant neutral-current and charged-current neutrino-nucleus scattering occurs, even though the corresponding cross sections are rather small. The neutral-current excitations and the subsequent multi-particle breakup determine the ν-process nucleosynthesis (Woosley *et al.*, 1990), while the competition between neutron capture and charged-current neutrino scattering is one of the key ingredients for determining the r-process nucleosynthesis (Langanke and Martínez-Pinedo, 2003), which is responsible for the formation of half of the elements with $A > 70$. Concerning the nuclear physics aspect, the neutrino-nucleus cross sections are found to be very sensitive to the nuclear spin-isospin excitations in such low neutrino energy region (Kolbe *et al.*, 2003).

So far, inclusive and exclusive charged-current neutrino-nucleus cross sections data for the ^{12}C (Krakauer *et al.*, 1992; Bodmann *et al.*, 1994; Athanassopoulos *et al.*, 1998; Auerbach *et al.*, 2001, 2002) and ^{56}Fe (Maschuw, 1998) targets have been obtained by the Liquid Scintillator Neutrino Detector (LSND), and Karlsruhe Rutherford Medium Energy Neutrino (KARMEN) Collaborations. More ambitious experiments using the neutrinos generated at the spallation sources are under construction, planning, or study. These facilities include the Spallation Neutron Source (SNS) at Oak Ridge, the European Spallation Source (ESS) in Lund, the Japanese Spallation Neutron Source (JSNS) at JPARC, and the China Spallation Neutron Source (CSNS) in Guangdong. Another kind of promising neutrino experiments would be that using the neutrinos generated with low energy beta-beams (Zucchelli, 2002; Volpe, 2004, 2007). The beta decays of boosted radioactive ions can

produce pure and collimated beams of electron (anti-)neutrinos, and the average energy of the neutrino beams can be controlled. Therefore, it is expected that more accurate neutrino-nucleus scattering data on various targets will be available in the near future.

On the other hand, it has been shown that the theoretical predictions of the neutrino-nucleus cross sections with sufficiently high accuracy are crucial to calibrate the neutrino detectors and interpret the neutrino experiments. One example is the reanalysis of the LSND neutrino oscillation experiment (Samana *et al.*, 2006). Based on the lepton-hadron weak interaction in the standard current-current form, the pioneering investigations of low energy neutrino-nucleus reactions were done in the 1970s (O'Connell *et al.*, 1972; Walecka, 1975). At present, a variety of microscopic approaches for evaluating the charged-current neutrino-nucleus cross sections include the nuclear shell model (Haxton, 1987; Auerbach and Brown, 2002), the RPA and QRPA (Auerbach *et al.*, 1997; Volpe *et al.*, 2000, 2002; Sajjad Athar *et al.*, 2006; Lazauskas and Volpe, 2007), continuum RPA (CRPA) (Jachowicz *et al.*, 2002; Kolbe *et al.*, 2002), projected quasiparticle RPA (PQRPA) (Krmpotić *et al.*, 2005), and relativistic RPA (RRPA) (Paar *et al.*, 2008). Comparing the above investigations, apart from the difference in the nuclear models used to describe the transitions from the parent ground-state to the excited daughter states, there are also important differences in the choice of recipes for the axial vector coupling strength g_A and the theoretical low-lying excited states of the daughter nucleus. Thus, we find it useful to discuss in this chapter the consequences of the various choices.

Comparing with the shell model calculations, the RPA calculations based on the mean field can be, in principle, implemented for the whole nuclear chart, and the relatively large p-h configuration space allows for the description of the high-J excitations up to ~ 100 MeV. Furthermore, it has been shown that the self-consistency of the RPA approach is an important requirement for restoring the symmetries which are broken by the mean field approximation, and for separating the spurious states from the physical states, as well as for extrapolating the theoretical analysis towards the nucleon drip lines. Nevertheless, the present CRPA calculations (Jachowicz *et al.*, 2002; Kolbe *et al.*, 2002) are not self-consistent since they employ different interactions for the description of the ground-state and excited states, and the (Q)RPA calculations based on the SHF theory (Lazauskas and Volpe, 2007) still exclude some terms in the p-h residual interaction, e.g., the spin-orbit term. Only recently, a fully self-consistent SHF+RPA in the charge-exchange channels was developed (Fracasso and Colò, 2005; Fracasso and Colò, 2007), but not yet used in the analysis of neutrino-nucleus reactions. On the relativistic side, it has been shown in **Chapter 4** that the nuclear spin-flip responses, e.g., SDR, SQR, and so on, are sensitive to the additional g' parameter within the RH+RPA framework. Therefore, it is interesting to investigate the properties of low energy neutrino-nucleus reactions within the fully self-consistent RHF+RPA framework.

In this chapter, the RHF+RPA approach will be applied to calculate the inclusive charged-current neutrino-nucleus cross sections, by taking the $^{16}\mathrm{O}(\nu_e,e^-)^{16}\mathrm{F}$ reaction as an illustrative example. Following the prescription given by Walecka (Walecka, 1975), the key expressions for calculating the cross sections in the extreme relativistic limit will be summarized in the next

section, and the Coulomb corrections to the inclusive cross section given by the Fermi function correction and effective momentum approximation (EMA) will be explained in details as well. The main effort will be dedicated to discussing the substantial influence of different recipes for the axial vector coupling strength and the choice of theoretical low-lying excited states of the daughter nucleus. Then, the reason why we favor the value of $g_A = 1.262$ and the inclusion of all RPA excited states will be explained. Finally, the inclusive cross sections averaged over the Michel flux and the supernova neutrino flux will be shown, in comparison with the previous theoretical studies by other authors.

6.2 Inclusive neutrino-nucleus cross sections

In the present study, we consider the charged-current neutrino-nucleus reactions

$$\nu_l +_Z X_N \rightarrow_{Z+1} X^*_{N-1} + l^-, \tag{6.1}$$

where l denotes the charged lepton, e.g., electron or muon. The charged-current neutrino-nucleus cross section reads (Walecka, 1975; O'Connell *et al.*, 1972)

$$\frac{d\sigma_\nu}{d\Omega} = \frac{V^2}{(2\pi)^2} p_l E_l \sum_{\text{lepton spins}} \frac{1}{2J_i+1} \sum_{M_i M_f} \left| \langle f|\hat{H}_W|i\rangle \right|^2, \tag{6.2}$$

where p_l and E_l are the momentum and energy of the outgoing lepton, respectively. The Hamiltonian $\hat{H}_W$ of the weak interaction is expressed in the standard current-current form, i.e., in terms of the nucleon $\mathcal{J}_\lambda(\boldsymbol{x})$ and lepton $j_\lambda(\boldsymbol{x})$ currents (Walecka, 1975; O'Connell *et al.*, 1972)

$$\hat{H}_W = -\frac{G}{\sqrt{2}} \int d\boldsymbol{x} \mathcal{J}^\lambda(\boldsymbol{x}) j_\lambda(\boldsymbol{x}), \tag{6.3}$$

Denoting the leptonic matrix current as $l_\lambda e^{-i\boldsymbol{q}\cdot\boldsymbol{x}}$, the transition matrix elements read

$$\langle f|\hat{H}_W|i\rangle = -\frac{G}{\sqrt{2}} l_\lambda \int d\boldsymbol{x} e^{-i\boldsymbol{q}\cdot\boldsymbol{x}} \langle f|\mathcal{J}^\lambda(\boldsymbol{x})|i\rangle, \tag{6.4}$$

with the four-momentum transfer

$$(q_0, \boldsymbol{q}) = (E_l, \boldsymbol{p}_l) - (E_\nu, \boldsymbol{p}_\nu), \tag{6.5}$$

which must be space-like, i.e.,

$$q^2 = q_0^2 - \boldsymbol{q}^2 \leqslant 0. \tag{6.6}$$

In the extreme relativistic limit (ERL), in which the energy of the outgoing lepton is considered much larger than its rest mass, the differential neutrino-nucleus cross section takes the form

(Walecka, 1975; O'Connell *et al.*, 1972)

$$\begin{aligned}\left(\frac{d\sigma_\nu}{d\Omega}\right)_{\mathrm{ERL}} &= \frac{2G_F^2\cos^2\theta_c}{\pi}\frac{E_l^2}{2J_i+1}\left\{\cos^2\frac{\theta}{2}\sum_{J\geqslant 0}\left|\langle J_f||\hat{\mathcal{M}}_J-\frac{q_0}{|\boldsymbol{q}|}\hat{\mathcal{L}}_J||J_i\rangle\right|^2\right.\\ &+\left(\frac{-q^2}{2\boldsymbol{q}^2}\cos^2\frac{\theta}{2}+\sin^2\frac{\theta}{2}\right)\sum_{J\geqslant 1}\left[\left|\langle J_f||\hat{\mathcal{T}}_J^{\mathrm{MAG}}||J_i\rangle\right|^2+\left|\langle J_f||\hat{\mathcal{T}}_J^{\mathrm{EL}}||J_i\rangle\right|^2\right]\\ &\left.-\sin\frac{\theta}{2}\sqrt{\frac{-q^2}{\boldsymbol{q}^2}\cos^2\frac{\theta}{2}+\sin^2\frac{\theta}{2}}\sum_{J\geqslant 1}2\mathrm{Re}\langle J_f||\hat{\mathcal{T}}_J^{\mathrm{MAG}}||J_i\rangle\langle J_f||\hat{\mathcal{T}}_J^{\mathrm{EL}}||J_i\rangle^*\right\} \quad (6.7)\end{aligned}$$

with $\kappa=|\boldsymbol{q}|$, where G_F is the Fermi constant for the weak interaction, θ_c is the Cabbibo's angel (Amsler *et al.*, 2008), and θ denotes the angle between the incoming and outgoing leptons. The nuclear multipole operators are the Coulomb operator

$$\hat{\mathcal{M}}_{JM}(\boldsymbol{x})=F_1^V M_J^M(\boldsymbol{x})-\frac{i\kappa}{m_N}\left[F_A\Omega_J^M(\boldsymbol{x})+\frac{1}{2}(F_A+q_0F_P)\Sigma''^M_J(\boldsymbol{x})\right], \quad (6.8)$$

the longitudinal operator

$$\hat{\mathcal{L}}_{JM}(\boldsymbol{x})=\frac{q_0}{\kappa}F_1^V M_J^M(\boldsymbol{x})+i\left[F_A-\frac{1}{2}\frac{\kappa^2}{m_N}F_P\right]\Sigma''^M_J(\boldsymbol{x}), \quad (6.9)$$

the transverse electric operator

$$\hat{\mathcal{T}}^{\mathrm{EL}}_{JM}(\boldsymbol{x})=\frac{\kappa}{m_N}\left[F_1^V\Delta'^M_J(\boldsymbol{x})+\frac{1}{2}\mu^V\Sigma_J^M(\boldsymbol{x})\right]+iF_A\Sigma'^M_J(\boldsymbol{x}), \quad (6.10)$$

and the transverse magnetic operator

$$\hat{\mathcal{T}}^{\mathrm{MAG}}_{JM}(\boldsymbol{x})=-\frac{i\kappa}{m_N}\left[F_1^V\Delta_J^M(\boldsymbol{x})-\frac{1}{2}\mu^V\Sigma'^M_J(\boldsymbol{x})\right]+F_A\Sigma_J^M(\boldsymbol{x}), \quad (6.11)$$

where m_N is the mass of nucleon. The form factors are the functions of q^2 (Kuramoto *et al.*, 1990),

$$F_1^V(q^2) = \left(1-\frac{q^2}{(840\ \mathrm{MeV})^2}\right)^{-2}, \quad (6.12a)$$

$$\mu^V(q^2) = 4.706\left(1-\frac{q^2}{(840\ \mathrm{MeV})^2}\right)^{-2}, \quad (6.12b)$$

$$F_A(q^2) = -g_A\left(1-\frac{q^2}{(1032\ \mathrm{MeV})^2}\right)^{-2}, \quad (6.12c)$$

$$F_P(q^2) = \frac{2m_NF_A(q^2)}{-q^2+m_\pi^2}, \quad (6.12d)$$

where m_π is the mass of pion, and $g_A=1.262$ is the axial vector coupling strength. To account for the universal quenching of the Gamow-Teller strength function, the effective axial vector coupling $g_A^{\mathrm{eff}}=1$ is sometimes proposed (Bohr and Mottelson, 1969). We will come back to this point in

Section 6.3. The short-hand notations of the fundamental operators read

$$
\begin{aligned}
& M_J^M(\boldsymbol{x}), && (6.13a)\\
\Delta_J^M(\boldsymbol{x}) &\equiv \boldsymbol{M}_{JJ}^M(\boldsymbol{x})\cdot\frac{1}{\kappa}\boldsymbol{\nabla}, && (6.13b)\\
\Delta'^M_J(\boldsymbol{x}) &\equiv -i\left[\frac{1}{\kappa}\boldsymbol{\nabla}\times\boldsymbol{M}_{JJ}^M(\boldsymbol{x})\right]\cdot\frac{1}{\kappa}\boldsymbol{\nabla}\\
&= \left[-\sqrt{\frac{J}{2J+1}}\boldsymbol{M}_{JJ+1}^M(\boldsymbol{x})+\sqrt{\frac{J+1}{2J+1}}\boldsymbol{M}_{JJ-1}^M(\boldsymbol{x})\right]\cdot\frac{1}{\kappa}\boldsymbol{\nabla}, && (6.13c)\\
\Sigma_J^M(\boldsymbol{x}) &\equiv \boldsymbol{M}_{JJ}^M(\boldsymbol{x})\cdot\boldsymbol{\sigma}, && (6.13d)\\
\Sigma'^M_J(\boldsymbol{x}) &\equiv -i\left[\frac{1}{\kappa}\boldsymbol{\nabla}\times\boldsymbol{M}_{JJ}^M(\boldsymbol{x})\right]\cdot\boldsymbol{\sigma}\\
&= \left[-\sqrt{\frac{J}{2J+1}}\boldsymbol{M}_{JJ+1}^M(\boldsymbol{x})+\sqrt{\frac{J+1}{2J+1}}\boldsymbol{M}_{JJ-1}^M(\boldsymbol{x})\right]\cdot\boldsymbol{\sigma}, && (6.13e)\\
\Sigma''^M_J(\boldsymbol{x}) &\equiv \left[\frac{1}{\kappa}\boldsymbol{\nabla}M_J^M(\boldsymbol{x})\right]\cdot\boldsymbol{\sigma}\\
&= \left[\sqrt{\frac{J+1}{2J+1}}\boldsymbol{M}_{JJ+1}^M(\boldsymbol{x})+\sqrt{\frac{J}{2J+1}}\boldsymbol{M}_{JJ-1}^M(\boldsymbol{x})\right]\cdot\boldsymbol{\sigma}, && (6.13f)\\
\Omega_J^M(\boldsymbol{x}) &\equiv M_J^M(\boldsymbol{x})\boldsymbol{\sigma}\cdot\frac{1}{\kappa}\boldsymbol{\nabla}, && (6.13g)
\end{aligned}
$$

where

$$M_J^M(\boldsymbol{x})\equiv j_J(kx)Y_{JM}(\hat{x}),\qquad \boldsymbol{M}_{JL}^M(\boldsymbol{x})\equiv j_J(kx)\mathcal{Y}_{JL1}^M(\hat{x}) \tag{6.14}$$

with the spherical Bessel function $j_J(kx)$, the spherical harmonics $Y_{JM}(\hat{x})$, and the vector spherical harmonics $\mathcal{Y}_{JL1}^M(\hat{x})$ defined as

$$\mathcal{Y}_{JL1}^M=\sum_{\mu\nu}C_{L\mu1\nu}^{JM}Y_{1\mu}e_\nu. \tag{6.15}$$

The reduced matrix elements concerning the above operators read (see **Remark 14**),

$$\langle n'l'j'||M_J||nlj\rangle = (-)^{j-J-\frac{1}{2}}\frac{\hat{j}\hat{j}'\hat{J}}{\sqrt{4\pi}}\begin{pmatrix} j' & j & J\\ \frac{1}{2} & -\frac{1}{2} & 0\end{pmatrix}\langle n'l'|j_J(kr)|nl\rangle, \tag{6.16}$$

$$\langle n'l'j'||\boldsymbol{M}_{JL}\cdot\boldsymbol{\sigma}||nlj\rangle = (-)^{l'}\frac{\sqrt{6}}{\sqrt{4\pi}}\hat{j}\hat{j}'\hat{l}\hat{l}'\hat{L}\hat{J}\begin{pmatrix} l' & L & l\\ 0 & 0 & 0\end{pmatrix}\begin{Bmatrix} j' & j & J\\ l' & l & L\\ \frac{1}{2} & \frac{1}{2} & 1\end{Bmatrix}\langle n'l'|j_L(kr)|nl\rangle, \tag{6.17}$$

$$\langle n'l'j'||\boldsymbol{M}_{JL}\cdot\boldsymbol{\nabla}||nlj\rangle = (-)^{l'+\frac{1}{2}+j+J}\hat{j}\hat{j}'\begin{Bmatrix} l' & j' & \frac{1}{2}\\ j & l & J\end{Bmatrix}\langle n'l'||\boldsymbol{M}_{JL}\cdot\boldsymbol{\nabla}||nl\rangle, \tag{6.18}$$

with

$$\begin{aligned}\langle n'l'||\boldsymbol{M}_{JL}\cdot\boldsymbol{\nabla}||nl\rangle &= (-)^{J+l}\frac{\hat{l}'\hat{L}\hat{J}}{\sqrt{4\pi}}\times\left[\sqrt{(l+1)(2l+3)}\left\{\begin{array}{ccc} L & 1 & J \\ l & l' & l+1\end{array}\right\}\left(\begin{array}{ccc} l' & L & l+1 \\ 0 & 0 & 0\end{array}\right)\right.\\ &\times\langle n'l'|j_L(kr)\left(\frac{d}{dr}-\frac{l}{r}\right)|nl\rangle\\ &-\sqrt{l(2l-1)}\left\{\begin{array}{ccc} L & 1 & J \\ l & l' & l-1\end{array}\right\}\left(\begin{array}{ccc} l' & L & l-1 \\ 0 & 0 & 0\end{array}\right)\\ &\left.\times\langle n'l'|j_L(kr)\left(\frac{d}{dr}+\frac{l+1}{r}\right)|nl\rangle\right], \end{aligned} \tag{6.19}$$

and

$$\begin{aligned}\langle n'l'j'||M_J\boldsymbol{\nabla}\cdot\boldsymbol{\sigma}||nlj\rangle &= (-)^{l'}\frac{\hat{j}'\hat{j}\hat{l}'\hat{J}}{\sqrt{4\pi}}\times\left[-\delta_{j,l+1/2}\sqrt{2l+3}\left\{\begin{array}{ccc} J & l' & l+1 \\ \frac{1}{2} & j & j'\end{array}\right\}\left(\begin{array}{ccc} l' & J & l+1 \\ 0 & 0 & 0\end{array}\right)\right.\\ &\times\langle n'l'|j_J(kr)\left(\frac{d}{dr}-\frac{l}{r}\right)|nl\rangle\\ &+\delta_{j,l-1/2}\sqrt{2l-1}\left\{\begin{array}{ccc} J & l' & l-1 \\ \frac{1}{2} & j & j'\end{array}\right\}\left(\begin{array}{ccc} l' & J & l-1 \\ 0 & 0 & 0\end{array}\right)\\ &\left.\times\langle n'l'|j_J(kr)\left(\frac{d}{dr}+\frac{l+1}{r}\right)|nl\rangle\right]. \end{aligned} \tag{6.20}$$

In the above expressions, the Wigner-Eckart Theorem with composite tensors is used (see **Remark 13**).

With the definition of four-momentum transfer $q=(q_0,\boldsymbol{q})$ in Eq. (6.5), one has

$$q_0 = E_l - E_\nu = E_i - E_f, \tag{6.21}$$

where E_i and E_f are the energies of the parent and daughter nuclei, respectively. Assuming the parent nucleus is in the ground-state, and neglecting the kinetic energy of the nuclei,

$$E_i = m_i, \qquad \text{and} \qquad E_f = m_f + E^*, \tag{6.22}$$

where m_i and m_f are the masses of the parent and daughter nuclei, respectively, and E^* is the excitation energy with respect to the ground-state of the daughter nucleus. The excitation energy E^* can be obtained with the RPA calculations by

$$E^* = E_{\rm RPA} - \left[(m_f - m_i) + (m_n - m_p)\right], \tag{6.23}$$

where $E_{\rm RPA}$ is the excitation energy with respect to the ground-state of the parent nucleus, and $(m_n - m_p)$ is the neutron-proton mass difference which is missing when neutron hole and proton particle configurations are built. In principle, E^* should be $\geqslant 0$, which indicates the energetically possible final states in the daughter nucleus. In some literature, the experimental mass data

$$Q_{\rm th}^{\rm exp} = (m_f^{\rm exp} - m_i^{\rm exp}) + (m_n - m_p) \tag{6.24}$$

is taken as the threshold in the theoretical calculations. We will also come back to this point in **Section 6.3**. Combining Eqs. (6.21), (6.22), and (6.23), one has

$$q_0 = E_l - E_\nu = -E_{\rm RPA} + (m_n - m_p), \tag{6.25}$$

i.e., for a given energy of the neutrino, the energy of the outgoing lepton reads

$$E_l = E_\nu - E_{\rm RPA} + (m_n - m_p). \tag{6.26}$$

On the other hand, the momenta of the incoming neutrino and the outgoing lepton in Eq. (6.5) are

$$|\boldsymbol{p}_\nu| = E_\nu, \qquad \text{and} \qquad |\boldsymbol{p}_l| = \sqrt{E_l^2 - m_l^2}. \tag{6.27}$$

Since the angle between the incoming and outgoing leptons is θ, the momentum transfer is

$$\kappa = |\boldsymbol{q}| = \sqrt{\boldsymbol{p}_\nu^2 + \boldsymbol{p}_l^2 - 2|\boldsymbol{p}_\nu||\boldsymbol{p}_l|\cos\theta}. \tag{6.28}$$

Furthermore, the reduced matrix elements $\langle J_f||\hat{O}_J||J_i\rangle$ for a given operator can be written in terms of the (X, Y) solutions of the angular momentum coupled RPA equations (Eq. (2.49)) as

$$\langle J_f||\hat{O}_J||J_i\rangle = \sum_{ph} \left\{ X_{ph}^{J\nu} \langle p||\hat{O}_J||h\rangle + (-)^{j_p+j_h} Y_{ph}^{J\nu} \langle h||\hat{O}_J||p\rangle \right\}. \tag{6.29}$$

Therefore, corresponding to a specific excited state, the differential neutrino-nucleus cross section in Eq. (6.7) is just a function of the neutrino energy E_ν and the angle θ. The total cross section is the integral over the angle θ, which reads

$$\sigma_\nu = \int_0^\pi 2\pi \left(\frac{d\sigma_\nu}{d\Omega}\right) \sin\theta d\theta. \tag{6.30}$$

For charged-current reactions, the cross section in Eq. (6.2) must be corrected for the distortion of the outgoing lepton wave function by the Coulomb field of the daughter nucleus. In the low energy region, the cross section can be multiplied by a Fermi function, which reads (Engel, 1998; Kolbe *et al.*, 2003), (also see Eq. (7.15) in Ref. (Behrens and Bühring, 1982)),

$$F(Z, E_l) = 2(1+\gamma)(2p_l R_c)^{2(\gamma-1)} e^{\pi y} \left| \frac{\Gamma(\gamma + iy)}{\Gamma(2\gamma+1)} \right|^2. \tag{6.31}$$

Here, Z denotes the proton number of the daughter nucleus, $R_c = \sqrt{R_p^2 + 0.64\ \text{fm}^2}$ is the charge rms radius calculated with the ground-state density, α is the fine structure constant, and γ and y are given by

$$\gamma = \sqrt{1 - \alpha^2 Z^2}, \qquad \text{and} \qquad y = \alpha Z \frac{E_l}{p_l}. \tag{6.32}$$

In the high energy region, the effect of the Coulomb field can be described by the EMA (Engel, 1998), in which all the lepton momentum p_l and energy E_l in Eq. (6.2) are replaced by

$$p_l^{\rm eff} = \sqrt{E_l^{\rm eff\,2} - m_l^2}, \qquad \text{and} \qquad E_l^{\rm eff} = E_l - V_C^{\rm eff}, \tag{6.33}$$

where $V_C^{\rm eff} = 4V_C(0)/5$ with $V_C(0) = -3Z\alpha/(2R_c)$ being the effective Coulomb potential (Aste and Trautmann, 2007). As discussed in previous investigations (Volpe *et al.*, 2002; Paar *et al.*, 2008), the cross section calculated with the Fermi function is taken at low neutrino energies, and the one calculated with EMA is taken when the latter becomes smaller than the former for each J^π contribution.

6.3 Results and discussion

As the first application, we focus on the neutrino-nucleus reaction $^{16}\mathrm{O}(\nu_e,e^-)^{16}\mathrm{F}$ in the following discussion. The Dirac equations for ^{16}O are solved in coordinate space within a spherical box with a box radius $R = 15$ fm and a mesh size $dr = 0.1$ fm. The single-particle wave functions thus obtained are used to construct the RPA matrix elements $\mathcal{A}^J$ and $\mathcal{B}^J$ in Eq. (2.53) with the single-particle energy truncation $[-M, M + 150$ MeV$]$. For each given neutrino energy E_ν, the angular integral over $\cos\theta$ in Eq. (6.30) is performed with the 8-point Gauss-Legendre integration. We have checked that the final results of neutrino-nucleus cross sections are stable with respect to variations of the above numerical inputs.

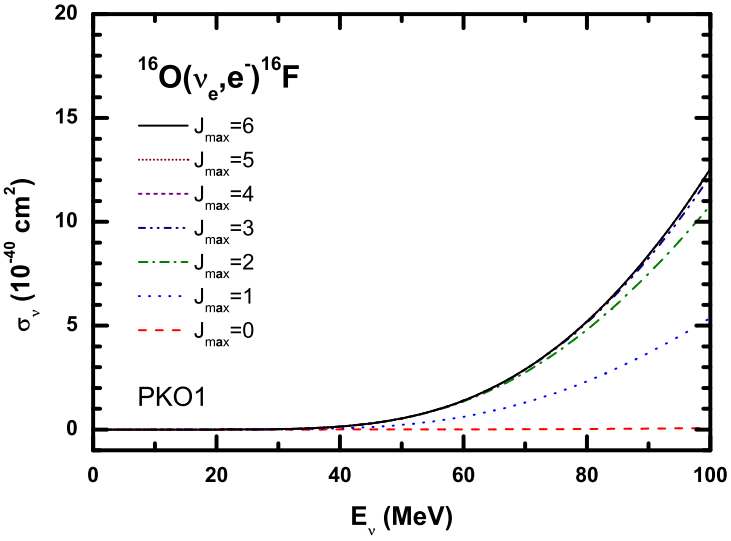

Figure 6.1: Uncorrected inclusive cross sections of the reactions $^{16}\mathrm{O}(\nu_e,e^-)^{16}\mathrm{F}$, where $g_A = 1.262$ and all the RPA excited states are taken into account. The different curves correspond to cross sections evaluated by successively increasing the maximal allowed angular momentum $J_{\max}$.

First of all, in order to illustrate the contributions of different multipole excitations and check the convergence with increasing $J_{\max}$, the uncorrected inclusive $^{16}\mathrm{O}(\nu_e,e^-)^{16}\mathrm{F}$ cross sections are shown as a function of the neutrino energy E_ν in Fig. 6.1. The different curves correspond to cross sections evaluated by successively increasing the maximal allowed angular momentum $J_{\max}$. It is found that the largest contributions come from the $J^\pi = 1^-$ and $J^\pi = 2^-$ excitations, because any other multipole excitation of ^{16}O requires the energies of at least $2\hbar\omega$. It is also found that the contributions of higher multipoles gradually decrease, and it is well converged when the contributions of up to $J = 6$ are taken into account.

Due to the distortion of the outgoing lepton wave function by the Coulomb field of the daughter nucleus, the Coulomb corrections to the inclusive cross sections must be carried out. In Fig. 6.2, we show the results with Fermi function correction and EMA, comparing with the uncorrected results. For the daughter nucleus ^{16}F, the value of the Fermi function $F(Z, E_l)$ is around 1.25 for the whole energy region considered in the present calculations, while the EMA correction is rather large for

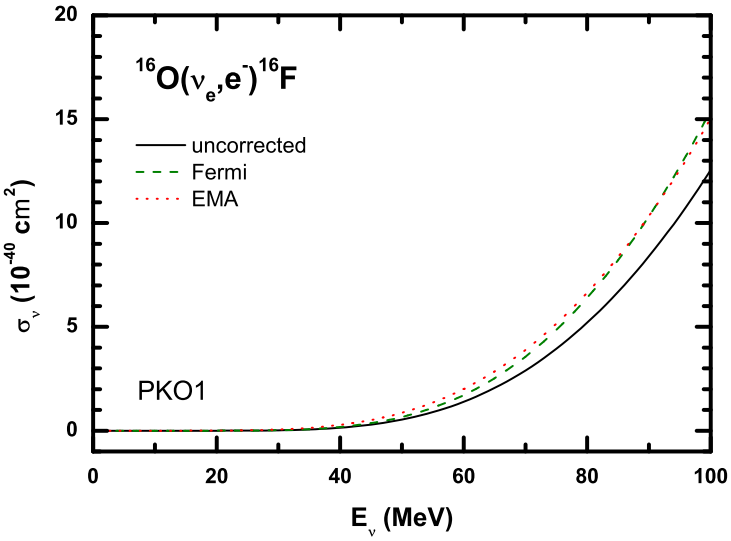

Figure 6.2: Coulomb corrections to the inclusive cross sections of the reactions ^{16}O(ν_e,e^-)^{16}F, where $g_A = 1.262$ and all the RPA excited states are taken into account. The uncorrected result as well as those with Fermi function correction and effective momentum approximation are shown with solid, dashed, and dotted lines, respectively.

the small neutrino energy and decreases gradually with increasing neutrino energy. It is shown that the EMA correction becomes smaller than the Fermi function correction when $E_\nu > 90$ MeV. As mentioned in the previous section, for each J^π contribution, one takes the smaller results given either by the Fermi function correction or EMA, then the final corrected inclusive cross sections can be obtained.

So far, it is still an open question that one should use the empirical value of the axial vector coupling strength, i.e., $g_A = 1.262$ (Amsler *et al.*, 2008), or its effective value $g_A^{\rm eff} = 1$ (Bohr and Mottelson, 1969), in the nuclear weak interaction calculations. Furthermore, as discussed in the previous section, the ground-state and all the excited states of daughter nucleus should be included for the inclusive neutrino-nucleus cross sections. In some investigations, e.g., in Ref. (Lazauskas and Volpe, 2007), each RPA eigenstate is regarded as a possible excitation, and all of them generate the complete spectrum of the daughter nuclei. On the other hand, in some other investigations, e.g., in Refs. (Kolbe *et al.*, 2002; Jachowicz *et al.*, 2002), the experimental mass difference is used to defined the ground-state of the daughter nucleus, and only the excited states that satisfy $E_{\rm RPA} \geqslant Q_{\rm th}^{\rm exp}$ are taken into account, while the others are regarded as the energetically impossible excitations. In the following, we denote the former case as *all* $E_{\rm RPA}$ and the later case as $E_{\rm RPA} \geqslant Q_{\rm th}^{\rm exp}$.

In order to investigate the effects of different recipes for g_A and $E_{\rm RPA}$, we perform the calculations for these four cases based on the RHF+RPA framework. In Fig. 6.3, the inclusive cross sections of the reactions ^{16}O(ν_e,e^-)^{16}F by RHF+RPA with PKO1 are shown in comparison the results with the SHF+RPA (Lazauskas and Volpe, 2007) and CRPA (Kolbe *et al.*, 2002) calculations. Different curves represent different recipes for g_A and $E_{\rm RPA}$.

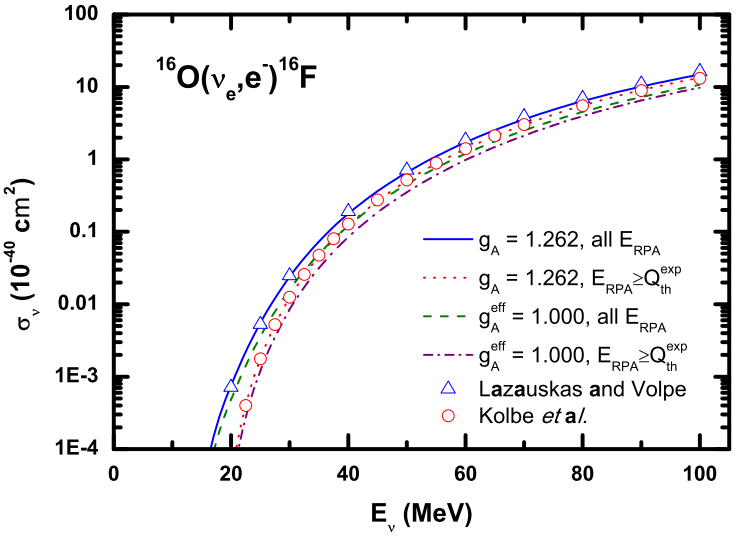

Figure 6.3: Inclusive cross sections of the reactions $^{16}\mathrm{O}(\nu_e,e^-)^{16}\mathrm{F}$ with different recipes for g_A and E_{RPA}. The RHF+RPA results are compared with those obtained by SHF+RPA (Lazauskas and Volpe, 2007) and CRPA (Kolbe *et al.*, 2002) calculations.

From the structure of the expression (6.7), it can be found that, when the quenching of g_A is considered, the unnatural parity terms of the operators $\hat{\mathcal{M}}$, $\hat{\mathcal{L}}$ and $\hat{\mathcal{T}}^{\mathrm{EL}}$ as well as the natural parity terms of the operator $\hat{\mathcal{T}}^{\mathrm{MAG}}$ are quenched with the factor $(g_A^{\mathrm{eff}}/g_A)^2 = 0.628$, and the mixing terms of the operators $\hat{\mathcal{T}}^{\mathrm{EL}}$ and $\hat{\mathcal{T}}^{\mathrm{MAG}}$ are quenched with the factor $g_A^{\mathrm{eff}}/g_A = 0.792$, while the rest terms are not affected. Therefore, the total quenching effect depends on the dominant contributions to the cross sections. Comparing the solid and dashed lines or the dotted and dash-dotted lines in Fig. 6.3, it is found that the quenching effect is slightly larger in the low neutrino energy region. For example, in the case of *all* E_{RPA} the ratio between the results with g_A^{eff} and g_A is 0.637 at $E_\nu = 20$ MeV and 0.721 at $E_\nu = 100$ MeV.

Since the difference between the cases of *all* E_{RPA} and $E_{\mathrm{RPA}} \geqslant Q_{\mathrm{th}}^{\mathrm{exp}}$ is whether the low-lying states are taken into account or not in the cross sections, it is not surprising that the effect of different recipes for E_{RPA} is much more visible in the low neutrino energy region than in the high neutrino energy region. For example, in the case of $g_A = 1.262$ the ratio between the $E_{\mathrm{RPA}} \geqslant Q_{\mathrm{th}}^{\mathrm{exp}}$ and *all* E_{RPA} results is 0.063 at $E_\nu = 20$ MeV and 0.908 at $E_\nu = 100$ MeV. Furthermore, it is shown that the present RHF+RPA results with $g_A = 1.262$ and *all* E_{RPA} are in a good agreement with those obtained with SHF+RPA calculations by Lazauskas and Volpe (Lazauskas and Volpe, 2007), while the present results with $g_A = 1.262$ and $E_{\mathrm{RPA}} \geqslant Q_{\mathrm{th}}^{\mathrm{exp}}$ are in a good agreement with those obtained with CRPA calculation by Kolbe *et al.* (Kolbe *et al.*, 2002). In other words, with the guidelines provided by the present calculations, it is clearly shown that the discrepancy between the results in Refs. (Lazauskas and Volpe, 2007) and (Kolbe *et al.*, 2002) is mainly due to the different recipes for E_{RPA}, rather than the difference of the RPA approaches.

In our opinion, we favor the case of $g_A = 1.262$ and *all* E_{RPA} due to the following reasons.

First of all, the effective axial vector coupling $g_A^{\rm eff} = 1$ was proposed to account for the universal quenching $Q \sim 60\%$ of the Gamow-Teller strength function (Bohr and Mottelson, 1969). However, recent experiments performed in both ^{90}Zr(p,n) and ^{90}Zr(n,p) channels and more reliably analyzed by multipole decomposition analysis detected $Q = 88\% \pm 6\%$ of the $3(N-Z)$ sum rule (Yako *et al.*, 2005). As another argument for using $g_A^{\rm eff}$, it was found that the $0\hbar\omega$ ground-state shell model calculations could reproduce the total μ^- capture rate in ^{16}O, the only weak interaction data in ^{16}O, with an overall reduction factor about 0.64, which corresponds to $g_A^{\rm eff}/g_A \sim 0.8$ (Auerbach and Brown, 2002). However, it was shown that the total μ^- capture rate in ^{16}O could be reproduced without quenching in g_A within the mean field plus RPA approaches (Van Giai *et al.*, 1981; Marketin *et al.*, 2009). Second, from the self-consistent point of view, it is more correct to include contributions of all the RPA excited states, since every RPA eigenstate stands for a theoretically energetically possible excitations to the daughter nucleus. If some of these excitations are eliminated, the non-energy weighted sum rule for each J^π component is no longer conserved. Furthermore, even though the spectrum of the daughter odd-odd nucleus might not be well reproduced by RPA calculations, it is inherent to the limitation of the p-h configurations or the disease of the effective interactions. Just eliminating the states under the threshold $Q_{\rm th}^{\rm exp}$ defined with the experimental mass difference cannot cure this problem. Last but not least, the present density functional theory should be extended to the exotic nuclei region where no experimental mass data is available. Therefore, we favor the empirical value of the axial vector coupling strength $g_A = 1.262$, and suggest to include all the RPA excitation states for the sake of the consistency of the model.

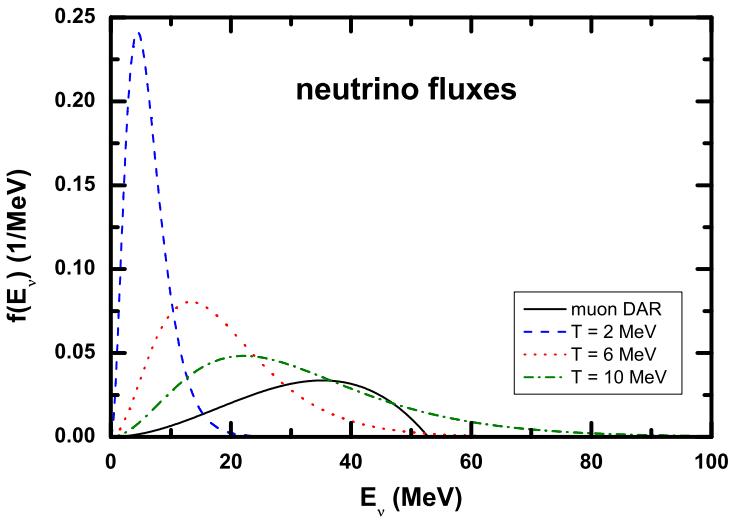

Figure 6.4: Michel flux from the decay at rest (DAR) of μ^+ (solid line) and supernova neutrino flux for $T = 2$ MeV (dashed line), $T = 6$ MeV (dotted line), and $T = 10$ MeV (dash-dotted line) with $\alpha = 0$.

The theoretical results could be compared with the future data by averaging the cross sections

over the neutrino flux $f(E_\nu)$ provided by specific neutrino source,

$$\langle\sigma_\nu\rangle = \frac{\int f(E_\nu)\sigma_\nu(E_\nu)dE_\nu}{\int f(E_\nu)dE_\nu}. \tag{6.34}$$

Two important neutrino sources are the Michel flux from the decay at rest (DAR) of μ^+ (Krakauer *et al.*, 1992) which reads

$$f(E_\nu) = \frac{96E_\nu^2}{m_\mu^4}(m_\mu - 2E_\nu), \tag{6.35}$$

and the supernova neutrino flux usually described by the Fermi-Dirac spectrum,

$$f(E_\nu) = \frac{1}{T^3}\frac{E_\nu^2}{\exp[(E_\nu/T) - \alpha] + 1}, \tag{6.36}$$

where T is the temperature and α is the chemical potential. In Fig. 6.4, the Michel flux and the supernova neutrino flux for $T = 2$ MeV, $T = 6$ MeV, and $T = 10$ MeV with $\alpha = 0$ are illustrated. It is shown that the Michel flux is dominant around $E_\nu = 35$ MeV and vanishes when $E_\nu > 53$ MeV, and increasing the temperature, the supernova neutrino flux is pushed into higher neutrino energy region and becomes more spread.

Table 6.1: Inclusive cross sections of the reactions ^{16}O(ν_e,e^-)^{16}F averaged over Michel flux from the DAR of μ^+ (Krakauer *et al.*, 1992). The RHF+RPA results are compared with those from Refs. (Paar *et al.*, 2008; Paar, 2010; Auerbach and Brown, 2002; Lazauskas and Volpe, 2007; Jachowicz *et al.*, 2002; Sajjad Athar *et al.*, 2006). All units are in 10^{-42} cm^2.

	$g_A = 1.262$		$g_A^{\rm eff} = 1.000$	
	all $E_{\rm RPA}$	$E_{\rm RPA} \geqslant Q_{\rm th}^{\rm exp}$	all $E_{\rm RPA}$	$E_{\rm RPA} \geqslant Q_{\rm th}^{\rm exp}$
PKO1	12.19	8.67	8.31	6.00
PKO2	12.12	8.77	8.24	6.05
DD-ME2 (Paar *et al.*, 2008; Paar, 2010)	12.49	8.76	8.44	6.00
shell model (Auerbach and Brown, 2002)	16.9		10.8	
SIII (Lazauskas and Volpe, 2007)	13.1			
HFSk (Jachowicz *et al.*, 2002)		9.43		
WSSk (Jachowicz *et al.*, 2002)		6.67		
RPA (Sajjad Athar *et al.*, 2006)		14.55		

In Table 6.1, the inclusive cross sections of the reactions ^{16}O(ν_e,e^-)^{16}F averaged over Michel flux by RHF+RPA with PKO1 and PKO2 are listed. First of all, comparing the results by PKO1 and PKO2, it can be found that these two parametrizations lead to almost the same results for all the cases. Recalling the discussion in **Section 4.2**, this indicates the isoscalar σ- and ω-mesons play an essential role, while the pion just stands on a marginal position in determining the neutrino-nucleus cross sections. It is also found that different recipes for g_A and $E_{\rm RPA}$ lead to quite different results. For example, the values in the last column are just 50% of those with $g_A = 1.262$ and

all $E_{\rm RPA}$. For this reason, one must be careful in comparing the results of different authors. The results from Refs. (Paar *et al.*, 2008; Paar, 2010; Auerbach and Brown, 2002; Auerbach *et al.*, 1997; Jachowicz *et al.*, 2002; Sajjad Athar *et al.*, 2006) are classified according to the recipes for g_A and $E_{\rm RPA}$. It is found that the present RHF+RPA results are similar to the RH+RPA results with DD-ME2 parametrization, and in a good agreement with the SHF+RPA (SIII) and CRPA (HFSk and WSSk) results, while somewhat smaller than those predicted by shell model and RPA approaches.

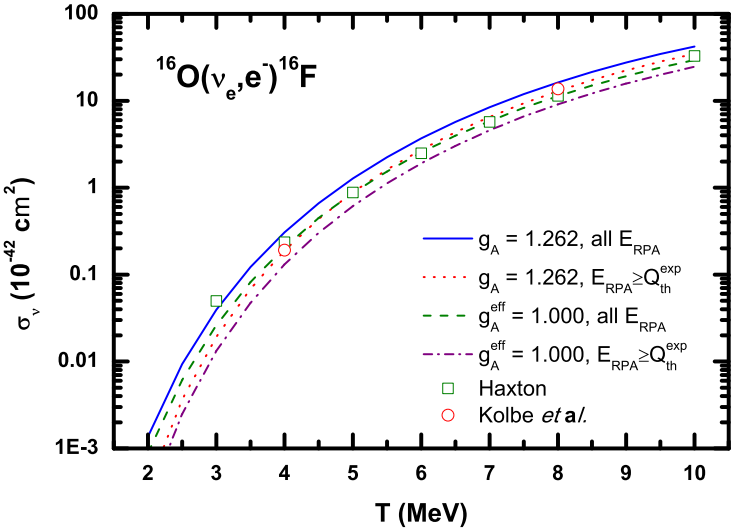

Figure 6.5: Inclusive cross sections of the reactions ^{16}O(ν_e,e^-)^{16}F averaged over supernova neutrino flux. The RHF+RPA results are compared with those obtained by shell model (Haxton, 1987) and CRPA (Kolbe *et al.*, 2002) calculations.

In Fig. 6.5, the inclusive cross sections of the reactions ^{16}O(ν_e,e^-)^{16}F averaged over supernova neutrino flux are shown as a function of the temperature T, where the chemical potential is $\alpha = 0$. The difference caused by different recipes can be seen. Since the peak of the supernova neutrino flux with lower temperature lies in the lower neutrino energy region, the effect of eliminating the states below $Q_{\rm th}^{\rm exp}$ is more pronounced with lower temperature. Comparing the present results with those from shell model by Haxton (Haxton, 1987) and CRPA by Kolbe *et al.* (Kolbe *et al.*, 2002), one must be careful about the adopted recipes for g_A and $E_{\rm RPA}$. It is found that the present results are in a very good agreement with the CRPA results, and consistent with the shell model results beyond $T = 4$ MeV, which indicates that the low-lying excitations are somewhat different between these two models. It should be emphasized again that the results by shell model and CRPA should not be compared directly to each other.

In summary, in this chapter the RHF+RPA approach is applied to calculate the inclusive charged-current neutrino-nucleus cross sections. Taking the reaction ^{16}O(ν_e,e^-)^{16}F as an example, first of all, the contributions of different multipole excitations are shown, and the total cross section is found to be well converged when the contributions of up to $J = 6$ are included for E_ν below 100 MeV. Furthermore, the Coulomb corrections to the inclusive cross section given by Fermi

function correction and EMA are explained in details and illustrated for the daughter nucleus ^{16}F. The main effort is dedicated to discussing the effects of different recipes for the axial vector coupling strength and the theoretical low-lying excited states of the daughter nucleus proposed in different literature. The calculations based on RHF+RPA for all four cases have been performed to examine their effects, and substantial difference is found in the resulting cross sections. This indicates one must be careful in comparing the results of different authors. Among these four cases, we favor the value of $g_A = 1.262$ and the inclusion of all RPA excited states for the sake of the model consistency and the present status of the GT quenching problem. Finally, the inclusive cross sections averaged over the Michel flux and the supernova neutrino flux are shown, a good agreement with the previous theoretical studies is obtained.

Chapter 7

Summary and Perspectives

In the last five years, the success of covariant effective Lagrangians in describing nuclear ground-states in the RHF theory have opened the way to the study of nuclear excitations within a relativistic RPA framework. In this work, we have established a fully self-consistent relativistic RPA scheme based on these effective Lagrangians. This scheme is then applied to charge-exchange excitations in various nuclei. The complete self-consistency has been demonstrated by the numerical checks for restoring the translational and isospin symmetries in non-charge-exchange and charge-exchange channels, respectively. We have focused our investigations on the problems of the nuclear spin-isospin resonances, isospin symmetry-breaking corrections for the superallowed β decays, and the charged-current neutrino-nucleus cross sections.

For the nuclear spin-isospin resonances, we have shown that the experimental data on the IAS and GTR in doubly magic nuclei ^{48}Ca, ^{90}Zr, ^{208}Pb can be well reproduced by the present RHF+RPA approach without any readjustment of the energy functional. Compared with the RH+RPA approach, the isoscalar σ- and ω-mesons are found to play an essential role in spin-isospin resonances via the exchange terms. This physical mechanism is clearly demonstrated in the properties of other charge-exchange spin-flip modes, e.g., the energy hierarchies of different components of SDR and SQR. Furthermore, the effects of the negative energy states on the non-energy weighted sum rules are discussed. It is explicitly shown that for the spin-flip modes the non-energy weighted sum rules can be 100% exhausted, only when the strengths of the transition from the occupied positive energy states to the empty negative energy states are included.

In the investigation of the isospin symmetry-breaking corrections for the superallowed β decays, it is found that the corrections δ_c are sensitive to the proper treatment of the Coulomb interaction, especially the Coulomb exchange contributions to the mean field, but not so much to specific effective nuclear interactions. With these corrections δ_c, the nucleus-independent $\mathcal{F}t$ values are obtained in combination with the experimental ft values from the most recent survey and the improved radiative corrections. The values of the CKM matrix element $|V_{ud}|$ thus obtained agree well with those obtained in neutron decay, pion β decay, and nuclear mirror transitions, while the sum of squared top-row elements somehow deviates from the unitarity condition.

Expressing the weak lepton-hadron interaction in the standard current-current form, the rele-

vant transitions from the nuclear ground state to the excited states are calculated with RHF+RPA approach. Illustrative calculations of the inclusive neutrino-nucleus cross section are performed for the ^{16}O(ν_e,e^-)^{16}F reaction, and a good agreement with the previous theoretical studies is obtained. The main effort is dedicated to discussing the substantial influence of different recipes for the axial vector coupling strength and the theoretical low-lying excited states of the daughter nucleus. The reason why we favor the value of $g_A = 1.262$ and the inclusion of all RPA excited states is explained. Meanwhile, we emphasize that one must be careful in comparing the results of different authors.

In this work, the applications of the present RHF+RPA approach are mainly focused on the charge-exchange channels. As a perspective for the future studies, a systematic research in the non-charge-exchange channel should be performed. Especially, the description of the magnetic transitions, which contain the spin operators, may be one of the most interesting points.

For the extensions of the present work, the following points could be considered:

- The ρ-N tensor interaction is not present in all DDRHF parametrizations used in the present work. However, it has been demonstrated that this interaction plays an important role in the shell structures and their evolution (Long *et al.*, 2007). On the other hand, a satisfactory description of GTR has not been achieved when the ρ-N tensor interaction is taken into account in the RH+RPA approach (De Conti *et al.*, 2000). Therefore, it is worthwhile to investigate its effects on the spin-isospin resonances when the exchange terms are included, i.e., in the RHF+RPA framework.

- For the open shell nuclei, it is a natural extension to establish the self-consistent QRPA based on the newly developed relativistic Hartree-Fock-Bogoliubov (RHFB) theory (Long *et al.*, 2010). The main challenge to fulfill the model self-consistency lies in determining the $T = 0$ component of the proton-neutron pairing. Since the information on that is quite limited, so far, the pairing strengths have to be treated as additional parameters in both non-relativistic and relativistic charge-exchange QRPA approaches (Fracasso and Colò, 2007; Paar *et al.*, 2004).

- In order to access most nuclei in the nuclear chart, deformation effects should be included. The main challenge will be the time consuming numerical calculations for constructing the RPA matrix elements and diagonalizing the relatively large RPA matrix when one deals with deformed nuclei.

Carrying out such investigations, one could really have microscopic and precise nuclear inputs for the most interesting issues of nuclear astrophysics: the information on nucleon separation energies, β decay rates, lepton capture rates, and neutrino-nucleus scattering for the r-process of stellar nucleosynthesis.

Finally, an alternative route to that adopted here would be to determine new effective Lagrangians where the meson-nucleon couplings would contain form factors (Hu *et al.*, 2010a,b) such that contact terms would be avoided. These new Lagrangians need to be adjusted to reproduce

nuclear ground-state properties at the same quantitative level as obtained with the Lagrangians used here. Then, alternative RHF+RPA studies could be envisaged.

Appendix A

Detailed Derivations of RHF+RPA expressions

A.1 RHF energy contributions in spherical nuclei

In this section, the energy contributions in Eq. (2.20) for the case of spherical nuclei are listed. The detailed derivations are given in W. H. Long's Ph.D. thesis (Long, 2005).

First, the kinetic energy E_k reads

$$E_k = \int dr \sum_a \hat{j}_a^2 \left\{ G_a \left[-\frac{d}{dr} F_a + \frac{\kappa_a}{r} F_a + M G_a \right] - F_a \left[-\frac{d}{dr} G_a - \frac{\kappa_a}{r} G_a + M F_a \right] \right\}. \tag{A.1}$$

Second, the energy contributions from the Hartree terms read

$$E_\sigma^D = \frac{1}{2} 4\pi \int r^2 g_\sigma \sigma(r) \rho_s(r) dr, \qquad \sigma(r) = -\int r'^2 g_\sigma \rho_s(r') R_{00}(m_\sigma; r, r') dr', \tag{A.2a}$$

$$E_\omega^D = \frac{1}{2} 4\pi \int r^2 g_\omega \omega(r) \rho_b(r) dr, \qquad \omega(r) = +\int r'^2 g_\omega \rho_b(r') R_{00}(m_\omega; r, r') dr', \tag{A.2b}$$

$$E_\rho^D = \frac{1}{2} 4\pi \int r^2 g_\rho \rho(r) \rho_b^{(3)}(r) dr, \qquad \rho(r) = +\int r'^2 g_\rho \rho_b^{(3)}(r') R_{00}(m_\rho; r, r') dr', \tag{A.2c}$$

$$E_A^D = \frac{1}{2} 4\pi \int r^2 e A(r) \rho_c(r) dr, \qquad A(r) = +\int r'^2 e \rho_c(r') \frac{1}{r_>} dr', \tag{A.2d}$$

where the densities appearing in the source terms are given by Eqs. (2.18).

The Fock contributions are more complicated. For the isoscalar σ- and ω-mesons, the exchange

contributions are

$$
\begin{aligned}
E^E_\sigma &= +\frac{1}{2}\sum_{ab}\delta_{q_aq_b}\frac{\hat{j}_a^2\hat{j}_b^2}{4\pi}\sum_L{}' C^{L0}_{j_a\frac{1}{2}j_b-\frac{1}{2}}C^{L0}_{j_a\frac{1}{2}j_b-\frac{1}{2}} \\
&\quad\times\int dr_1dr_2[g_\sigma(G_aG_b-F_aF_b)]_{r_1}R_{LL}(m_\sigma;r_1,r_2)[g_\sigma(G_aG_b-F_aF_b)]_{r_2}, \qquad \text{(A.3a)}\\
\bar{E}^E_\omega &= -\frac{1}{2}\sum_{ab}\delta_{q_aq_b}\frac{\hat{j}_a^2\hat{j}_b^2}{4\pi}\sum_L{}' C^{L0}_{j_a\frac{1}{2}j_b-\frac{1}{2}}C^{L0}_{j_a\frac{1}{2}j_b-\frac{1}{2}} \\
&\quad\times\int dr_1dr_2[g_\omega(G_aG_b+F_aF_b)]_{r_1}R_{LL}(m_\omega;r_1,r_2)[g_\omega(G_aG_b+F_aF_b)]_{r_2}, \qquad \text{(A.3b)}\\
\bar{\bar{E}}^E_\omega &= +\sum_{ab}\delta_{q_aq_b}\frac{\hat{j}_a^2\hat{j}_b^2}{4\pi}\sum_L{}'' \int dr_1dr_2[g_\omega F_aG_b]_{r_1}R_{LL}(m_\omega;r_1,r_2) \\
&\quad\times\left\{g_\omega\left[(C^{L0}_{j_a\frac{1}{2}j_b-\frac{1}{2}})^2(F_bG_a-G_bF_a)+2(C^{L0}_{l'_a0l_b0})^2G_bF_a\right]\right\}_{r_2}, \qquad \text{(A.3c)}
\end{aligned}
$$

where $\bar{E}^E_\omega$ represents the contribution from the time component and $\bar{\bar{E}}^E_\omega$ that from the space components. The notation $\sum_L{}'(\sum_L{}'')$ means that $L+l_a+l_b$ must be even (odd). For the ρ-meson, the potential energy of the exchange part can be obtained by making the following replacements:

$$
g_\omega, m_\omega \to g_\rho, m_\rho, \qquad \text{and} \qquad \sum_{ab}\delta_{q_aq_b} \to \sum_{ab}(2-\delta_{q_aq_b}). \qquad \text{(A.4)}
$$

The exchange contribution from the photon field can be obtained in a similar way,

$$
\begin{aligned}
\bar{E}^E_A &= -\frac{1}{2}e^2\sum_{ab}^{Z}\frac{\hat{j}_a^2\hat{j}_b^2}{4\pi}\sum_L{}'\hat{L}^{-2}(C^{L0}_{j_a\frac{1}{2}j_b-\frac{1}{2}})^2 \\
&\quad\times\int dr_1dr_2[(G_aG_b+F_aF_b)]_{r_1}\frac{r_<^L}{r_>^{L+1}}[(G_aG_b+F_aF_b)]_{r_2}, \qquad \text{(A.5a)}\\
\bar{\bar{E}}^E_A &= +e^2\sum_{ab}^{Z}\frac{\hat{j}_a^2\hat{j}_b^2}{4\pi}\sum_L{}''\hat{L}^{-2}\int dr_1dr_2[F_aG_b]_{r_1}\frac{r_<^L}{r_>^{L+1}} \\
&\quad\times\left[(C^{L0}_{j_a\frac{1}{2}j_b-\frac{1}{2}})^2(F_bG_a-F_aG_b)+2(C^{L0}_{l'_a0l_b0})^2G_bF_a\right]_{r_2}. \qquad \text{(A.5b)}
\end{aligned}
$$

For the π-meson contributions with pseudo-vector coupling, the gradients of the Yukawa propagator with respect to $\boldsymbol{r}_1$ and $\boldsymbol{r}_2$ are needed (see **Remark 10**), then

$$
\begin{aligned}
E^E_\pi &= \frac{1}{2}\sum_{ab}(2-\delta_{q_aq_b})\frac{\hat{j}_a^2\hat{j}_b^2}{4\pi}\left\{\int dr\frac{f_\pi^2(G_aG_b+F_aF_b)^2}{2m_\pi^2r^2}-\sum_L{}''\hat{L}^{-4}(C^{L0}_{j_a\frac{1}{2}j_b-\frac{1}{2}})^2\right. \\
&\quad\left.\times\sum_{L_1L_2}^{L\pm1}i^{L_2-L_1}\int dr_1dr_2\left[f_\pi\mathscr{Y}^{LL_1}_{ab}\right]_{r_1}R_{L_1L_2}(m_\pi;r_1,r_2)\left[f_\pi\mathscr{Y}^{LL_2}_{ab}\right]_{r_2}, \qquad \text{(A.6)}\right.
\end{aligned}
$$

where

$$
\mathscr{Y}^{LL_1}_{ab}(r) \equiv (\kappa_{ab}+\beta_{LL_1})G_aG_b-(\kappa_{ab}-\beta_{LL_1})F_aF_b, \qquad \text{(A.7)}
$$

with κ_{ab} and β_{LL_1} defined in **Remark 16**. The $\delta(\boldsymbol{r}_1-\boldsymbol{r}_2)$ term which arises in pseudo-vector coupling can be removed by adding,

$$E^E_{\pi\delta}=-\frac{1}{2}\sum_{ab}(2-\delta_{q_aq_b})\frac{\hat{j}_a^2\hat{j}_b^2}{4\pi}\int dr\frac{f_\pi^2}{2m_\pi^2r^2}\left\{G_a^2G_b^2-\frac{2}{3}G_aG_bF_aF_b+F_a^2F_b^2\right\}. \tag{A.8}$$

Finally, the total energy for spherical nuclei is

$$E=E_k+E^D_\sigma+E^E_\sigma+E^D_\omega+E^E_\omega+E^D_\rho+E^E_\rho+E^E_\pi+E^D_A+E^E_A. \tag{A.9}$$

A.2 $\sigma-$meson contribution to the p-h matrix elements

In this section, the derivations for the quantities $H^J(1234)$ in Eq. (2.85) induced by the σ-meson will be given in details.

For the σ-meson, the two-body interaction reads

$$\begin{aligned}V^\sigma(1,2) &= -g_\sigma(1)\gamma_0(1)g_\sigma(2)\gamma_0(2)D_\sigma(1,2)\\ &= -\sum_{L\nu}g_\sigma(1)\gamma_0(1)g_\sigma(2)\gamma_0(2)R_{LL}(m_\sigma;1,2)(-)^\nu Y_L^\nu(\hat{r}_1)Y_L^{-\nu}(\hat{r}_2).\end{aligned} \tag{A.10}$$

In the following, the short-hand notation for the σ-field

$$\sigma(1)=\int dr_2r_2^2R_{00}(m_\sigma;1,2)\rho_s(2)g_\sigma(2) \tag{A.11}$$

is employed, where the scalar density is

$$\rho_s(r)=\sum_d\frac{1}{4\pi r^2}[G_d^2(r)-F_d^2(r)]. \tag{A.12}$$

For the Term1 in Eq. (2.78),

$$\begin{aligned}\text{Term1} &= \int d\boldsymbol{r}_1d\boldsymbol{r}_2f_A^\dagger(1)f_b^\dagger(2)g_\sigma(1)g_\sigma(2)I(1,2)f_B(2)f_a(1)\\ &= -\int d\boldsymbol{r}_1d\boldsymbol{r}_2g_\sigma(1)g_\sigma(2)\sum_{L\nu}(-)^\nu R_{LL}(m_\sigma;1,2)\langle f_A|\gamma_0Y_{L\nu}|f_a\rangle_{r_1}\langle f_b|\gamma_0Y_{L-\nu}|f_B\rangle_{r_2}.\end{aligned} \tag{A.13}$$

Using the Wigner-Eckart Theorem (see **Remark 13**) and the symmetry and orthogonality relations of 3-j Symbols (see **Remarks 2 and 3**), the summation over m_A, m_a gives

$$\begin{aligned}&\sum_{m_Am_a}(-)^{j_A-m_A}\begin{pmatrix}j_A & j_a & J\\ m_A & -m_a & -M\end{pmatrix}\langle f_A|\gamma_0Y_{L\nu}|f_a\rangle\\ =\;&\frac{1}{r_1^2}\sum_{m_Am_a}\begin{pmatrix}j_A & j_a & J\\ m_A & -m_a & -M\end{pmatrix}\begin{pmatrix}j_A & L & j_a\\ -m_A & \nu & m_a\end{pmatrix}[G_AG_a-F_AF_a]\langle A||Y_L||a\rangle\delta_{q_Aq_a}\\ =\;&\delta_{q_Aq_a}\delta_{JL}\delta_{M\nu}\hat{J}^{-2}\langle A||Y_L||a\rangle\frac{(G_AG_a-F_AF_a)_{r_1}}{r_1^2}.\end{aligned} \tag{A.14}$$

The summation over m_B, m_b gives

$$\begin{aligned}
&\sum_{m_B m_b}(-)^{j_B-m_B}\begin{pmatrix} j_B & j_b & J \\ m_B & -m_b & -M \end{pmatrix}\langle f_b|\gamma_0 Y_{L-\nu}|f_B\rangle \\
&= \delta_{q_B q_b}\sum_{m_B m_b}(-)^{j_B-m_B}\begin{pmatrix} j_B & j_b & J \\ m_B & -m_b & -M \end{pmatrix} \\
&\times(-)^{j_b-m_b}\begin{pmatrix} j_b & L & j_B \\ -m_b & -\nu & m_B \end{pmatrix}\langle b||Y_L||B\rangle\frac{(G_BG_b-F_BF_b)_{r_2}}{r_2^2} \\
&= \delta_{q_B q_b}\delta_{JL}\delta_{M\nu}\hat{J}^{-2}(-)^M\langle B||Y_L||b\rangle\frac{(G_BG_b-F_BF_b)_{r_2}}{r_2^2},
\end{aligned} \tag{A.15}$$

where $\langle a||Y_L||b\rangle = (-)^{j_a-j_b}\langle b||Y_L||a\rangle$ in **Remark 14** is used. Finally, $H_1^{J\sigma}(AaBb)$ can be expressed as,

$$\begin{aligned}
H_1^{J\sigma}(AaBb) &= -\delta_{q_A q_a}\delta_{q_B q_b}\hat{J}^{-2}\langle A||Y_J||a\rangle\langle B||Y_J||b\rangle \\
&\times\int dr_1 dr_2 R_{JJ}(m_\sigma;r_1,r_2)[g_\sigma(G_AG_a-F_AF_a)]_{r_1}[g_\sigma(G_bG_B-F_bF_B)]_{r_2}.
\end{aligned} \tag{A.16}$$

where $\sum_M$ brings in a factor $\hat{J}^2$.

For the Term2 in Eq. (2.78),

$$\begin{aligned}
\text{Term2} &= \sum_d\int d\boldsymbol{r}_1 d\boldsymbol{r}_2 f_A^\dagger(1)f_d^\dagger(2)g'_\sigma(1)f_b^\dagger(1)f_B(1)g_\sigma(2)I(1,2)f_d(2)f_a(1) \\
&= -\sum_d\int d\boldsymbol{r}_1 d\boldsymbol{r}_2 d\boldsymbol{r}'_1 g'_\sigma(1)g_\sigma(2)\frac{\delta(r_1-r'_1)}{r'^2_1}\sum_{L\nu}\sum_{L'\nu'}(-)^{\nu+\nu'}R_{LL}(m_\sigma;1,2) \\
&\times\langle f_b|Y_{L'-\nu'}|f_B\rangle_{r'_1}\langle f_A|\gamma_0 Y_{L\nu}Y_{L'\nu'}|f_a\rangle_{r_1}\langle f_d|\gamma_0 Y_{L-\nu}|f_d\rangle_{r_2},
\end{aligned} \tag{A.17}$$

where the expansion of the Delta function is used (see **Remark 11**). For the expectation $\langle f_d|\gamma_0 Y_{L-\nu}|f_d\rangle_{r_2}$, all terms will vanish with the summation over m_d, except the term with $L=0$. So the above quantity can be expressed as,

$$\text{Term2} = -\sum_{L'\nu'}\int d\boldsymbol{r}_1 d\boldsymbol{r}'_1(-)^{\nu'}g'_\sigma(1)\frac{\delta(r_1-r'_1)}{r'^2_1}\times\langle f_b|Y_{L'-\nu'}|f_B\rangle_{r'_1}\langle f_A|\gamma_0 Y_{L'\nu'}|f_a\rangle_{r_1}\sigma(1). \tag{A.18}$$

In analogy with $H_1^{J\sigma}(AaBb)$,

$$\begin{aligned}
H_2^{J\sigma}(AaBb) &= -\delta_{q_A q_a}\delta_{q_B q_b}\hat{J}^{-2}\langle A||Y_J||a\rangle\langle B||Y_J||b\rangle \\
&\times\int dr\frac{1}{r^2}g'_\sigma(r)\sigma(r)(G_AG_a-F_AF_a)(G_BG_b+F_BF_b).
\end{aligned} \tag{A.19}$$

For the Term3 in Eq. (2.78),

$$\begin{aligned}
\text{Term3} &= \sum_d\int d\boldsymbol{r}_1 d\boldsymbol{r}_2 f_A^\dagger(1)f_d^\dagger(2)g_\sigma(1)g'_\sigma(2)f_b^\dagger(2)f_B(2)I(1,2)f_d(2)f_a(1) \\
&= -\sum_d\int d\boldsymbol{r}_1 d\boldsymbol{r}_2 d\boldsymbol{r}'_2 g_\sigma(1)g'_\sigma(2)\frac{\delta(r_2-r'_2)}{r'^2_2}\sum_{L\nu}\sum_{L'\nu'}(-)^{\nu+\nu'}R_{LL}(m_\sigma;1,2) \\
&\times\langle f_A|\gamma_0 Y_{L\nu}|f_a\rangle_{r_1}\langle f_d|\gamma_0 Y_{L-\nu}Y_{L'\nu'}|f_d\rangle_{r_2}\langle f_b|Y_{L'-\nu'}|f_B\rangle_{r'_2}.
\end{aligned} \tag{A.20}$$

For the expectation $\langle f_d|\gamma_0 Y_{L-\nu}Y_{L'\nu'}|f_d\rangle_{r_2}$, the spherical harmonics $Y_{L-\nu}Y_{L'\nu'}$ should couple to Y_{00}, i.e.,

$$Y_{L-\nu}Y_{L'\nu'} = \delta_{LL'}\delta_{\nu\nu'}(-)^{\nu}\frac{1}{\sqrt{4\pi}}Y_{00}, \tag{A.21}$$

where the relation of the direct product of two spherical harmonics in **Remark 12** and the 3-j symbol value in **Remark 4** are used. Hence,

$$\begin{aligned}\text{Term3} &= -\int d\boldsymbol{r}_1 d\boldsymbol{r}_2 g_\sigma(1)g'_\sigma(2)\rho_s(2)\sum_{L\nu}(-)^{\nu}R_{LL}(m_\sigma;1,2)\\ &\quad\times\langle f_A|\gamma_0 Y_{L\nu}|f_a\rangle_{r_1}\langle f_b|Y_{L-\nu}|f_B\rangle_{r_2}.\end{aligned} \tag{A.22}$$

Therefore,

$$\begin{aligned}H_3^{J^\sigma}(AaBb) &= -\delta_{q_Aq_a}\delta_{q_Bq_b}\hat{J}^{-2}\langle A||Y_J||a\rangle\langle B||Y_J||b\rangle\\ &\quad\times\int dr_1 dr_2 R_{JJ}(m_\sigma;r_1,r_2)[g_\sigma(G_AG_a-F_AF_a)]_{r_1}[g'_\sigma\rho_s(G_BG_b+F_BF_b)]_{r_2}.\end{aligned} \tag{A.23}$$

For the Term6 in Eq. (2.78),

$$\begin{aligned}\text{Term6} &= \sum_{cd}\int d\boldsymbol{r}_1 d\boldsymbol{r}_2 f_A^\dagger(1)f_c^\dagger(1)f_d^\dagger(2)g''_\sigma(1)f_b^\dagger(1)f_B(1)g_\sigma(2)I(1,2)f_d(2)f_c(1)f_a(1)\\ &= -\sum_{cd}\int d\boldsymbol{r}_1 d\boldsymbol{r}'_1 d\boldsymbol{r}''_1 d\boldsymbol{r}_2 g''_\sigma(1)g_\sigma(2)\frac{\delta(r_1-r'_1)}{r'^2_1}\frac{\delta(r_1-r''_1)}{r''^2_1}\sum_{LL'L''\nu\nu'\nu''}(-)^{\nu+\nu'+\nu''}R_{LL}(m_\sigma;1,2)\\ &\quad\times\langle f_A|Y_{L'\nu'}|f_a\rangle_{r'_1}\langle f_b|Y_{L'-\nu'}Y_{L''\nu''}|f_B\rangle_{r''_1}\langle f_c|\gamma_0 Y_{L''-\nu''}Y_{L\nu}|f_c\rangle_{r_1}\langle f_d|\gamma_0 Y_{L-\nu}|f_d\rangle_{r_2}.\end{aligned} \tag{A.24}$$

For the same reason as in the Term2, the spherical harmonics $Y_{L\nu}$ should be Y_{00}, then the spherical harmonics $Y_{L''\nu''}$ should be Y_{00} as well. The Term6 can be rewritten as

$$\begin{aligned}\text{Term6} &= -\int r_1^2 dr_1 d\boldsymbol{r}'_1 d\boldsymbol{r}''_1 r_2^2 dr_2 g''_\sigma(1)g_\sigma(2)\frac{\delta(r_1-r'_1)}{r'^2_1}\frac{\delta(r_1-r''_1)}{r''^2_1}\sum_{L'\nu'}(-)^{\nu'}R_{00}(m_\sigma;1,2)\\ &\quad\times\langle f_A|Y_{L'\nu'}|f_a\rangle_{r'_1}\langle f_b|Y_{L'-\nu'}|f_B\rangle_{r''_1}\rho_s(1)\rho_s(2).\end{aligned} \tag{A.25}$$

Finally,

$$\begin{aligned}H_6^{J^\sigma}(AaBb) &= -\delta_{q_Aq_a}\delta_{q_Bq_b}\hat{J}^{-2}\langle A||Y_J||a\rangle\langle B||Y_J||b\rangle\\ &\quad\times\int dr\frac{1}{r^2}g''_\sigma(r)\rho_s(r)\sigma(r)(G_AG_a+F_AF_a)(G_BG_b+F_BF_b).\end{aligned} \tag{A.26}$$

For the Term7 in Eq. (2.78),

$$\begin{aligned}\text{Term7} &= \sum_{cd}\int d\boldsymbol{r}_1 d\boldsymbol{r}_2 f_A^\dagger(1)f_c^\dagger(1)f_d^\dagger(2)g'_\sigma(1)g'_\sigma(2)f_b^\dagger(2)f_B(2)I(1,2)f_d(2)f_c(1)f_a(1)\\ &= -\sum_{cd}\int d\boldsymbol{r}_1 d\boldsymbol{r}'_1 d\boldsymbol{r}_2 d\boldsymbol{r}'_2 g'_\sigma(1)g'_\sigma(2)\frac{\delta(r_1-r'_1)}{r'^2_1}\frac{\delta(r_2-r'_2)}{r_2^2}\sum_{LL'L''\nu\nu'\nu''}(-)^{\nu+\nu'+\nu''}R_{LL}(m_\sigma;1,2)\\ &\quad\times\langle f_A|Y_{L'\nu'}|f_a\rangle_{r'_1}\langle f_c|\gamma_0 Y_{L'-\nu'}Y_{L\nu}|f_c\rangle_{r_1}\langle f_d|\gamma_0 Y_{L-\nu}Y_{L''\nu''}|f_d\rangle_{r_2}\langle f_b|Y_{L''-\nu''}|f_B\rangle_{r'_2}.\end{aligned} \tag{A.27}$$

Using the same trick in calculating $H_3^{J\sigma}(AaBb)$, we can obtain

$$\begin{aligned} H_7^{J\sigma}(AaBb) &= -\delta_{q_Aq_a}\delta_{q_Bq_b}\hat{J}^{-2}\langle A||Y_J||a\rangle\langle B||Y_J||b\rangle \\ &\quad\times\int dr_1dr_2R_{JJ}(m_\sigma;r_1,r_2)[g'_\sigma\rho_s(G_AG_a+F_AF_a)]_{r_1}[g'_\sigma\rho_s(G_BG_b+F_BF_b)]_{r_2}. \end{aligned} \tag{A.28}$$

Next we consider the contributions from the exchange terms. For the Term9 in Eq. (2.79),

$$\begin{aligned} \text{Term9} &= -\sum_d\int d\boldsymbol{r}_1d\boldsymbol{r}_2f_A^\dagger(1)f_d^\dagger(2)g'_\sigma(1)f_b^\dagger(1)f_B(1)g_\sigma(2)I(1,2)f_a(2)f_d(1) \\ &= \sum_d\int d\boldsymbol{r}_1d\boldsymbol{r}'_1d\boldsymbol{r}_2g'_\sigma(1)g_\sigma(2)\frac{\delta(r_1-r'_1)}{r_1^2}\sum_{LL'\nu\nu'}(-)^{\nu+\nu'}R_{LL}(m_\sigma;1,2) \\ &\quad\times\langle f_b|Y_{L'-\nu'}|f_B\rangle_{r'_1}\langle f_A|\gamma_0Y_{L'\nu'}Y_{L\nu}|f_d\rangle_{r_1}\langle f_d|\gamma_0Y_{L-\nu}|f_a\rangle_{r_2}. \end{aligned} \tag{A.29}$$

Then

$$\begin{aligned} H_9^{J\sigma}(AaBb) &= \sum_d\sum_{mM}(-)^{j_A+j_B-m_A-m_B}\begin{pmatrix} j_A & j_a & J \\ m_A & -m_a & -M\end{pmatrix}\begin{pmatrix} j_B & j_b & J \\ m_B & -m_b & -M\end{pmatrix} \\ &\quad\times\int d\boldsymbol{r}_1d\boldsymbol{r}'_1d\boldsymbol{r}_2g'_\sigma(1)g_\sigma(2)\frac{\delta(r_1-r'_1)}{r_1^2}\sum_{LL'\nu\nu'}(-)^{\nu+\nu'}R_{LL}(m_\sigma;1,2) \\ &\quad\times\langle f_b|Y_{L'-\nu'}|f_B\rangle_{r'_1}\langle f_A|\gamma_0Y_{L'\nu'}Y_{L\nu}|f_d\rangle_{r_1}\langle f_d|\gamma_0Y_{L-\nu}|f_a\rangle_{r_2}, \end{aligned} \tag{A.30}$$

with

$$\begin{aligned} &\sum_{m_bm_B}(-)^{j_B-m_B+\nu'}\begin{pmatrix} j_B & j_b & J \\ m_B & -m_b & -M\end{pmatrix}\langle f_b|Y_{L'-\nu'}|f_B\rangle \\ &= \delta_{q_Bq_b}\delta_{L'J}\delta_{\nu'M}\hat{J}^{-2}\langle B||Y_J||b\rangle\frac{(G_BG_b+F_BF_b)_{r'_1}}{{r'_1}^2}. \end{aligned} \tag{A.31}$$

Using the direct product of the spherical harmonics (see **Remark 12**)

$$Y_{JM}Y_{L\nu}=\sum_{L'\nu'}(-)^{\nu'}\frac{\hat{J}\hat{L}\hat{L}'}{\sqrt{4\pi}}\begin{pmatrix} J & L & L' \\ 0 & 0 & 0\end{pmatrix}\begin{pmatrix} J & L & L' \\ M & \nu & \nu'\end{pmatrix}Y_{L'-\nu'}, \tag{A.32}$$

we can obtain that

$$\begin{aligned} \langle f_A|\gamma_0Y_{JM}Y_{L\nu}|f_d\rangle &= \delta_{q_Aq_d}\sum_{L'\nu'}(-)^{\nu'+j_A-m_A}\frac{\hat{J}\hat{L}\hat{L}'}{\sqrt{4\pi}}\begin{pmatrix} J & L & L' \\ 0 & 0 & 0\end{pmatrix}\begin{pmatrix} J & L & L' \\ M & \nu & \nu'\end{pmatrix} \\ &\quad\times\begin{pmatrix} j_A & L' & j_d \\ -m_A & -\nu' & m_d\end{pmatrix}\langle A||Y_{L'}||d\rangle\frac{(G_AG_d-F_AF_d)_{r_1}}{{r_1}^2}. \end{aligned} \tag{A.33}$$

Therefore $H_9^{J\sigma}(AaBb)$ can be rewritten as

$$\begin{aligned}
& H_9^{J\sigma}(AaBb) \\
= & \sum_{j_d m_d} \sum_{m_A m_a M} \sum_{L\nu L'\nu'} \delta_{q_B q_b}\delta_{q_A q_d}\delta_{q_d q_a}(-)^{\nu+\nu'+j_d-m_d}\frac{\hat{J}^{-1}\hat{L}\hat{L}'}{\sqrt{4\pi}}\begin{pmatrix} J & L & L' \\ 0 & 0 & 0 \end{pmatrix} \\
& \times \begin{pmatrix} j_A & j_a & J \\ m_A & -m_a & -M \end{pmatrix}\begin{pmatrix} J & L & L' \\ M & \nu & \nu' \end{pmatrix}\begin{pmatrix} j_A & L' & j_d \\ -m_A & -\nu' & m_d \end{pmatrix}\begin{pmatrix} j_d & L & j_a \\ -m_d & -\nu & m_a \end{pmatrix} \\
& \times \langle B||Y_J||b\rangle\langle A||Y_{L'}||d\rangle\langle d||Y_L||a\rangle \\
& \times \int dr_1 dr_2 R_{LL}(m_\sigma; r_1, r_2)\left[g'_\sigma \frac{(G_b G_B + F_b F_B)(G_A G_d - F_A F_d)}{r^2}\right]_{r_1}[g_\sigma(G_d G_a - F_d F_a)]_{r_2}.
\end{aligned} \tag{A.34}$$

Then we can carry out all the m summations,

$$\begin{aligned}
& \sum_{m_d m_A m_a M \nu\nu'} (-)^{\nu+\nu'+j_d-m_d} \\
& \times \begin{pmatrix} j_A & j_a & J \\ m_A & -m_a & -M \end{pmatrix}\begin{pmatrix} J & L & L' \\ M & \nu & \nu' \end{pmatrix}\begin{pmatrix} j_A & L' & j_d \\ -m_A & -\nu' & m_d \end{pmatrix}\begin{pmatrix} j_d & L & j_a \\ -m_d & -\nu & m_a \end{pmatrix} \\
= & (-)^{j_A+j_a}\begin{Bmatrix} j_A & j_a & J \\ L & L' & j_d \end{Bmatrix},
\end{aligned} \tag{A.35}$$

where the relation of contracting 3-j symbols to 6-j symbols in **Remark 7** is used. Finally, $H_9^{J\sigma}(AaBb)$ can be expressed as

$$\begin{aligned}
& H_9^{J\sigma}(AaBb) \\
= & \delta_{q_B q_b}\delta_{q_A q_a}(-)^{j_A+j_a}\frac{\hat{J}^{-1}}{\sqrt{4\pi}}\sum_{j_d LL'}\delta_{q_d q_a}\hat{L}\hat{L}'\begin{pmatrix} J & L & L' \\ 0 & 0 & 0 \end{pmatrix}\begin{Bmatrix} j_A & j_a & J \\ L & L' & j_d \end{Bmatrix} \\
& \times \langle B||Y_J||b\rangle\langle A||Y_{L'}||d\rangle\langle d||Y_L||a\rangle \\
& \times \int dr_1 dr_2 R_{LL}(m_\sigma; r_1, r_2)\left[g'_\sigma \frac{(G_b G_B + F_b F_B)(G_A G_d - F_A F_d)}{r^2}\right]_{r_1}[g_\sigma(G_d G_a - F_d F_a)]_{r_2}.
\end{aligned} \tag{A.36}$$

For the Term13 in Eq. (2.79),

$$\begin{aligned}
\text{Term13} = & -\sum_{cd}\int d\boldsymbol{r}_1 d\boldsymbol{r}_2 f_A^\dagger(1) f_c^\dagger(1) f_d^\dagger(2) g''_\sigma(1) f_b^\dagger(1) f_B(1) g_\sigma(2) I(1,2) f_c(2) f_d(1) f_a(1) \\
= & \sum_{cd}\int d\boldsymbol{r}_1 d\boldsymbol{r}'_1 d\boldsymbol{r}''_1 d\boldsymbol{r}_2 g''_\sigma(1) g_\sigma(2)\frac{\delta(r_1 - r'_1)}{r_1^2}\frac{\delta(r_1 - r''_1)}{r_1^2}\sum_{LL'L''\nu\nu'\nu''}(-)^{\nu+\nu'+\nu''} R_{LL}(m_\sigma; 1, 2) \\
& \times \langle f_A|Y_{L'\nu'}|f_a\rangle_{r''_1}\langle f_b|Y_{L'-\nu'}Y_{L''\nu''}|f_B\rangle_{r'_1}\langle f_c|\gamma_0 Y_{L''-\nu''}Y_{L\nu}|f_d\rangle_{r_1}\langle f_d|\gamma_0 Y_{L-\nu}|f_c\rangle_{r_2}.
\end{aligned} \tag{A.37}$$

Due to the same argument in the derivation of Term3, it is not difficult to prove that the spherical harmonics $Y_{L''-\nu''}Y_{L\nu}$ couple to $Y_{L\nu}$, $Y_{L'\nu'}$ is just Y_{JM}, and $Y_{L'-\nu'}Y_{L''\nu''}$ must couple to Y_{J-M}, then

$Y_{L''\nu''}$ is thus Y_{00}. Therefore,

$$\begin{aligned}
H_{13}^{J\,\sigma}(AaBb) =& \sum_{cd}\sum_{mM}(-)^{j_A+j_B-m_A-m_B}\begin{pmatrix} j_A & j_a & J \\ m_A & -m_a & -M \end{pmatrix}\begin{pmatrix} j_B & j_b & J \\ m_B & -m_b & -M \end{pmatrix} \\
&\times \frac{1}{4\pi}\int d\boldsymbol{r}_1 d\boldsymbol{r}_1' d\boldsymbol{r}_1'' d\boldsymbol{r}_2 g_\sigma''(1) g_\sigma(2)\frac{\delta(r_1-r_1')}{r_1^2}\frac{\delta(r_1-r_1'')}{r_1^2}\sum_{LL'\nu\nu'}(-)^{\nu+\nu'}R_{LL}(m_\sigma;1,2) \\
&\times \langle f_A|Y_{L'\nu'}|f_a\rangle_{r_1''}\langle f_b|Y_{L'-\nu'}|f_B\rangle_{r_1'}\langle f_c|\gamma_0 Y_{L\nu}|f_d\rangle_{r_1}\langle f_d|\gamma_0 Y_{L-\nu}|f_c\rangle_{r_2} \\
=&\delta_{q_Aq_a}\delta_{q_Bq_b}\frac{\hat{J}^{-2}}{4\pi}\langle A||Y_J||a\rangle\langle B||Y_J||b\rangle\sum_{j_cj_dL}\delta_{q_cq_d}\langle c||Y_L||d\rangle^2 \\
&\times\int dr_1 dr_2 R_{LL}(m_\sigma;r_1,r_2)\left[g_\sigma''\frac{(G_AG_a+F_AF_a)(G_BG_b+F_BF_b)(G_cG_d-F_cF_d)}{r^4}\right]_{r_1} \\
&\times[g_\sigma(G_cG_d-F_cF_d)]_{r_2}. \qquad \text{(A.38)}
\end{aligned}$$

For the Term14 in Eq. (2.79),

$$\begin{aligned}
\text{Term14} =& -\sum_{cd}\int d\boldsymbol{r}_1 d\boldsymbol{r}_2 f_A^\dagger(1) f_c^\dagger(1) f_d^\dagger(2) g_\sigma'(1) g_\sigma'(2) f_b^\dagger(2) f_B(2) I(1,2) f_c(2) f_d(1) f_a(1) \\
=&\sum_{cd}\int d\boldsymbol{r}_1 d\boldsymbol{r}_1' d\boldsymbol{r}_2 d\boldsymbol{r}_2' g_\sigma'(1) g_\sigma'(2)\frac{\delta(r_1-r_1')}{r_1^2}\frac{\delta(r_2-r_2')}{r_2^2}\sum_{LL'L''\nu\nu'\nu''}(-)^{\nu+\nu'+\nu''}R_{LL}(m_\sigma;1,2) \\
&\times\langle f_A|Y_{L'\nu'}|f_a\rangle_{r_1'}\langle f_c|\gamma_0 Y_{L'-\nu'}Y_{L\nu}|f_d\rangle_{r_1}\langle f_d|\gamma_0 Y_{L''\nu''}Y_{L-\nu}|f_c\rangle_{r_2}\langle f_b|Y_{L''-\nu''}|f_B\rangle_{r_2'}.
\end{aligned} \qquad \text{(A.39)}$$

Then,

$$\begin{aligned}
H_{14}^{J\,\sigma}(AaBb) =&\delta_{q_Aq_a}\delta_{q_Bq_b}\hat{J}^{-4}\langle A||Y_J||a\rangle\langle B||Y_J||b\rangle \\
&\times\int d\boldsymbol{r}_1 d\boldsymbol{r}_2 g_\sigma'(1) g_\sigma'(2)\sum_{L\nu M}\sum_{j_cm_cj_dm_d}(-)^{\nu+M}R_{LL}(m_\sigma;1,2)\left[\frac{G_AG_a+F_AF_a}{r^2}\right]_{r_1} \\
&\times\langle f_c|\gamma_0 Y_{J-M}Y_{L\nu}|f_d\rangle_{r_1}\langle f_d|\gamma_0 Y_{JM}Y_{L-\nu}|f_c\rangle_{r_2}\left[\frac{G_BG_b+F_BF_b}{r^2}\right]_{r_2}.
\end{aligned} \qquad \text{(A.40)}$$

With

$$\begin{aligned}
\langle f_c|\gamma_0 Y_{J-M}Y_{L\nu}|f_d\rangle_{r_1} =&\sum_{L'\nu'}(-)^{\nu'}\frac{\hat{J}\hat{L}\hat{L}'}{\sqrt{4\pi}}\begin{pmatrix} J & L & L' \\ 0 & 0 & 0 \end{pmatrix}\begin{pmatrix} J & L & L' \\ -M & \nu & \nu' \end{pmatrix} \\
&\times(-)^{j_c-m_c}\begin{pmatrix} j_c & L' & j_d \\ -m_c & -\nu' & m_d \end{pmatrix}\langle c||Y_{L'}||d\rangle\left[\frac{G_cG_d-F_cF_d}{r^2}\right]_{r_1}, \qquad \text{(A.41)} \\
\langle f_d|\gamma_0 Y_{JM}Y_{L-\nu}|f_c\rangle_{r_2} =&\sum_{L''\nu''}(-)^{-\nu''}\frac{\hat{J}\hat{L}\hat{L}''}{\sqrt{4\pi}}\begin{pmatrix} J & L & L'' \\ 0 & 0 & 0 \end{pmatrix}\begin{pmatrix} J & L & L'' \\ M & -\nu & -\nu'' \end{pmatrix} \\
&\times(-)^{j_d-m_d}\begin{pmatrix} j_d & L'' & j_c \\ -m_d & \nu'' & m_c \end{pmatrix}\langle d||Y_{L''}||c\rangle\left[\frac{G_cG_d-F_cF_d}{r^2}\right]_{r_2}, \qquad \text{(A.42)}
\end{aligned}$$

we can finally obtain that

$$\begin{aligned} H_{14}^{J\,\sigma}(AaBb) &= \delta_{q_Aq_a}\delta_{q_Bq_b}\frac{\hat{J}^{-2}}{4\pi}\langle A||Y_J||a\rangle\langle B||Y_J||b\rangle\sum_{j_cj_dLL'}\delta_{q_cq_d}\hat{L}^2\begin{pmatrix} J & L & L' \\ 0 & 0 & 0\end{pmatrix}^2\langle c||Y_{L'}||d\rangle^2 \\ &\times\int dr_1dr_2R_{LL}(m_\sigma;r_1,r_2)\left[g'_\sigma\frac{(G_AG_a+F_AF_a)(G_cG_d-F_cF_d)}{r^2}\right]_{r_1} \\ &\times\left[g'_\sigma\frac{(G_BG_b+F_BF_b)(G_cG_d-F_cF_d)}{r^2}\right]_{r_2}. \end{aligned} \tag{A.43}$$

In summary,

$$\begin{aligned} H_1^{J\sigma}(1234) &= -\delta_{q_1q_2}\delta_{q_3q_4}\hat{J}^{-2}\langle 1||Y_J||2\rangle\langle 3||Y_J||4\rangle \\ &\times\int dr_1dr_2R_{JJ}(m_\sigma;r_1,r_2)[g_\sigma(G_1G_2-F_1F_2)]_{r_1}[g_\sigma(G_3G_4-F_3F_4)]_{r_2}, \end{aligned} \tag{A.44}$$

$$\begin{aligned} H_2^{J\sigma}(1234) &= -\delta_{q_1q_2}\delta_{q_3q_4}\hat{J}^{-2}\langle 1||Y_J||2\rangle\langle 3||Y_J||4\rangle \\ &\times\int dr\frac{1}{r^2}g'_\sigma(r)\sigma(r)(G_1G_2-F_1F_2)(G_3G_4+F_3F_4), \end{aligned} \tag{A.45}$$

$$\begin{aligned} H_3^{J\sigma}(1234) &= -\delta_{q_1q_2}\delta_{q_3q_4}\hat{J}^{-2}\langle 1||Y_J||2\rangle\langle 3||Y_J||4\rangle \\ &\times\int dr_1dr_2R_{JJ}(m_\sigma;r_1,r_2)[g_\sigma(G_1G_2-F_1F_2)]_{r_1}[g'_\sigma\rho_s(G_3G_4+F_3F_4)]_{r_2}, \end{aligned} \tag{A.46}$$

$$\begin{aligned} H_6^{J\sigma}(1234) &= -\delta_{q_1q_2}\delta_{q_3q_4}\hat{J}^{-2}\langle 1||Y_J||2\rangle\langle 3||Y_J||4\rangle \\ &\times\int dr\frac{1}{r^2}g''_\sigma(r)\rho_s(r)\sigma(r)(G_1G_2+F_1F_2)(G_3G_4+F_3F_4), \end{aligned} \tag{A.47}$$

$$\begin{aligned} H_7^{J\sigma}(1234) &= -\delta_{q_1q_2}\delta_{q_3q_4}\hat{J}^{-2}\langle 1||Y_J||2\rangle\langle 3||Y_J||4\rangle \\ &\times\int dr_1dr_2R_{JJ}(m_\sigma;r_1,r_2)[g'_\sigma\rho_s(G_1G_2+F_1F_2)]_{r_1}[g'_\sigma\rho_s(G_3G_4+F_3F_4)]_{r_2}, \end{aligned} \tag{A.48}$$

$$\begin{aligned} H_9^{J\sigma}(1234) &= \delta_{q_1q_2}\delta_{q_3q_4}(-)^{j_1+j_2}\frac{\hat{J}^{-1}}{\sqrt{4\pi}}\sum_{j_dLL'}\delta_{q_dq_2}\hat{L}\hat{L}'\begin{pmatrix} J & L & L' \\ 0 & 0 & 0\end{pmatrix}\begin{Bmatrix} j_1 & j_2 & J \\ L & L' & j_d\end{Bmatrix} \\ &\times\langle 3||Y_J||4\rangle\langle 1||Y_{L'}||d\rangle\langle d||Y_L||2\rangle \\ &\times\int dr_1dr_2R_{LL}(m_\sigma;r_1,r_2)\left[g'_\sigma\frac{(G_3G_4+F_3F_4)(G_1G_d-F_1F_d)}{r^2}\right]_{r_1} \\ &\times[g_\sigma(G_dG_2-F_dF_2)]_{r_2}, \end{aligned} \tag{A.49}$$

$$\begin{aligned} H_{13}^{J\,\sigma}(1234) &= \delta_{q_1q_2}\delta_{q_3q_4}\frac{\hat{J}^{-2}}{4\pi}\langle 1||Y_J||2\rangle\langle 3||Y_J||4\rangle\sum_{j_cj_dL}\delta_{q_cq_d}\langle c||Y_L||d\rangle^2 \\ &\times\int dr_1dr_2R_{LL}(m_\sigma;r_1,r_2)\left[g''_\sigma\frac{(G_1G_2+F_1F_2)(G_3G_4+F_3F_4)(G_cG_d-F_cF_d)}{r^4}\right]_{r_1} \\ &\times[g_\sigma(G_cG_d-F_cF_d)]_{r_2}, \end{aligned} \tag{A.50}$$

$$
\begin{aligned}
H_{14}^{J\ \sigma}(1234) &= \delta_{q_1q_2}\delta_{q_3q_4}\frac{\hat{J}^{-2}}{4\pi}\langle 1||Y_J||2\rangle\langle 3||Y_J||4\rangle \sum_{j_cj_dLL'}\delta_{q_cq_d}\hat{L}^2\begin{pmatrix} J & L & L' \\ 0 & 0 & 0 \end{pmatrix}^2\langle c||Y_{L'}||d\rangle^2 \\
&\times \int dr_1dr_2R_{LL}(m_\sigma;r_1,r_2)\left[g'_\sigma\frac{(G_1G_2+F_1F_2)(G_cG_d-F_cF_d)}{r^2}\right]_{r_1} \\
&\times \left[g'_\sigma\frac{(G_3G_4+F_3F_4)(G_cG_d-F_cF_d)}{r^2}\right]_{r_2}, \qquad (A.51)
\end{aligned}
$$

where summations over c,d stand for summations over all the occupied states.

A.3 $\omega-$meson contribution to the p-h matrix elements

In this section, the derivations for the quantities $H^J(1234)$ in Eq. (2.85) induced by the ω-meson will be given in details.

For the ω-meson, the two-body interaction reads

$$
\begin{aligned}
V^\omega(1,2) &= g_\omega(1)\gamma_0(1)\gamma^\mu(1)g_\omega(2)\gamma_0(2)\gamma_\mu(2)D_\omega(1,2) \\
&= \sum_{L\nu} g_\omega(1)\gamma_0(1)\gamma^\mu(1)g_\omega(2)\gamma_0(2)\gamma_\mu(2)R_{LL}(m_\omega;1,2)(-)^\nu Y_L^\nu(\hat{r}_1)Y_L^{-\nu}(\hat{r}_2). \qquad (A.52)
\end{aligned}
$$

It is convenient to divide the $H^{J\omega}(1234)$ into two parts, where the time component with $\mu=0$ is denoted as $\bar{H}^{J\omega}(1234)$, and the space component with $\mu=1,2,3$ is denoted as $\bar{\bar{H}}^{J\omega}(1234)$.

For time component with $\mu=0$, the $\bar{H}^{J\omega}(1234)$ values in Eq. (2.85) can be derived in analogy with the derivation of the σ-meson in **Section A.2**.

For the space component with $\mu=1,2,3$, one has

$$
\bar{\bar{V}}^\omega(1,2) = -\sum_{L\nu k}(-)^{\nu+k}g_\omega(1)\alpha_k(1)g_\omega(2)\alpha_{-k}(2)R_{LL}(m_\omega;1,2)Y_L^\nu(\hat{r}_1)Y_L^{-\nu}(\hat{r}_2). \qquad (A.53)
$$

For the Term1 in Eq. (2.78),

$$
\begin{aligned}
\text{Term1} &= \int d\boldsymbol{r}_1d\boldsymbol{r}_2f_A^\dagger(1)f_b^\dagger(2)g_\omega(1)g_\omega(2)I(1,2)f_B(2)f_a(1) \\
&= -\int d\boldsymbol{r}_1d\boldsymbol{r}_2g_\omega(1)g_\omega(2)\sum_{L\nu k}(-)^{\nu+k}R_{LL}(m_\omega;1,2)\langle f_A|Y_{L\nu}\alpha_k|f_a\rangle_{r_1}\langle f_b|Y_{L-\nu}\alpha_{-k}|f_B\rangle_{r_2}.
\end{aligned} \qquad (A.54)
$$

The summation over m_A, m_a gives

$$
\begin{aligned}
&\sum_{m_Am_a}(-)^{j_A-m_A}\begin{pmatrix} j_A & j_a & J \\ m_A & -m_a & -M \end{pmatrix}\langle f_A|Y_{L\nu}\alpha_k|f_a\rangle \\
&= \frac{1}{r_1^2}\delta_{q_Aq_a}\sum_{m_Am_a}(-)^{j_A-m_A}\begin{pmatrix} j_A & j_a & J \\ m_A & -m_a & -M \end{pmatrix}\left[iG_AF_a\langle A|Y_{L\nu}\sigma_k|a'\rangle - iF_AG_a\langle A'|Y_{L\nu}\sigma_k|a\rangle\right].
\end{aligned} \qquad (A.55)
$$

With the definition of the vector spherical harmonics

$$
Y_{L\nu}\sigma_k = \sum_{J'M'}(-)^{L-1+M'}\hat{J}'\begin{pmatrix} L & 1 & J' \\ \nu & k & -M' \end{pmatrix}\mathscr{T}_{J'M'}, \qquad (A.56)
$$

$$\begin{aligned}
&\sum_{m_A m_a}(-)^{j_A-m_A}\begin{pmatrix} j_A & j_a & J \\ m_A & -m_a & -M \end{pmatrix}\langle f_A|Y_{L\nu}\alpha_k|f_a\rangle \\
&= \frac{1}{r_1^2}\delta_{q_Aq_a}(-)^{L-1+M}\hat{J}^{-1}\begin{pmatrix} L & 1 & J \\ \nu & k & -M \end{pmatrix} i\left[G_AF_a\langle A||\mathscr{T}_{JL}||a'\rangle - F_AG_a\langle A'||\mathscr{T}_{JL}||a\rangle\right],
\end{aligned} \tag{A.57}$$

where the Wigner-Eckart Theorem (see **Remark 13**) and the symmetry and orthogonality relations of 3-j Symbols (see **Remarks 2 and 3**) are used. The summation over m_B, m_b gives

$$\begin{aligned}
&\sum_{m_B m_b}(-)^{j_B-m_B}\begin{pmatrix} j_B & j_b & J \\ m_B & -m_b & -M \end{pmatrix}\langle f_b|Y_{L-\nu}\alpha_{-k}|f_B\rangle \\
&= \frac{1}{r_2^2}\delta_{q_Bq_b}(-)^{j_B+j_b+L}\hat{J}^{-1}\begin{pmatrix} L & 1 & J \\ -\nu & -k & M \end{pmatrix} i\left[G_bF_B\langle b||\mathscr{T}_{JL}||B'\rangle - F_bG_B\langle b'||\mathscr{T}_{JL}||B\rangle\right]
\end{aligned} \tag{A.58}$$

Finally, the quantity $\bar{\bar{H}}_J^{\omega}(AaBb)$ can be expressed as

$$\begin{aligned}
\bar{\bar{H}}_1^{J\omega}(AaBb) &= -\delta_{q_Aq_a}\delta_{q_Bq_b}\hat{J}^{-2} \\
&\times\sum_L\int dr_1dr_2R_{LL}(m_\omega;r_1,r_2)\left[g_\omega\left(G_AF_a\langle A||\mathscr{T}_{JL}||a'\rangle - F_AG_a\langle A'||\mathscr{T}_{JL}||a\rangle\right)\right]_{r_1} \\
&\times\left[g_\omega\left(G_BF_b\langle B||\mathscr{T}_{JL}||b'\rangle - F_BG_b\langle B'||\mathscr{T}_{JL}||b\rangle\right)\right]_{r_2},
\end{aligned} \tag{A.59}$$

where the symmetry property of the reduced matrix element $\langle b||\mathscr{T}_{JL}||a\rangle = (-)^{j_a+j_b+J+L}\langle a||\mathscr{T}_{JL}||b\rangle$ in **Remark 14** is used.

It is easy to prove that $\sum_d\langle f_d|Y_{L\nu}\alpha_k|f_d\rangle = 0$ due to the parity conservation. In fact, this is the reason why the space components of vector mesons do not contribute to the energy functional in the spherical RH theory. Therefore,

$$\bar{\bar{H}}_i^{J\omega}(AaBb) = 0, \qquad \text{for} \quad i = 2,3,\cdots,7. \tag{A.60}$$

For the exchange rearrangement contributions, the Term9 in Eq. (2.79),

$$\begin{aligned}
\text{Term9} &= -\sum_d\int d\boldsymbol{r}_1d\boldsymbol{r}_2f_A^\dagger(1)f_d^\dagger(2)g'_\omega(1)f_b^\dagger(1)f_B(1)g_\omega(2)I(1,2)f_a(2)f_d(1) \\
&= \sum_d\int d\boldsymbol{r}_1d\boldsymbol{r}'_1d\boldsymbol{r}_2g'_\omega(1)g_\omega(2)\frac{\delta(r_1-r'_1)}{r_1^2}\sum_{LL'\nu\nu'k}(-)^{\nu+\nu'+k}R_{LL}(m_\omega;r_1,r_2) \\
&\times\langle f_b|Y_{L'-\nu'}|f_B\rangle_{r'_1}\langle f_A|Y_{L'\nu'}Y_{L\nu}\alpha_k|f_d\rangle_{r_1}\langle f_d|Y_{L-\nu}\alpha_{-k}|f_a\rangle_{r_2}.
\end{aligned} \tag{A.61}$$

Then

$$\begin{aligned}
\bar{\bar{H}}_9^{J\omega}(AaBb) &= \sum_d\sum_{mM}(-)^{j_A+j_B-m_A-m_B}\begin{pmatrix} j_A & j_a & J \\ m_A & -m_a & -M \end{pmatrix}\begin{pmatrix} j_B & j_b & J \\ m_B & -m_b & -M \end{pmatrix} \\
&\times\int d\boldsymbol{r}_1d\boldsymbol{r}'_1d\boldsymbol{r}_2g'_\omega(1)g_\omega(2)\frac{\delta(r_1-r'_1)}{r_1^2}\sum_{LL'\nu\nu'k}(-)^{\nu+\nu'+k}R_{LL}(m_\omega;r_1,r_2) \\
&\times\langle f_b|Y_{L'-\nu'}|f_B\rangle_{r'_1}\langle f_A|Y_{L'\nu'}Y_{L\nu}\alpha_k|f_d\rangle_{r_1}\langle f_d|Y_{L-\nu}\alpha_{-k}|f_a\rangle_{r_2},
\end{aligned} \tag{A.62}$$

with

$$\begin{aligned}
&\sum_{m_b m_B} (-)^{j_B - m_B + \nu'} \begin{pmatrix} j_B & j_b & J \\ m_B & -m_b & -M \end{pmatrix} \langle f_b | Y_{L'-\nu'} | f_B \rangle \\
&= \delta_{q_B q_b} \delta_{L'J} \delta_{\nu' M} (-)^{j_B + j_b + 1} \hat{J}^{-2} \langle b || Y_J || B \rangle \frac{(G_B G_b + F_B F_b)_{r_1'}}{{r_1'}^2}. \qquad \text{(A.63)}
\end{aligned}$$

Using the direct product of the spherical harmonics (see **Remark 12**)

$$Y_{JM} Y_{L\nu} = \sum_{L'\nu'} (-)^{\nu'} \frac{\hat{J}\hat{L}\hat{L}'}{\sqrt{4\pi}} \begin{pmatrix} J & L & L' \\ 0 & 0 & 0 \end{pmatrix} \begin{pmatrix} J & L & L' \\ M & \nu & \nu' \end{pmatrix} Y_{L'-\nu'}, \qquad \text{(A.64)}$$

and

$$Y_{L'-\nu'} \sigma_k = \sum_{J'M'} (-)^{L'-1+M'} \hat{J}' \begin{pmatrix} L' & 1 & J' \\ -\nu' & k & -M' \end{pmatrix} \mathscr{T}_{J'M'}, \qquad \text{(A.65)}$$

we can obtain that

$$\begin{aligned}
&\langle f_A | Y_{JM} Y_{L\nu} \alpha_k | f_d \rangle_{r_1} \\
&= \delta_{q_A q_d} \sum_{L'\nu' J'M'} (-)^{\nu' + j_A - m_A + L' - 1 + M'} \frac{\hat{J}\hat{L}\hat{L}'\hat{J}'}{\sqrt{4\pi}} \\
&\times \begin{pmatrix} J & L & L' \\ 0 & 0 & 0 \end{pmatrix} \begin{pmatrix} J & L & L' \\ M & \nu & \nu' \end{pmatrix} \begin{pmatrix} L' & 1 & J' \\ -\nu' & k & -M' \end{pmatrix} \begin{pmatrix} j_A & J' & j_d \\ -m_A & M' & m_d \end{pmatrix} \\
&\times \frac{1}{r_1^2} \left[i G_A F_d \langle A || \mathscr{T}_{J'L'} || d' \rangle - i F_A G_d \langle A' || \mathscr{T}_{J'L'} || d \rangle \right]_{r_1}, \qquad \text{(A.66)}
\end{aligned}$$

as well as

$$\begin{aligned}
&\langle f_d | Y_{L-\nu} \alpha_{-k} | f_a \rangle_{r_2} \\
&= \delta_{q_d q_a} \sum_{J''M''} (-)^{L-1+M''+j_d-m_d} \hat{J}'' \begin{pmatrix} L & 1 & J'' \\ -\nu & -k & -M'' \end{pmatrix} \\
&\times \begin{pmatrix} j_d & J'' & j_a \\ -m_d & M'' & m_a \end{pmatrix} \frac{1}{r_2^2} \left[i G_d F_a \langle d || \mathscr{T}_{J''L} || a' \rangle - i F_d G_a \langle d' || \mathscr{T}_{J''L} || a \rangle \right]_{r_2}. \qquad \text{(A.67)}
\end{aligned}$$

Putting all the angular parts together, i.e., the 3-j symbols and phases, one has

$$\begin{aligned}
&\sum_{j_d L L' J' J''} \sum_{m_d m_A m_a M \nu k \nu' M' M''} (-)^{j_A - m_A + \nu + k + \nu' + j_A - m_A + L' - 1 + M' + L - 1 + M'' + j_d - m_d} \\
&\times \delta_{q_d q_a} \delta_{q_A q_a} \frac{\hat{J}\hat{L}\hat{L}'\hat{J}'\hat{J}''}{\sqrt{4\pi}} \begin{pmatrix} J & L & L' \\ 0 & 0 & 0 \end{pmatrix} \\
&\times \begin{pmatrix} j_A & j_a & J \\ m_A & -m_a & -M \end{pmatrix} \begin{pmatrix} J & L & L' \\ M & \nu & \nu' \end{pmatrix} \begin{pmatrix} L' & 1 & J' \\ -\nu' & k & -M' \end{pmatrix} \\
&\times \begin{pmatrix} j_A & J' & j_d \\ -m_A & M' & m_d \end{pmatrix} \begin{pmatrix} L & 1 & J'' \\ -\nu & -k & -M'' \end{pmatrix} \begin{pmatrix} j_d & J'' & j_a \\ -m_d & M'' & m_a \end{pmatrix}. \qquad \text{(A.68)}
\end{aligned}$$

With the contraction of 3-j symbols to 6-j symbols (see **Remark 7**)

$$\begin{aligned}
&\sum_{\nu\nu' k}(-)^{L+L'+1+\nu-\nu'-k}\begin{pmatrix} L & L' & J \\ \nu & \nu' & M\end{pmatrix}\begin{pmatrix} L' & 1 & J' \\ -\nu' & k & -M'\end{pmatrix}\begin{pmatrix} 1 & L & J'' \\ -k & -\nu & -M''\end{pmatrix} \\
&= \begin{pmatrix} J' & J'' & J \\ -M' & -M'' & M\end{pmatrix}\begin{Bmatrix} J' & J'' & J \\ L & L' & 1\end{Bmatrix},
\end{aligned} \tag{A.69}$$

and

$$\begin{aligned}
&\sum_{m_A m_a m_d M M' M''}(-)^{J'+J''+j_d-M'+M''+m_d}\begin{pmatrix} J' & J'' & J \\ -M' & -M'' & M\end{pmatrix} \\
&\times\begin{pmatrix} J'' & j_d & j_a \\ M'' & -m_d & m_a\end{pmatrix}\begin{pmatrix} j_d & J' & j_A \\ m_d & M' & -m_A\end{pmatrix}\begin{pmatrix} j_a & j_A & J \\ m_a & -m_A & M\end{pmatrix} \\
&= \begin{Bmatrix} j_a & j_A & J \\ J' & J'' & j_d\end{Bmatrix},
\end{aligned} \tag{A.70}$$

the expression of angular parts can be rewritten again as,

$$\sum_{j_d LL'J'J''}(-)^{J''+L+j_A+j_a}\delta_{q_d q_a}\delta_{q_A q_a}\frac{\hat{J}\hat{L}\hat{L}'\hat{J}'\hat{J}''}{\sqrt{4\pi}}\begin{pmatrix} J & L & L' \\ 0 & 0 & 0\end{pmatrix}\begin{Bmatrix} j_a & j_A & J \\ J' & J'' & j_d\end{Bmatrix}\begin{Bmatrix} J' & J'' & J \\ L & L' & 1\end{Bmatrix}. \tag{A.71}$$

Finally, one obtains

$$\begin{aligned}
&\bar{\bar{H}}_9^{J\omega}(AaBb) \\
&= \delta_{q_A q_a}\delta_{q_B q_b}(-)^{j_A+j_a+j_B+j_b}\frac{\hat{J}^{-1}}{\sqrt{4\pi}}\sum_{j_d LL'J'J''}\delta_{q_d q_a}(-)^{J''+L}\hat{L}\hat{L}'\hat{J}'\hat{J}'' \\
&\times\begin{pmatrix} J & L & L' \\ 0 & 0 & 0\end{pmatrix}\begin{Bmatrix} j_a & j_A & J \\ J' & J'' & j_d\end{Bmatrix}\begin{Bmatrix} J' & J'' & J \\ L & L' & 1\end{Bmatrix}\langle b||Y_J||B\rangle \\
&\times\int dr_1 dr_2 R_{LL}(m_\omega;r_1,r_2)\left[g'_\omega\frac{(G_B G_b+F_B F_b)}{r^2}\left(G_A F_d\langle A||\mathscr{T}_{J'L'}||d'\rangle - F_A G_d\langle A'||\mathscr{T}_{J'L'}||d\rangle\right)\right]_{r_1} \\
&\quad\times\left[g_\omega\left(G_d F_a\langle d||\mathscr{T}_{J''L}||a'\rangle - F_d G_a\langle d'||\mathscr{T}_{J''L}||a\rangle\right)\right]_{r_2}.
\end{aligned} \tag{A.72}$$

For the Term13 in Eq. (2.79), according to the discussion in the previous section,

$$
\begin{aligned}
&\bar{\bar{H}}_{13}^{J\omega}(AaBb) \\
=\;& \sum_{cd}\sum_{mM}(-)^{j_A+j_B-m_A-m_B}\begin{pmatrix} j_A & j_a & J \\ m_A & -m_a & -M \end{pmatrix}\begin{pmatrix} j_B & j_b & J \\ m_B & -m_b & -M \end{pmatrix} \\
&\times\frac{1}{4\pi}\int d\boldsymbol{r}_1 d\boldsymbol{r}'_1 d\boldsymbol{r}''_1 d\boldsymbol{r}_2 g''_\omega(1)g_\omega(2)\frac{\delta(r_1-r'_1)}{r_1^2}\frac{\delta(r_1-r''_1)}{r_1^2}\sum_{LL'\nu\nu'k}(-)^{\nu+\nu'+k}R_{LL}(m_\omega;r_1,r_2) \\
&\times\langle f_A|Y_{L'\nu'}|f_a\rangle_{r''_1}\langle f_b|Y_{L'-\nu'}|f_B\rangle_{r'_1}\langle f_c|Y_{L\nu}\alpha_k|f_d\rangle_{r_1}\langle f_d|Y_{L-\nu}\alpha_{-k}|f_c\rangle_{r_2} \\
=\;& \delta_{q_Aq_a}\delta_{q_Bq_b}\frac{\hat{J}^{-2}}{4\pi}\langle A||Y_J||a\rangle\langle B||Y_J||b\rangle\sum_{cd}\int d\boldsymbol{r}_1 d\boldsymbol{r}_2 g''_\omega(1)g_\omega(2)\sum_{L\nu k}(-)^{\nu+k}R_{LL}(m_\omega;r_1,r_2) \\
&\times\left[\frac{(G_AG_a+F_AF_a)(G_BG_b+F_BF_b)}{r^4}\right]_{r_1}\langle f_c|Y_{L\nu}\alpha_k|f_d\rangle_{r_1}\langle f_d|Y_{L-\nu}\alpha_{-k}|f_c\rangle_{r_2} \\
=\;& \delta_{q_Aq_a}\delta_{q_Bq_b}\frac{\hat{J}^{-2}}{4\pi}\langle A||Y_J||a\rangle\langle B||Y_J||b\rangle\sum_{j_cj_dLJ'}\delta_{q_cq_d}\int dr_1 dr_2 R_{LL}(m_\omega;r_1,r_2) \\
&\times\left[g''_\omega\frac{(G_AG_a+F_AF_a)(G_BG_b+F_BF_b)}{r^4}\left(G_cF_d\langle c||\mathscr{T}_{J'L}||d'\rangle-F_cG_d\langle c'||\mathscr{T}_{J'L}||d\rangle\right)\right]_{r_1} \\
&\times\left[g_\omega\left(G_cF_d\langle c||\mathscr{T}_{J'L}||d'\rangle-F_cG_d\langle c'||\mathscr{T}_{J'L}||d\rangle\right)\right]_{r_2},
\end{aligned}
\tag{A.73}
$$

where $\langle b||\mathscr{T}_{JL}||a\rangle=(-)^{j_a+j_b+J+L}\langle a||\mathscr{T}_{JL}||b\rangle$ in **Remark 14** is used.

For the Term14 in Eq. (2.79),

$$
\begin{aligned}
&\bar{\bar{H}}_{14}^{J\omega}(AaBb) \\
=\;& \sum_{cd}\sum_{mM}(-)^{j_A+j_B-m_A-m_B}\begin{pmatrix} j_A & j_a & J \\ m_A & -m_a & -M \end{pmatrix}\begin{pmatrix} j_B & j_b & J \\ m_B & -m_b & -M \end{pmatrix} \\
&\times\int d\boldsymbol{r}_1 d\boldsymbol{r}'_1 d\boldsymbol{r}_2 d\boldsymbol{r}'_2 g'_\omega(1)g'_\omega(2)\frac{\delta(r_1-r'_1)}{r_1^2}\frac{\delta(r_2-r'_2)}{r_2^2}\sum_{LL'L''\nu\nu'\nu''k}(-)^{\nu+\nu'+\nu''+k}R_{LL}(m_\omega;r_1,r_2) \\
&\times\langle f_A|Y_{L'\nu'}|f_a\rangle_{r'_1}\langle f_c|Y_{L'-\nu'}Y_{L-\nu}\alpha_{-k}|f_d\rangle_{r_1}\langle f_d|Y_{L''\nu''}Y_{L\nu}\alpha_k|f_c\rangle_{r_2}\langle f_b|Y_{L''-\nu''}|f_B\rangle_{r'_2} \\
=\;& \delta_{q_Aq_a}\delta_{q_Bq_b}\hat{J}^{-4}\langle A||Y_J||a\rangle\langle B||Y_J||b\rangle\sum_{cd}\int d\boldsymbol{r}_1 d\boldsymbol{r}_2 g'_\omega(1)g'_\omega(2)\sum_{L\nu Mk}(-)^{\nu+M+k}R_{LL}(m_\omega;r_1,r_2) \\
&\times\left[\frac{(G_AG_a+F_AF_a)}{r^2}\right]_{r_1}\left[\frac{(G_BG_b+F_BF_b)}{r^2}\right]_{r_2}\langle f_c|Y_{J-M}Y_{L-\nu}\alpha_{-k}|f_d\rangle_{r_1}\langle f_d|Y_{JM}Y_{L\nu}\alpha_k|f_c\rangle_{r_2}.
\end{aligned}
\tag{A.74}
$$

As calculated before,

$$
\begin{aligned}
&\langle f_c|Y_{J-M}Y_{L-\nu}\alpha_{-k}|f_d\rangle_{r_1} \\
=\;& \delta_{q_cq_d}\sum_{L'\nu'J'M'}(-)^{\nu'+j_c-m_c+L'-1+M'}\frac{\hat{J}\hat{L}\hat{L}'\hat{J}'}{\sqrt{4\pi}} \\
&\times\begin{pmatrix} J & L & L' \\ 0 & 0 & 0 \end{pmatrix}\begin{pmatrix} J & L & L' \\ -M & -\nu & \nu' \end{pmatrix}\begin{pmatrix} L' & 1 & J' \\ -\nu' & -k & -M' \end{pmatrix}\begin{pmatrix} j_c & J' & j_d \\ -m_c & M' & m_d \end{pmatrix} \\
&\times\frac{1}{r_1^2}\left[iG_cF_d\langle c||\mathscr{T}_{J'L'}||d'\rangle-iF_cG_d\langle c'||\mathscr{T}_{J'L'}||d\rangle\right]_{r_1},
\end{aligned}
\tag{A.75}
$$

and

$$\begin{aligned}
&\langle f_d|Y_{JM}Y_{L\nu}\alpha_k|f_c\rangle_{r_2} \\
&= \delta_{q_cq_d}\sum_{L''\nu''J''M''}(-)^{\nu''+j_d-m_d+L''-1+M''}\frac{\hat{J}\hat{L}\hat{L}''\hat{J}''}{\sqrt{4\pi}} \\
&\times\begin{pmatrix} J & L & L'' \\ 0 & 0 & 0\end{pmatrix}\begin{pmatrix} J & L & L'' \\ M & \nu & \nu''\end{pmatrix}\begin{pmatrix} L'' & 1 & J'' \\ -\nu'' & k & -M''\end{pmatrix}\begin{pmatrix} j_d & J'' & j_c \\ -m_d & M'' & m_c\end{pmatrix} \\
&\times\frac{1}{r_2^2}\left[iG_dF_c\langle d||\mathscr{T}_{J''L''}||c'\rangle - iF_dG_c\langle d'||\mathscr{T}_{J''L''}||c\rangle\right]_{r_2}, \qquad (A.76)
\end{aligned}$$

the final result reads

$$\begin{aligned}
&\bar{\bar{H}}_{14}^{J\omega}(AaBb) \\
&= \delta_{q_Aq_a}\delta_{q_Bq_b}\frac{\hat{J}^{-2}}{4\pi}\langle A||Y_J||a\rangle\langle B||Y_J||b\rangle\sum_{j_cj_dLL'J'}\delta_{q_cq_d}\hat{L}^2\begin{pmatrix} J & L & L' \\ 0 & 0 & 0\end{pmatrix}^2 \\
&\times\int dr_1dr_2R_{LL}(m_\omega;r_1,r_2)\left[g'_\omega\frac{(G_AG_a+F_AF_a)}{r^2}\left(G_cF_d\langle c||\mathscr{T}_{J'L'}||d'\rangle - F_cG_d\langle c'||\mathscr{T}_{J'L'}||d\rangle\right)\right]_{r_1} \\
&\times\left[g'_\omega\frac{(G_BG_b+F_BF_b)}{r^2}\left(G_cF_d\langle c||\mathscr{T}_{J'L'}||d'\rangle - F_cG_d\langle c'||\mathscr{T}_{J'L'}||d\rangle\right)\right]_{r_2}. \qquad (A.77)
\end{aligned}$$

In summary, the contributions from the time component are

$$\begin{aligned}
\bar{H}_1^{J\omega}(1234) &= \delta_{q_1q_2}\delta_{q_3q_4}\hat{J}^{-2}\langle 1||Y_J||2\rangle\langle 3||Y_J||4\rangle \\
&\times\int dr_1dr_2R_{JJ}(m_\omega;r_1,r_2)[g_\omega(G_1G_2+F_1F_2)]_{r_1} \\
&\times[g_\omega(G_3G_4+F_3F_4)]_{r_2}, \qquad (A.78)
\end{aligned}$$

$$\begin{aligned}
\bar{H}_2^{J\omega}(1234) &= \delta_{q_1q_2}\delta_{q_3q_4}\hat{J}^{-2}\langle 1||Y_J||2\rangle\langle 3||Y_J||4\rangle \\
&\times\int dr\frac{1}{r^2}g'_\omega(r)\omega(r)(G_1G_2+F_1F_2)(G_3G_4+F_3F_4), \qquad (A.79)
\end{aligned}$$

$$\begin{aligned}
\bar{H}_3^{J\omega}(1234) &= \delta_{q_1q_2}\delta_{q_3q_4}\hat{J}^{-2}\langle 1||Y_J||2\rangle\langle 3||Y_J||4\rangle \\
&\times\int dr_1dr_2R_{JJ}(m_\omega;r_1,r_2)[g_\omega(G_1G_2+F_1F_2)]_{r_1} \\
&\times[g'_\omega\rho_v(G_3G_4+F_3F_4)]_{r_2}, \qquad (A.80)
\end{aligned}$$

$$\begin{aligned}
\bar{H}_6^{J\omega}(1234) &= \delta_{q_1q_2}\delta_{q_3q_4}\hat{J}^{-2}\langle 1||Y_J||2\rangle\langle 3||Y_J||4\rangle \\
&\times\int dr\frac{1}{r^2}g''_\omega(r)\rho_v(r)\omega(r)(G_1G_2+F_1F_2)(G_3G_4+F_3F_4), \qquad (A.81)
\end{aligned}$$

$$\begin{aligned}
\bar{H}_7^{J\omega}(1234) &= \delta_{q_1q_2}\delta_{q_3q_4}\hat{J}^{-2}\langle 1||Y_J||2\rangle\langle 3||Y_J||4\rangle \\
&\times\int dr_1dr_2R_{JJ}(m_\omega;r_1,r_2)[g'_\omega\rho_v(G_1G_2+F_1F_2)]_{r_1} \\
&\times[g'_\omega\rho_v(G_3G_4+F_3F_4)]_{r_2}, \qquad (A.82)
\end{aligned}$$

$$\begin{aligned}\bar{H}_9^{J\omega}(1234) &= \delta_{q_1q_2}\delta_{q_3q_4}(-)^{j_1+j_2+1}\frac{\hat{J}^{-1}}{\sqrt{4\pi}}\sum_{j_dLL'}\delta_{q_dq_2}\hat{L}\hat{L}'\begin{pmatrix} J & L & L' \\ 0 & 0 & 0\end{pmatrix}\begin{Bmatrix} j_1 & j_2 & J \\ L & L' & j_d\end{Bmatrix} \\ &\times\langle 3||Y_J||4\rangle\langle 1||Y_{L'}||d\rangle\langle d||Y_L||2\rangle \\ &\times\int dr_1dr_2R_{LL}(m_\omega;r_1,r_2)\left[g'_\omega\frac{(G_3G_4+F_3F_4)(G_1G_d+F_1F_d)}{r^2}\right]_{r_1} \\ &\times[g_\omega(G_dG_2+F_dF_2)]_{r_2}, \end{aligned} \tag{A.83}$$

$$\begin{aligned}\bar{H}_{13}^{J\omega}(1234) &= -\delta_{q_1q_2}\delta_{q_3q_4}\frac{\hat{J}^{-2}}{4\pi}\langle 1||Y_J||2\rangle\langle 3||Y_J||4\rangle\sum_{j_cj_dL}\delta_{q_cq_d}\langle c||Y_L||d\rangle^2 \\ &\times\int dr_1dr_2R_{LL}(m_\omega;r_1,r_2)\left[g''_\omega\frac{(G_1G_2+F_1F_2)(G_3G_4+F_3F_4)(G_cG_d+F_cF_d)}{r^4}\right]_{r_1} \\ &\times[g_\omega(G_cG_d+F_cF_d)]_{r_2}, \end{aligned} \tag{A.84}$$

$$\begin{aligned}\bar{H}_{14}^{J\omega}(1234) &= -\delta_{q_1q_2}\delta_{q_3q_4}\frac{\hat{J}^{-2}}{4\pi}\langle 1||Y_J||2\rangle\langle 3||Y_J||4\rangle\sum_{j_cj_dLL'}\delta_{q_cq_d}\hat{L}^2\begin{pmatrix} J & L & L' \\ 0 & 0 & 0\end{pmatrix}^2\langle c||Y_{L'}||d\rangle^2 \\ &\times\int dr_1dr_2R_{LL}(m_\omega;r_1,r_2)\left[g'_\omega\frac{(G_1G_2+F_1F_2)(G_cG_d+F_cF_d)}{r^2}\right]_{r_1} \\ &\times\left[g'_\omega\frac{(G_3G_4+F_3F_4)(G_cG_d+F_cF_d)}{r^2}\right]_{r_2}, \end{aligned} \tag{A.85}$$

with the short-hand notation for the ω-field

$$\omega(1)=\int dr_2r_2^2R_{00}(m_\omega;1,2)\rho_v(2)g_\omega(2), \tag{A.86}$$

where the baryonic density is

$$\rho_v(r)=\sum_d\frac{1}{4\pi r^2}[G_d^2(r)+F_d^2(r)]. \tag{A.87}$$

Moreover, the contributions from the space component are

$$\begin{aligned}\bar{\bar{H}}_1^{J\omega}(1234) &= -\delta_{q_1q_2}\delta_{q_3q_4}\hat{J}^{-2} \\ &\times\sum_L\int dr_1dr_2R_{LL}(m_\omega;r_1,r_2)\left[g_\omega\left(G_1F_2\langle 1||\mathscr{T}_{JL}||2'\rangle-F_1G_2\langle 1'||\mathscr{T}_{JL}||2\rangle\right)\right]_{r_1} \\ &\times\left[g_\omega\left(G_3F_4\langle 3||\mathscr{T}_{JL}||4'\rangle-F_3G_4\langle 3'||\mathscr{T}_{JL}||4\rangle\right)\right]_{r_2}, \end{aligned} \tag{A.88}$$

$$\bar{\bar{H}}_i^{J\omega}(1234)=0, \qquad \text{for} \quad i=2,3,\cdots,7, \tag{A.89}$$

$$
\begin{aligned}
&\bar{\bar{H}}_9^{J\omega}(1234) \\
&= \delta_{q_1q_2}\delta_{q_3q_4}(-)^{j_1+j_2+1}\frac{\hat{J}^{-1}}{\sqrt{4\pi}}\sum_{j_dLL'J'J''}\delta_{q_dq_2}(-)^{J''+L}\hat{L}\hat{L}'\hat{J}'\hat{J}'' \\
&\times\begin{pmatrix} J & L & L' \\ 0 & 0 & 0 \end{pmatrix}\begin{Bmatrix} j_2 & j_1 & J \\ J' & J'' & j_d \end{Bmatrix}\begin{Bmatrix} J' & J'' & J \\ L & L' & 1 \end{Bmatrix}\langle 3||Y_J||4\rangle \\
&\times\int dr_1dr_2R_{LL}(m_\omega;r_1,r_2) \\
&\quad\times\left[g'_\omega\frac{(G_3G_4+F_3F_4)}{r^2}\left(G_1F_d\langle 1||\mathscr{T}_{J'L'}||d'\rangle - F_1G_d\langle 1'||\mathscr{T}_{J'L'}||d\rangle\right)\right]_{r_1} \\
&\quad\times\left[g_\omega\left(G_dF_2\langle d||\mathscr{T}_{J''L}||2'\rangle - F_dG_2\langle d'||\mathscr{T}_{J''L}||2\rangle\right)\right]_{r_2}, \qquad (A.90)
\end{aligned}
$$

$$
\begin{aligned}
&\bar{\bar{H}}_{13}^{J\omega}(1234) \\
&= \delta_{q_1q_2}\delta_{q_3q_4}\frac{\hat{J}^{-2}}{4\pi}\langle 1||Y_J||2\rangle\langle 3||Y_J||4\rangle\sum_{j_cj_dLJ'}\delta_{q_cq_d}\int dr_1dr_2R_{LL}(m_\omega;r_1,r_2) \\
&\times\left[g''_\omega\frac{(G_1G_2+F_1F_2)(G_3G_4+F_3F_4)}{r^4}\left(G_cF_d\langle c||\mathscr{T}_{J'L}||d'\rangle - F_cG_d\langle c'||\mathscr{T}_{J'L}||d\rangle\right)\right]_{r_1} \\
&\times\left[g_\omega\left(G_cF_d\langle c||\mathscr{T}_{J'L}||d'\rangle - F_cG_d\langle c'||\mathscr{T}_{J'L}||d\rangle\right)\right]_{r_2}, \qquad (A.91)
\end{aligned}
$$

$$
\begin{aligned}
&\bar{\bar{H}}_{14}^{J\omega}(1234) \\
&= \delta_{q_1q_2}\delta_{q_3q_4}\frac{\hat{J}^{-2}}{4\pi}\langle 1||Y_J||2\rangle\langle 3||Y_J||4\rangle\sum_{j_cj_dLL'J'}\delta_{q_cq_d}\hat{L}^2\begin{pmatrix} J & L & L' \\ 0 & 0 & 0 \end{pmatrix}^2 \\
&\times\int dr_1dr_2R_{LL}(m_\omega;r_1,r_2)\left[g'_\omega\frac{(G_1G_2+F_1F_2)}{r^2}\left(G_cF_d\langle c||\mathscr{T}_{J'L'}||d'\rangle - F_cG_d\langle c'||\mathscr{T}_{J'L'}||d\rangle\right)\right]_{r_1} \\
&\quad\times\left[g'_\omega\frac{(G_3G_4+F_3F_4)}{r^2}\left(G_cF_d\langle c||\mathscr{T}_{J'L'}||d'\rangle - F_cG_d\langle c'||\mathscr{T}_{J'L'}||d\rangle\right)\right]_{r_2}. \qquad (A.92)
\end{aligned}
$$

A.4 ρ-meson contribution to the p-h matrix elements

In this section, the quantities $H^J(1234)$ in Eq. (2.85) induced by the ρ-meson with vector coupling will be summarized.

For the ρ-meson with vector coupling, the two-body interaction reads

$$V^\rho(1,2) = [g_\rho\gamma_0\gamma^\mu\vec{\tau}]_1\cdot[g_\rho\gamma_0\gamma_\mu\vec{\tau}]_2D_\rho(1,2). \qquad (A.93)$$

The quantities $H^{J\rho}(1234)$ in Eq. (2.85) can be derived in analogy with the derivations of the $\omega-$meson, with the two following replacements are needed. First, one should replace the mass of the meson and the coupling strength,

$$g_\omega, m_\omega \to g_\rho, m_\rho. \qquad (A.94)$$

Second, one should be careful about the isospin properties at the interaction vertices. For example, in $\bar{H}_1^{J\rho}(1234)$, the following substitution is needed,

$$\delta_{q_1q_2}\delta_{q_4q_3} \to \langle q_1|\vec{\tau}|q_2\rangle\cdot\langle q_4|\vec{\tau}|q_3\rangle. \qquad (A.95)$$

The final results are summarized as follows,

$$\begin{aligned}\bar{H}_1^{J\rho V}(1234) &= \langle q_1|\vec{\tau}|q_2\rangle\cdot\langle q_4|\vec{\tau}|q_3\rangle\hat{J}^{-2}\langle 1||Y_J||2\rangle\langle 3||Y_J||4\rangle \\ &\quad\times\int dr_1dr_2R_{JJ}(m_\rho;r_1,r_2)[g_\rho(G_1G_2+F_1F_2)]_{r_1} \\ &\quad\times[g_\rho(G_3G_4+F_3F_4)]_{r_2}, \end{aligned} \tag{A.96}$$

$$\begin{aligned}\bar{H}_2^{J\rho V}(1234) &= \delta_{q_1q_2}\delta_{q_3q_4}\tau_{q_1}\hat{J}^{-2}\langle 1||Y_J||2\rangle\langle 3||Y_J||4\rangle \\ &\quad\times\int dr\frac{1}{r^2}g'_\rho(r)\rho(r)(G_1G_2+F_1F_2)(G_3G_4+F_3F_4), \end{aligned} \tag{A.97}$$

$$\begin{aligned}\bar{H}_3^{J\rho V}(1234) &= \delta_{q_1q_2}\delta_{q_3q_4}\tau_{q_1}\hat{J}^{-2}\langle 1||Y_J||2\rangle\langle 3||Y_J||4\rangle \\ &\quad\times\int dr_1dr_2R_{JJ}(m_\rho;r_1,r_2)[g_\rho(G_1G_2+F_1F_2)]_{r_1} \\ &\quad\times[g'_\rho\rho_v^{(3)}(G_3G_4+F_3F_4)]_{r_2}, \end{aligned} \tag{A.98}$$

$$\begin{aligned}\bar{H}_6^{J\rho V}(1234) &= \delta_{q_1q_2}\delta_{q_3q_4}\hat{J}^{-2}\langle 1||Y_J||2\rangle\langle 3||Y_J||4\rangle \\ &\quad\times\int dr\frac{1}{r^2}g''_\rho(r)\rho_v^{(3)}(r)\rho(r)(G_1G_2+F_1F_2)(G_3G_4+F_3F_4), \end{aligned} \tag{A.99}$$

$$\begin{aligned}\bar{H}_7^{J\rho V}(1234) &= \delta_{q_1q_2}\delta_{q_3q_4}\hat{J}^{-2}\langle 1||Y_J||2\rangle\langle 3||Y_J||4\rangle \\ &\quad\times\int dr_1dr_2R_{JJ}(m_\rho;r_1,r_2)[g'_\rho\rho_v^{(3)}(G_1G_2+F_1F_2)]_{r_1} \\ &\quad\times[g'_\rho\rho_v^{(3)}(G_3G_4+F_3F_4)]_{r_2}, \end{aligned} \tag{A.100}$$

$$\begin{aligned}\bar{H}_9^{J\rho V}(1234) &= \delta_{q_1q_2}\delta_{q_3q_4}(-)^{j_1+j_2+1}\frac{\hat{J}^{-1}}{\sqrt{4\pi}}\sum_{j_dLL'}(2-\delta_{q_dq_2})\hat{L}\hat{L}'\begin{pmatrix} J & L & L' \\ 0 & 0 & 0\end{pmatrix}\begin{Bmatrix} j_1 & j_2 & J \\ L & L' & j_d\end{Bmatrix} \\ &\quad\times\langle 3||Y_J||4\rangle\langle 1||Y_{L'}||d\rangle\langle d||Y_L||2\rangle \\ &\quad\times\int dr_1dr_2R_{LL}(m_\rho;r_1,r_2)\left[g'_\rho\frac{(G_3G_4+F_3F_4)(G_1G_d+F_1F_d)}{r^2}\right]_{r_1} \\ &\quad\times[g_\rho(G_dG_2+F_dF_2)]_{r_2}, \end{aligned} \tag{A.101}$$

$$\begin{aligned}\bar{H}_{13}^{J\rho V}(1234) &= -\delta_{q_1q_2}\delta_{q_3q_4}\frac{\hat{J}^{-2}}{4\pi}\langle 1||Y_J||2\rangle\langle 3||Y_J||4\rangle\sum_{j_cj_dL}(2-\delta_{q_cq_d})\langle c||Y_L||d\rangle^2 \\ &\quad\times\int dr_1dr_2R_{LL}(m_\rho;r_1,r_2)\left[g''_\rho\frac{(G_1G_2+F_1F_2)(G_3G_4+F_3F_4)(G_cG_d+F_cF_d)}{r^4}\right]_{r_1} \\ &\quad\times[g_\rho(G_cG_d+F_cF_d)]_{r_2}, \end{aligned} \tag{A.102}$$

$$\begin{aligned}\bar{H}_{14}^{J\rho V}(1234) &= -\delta_{q_1q_2}\delta_{q_3q_4}\frac{\hat{J}^{-2}}{4\pi}\langle 1||Y_J||2\rangle\langle 3||Y_J||4\rangle\sum_{j_cj_dLL'}(2-\delta_{q_cq_d})\hat{L}^2\begin{pmatrix} J & L & L' \\ 0 & 0 & 0\end{pmatrix}^2\langle c||Y_{L'}||d\rangle^2 \\ &\quad\times\int dr_1dr_2R_{LL}(m_\rho;r_1,r_2)\left[g'_\rho\frac{(G_1G_2+F_1F_2)(G_cG_d+F_cF_d)}{r^2}\right]_{r_1} \\ &\quad\times\left[g'_\rho\frac{(G_3G_4+F_3F_4)(G_cG_d+F_cF_d)}{r^2}\right]_{r_2}, \end{aligned} \tag{A.103}$$

with the short-hand notation for the ρ-field

$$\rho(1) = \int dr_2 r_2^2 R_{00}(m_\rho; 1, 2)\rho_v^{(3)}(2) g_\rho(2), \tag{A.104}$$

where the isovector baryonic density is

$$\rho_v^{(3)} = \sum_d \frac{\tau_d}{4\pi r^2}[G_d^2(r) + F_d^2(r)]. \tag{A.105}$$

Moreover,

$$\begin{aligned}
\bar{\bar{H}}_1^{J\rho V}(1234) &= -\langle q_1|\vec{\tau}|q_2\rangle \cdot \langle q_4|\vec{\tau}|q_3\rangle \hat{J}^{-2} \\
&\quad \times \sum_L \int dr_1 dr_2 R_{LL}(m_\rho; r_1, r_2) \left[g_\rho \left(G_1 F_2 \langle 1||\mathscr{T}_{JL}||2'\rangle - F_1 G_2 \langle 1'||\mathscr{T}_{JL}||2\rangle \right) \right]_{r_1} \\
&\quad \times \left[g_\rho \left(G_3 F_4 \langle 3||\mathscr{T}_{JL}||4'\rangle - F_3 G_4 \langle 3'||\mathscr{T}_{JL}||4\rangle \right) \right]_{r_2}, \qquad \text{(A.106)} \\
&\bar{\bar{H}}_i^{J\rho V}(1234) = 0, \qquad \text{for} \quad i = 2, 3, \cdots, 7, \qquad \text{(A.107)}
\end{aligned}$$

$$\begin{aligned}
&\bar{\bar{H}}_9^{J\rho V}(1234) \\
&= \delta_{q_1 q_2}\delta_{q_3 q_4}(-)^{j_1+j_2+1}\frac{\hat{J}^{-1}}{\sqrt{4\pi}} \sum_{j_d L L' J' J''} (2 - \delta_{q_d q_2})(-)^{J''+L} \hat{L}\hat{L}'\hat{J}'\hat{J}'' \\
&\quad \times \begin{pmatrix} J & L & L' \\ 0 & 0 & 0 \end{pmatrix} \begin{Bmatrix} j_2 & j_1 & J \\ J' & J'' & j_d \end{Bmatrix} \begin{Bmatrix} J' & J'' & J \\ L & L' & 1 \end{Bmatrix} \langle 3||Y_J||4\rangle \\
&\quad \times \int dr_1 dr_2 R_{LL}(m_\rho; r_1, r_2) \\
&\qquad \times \left[g'_\rho \frac{(G_3 G_4 + F_3 F_4)}{r^2} \left(G_1 F_d \langle 1||\mathscr{T}_{J'L'}||d'\rangle - F_1 G_d \langle 1'||\mathscr{T}_{J'L'}||d\rangle \right) \right]_{r_1} \\
&\qquad \times \left[g_\rho \left(G_d F_2 \langle d||\mathscr{T}_{J''L}||2'\rangle - F_d G_2 \langle d'||\mathscr{T}_{J''L}||2\rangle \right) \right]_{r_2}, \qquad \text{(A.108)}
\end{aligned}$$

$$\begin{aligned}
&\bar{\bar{H}}_{13}^{J\rho V}(1234) \\
&= \delta_{q_1 q_2}\delta_{q_3 q_4}\frac{\hat{J}^{-2}}{4\pi}\langle 1||Y_J||2\rangle\langle 3||Y_J||4\rangle \sum_{j_c j_d L J'} (2 - \delta_{q_c q_d}) \int dr_1 dr_2 R_{LL}(m_\rho; r_1, r_2) \\
&\quad \times \left[g''_\rho \frac{(G_1 G_2 + F_1 F_2)(G_3 G_4 + F_3 F_4)}{r^4} \left(G_c F_d \langle c||\mathscr{T}_{J'L}||d'\rangle - F_c G_d \langle c'||\mathscr{T}_{J'L}||d\rangle \right) \right]_{r_1} \\
&\quad \times \left[g_\rho \left(G_c F_d \langle c||\mathscr{T}_{J'L}||d'\rangle - F_c G_d \langle c'||\mathscr{T}_{J'L}||d\rangle \right) \right]_{r_2}, \qquad \text{(A.109)}
\end{aligned}$$

$$\begin{aligned}
&\bar{\bar{H}}_{14}^{J\rho V}(1234) \\
&= \delta_{q_1 q_2}\delta_{q_3 q_4}\frac{\hat{J}^{-2}}{4\pi}\langle 1||Y_J||2\rangle\langle 3||Y_J||4\rangle \sum_{j_c j_d L L' J'} (2 - \delta_{q_c q_d})\hat{L}^2 \begin{pmatrix} J & L & L' \\ 0 & 0 & 0 \end{pmatrix}^2 \\
&\quad \times \int dr_1 dr_2 R_{LL}(m_\rho; r_1, r_2) \\
&\qquad \times \left[g'_\rho \frac{(G_1 G_2 + F_1 F_2)}{r^2} \left(G_c F_d \langle c||\mathscr{T}_{J'L'}||d'\rangle - F_c G_d \langle c'||\mathscr{T}_{J'L'}||d\rangle \right) \right]_{r_1} \\
&\qquad \times \left[g'_\rho \frac{(G_3 G_4 + F_3 F_4)}{r^2} \left(G_c F_d \langle c||\mathscr{T}_{J'L'}||d'\rangle - F_c G_d \langle c'||\mathscr{T}_{J'L'}||d\rangle \right) \right]_{r_2}. \qquad \text{(A.110)}
\end{aligned}$$

A.5 Pion contribution to the p-h matrix elements

In this section, the derivations for the quantities $H^J(1234)$ in Eq. (2.85) induced by the pseudo-vector pion will be given in details.

The two-body interaction reads

$$V^\pi(1,2) = -[\frac{f_\pi}{m_\pi}\vec{\tau}\gamma_0\gamma_5\gamma^\mu\partial_\mu]_1 \cdot [\frac{f_\pi}{m_\pi}\vec{\tau}\gamma_0\gamma_5\gamma^\nu\partial_\nu]_2 D_\pi(1,2). \tag{A.111}$$

Because the retardation effect is neglected, the meson propagator is time independent. The interaction can be expressed as,

$$V^\pi(1,2) = -[\frac{f_\pi}{m_\pi}\vec{\tau}\gamma_0\gamma_5\gamma^k\partial_k]_1 \cdot [\frac{f_\pi}{m_\pi}\vec{\tau}\gamma_0\gamma_5\gamma^l\partial_l]_2 D_\pi(1,2). \tag{A.112}$$

The gradients acting on the propagator give (see **Remark 10**)

$$\begin{aligned}\nabla_2\nabla_1 D(\mu;\boldsymbol{r}_1,\boldsymbol{r}_2) &= \mu^2\sum_L\sum_{L_1L_2}^{L\pm1}\hat{L}_1\hat{L}_2\begin{pmatrix} L & 1 & L_1\\ 0 & 0 & 0\end{pmatrix}\begin{pmatrix} L & 1 & L_2\\ 0 & 0 & 0\end{pmatrix}\\ &\times\mathscr{V}_L^{L_1L_2}(\mu;r_1,r_2)\boldsymbol{Y}_{LL_1}(\hat{\boldsymbol{r}}_1)\cdot\boldsymbol{Y}_{LL_2}(\hat{\boldsymbol{r}}_2),\end{aligned} \tag{A.113}$$

where

$$\mathscr{V}_L^{L_1L_2}(\mu;r_1,r_2) \equiv -R_{L_1L_2}(\mu;r_1,r_2) + \frac{1}{\mu^2 r_1^2}\delta(r_1-r_2), \tag{A.114}$$

and the scalar product of vector spherical harmonics $\boldsymbol{Y}^{L_1}_{LM} \equiv \sum_{M_1\mu} C^{LM}_{L_1M_1 1\mu}Y_{L_1M_1}\boldsymbol{e}_\mu$ reads

$$\boldsymbol{Y}_{LL_1}(\hat{\boldsymbol{r}}_1)\cdot\boldsymbol{Y}_{LL_2}(\hat{\boldsymbol{r}}_2) = \sum_M(-)^M\boldsymbol{Y}^{L_1}_{LM}(\hat{\boldsymbol{r}}_1)\boldsymbol{Y}^{L_2}_{L-M}(\hat{\boldsymbol{r}}_2). \tag{A.115}$$

Therefore, the potential can be expressed as,

$$\begin{aligned}V^\pi(1,2) &= -\sum_{L\nu}\sum_{L_1L_2}^{L\pm1}(-)^\nu\hat{L}_1\hat{L}_2\begin{pmatrix} L & 1 & L_1\\ 0 & 0 & 0\end{pmatrix}\begin{pmatrix} L & 1 & L_2\\ 0 & 0 & 0\end{pmatrix}\\ &\times\left(f_\pi\vec{\tau}\gamma_0\gamma_5\boldsymbol{\gamma}\cdot\boldsymbol{Y}^{L_1}_{L\nu}\right)_{r_1}\mathscr{V}_L^{L_1L_2}(m_\pi;r_1,r_2)\left(f_\pi\vec{\tau}\gamma_0\gamma_5\boldsymbol{\gamma}\cdot\boldsymbol{Y}^{L_2}_{L-\nu}\right)_{r_2}.\end{aligned} \tag{A.116}$$

For the Term1 in Eq. (2.78),

$$\begin{aligned}\text{Term1} &= \int d\boldsymbol{r}_1 d\boldsymbol{r}_2 f_A^\dagger(1)f_b^\dagger(2)g(1)g(2)I(1,2)f_B(2)f_a(1)\\ &= -\int d\boldsymbol{r}_1 d\boldsymbol{r}_2 f_\pi(1)f_\pi(2)\sum_{L\nu}\sum_{L_1L_2}^{L\pm1}(-)^\nu\hat{L}_1\hat{L}_2\begin{pmatrix} L & 1 & L_1\\ 0 & 0 & 0\end{pmatrix}\begin{pmatrix} L & 1 & L_2\\ 0 & 0 & 0\end{pmatrix}\\ &\times\mathscr{V}_L^{L_1L_2}(m_\pi;r_1,r_2)\langle f_A|\vec{\tau}\gamma_0\gamma_5\boldsymbol{\gamma}\cdot\boldsymbol{Y}^{L_1}_{L\nu}|f_a\rangle_{r_1}\langle f_b|\vec{\tau}\gamma_0\gamma_5\boldsymbol{\gamma}\cdot\boldsymbol{Y}^{L_2}_{L-\nu}|f_B\rangle_{r_2}.\end{aligned} \tag{A.117}$$

The summation over m_A, m_a gives,

$$\begin{aligned}&\sum_{m_Am_a}(-)^{j_A-m_A}\begin{pmatrix} j_A & j_a & J\\ m_A & -m_a & -M\end{pmatrix}\langle f_A|\vec{\tau}\gamma_0\gamma_5\boldsymbol{\gamma}\cdot\boldsymbol{Y}^{L_1}_{L\nu}|f_a\rangle\\ =&\sum_{m_Am_a}(-)^{j_A-m_A}\begin{pmatrix} j_A & j_a & J\\ m_A & -m_a & -M\end{pmatrix}\frac{1}{r_1^2}\langle q_A|\vec{\tau}|q_a\rangle\\ &\times(-1)\left[G_AG_a\langle A|\boldsymbol{\sigma}\cdot\boldsymbol{Y}^{L_1}_{L\nu}|a\rangle + F_AF_a\langle A'|\boldsymbol{\sigma}\cdot\boldsymbol{Y}^{L_1}_{L\nu}|a'\rangle\right].\end{aligned} \tag{A.118}$$

Using the relations

$$\boldsymbol{\sigma}\cdot\boldsymbol{Y}^{L_1}_{L\nu}=\sum_{k'}\sigma_{k'}\boldsymbol{e}^{k'}\sum_{\mu k}C^{L\nu}_{L_1\mu 1k}Y_{L_1\mu}\boldsymbol{e}_k, \tag{A.119}$$

and

$$\boldsymbol{e}^{\mu}\boldsymbol{e}_{\nu}=\delta_{\mu\nu},\qquad(\mu,\nu=\pm1,0), \tag{A.120}$$

we can define

$$\mathscr{T}^{L_1}_{L\nu}\equiv\boldsymbol{\sigma}\cdot\boldsymbol{Y}^{L_1}_{L\nu}=\sum_{\mu k}C^{L\nu}_{L_1\mu 1k}Y_{L_1\mu}\sigma_k. \tag{A.121}$$

Therefore,

$$\begin{aligned}&\sum_{m_Am_a}(-)^{j_A-m_A}\begin{pmatrix}j_A & j_a & J\\ m_A & -m_a & -M\end{pmatrix}\langle f_A|\vec{\tau}\gamma_0\gamma_5\boldsymbol{\gamma}\cdot\boldsymbol{Y}^{L_1}_{L\nu}|f_a\rangle\\ =\;&-\langle q_A|\vec{\tau}|q_a\rangle\hat{J}^{-2}\delta_{JL}\delta_{M\nu}\frac{\left[G_AG_a\langle A||\mathscr{T}_{LL_1}||a\rangle+F_AF_a\langle A'||\mathscr{T}_{LL_1}||a'\rangle\right]_{r_1}}{r_1^2},\end{aligned} \tag{A.122}$$

where the Wigner-Eckart Theorem (see **Remark 13**) and the symmetry and orthogonality relations of 3-j Symbols (see **Remarks 2 and 3**) are used. The summation over m_B, m_b gives,

$$\begin{aligned}&\sum_{m_Bm_b}(-)^{j_B-m_B}\begin{pmatrix}j_B & j_b & J\\ m_B & -m_b & -M\end{pmatrix}\langle f_b|\vec{\tau}\gamma_0\gamma_5\boldsymbol{\gamma}\cdot\boldsymbol{Y}^{L_2}_{L-\nu}|f_B\rangle\\ =\;&-\langle q_b|\vec{\tau}|q_B\rangle(-)^{j_B-j_b-M}\hat{J}^{-2}\delta_{JL}\delta_{M\nu}\frac{\left[G_bG_B\langle b||\mathscr{T}_{LL_2}||B\rangle+F_bF_B\langle b'||\mathscr{T}_{LL_2}||B'\rangle\right]_{r_2}}{r_2^2}.\end{aligned} \tag{A.123}$$

Finally, $H^{\pi}_J(AaBb)$ can be expressed as,

$$\begin{aligned}H^{J\pi}_1(AaBb)\;=\;&-\langle q_A|\vec{\tau}|q_a\rangle\cdot\langle q_b|\vec{\tau}|q_B\rangle\hat{J}^{-2}\\ &\times\sum_{L_1L_2}^{J\pm1}\hat{L}_1\hat{L}_2\begin{pmatrix}J & 1 & L_1\\ 0 & 0 & 0\end{pmatrix}\begin{pmatrix}J & 1 & L_2\\ 0 & 0 & 0\end{pmatrix}\\ &\times\int dr_1dr_2\mathscr{V}^{L_1L_2}_J(m_\pi;r_1,r_2)\left[f_\pi\left(G_AG_a\langle A||\mathscr{T}_{JL_1}||a\rangle+F_AF_a\langle A'||\mathscr{T}_{JL_1}||a'\rangle\right)\right]_{r_1}\\ &\quad\times\left[f_\pi\left(G_BG_b\langle B||\mathscr{T}_{JL_2}||b\rangle+F_BF_b\langle B'||\mathscr{T}_{JL_2}||b'\rangle\right)\right]_{r_2},\end{aligned} \tag{A.124}$$

where $\langle b||\mathscr{T}_{JL}||a\rangle=(-)^{j_a+j_b+J+L}\langle a||\mathscr{T}_{JL}||b\rangle$ in **Remark 14** is used.

Because of parity conservation, the pion does not contribute to direct rearrangement terms,

$$H^{J\pi}_i(1234)=0,\qquad\text{for}\quad i=2,3,\cdots,7. \tag{A.125}$$

For the Term9 in Eq. (2.79),

$$\begin{aligned}&H^{J\pi}_9(AaBb)\\ =\;&\sum_d\sum_{mM}(-)^{j_A+j_B-m_A-m_B}\begin{pmatrix}j_A & j_a & J\\ m_A & -m_a & -M\end{pmatrix}\begin{pmatrix}j_B & j_b & J\\ m_B & -m_b & -M\end{pmatrix}\\ &\times\int d\boldsymbol{r}_1d\boldsymbol{r}'_1d\boldsymbol{r}_2f'_\pi(1)f_\pi(2)\frac{\delta(r_1-r'_1)}{r_1^2}\sum_{LL'\nu\nu'L_1L_2}(-)^{\nu+\nu'}\\ &\times\hat{L}_1\hat{L}_2\begin{pmatrix}L & 1 & L_1\\ 0 & 0 & 0\end{pmatrix}\begin{pmatrix}L & 1 & L_2\\ 0 & 0 & 0\end{pmatrix}\mathscr{V}^{L_1L_2}_L(m_\pi;r_1,r_2)\\ &\times\langle f_b|Y_{L'-\nu'}|f_B\rangle_{r'_1}\langle f_A|Y_{L'\nu'}\vec{\tau}\gamma_0\gamma_5\boldsymbol{\gamma}\cdot\boldsymbol{Y}^{L_1}_{L\nu}|f_d\rangle_{r_1}\langle f_d|\vec{\tau}\gamma_0\gamma_5\boldsymbol{\gamma}\cdot\boldsymbol{Y}^{L_2}_{L-\nu}|f_a\rangle_{r_2},\end{aligned} \tag{A.126}$$

with

$$\begin{aligned}
&\sum_{m_b m_B}(-)^{j_B-m_B+\nu'}\begin{pmatrix} j_B & j_b & J \\ m_B & -m_b & -M\end{pmatrix}\langle f_b|Y_{L'-\nu'}|f_B\rangle \\
&= \delta_{q_B q_b}\delta_{L'J}\delta_{\nu' M}\hat{J}^{-2}\langle B||Y_J||b\rangle\frac{(G_BG_b+F_BF_b)_{r_1'}}{{r_1'}^2}. \qquad \text{(A.127)}
\end{aligned}$$

Using

$$\boldsymbol{\sigma}\cdot\boldsymbol{Y}^{L_1}_{L\nu}=\sum_{M_1 k}(-)^{L_1-1+\nu}\hat{L}\begin{pmatrix} L_1 & 1 & L \\ M_1 & k & -\nu\end{pmatrix}Y_{L_1M_1}\sigma_k, \qquad \text{(A.128)}$$

$$Y_{JM}Y_{L_1M_1}=\sum_{L'\nu'}(-)^{\nu'}\frac{\hat{J}\hat{L}_1\hat{L}'}{\sqrt{4\pi}}\begin{pmatrix} J & L_1 & L' \\ 0 & 0 & 0\end{pmatrix}\begin{pmatrix} J & L_1 & L' \\ M & M_1 & \nu'\end{pmatrix}Y_{L'-\nu'}, \qquad \text{(A.129)}$$

and

$$Y_{L'-\nu'}\sigma_k=\sum_{J'M'}(-)^{L'-1+M'}\hat{J}'\begin{pmatrix} L' & 1 & J' \\ -\nu' & k & -M'\end{pmatrix}\mathscr{T}_{J'M'}, \qquad \text{(A.130)}$$

we can obtain that

$$\begin{aligned}
&\langle f_A|Y_{JM}\vec{\tau}\gamma_0\gamma_5\boldsymbol{\gamma}\cdot\boldsymbol{Y}^{L_1}_{L\nu}|f_d\rangle_{r_1} \\
=\ &\langle q_A|\vec{\tau}|q_d\rangle\sum_{M_1kL'\nu'J'M'}(-)^{1+L_1-1+\nu+\nu'+L'-1+M'+j_A-m_A}\frac{\hat{L}\hat{J}\hat{L}_1\hat{L}'\hat{J}'}{\sqrt{4\pi}} \\
&\times\begin{pmatrix} L_1 & 1 & L \\ M_1 & k & -\nu\end{pmatrix}\begin{pmatrix} J & L_1 & L' \\ 0 & 0 & 0\end{pmatrix}\begin{pmatrix} J & L_1 & L' \\ M & M_1 & \nu'\end{pmatrix} \\
&\times\begin{pmatrix} L' & 1 & J' \\ -\nu' & k & -M'\end{pmatrix}\begin{pmatrix} j_A & J' & j_d \\ -m_A & M' & m_d\end{pmatrix} \\
&\times\frac{1}{r_1^2}\left[G_AG_d\langle A||\mathscr{T}_{J'L'}||d\rangle+F_AF_d\langle A'||\mathscr{T}_{J'L'}||d'\rangle\right]_{r_1} \\
=\ &\langle q_A|\vec{\tau}|q_d\rangle\sum_{L'J'M'}(-)^{M'+j_A-m_A}\frac{\hat{L}\hat{J}\hat{L}_1\hat{L}'\hat{J}'}{\sqrt{4\pi}} \\
&\begin{pmatrix} J & L_1 & L' \\ 0 & 0 & 0\end{pmatrix}\begin{pmatrix} j_A & J' & j_d \\ -m_A & M' & m_d\end{pmatrix}\begin{pmatrix} J' & J & L \\ M' & -M & -\nu\end{pmatrix}\begin{Bmatrix} J' & J & L \\ L_1 & 1 & L'\end{Bmatrix} \\
&\times\frac{1}{r_1^2}\left[G_AG_d\langle A||\mathscr{T}_{J'L'}||d\rangle+F_AF_d\langle A'||\mathscr{T}_{J'L'}||d'\rangle\right]_{r_1}. \qquad \text{(A.131)}
\end{aligned}$$

Another component reads,

$$\begin{aligned}
&\langle f_d|\vec{\tau}\gamma_0\gamma_5\boldsymbol{\gamma}\cdot\boldsymbol{Y}^{L_2}_{L-\nu}|f_a\rangle_{r_2} \\
=\ &\langle q_d|\vec{\tau}|q_a\rangle(-)^{j_d-m_d+1}\begin{pmatrix} j_d & L & j_a \\ -m_d & -\nu & m_a\end{pmatrix} \\
&\times\frac{1}{r_2^2}\left[G_dG_a\langle d||\mathscr{T}_{LL_2}||a\rangle+F_dF_a\langle d'||\mathscr{T}_{LL_2}||a'\rangle\right]_{r_2}. \qquad \text{(A.132)}
\end{aligned}$$

Finally,

$$
\begin{aligned}
& H_9^{J\pi}(AaBb) \\
= \; & \delta_{q_Aq_a}\delta_{q_Bq_b}(-)^{j_A+j_a+1}\frac{\hat{J}^{-1}}{\sqrt{4\pi}}\sum_{j_dLL_1L_2L'J'}(2-\delta_{q_dq_a})\hat{L}\hat{L}_1^2\hat{L}_2\hat{L}'\hat{J}' \\
& \times\begin{pmatrix} L & 1 & L_1 \\ 0 & 0 & 0 \end{pmatrix}\begin{pmatrix} L & 1 & L_2 \\ 0 & 0 & 0 \end{pmatrix}\begin{pmatrix} J & L_1 & L' \\ 0 & 0 & 0 \end{pmatrix}\begin{Bmatrix} J' & J & L \\ L_1 & 1 & L' \end{Bmatrix}\begin{Bmatrix} j_A & j_a & J \\ L & J' & j_d \end{Bmatrix}\langle B||Y_J||b\rangle \\
& \times\int dr_1dr_2\mathscr{V}_L^{L_1L_2}(m_\pi;r_1,r_2)\left[f'_\pi\frac{(G_BG_b+F_BF_b)}{r^2}\left(G_AG_d\langle A||\mathscr{T}_{J'L'}||d\rangle+F_AF_d\langle A'||\mathscr{T}_{J'L'}||d'\rangle\right)\right]_{r_1} \\
& \quad\times\left[f_\pi\left(G_dG_a\langle d||\mathscr{T}_{LL_2}||a\rangle+F_dF_a\langle d'||\mathscr{T}_{LL_2}||a'\rangle\right)\right]_{r_2}. \qquad \text{(A.133)}
\end{aligned}
$$

For the Term13 in Eq. (2.79),

$$
\begin{aligned}
& H_{13}^{J\pi}(AaBb) \\
= \; & \sum_{cd}\sum_{mM}(-)^{j_A+j_B-m_A-m_B}\begin{pmatrix} j_A & j_a & J \\ m_A & -m_a & -M \end{pmatrix}\begin{pmatrix} j_B & j_b & J \\ m_B & -m_b & -M \end{pmatrix} \\
& \times\frac{1}{4\pi}\int d\boldsymbol{r}_1d\boldsymbol{r}'_1d\boldsymbol{r}''_1d\boldsymbol{r}_2f''_\pi(1)f_\pi(2)\frac{\delta(r_1-r'_1)}{r_1^2}\frac{\delta(r_1-r''_1)}{r_1^2}\sum_{LL'\nu\nu'L_1L_2}(-)^{\nu+\nu'} \\
& \times\hat{L}_1\hat{L}_2\begin{pmatrix} L & 1 & L_1 \\ 0 & 0 & 0 \end{pmatrix}\begin{pmatrix} L & 1 & L_2 \\ 0 & 0 & 0 \end{pmatrix}\mathscr{V}_L^{L_1L_2}(m_\pi;r_1,r_2) \\
& \times\langle f_A|Y_{L'\nu'}|f_a\rangle_{r''_1}\langle f_b|Y_{L'-\nu'}|f_B\rangle_{r'_1}\langle f_c|\vec{\tau}\gamma_0\gamma_5\boldsymbol{\gamma}\cdot\boldsymbol{Y}_{L\nu}^{L_1}|f_d\rangle_{r_1}\langle f_d|\vec{\tau}\gamma_0\gamma_5\boldsymbol{\gamma}\cdot\boldsymbol{Y}_{L-\nu}^{L_2}|f_c\rangle_{r_2} \\
= \; & \delta_{q_Aq_a}\delta_{q_Bq_b}\frac{\hat{J}^{-2}}{4\pi}\langle A||Y_J||a\rangle\langle B||Y_J||b\rangle\sum_{j_cj_dLL_1L_2}(2-\delta_{q_cq_d})\hat{L}_1\hat{L}_2\begin{pmatrix} L & 1 & L_1 \\ 0 & 0 & 0 \end{pmatrix}\begin{pmatrix} L & 1 & L_2 \\ 0 & 0 & 0 \end{pmatrix} \\
& \times\int dr_1dr_2\mathscr{V}_L^{L_1L_2}(m_\pi;r_1,r_2) \\
& \times\left[f''_\pi\frac{(G_AG_a+F_AF_a)(G_BG_b+F_BF_b)}{r^4}\left(G_cG_d\langle c||\mathscr{T}_{LL_1}||d\rangle+F_cF_d\langle c'||\mathscr{T}_{LL_1}||d'\rangle\right)\right]_{r_1} \\
& \times\left[f_\pi\left(G_cG_d\langle c||\mathscr{T}_{LL_2}||d\rangle+F_cF_d\langle c'||\mathscr{T}_{LL_2}||d'\rangle\right)\right]_{r_2}. \qquad \text{(A.134)}
\end{aligned}
$$

For the Term14 in Eq. (2.79),

$$
\begin{aligned}
& H_{14}^{J\pi}(AaBb) \\
= & \sum_{cd}\sum_{mM}(-)^{j_A+j_B-m_A-m_B}\begin{pmatrix} j_A & j_a & J \\ m_A & -m_a & -M \end{pmatrix}\begin{pmatrix} j_B & j_b & J \\ m_B & -m_b & -M \end{pmatrix} \\
& \times\int d\boldsymbol{r}_1 d\boldsymbol{r}'_1 d\boldsymbol{r}_2 d\boldsymbol{r}'_2 f'_\pi(1) f'_\pi(2)\frac{\delta(r_1-r'_1)}{r_1^2}\frac{\delta(r_2-r'_2)}{r_2^2}\sum_{LL'L''\nu\nu'\nu''L_1L_2}(-)^{\nu+\nu'+\nu''} \\
& \times\hat{L}_1\hat{L}_2\begin{pmatrix} L & 1 & L_1 \\ 0 & 0 & 0 \end{pmatrix}\begin{pmatrix} L & 1 & L_2 \\ 0 & 0 & 0 \end{pmatrix}\mathscr{V}_L^{L_1L_2}(m_\pi;r_1,r_2) \\
& \times\langle f_A|Y_{L'\nu'}|f_a\rangle_{r'_1}\langle f_c|Y_{L'-\nu'}\vec{\tau}\gamma_0\gamma_5\boldsymbol{\gamma}\cdot\boldsymbol{Y}^{L_1}_{L-\nu}|f_d\rangle_{r_1}\langle f_d|Y_{L''\nu''}\vec{\tau}\gamma_0\gamma_5\boldsymbol{\gamma}\cdot\boldsymbol{Y}^{L_2}_{L\nu}|f_c\rangle_{r_2}\langle f_b|Y_{L''-\nu''}|f_B\rangle_{r'_2} \\
= & \delta_{q_Aq_a}\delta_{q_Bq_b}\hat{J}^{-4}\langle A||Y_J||a\rangle\langle B||Y_J||b\rangle\sum_{cd}\int d\boldsymbol{r}_1 d\boldsymbol{r}_2 f'_\pi(1)f'_\pi(2)\sum_{L\nu ML_1L_2}(-)^{\nu+M} \\
& \times\hat{L}_1\hat{L}_2\begin{pmatrix} L & 1 & L_1 \\ 0 & 0 & 0 \end{pmatrix}\begin{pmatrix} L & 1 & L_2 \\ 0 & 0 & 0 \end{pmatrix}\mathscr{V}_L^{L_1L_2}(m_\pi;r_1,r_2)\left[\frac{(G_AG_a+F_AF_a)}{r^2}\right]_{r_1}\left[\frac{(G_BG_b+F_BF_b)}{r^2}\right]_{r_2} \\
& \times\langle f_c|Y_{J-M}\vec{\tau}\gamma_0\gamma_5\boldsymbol{\gamma}\cdot\boldsymbol{Y}^{L_1}_{L-\nu}|f_d\rangle_{r_1}\langle f_d|Y_{JM}\vec{\tau}\gamma_0\gamma_5\boldsymbol{\gamma}\cdot\boldsymbol{Y}^{L_2}_{L\nu}|f_c\rangle_{r_2}. \qquad \text{(A.135)}
\end{aligned}
$$

As calculated before,

$$
\begin{aligned}
& \langle f_c|Y_{J-M}\vec{\tau}\gamma_0\gamma_5\boldsymbol{\gamma}\cdot\boldsymbol{Y}^{L_1}_{L-\nu}|f_d\rangle_{r_1} \\
= & \langle q_c|\vec{\tau}|q_d\rangle\sum_{L'J'M'}(-)^{M'+j_c-m_c}\frac{\hat{L}\hat{J}\hat{L}_1\hat{L}'\hat{J}'}{\sqrt{4\pi}} \\
& \begin{pmatrix} J & L_1 & L' \\ 0 & 0 & 0 \end{pmatrix}\begin{pmatrix} j_c & J' & j_d \\ -m_c & M' & m_d \end{pmatrix}\begin{pmatrix} J' & J & L \\ M' & M & \nu \end{pmatrix}\begin{Bmatrix} J' & J & L \\ L_1 & 1 & L' \end{Bmatrix} \\
& \times\frac{1}{r_1^2}\left[G_cG_d\langle c||\mathscr{T}_{J'L'}||d\rangle + F_cF_d\langle c'||\mathscr{T}_{J'L'}||d'\rangle\right]_{r_1}, \qquad \text{(A.136)}
\end{aligned}
$$

$$
\begin{aligned}
& \langle f_d|Y_{JM}\vec{\tau}\gamma_0\gamma_5\boldsymbol{\gamma}\cdot\boldsymbol{Y}^{L_2}_{L\nu}|f_c\rangle_{r_2} \\
= & \langle q_d|\vec{\tau}|q_c\rangle\sum_{L''J''M''}(-)^{M''+j_d-m_d}\frac{\hat{L}\hat{J}\hat{L}_2\hat{L}''\hat{J}''}{\sqrt{4\pi}} \\
& \begin{pmatrix} J & L_2 & L'' \\ 0 & 0 & 0 \end{pmatrix}\begin{pmatrix} j_d & J'' & j_c \\ -m_d & M'' & m_c \end{pmatrix}\begin{pmatrix} J'' & J & L \\ M'' & -M & -\nu \end{pmatrix}\begin{Bmatrix} J'' & J & L \\ L_2 & 1 & L'' \end{Bmatrix} \\
& \times\frac{1}{r_2^2}\left[G_dG_c\langle d||\mathscr{T}_{J''L''}||c\rangle + F_dF_c\langle d'||\mathscr{T}_{J''L''}||c'\rangle\right]_{r_2}. \qquad \text{(A.137)}
\end{aligned}
$$

Finally,

$$
\begin{aligned}
& H_{14}^{J\pi}(AaBb) \\
= \; & \delta_{q_Aq_a}\delta_{q_Bq_b}\frac{\hat{J}^{-2}}{4\pi}\langle A||Y_J||a\rangle\langle B||Y_J||b\rangle \sum_{j_cj_dLL_1L_2L'J'L''}(2-\delta_{q_cq_d})\hat{L}^2\hat{L}_1^2\hat{L}_2^2\hat{L}'\hat{L}''\begin{pmatrix} L & 1 & L_1 \\ 0 & 0 & 0 \end{pmatrix} \\
& \times\begin{pmatrix} L & 1 & L_2 \\ 0 & 0 & 0 \end{pmatrix}\begin{pmatrix} J & L_1 & L' \\ 0 & 0 & 0 \end{pmatrix}\begin{pmatrix} J & L_2 & L'' \\ 0 & 0 & 0 \end{pmatrix}\begin{Bmatrix} J' & J & L \\ L_1 & 1 & L' \end{Bmatrix}\begin{Bmatrix} J' & J & L \\ L_2 & 1 & L'' \end{Bmatrix} \\
& \times\int dr_1dr_2\mathscr{V}_L^{L_1L_2}(m_\pi;r_1,r_2)\left[f'_\pi\frac{(G_AG_a+F_AF_a)}{r^2}\left(G_cG_d\langle c||\mathscr{T}_{J'L'}||d\rangle+F_cF_d\langle c'||\mathscr{T}_{J'L'}||d'\rangle\right)\right]_{r_1} \\
& \quad\times\left[f'_\pi\frac{(G_BG_b+F_BF_b)}{r^2}\left(G_cG_d\langle c||\mathscr{T}_{J'L''}||d\rangle+F_cF_d\langle c'||\mathscr{T}_{J'L''}||d'\rangle\right)\right]_{r_2}. \qquad \text{(A.138)}
\end{aligned}
$$

In conclusion, for the pion with pseudo-vector coupling, one has

$$
\begin{aligned}
H_1^{J\pi}(1234) \;=\; & -\langle q_1|\vec{r}|q_2\rangle\cdot\langle q_4|\vec{r}|q_3\rangle\hat{J}^{-2} \\
& \times\sum_{L_1L_2}^{J\pm1}\hat{L}_1\hat{L}_2\begin{pmatrix} J & 1 & L_1 \\ 0 & 0 & 0 \end{pmatrix}\begin{pmatrix} J & 1 & L_2 \\ 0 & 0 & 0 \end{pmatrix} \\
& \times\int dr_1dr_2\mathscr{V}_J^{L_1L_2}(m_\pi;r_1,r_2)\left[f_\pi\left(G_1G_2\langle 1||\mathscr{T}_{JL_1}||2\rangle+F_1F_2\langle 1'||\mathscr{T}_{JL_1}||2'\rangle\right)\right]_{r_1} \\
& \quad\times\left[f_\pi\left(G_3G_4\langle 3||\mathscr{T}_{JL_2}||4\rangle+F_3F_4\langle 3'||\mathscr{T}_{JL_2}||4'\rangle\right)\right]_{r_2}, \qquad \text{(A.139)}
\end{aligned}
$$

$$
\bar{\bar{H}}_i^{J\pi}(1234)=0, \qquad \text{for} \quad i=2,3,\cdots,7, \qquad \text{(A.140)}
$$

$$
\begin{aligned}
& H_9^{J\pi}(1234) \\
= \; & \delta_{q_1q_2}\delta_{q_3q_4}(-)^{j_1+j_2+1}\frac{\hat{J}^{-1}}{\sqrt{4\pi}}\sum_{j_dLL_1L_2L'J'}(2-\delta_{q_dq_2})\hat{L}\hat{L}_1^2\hat{L}_2\hat{L}'\hat{J}' \\
& \times\begin{pmatrix} L & 1 & L_1 \\ 0 & 0 & 0 \end{pmatrix}\begin{pmatrix} L & 1 & L_2 \\ 0 & 0 & 0 \end{pmatrix}\begin{pmatrix} J & L_1 & L' \\ 0 & 0 & 0 \end{pmatrix}\begin{Bmatrix} J' & J & L \\ L_1 & 1 & L' \end{Bmatrix}\begin{Bmatrix} j_2 & j_1 & J \\ J' & L & j_d \end{Bmatrix}\langle 3||Y_J||4\rangle \\
& \times\int dr_1dr_2\mathscr{V}_L^{L_1L_2}(m_\pi;r_1,r_2)\left[f'_\pi\frac{(G_3G_4+F_3F_4)}{r^2}\left(G_1G_d\langle 1||\mathscr{T}_{J'L'}||d\rangle+F_1F_d\langle 1'||\mathscr{T}_{J'L'}||d'\rangle\right)\right]_{r_1} \\
& \quad\times\left[f_\pi\left(G_dG_2\langle d||\mathscr{T}_{LL_2}||2\rangle+F_dF_2\langle d'||\mathscr{T}_{LL_2}||2'\rangle\right)\right]_{r_2}, \qquad \text{(A.141)}
\end{aligned}
$$

$$
\begin{aligned}
& H_{13}^{J\pi}(1234) \\
= \; & \delta_{q_1q_2}\delta_{q_3q_4}\frac{\hat{J}^{-2}}{4\pi}\langle 1||Y_J||2\rangle\langle 3||Y_J||4\rangle\sum_{j_cj_dLL_1L_2}(2-\delta_{q_cq_d})\hat{L}_1\hat{L}_2\begin{pmatrix} L & 1 & L_1 \\ 0 & 0 & 0 \end{pmatrix}\begin{pmatrix} L & 1 & L_2 \\ 0 & 0 & 0 \end{pmatrix} \\
& \times\int dr_1dr_2\mathscr{V}_L^{L_1L_2}(m_\pi;r_1,r_2) \\
& \times\left[f''_\pi\frac{(G_1G_2+F_1F_2)(G_3G_4+F_3F_4)}{r^4}\left(G_cG_d\langle c||\mathscr{T}_{LL_1}||d\rangle+F_cF_d\langle c'||\mathscr{T}_{LL_1}||d'\rangle\right)\right]_{r_1} \\
& \times\left[f_\pi\left(G_cG_d\langle c||\mathscr{T}_{LL_2}||d\rangle+F_cF_d\langle c'||\mathscr{T}_{LL_2}||d'\rangle\right)\right]_{r_2}, \qquad \text{(A.142)}
\end{aligned}
$$

$$
\begin{aligned}
& H_{14}^{J\pi}(1234) \\
= \;& \delta_{q_1q_2}\delta_{q_3q_4}\frac{\hat{J}^{-2}}{4\pi}\langle 1||Y_J||2\rangle\langle 3||Y_J||4\rangle \sum_{j_cj_dLL_1L_2L'J'L''}(2-\delta_{q_cq_d})\hat{L}^2\hat{L}_1^2\hat{L}_2^2\hat{L}'\hat{L}''\begin{pmatrix} L & 1 & L_1 \\ 0 & 0 & 0 \end{pmatrix} \\
& \times\begin{pmatrix} L & 1 & L_2 \\ 0 & 0 & 0 \end{pmatrix}\begin{pmatrix} J & L_1 & L' \\ 0 & 0 & 0 \end{pmatrix}\begin{pmatrix} J & L_2 & L'' \\ 0 & 0 & 0 \end{pmatrix}\begin{Bmatrix} J' & J & L \\ L_1 & 1 & L' \end{Bmatrix}\begin{Bmatrix} J' & J & L \\ L_2 & 1 & L'' \end{Bmatrix} \\
& \times\int dr_1dr_2\mathscr{V}_L^{L_1L_2}(m_\pi;r_1,r_2)\left[f'_\pi\frac{(G_1G_2+F_1F_2)}{r^2}\left(G_cG_d\langle c||\mathscr{T}_{J'L'}||d\rangle+F_cF_d\langle c'||\mathscr{T}_{J'L'}||d'\rangle\right)\right]_{r_1} \\
& \quad\times\left[f'_\pi\frac{(G_3G_4+F_3F_4)}{r^2}\left(G_cG_d\langle c||\mathscr{T}_{J'L''}||d\rangle+F_cF_d\langle c'||\mathscr{T}_{J'L''}||d'\rangle\right)\right]_{r_2}. \qquad \text{(A.143)}
\end{aligned}
$$

In order to cancel the contact interaction coming from the pion pseudo-vector coupling, a pionic zero-range counterterm should be included (Bouyssy *et al.*, 1987), which reads

$$
\begin{aligned}
V^{\pi\delta}(1,2) &= \frac{1}{3}[\frac{f_\pi}{m_\pi}\vec{\tau}\gamma_0\gamma_5\boldsymbol{\gamma}]_1\cdot[\frac{f_\pi}{m_\pi}\vec{\tau}\gamma_0\gamma_5\boldsymbol{\gamma}]_2\delta(\boldsymbol{r}_1-\boldsymbol{r}_2) \\
&= \frac{1}{3}\sum_{Lk\nu}(-)^{k+\nu}[\frac{f_\pi}{m_\pi}\vec{\tau}\gamma_0\gamma_5\gamma^kY_L^\nu]_1\cdot[\frac{f_\pi}{m_\pi}\vec{\tau}\gamma_0\gamma_5\gamma^{-k}Y_L^{-\nu}]_2\frac{\delta(r_1-r_2)}{r_1^2}. \qquad \text{(A.144)}
\end{aligned}
$$

It has a similar form as $\bar{\bar{V}}^\omega$, so we can calculate its p-h matrix elements in a similar way.

Therefore, we can easily obtain that

$$
\begin{aligned}
H_1^{J\pi\delta}(1234) =& \frac{1}{3m_\pi^2}\langle q_1|\vec{\tau}|q_2\rangle\cdot\langle q_4|\vec{\tau}|q_3\rangle\hat{J}^{-2} \\
& \times\sum_L\int dr\frac{f_\pi^2}{r^2}\left[G_1G_2\langle 1||\mathscr{T}_{JL}||2\rangle+F_1F_2\langle 1'||\mathscr{T}_{JL}||2'\rangle\right] \\
& \quad\times\left[G_3G_4\langle 3||\mathscr{T}_{JL}||4\rangle+F_3F_4\langle 3'||\mathscr{T}_{JL}||4'\rangle\right], \qquad \text{(A.145)}
\end{aligned}
$$

Furthermore, all the terms from Term2 to Term7 vanish due to the parity conservation.

For the Term9 in Eq. (2.79),

$$
\begin{aligned}
H_9^{J\pi\delta}(1234) =& \frac{1}{3m_\pi^2}\delta_{q_1q_2}\delta_{q_3q_4}(-)^{j_1+j_2+1}\frac{\hat{J}^{-1}}{\sqrt{4\pi}}\sum_{j_dLL'J'J''}(2-\delta_{q_dq_2})(-)^{J''+L}\hat{L}\hat{L}'\hat{J}'\hat{J}'' \\
& \times\begin{pmatrix} J & L & L' \\ 0 & 0 & 0 \end{pmatrix}\begin{Bmatrix} j_2 & j_1 & J \\ J' & J'' & j_d \end{Bmatrix}\begin{Bmatrix} J' & J'' & J \\ L & L' & 1 \end{Bmatrix}\langle 3||Y_J||4\rangle \\
& \times\int dr\frac{f'_\pi f_\pi}{r^4}(G_3G_4+F_3F_4)\left(G_1G_d\langle 1||\mathscr{T}_{J'L'}||d\rangle+F_1F_d\langle 1'||\mathscr{T}_{J'L'}||d'\rangle\right) \\
& \quad\times\left(G_dG_2\langle d||\mathscr{T}_{J''L}||2\rangle+F_dF_2\langle d'||\mathscr{T}_{J''L}||2'\rangle\right). \qquad \text{(A.146)}
\end{aligned}
$$

For the Term13 in Eq. (2.79),

$$
\begin{aligned}
& H_{13}^{J\pi\delta}(1234) \\
=& -\frac{1}{3m_\pi^2}\delta_{q_1q_2}\delta_{q_3q_4}\frac{\hat{J}^{-2}}{4\pi}\langle 1||Y_J||2\rangle\langle 3||Y_J||4\rangle\sum_{j_cj_dLJ'}(2-\delta_{q_cq_d})\int dr\frac{f''_\pi f_\pi}{r^6} \\
& \times(G_1G_2+F_1F_2)(G_3G_4+F_3F_4)\left[G_cG_d\langle c||\mathscr{T}_{J'L}||d\rangle+F_cF_d\langle c'||\mathscr{T}_{J'L}||d'\rangle\right]^2. \qquad \text{(A.147)}
\end{aligned}
$$

For the Term14 in Eq. (2.79),

$$
\begin{aligned}
&H_{14}^{J\pi\delta}(1234) \\
&= -\frac{1}{3m_\pi^2}\delta_{q_1q_2}\delta_{q_3q_4}\frac{\hat{J}^{-2}}{4\pi}\langle 1||Y_J||2\rangle\langle 3||Y_J||4\rangle \sum_{j_cj_dLL'J'}(2-\delta_{q_cq_d})\hat{L}^2\begin{pmatrix} J & L & L' \\ 0 & 0 & 0 \end{pmatrix}^2 \int dr \frac{{f'_\pi}^2}{r^6} \\
&\times (G_1G_2+F_1F_2)(G_3G_4+F_3F_4)\left[G_cG_d\langle c||\mathscr{T}_{J'L'}||d\rangle + F_cF_d\langle c'||\mathscr{T}_{J'L'}||d'\rangle\right]^2 . \qquad \text{(A.148)}
\end{aligned}
$$

Appendix B

Remarks

In this appendix, the main results concerning the angular momenta couplings, and the properties of the Yukawa propagator, as well as the conventional notations used in the thesis are gathered for reader's convenience. In particular, we follow the conventions of Wigner-Eckart Theorem and reduced matrix elements in the textbook (Varshalovich *et al.*, 1987).

Remark 1 Definitions of the 3-j, 6-j, 9-j Symbols (Brink and Satchler, 1968)

The Clebsch-Gordan coefficient is defined by the transformation

$$|abc\gamma\rangle = \sum_{\alpha\beta} C^{c\gamma}_{a\alpha b\beta} \, |a\alpha\rangle \, |b\beta\rangle \, , \tag{B.1}$$

and vanishes unless $\alpha + \beta = \gamma$.

The relation between 3-j symbols and C-G coefficients reads

$$C^{c-\gamma}_{a\alpha b\beta} = (-)^{a-b-\gamma} \hat{c} \begin{pmatrix} a & b & c \\ \alpha & \beta & \gamma \end{pmatrix}, \tag{B.2}$$

where $\hat{c}$ means $\sqrt{2c+1}$. Note the appearance of γ with a minus sign on the left, so that $\alpha+\beta+\gamma = 0$ for the 3-j symbols.

The 6-j symbol is defined by the transformation

$$|(ab)e, d; c\rangle = \sum_f (-)^{a+b+c+d} \hat{e}\hat{f} \begin{Bmatrix} a & b & e \\ d & c & f \end{Bmatrix} |a, (bd)f; c\rangle \, . \tag{B.3}$$

The 9-j symbol is defined by the transformation

$$|(ad)g, (be)h; i\rangle = \sum_{cf} \hat{c}\hat{f}\hat{g}\hat{h} \begin{Bmatrix} a & b & c \\ d & e & f \\ g & h & i \end{Bmatrix} |(ab)c, (de)f; i\rangle \, . \tag{B.4}$$

Remark 2 Symmetries of 3-j Symbols (Brink and Satchler, 1968)

The 3-j symbol is invariant under cyclic permutation of its columns and multipied by $(-)^{a+b+c}$ by non-cyclic ones

$$\begin{pmatrix} a & b & c \\ \alpha & \beta & \gamma \end{pmatrix} = \begin{pmatrix} b & c & a \\ \beta & \gamma & \alpha \end{pmatrix} = (-)^{a+b+c} \begin{pmatrix} b & a & c \\ \beta & \alpha & \gamma \end{pmatrix}, \quad \text{etc.} \tag{B.5}$$

and

$$\begin{pmatrix} a & b & c \\ -\alpha & -\beta & -\gamma \end{pmatrix} = (-)^{a+b+c} \begin{pmatrix} a & b & c \\ \alpha & \beta & \gamma \end{pmatrix}. \tag{B.6}$$

Remark 3 Orthogonality Relations of 3-j Symbols (Brink and Satchler, 1968)

The sums involving products of two 3-j symbols read as

$$\sum_{\alpha\beta} \hat{c}^2 \begin{pmatrix} a & b & c \\ \alpha & \beta & \gamma \end{pmatrix} \begin{pmatrix} a & b & c' \\ \alpha & \beta & \gamma' \end{pmatrix} = \delta_{cc'}\delta_{\gamma\gamma'}, \tag{B.7}$$

$$\sum_{c\gamma} \hat{c}^2 \begin{pmatrix} a & b & c \\ \alpha & \beta & \gamma \end{pmatrix} \begin{pmatrix} a & b & c \\ \alpha' & \beta' & \gamma \end{pmatrix} = \delta_{\alpha\alpha'}\delta_{\beta\beta'}. \tag{B.8}$$

Remark 4 Values of Some Special 3-j Symbols (Brink and Satchler, 1968)

$$\begin{pmatrix} L & L & 0 \\ M & -M & 0 \end{pmatrix} = \frac{(-)^{L-M}}{\hat{L}}, \tag{B.9}$$

$$\begin{pmatrix} a & b & a+b \\ 0 & 0 & 0 \end{pmatrix} = (-)^{a-b} \frac{(a+b)!}{a!b!} \left[\frac{(2a)!(2b)!}{(2a+2b+1)!}\right]^{1/2}. \tag{B.10}$$

Remark 5 Triangular Conditions of 6-j Symbols (Brink and Satchler, 1968)

The four triangular conditions which must be satisfied by the six angular momenta in the 6-j symbol may be illustrated in the following way:

$$\left\{ \begin{matrix} \bigcirc & \bigcirc & \bigcirc \\ & & \end{matrix} \right\}, \left\{ \begin{matrix} \bigcirc & & \\ & \bigcirc & \bigcirc \end{matrix} \right\}, \left\{ \begin{matrix} & \bigcirc & \\ \bigcirc & & \bigcirc \end{matrix} \right\}, \left\{ \begin{matrix} & & \bigcirc \\ \bigcirc & \bigcirc & \end{matrix} \right\}.$$

Remark 6 Symmetries of 6-j Symbols (Brink and Satchler, 1968)

The 6-j symbol is invariant under the interchange of any two columns, and also under the interchange of the upper and lower arguments in each of any two columns, e.g.,

$$\begin{Bmatrix} a & b & e \\ d & c & f \end{Bmatrix} = \begin{Bmatrix} a & e & b \\ d & f & c \end{Bmatrix} = \begin{Bmatrix} e & b & a \\ f & c & d \end{Bmatrix} = \begin{Bmatrix} a & c & f \\ d & b & e \end{Bmatrix} = \begin{Bmatrix} d & c & e \\ a & b & f \end{Bmatrix}. \tag{B.11}$$

Remark 7 Contraction of 3-j Symbols to 6-j Symbols (Brink and Satchler, 1968)

$$\sum_{\alpha\beta\gamma\alpha'\beta'}(-)^{A+B+C+\alpha+\beta+\gamma}\begin{pmatrix} A & B & c \\ \alpha & -\beta & \gamma' \end{pmatrix}\begin{pmatrix} B & C & a \\ \beta & -\gamma & \alpha' \end{pmatrix}\begin{pmatrix} C & A & b \\ \gamma & -\alpha & \beta' \end{pmatrix}\begin{pmatrix} a & b & c_1 \\ \alpha' & \beta' & \gamma_1' \end{pmatrix}$$

$$= \hat{c}^{-2}\delta_{cc_1}\delta_{\gamma'\gamma_1'}\begin{Bmatrix} a & b & c \\ A & B & C \end{Bmatrix}, \tag{B.12}$$

$$\sum_{\alpha\beta\gamma}(-)^{A+B+C+\alpha+\beta+\gamma}\begin{pmatrix} A & B & c \\ \alpha & -\beta & \gamma' \end{pmatrix}\begin{pmatrix} B & C & a \\ \beta & -\gamma & \alpha' \end{pmatrix}\begin{pmatrix} C & A & b \\ \gamma & -\alpha & \beta' \end{pmatrix}$$

$$= \begin{pmatrix} a & b & c \\ \alpha' & \beta' & \gamma' \end{pmatrix}\begin{Bmatrix} a & b & c \\ A & B & C \end{Bmatrix}, \tag{B.13}$$

$$\sum_{\gamma}(-)^{b+B-\alpha'-\alpha}\begin{pmatrix} a & B & C \\ \alpha' & \beta & -\gamma \end{pmatrix}\begin{pmatrix} b & A & C \\ \beta' & -\alpha & \gamma \end{pmatrix}$$

$$= \sum_{c\gamma'}\hat{c}^2\begin{Bmatrix} a & b & c \\ A & B & C \end{Bmatrix}\begin{pmatrix} a & b & c \\ \alpha' & \beta' & -\gamma' \end{pmatrix}\begin{pmatrix} B & A & c \\ \beta & -\alpha & \gamma' \end{pmatrix}, \tag{B.14}$$

Remark 8 Values of Some Special 6-j and 3-j Symbols (Brink and Satchler, 1968)

$$\begin{Bmatrix} a & b & a+b \\ a+b+e & e & a+e \end{Bmatrix} = (-)^{2(a+b+e)}\frac{1}{\sqrt{(2a+2b+1)(2a+2e+1)}}. \tag{B.15}$$

If $l+l'+J$ is even,

$$\begin{pmatrix} l' & l & J \\ 0 & 0 & 0 \end{pmatrix}\begin{Bmatrix} l' & l & J \\ j & j' & \frac{1}{2} \end{Bmatrix} = (-1)\hat{l'}^{-1}\hat{l}^{-1}\begin{pmatrix} j' & j & J \\ \frac{1}{2} & -\frac{1}{2} & 0 \end{pmatrix}. \tag{B.16}$$

Remark 9 Symmetries of 9-j Symbols (Brink and Satchler, 1968)

The 9-j symbol is invariant under cyclic permutations of rows and columns as well as reflection about a diagonal, and is multiplied by $(-)^R$ under non-cyclic permutations of rows and columns, where R is the sum of all arguments of the 9-j symbol.

Remark 10 Gradient of Propagator

In general, in the meson exchange model, the propagators for mesons are Yukawa functions

$$v(\mu;\boldsymbol{r}_1,\boldsymbol{r}_2) = \frac{1}{4\pi}\frac{e^{-\mu|\boldsymbol{r}_1-\boldsymbol{r}_2|}}{|\boldsymbol{r}_1-\boldsymbol{r}_2|}, \tag{B.17}$$

which can be expanded in terms of spherical modified Bessel functions combined with the spherical harmonics,

$$v(\mu;\boldsymbol{r}_1,\boldsymbol{r}_2) = \sum_{L=0}^{\infty}R_{LL}(\mu;r_1,r_2)\boldsymbol{Y}_L(\hat{\boldsymbol{r}}_1)\cdot\boldsymbol{Y}_L(\hat{\boldsymbol{r}}_2), \tag{B.18}$$

where

$$R_{L_1L_2}(\mu;r_1,r_2)=\mu\sqrt{\frac{1}{z_1z_2}}\left[I_{L_1+\frac{1}{2}}(z_1)K_{L_2+\frac{1}{2}}(z_2)\theta(z_2-z_1)+K_{L_1+\frac{1}{2}}(z_1)I_{L_2+\frac{1}{2}}(z_2)\theta(z_1-z_2)\right] \tag{B.19}$$

with $z=\mu r$.

The gradient on the propagator with respect to r_1 reads

$$\begin{aligned}\nabla_1 v(\mu;\boldsymbol{r}_1,\boldsymbol{r}_2) &= -\sum_{LM}\sum_{L_1}C_{L010}^{L_10}\mu\left[\frac{d}{dz_1}+\frac{\alpha_{LL_1}}{z_1}\right]R_{LL}(\mu;r_1,r_2)\boldsymbol{Y}_{LM}^{L_1}(\hat{\boldsymbol{r}}_1)Y_{LM}^*(\hat{\boldsymbol{r}}_2)\\ &= -\mu\sum_{LM}\sum_{L_1}C_{L010}^{L_10}S_{LL_1}(\mu;r_1,r_2)\boldsymbol{Y}_{LM}^{L_1}(\hat{\boldsymbol{r}}_1)Y_{LM}^*(\hat{\boldsymbol{r}}_2),\end{aligned} \tag{B.20}$$

where

$$S_{LL_1}(\mu;r_1,r_2)=\mu\sqrt{\frac{1}{z_1z_2}}\left[I_{L_1+\frac{1}{2}}(z_1)K_{L+\frac{1}{2}}(z_2)\theta(z_2-z_1)-K_{L_1+\frac{1}{2}}(z_1)I_{L+\frac{1}{2}}(z_2)\theta(z_1-z_2)\right], \tag{B.21}$$

and α_{ll_1} is defined in **Remark 16**. Obviously, one has $S_{LL_1}(\mu;r_1,r_2)=-S_{L_1L}(\mu;r_2,r_1)$.

The action of $\nabla_2\nabla_1$ on v reads

$$\begin{aligned}\nabla_2\nabla_1 v(\mu;\boldsymbol{r}_1,\boldsymbol{r}_2) &= +\mu^2\sum_{LM}\sum_{L_1L_2}C_{L010}^{L_10}C_{L010}^{L_20}\left[\frac{d}{dz_2}+\frac{\alpha_{LL_2}}{z_2}\right]S_{LL_1}(\mu;r_1,r_2)(-)^M\boldsymbol{Y}_{LM}^{L_1}(\hat{\boldsymbol{r}}_1)\boldsymbol{Y}_{L-M}^{L_2}(\hat{\boldsymbol{r}}_2)\\ &= \mu^2\sum_{L}\sum_{L_1L_2}C_{L010}^{L_10}C_{L010}^{L_20}\left[-R_{L_1L_2}+D_{LL_1}\delta(z_1-z_2)\right]\boldsymbol{Y}_{LL_1}(\hat{\boldsymbol{r}}_1)\cdot\boldsymbol{Y}_{LL_2}(\hat{\boldsymbol{r}}_2),\end{aligned} \tag{B.22}$$

where

$$D_{LL_1}(\mu;r_1,r_2)=\mu\sqrt{\frac{1}{z_1z_2}}\left[I_{L_1+\frac{1}{2}}(z_1)K_{L+\frac{1}{2}}(z_2)+K_{L_1+\frac{1}{2}}(z_1)I_{L+\frac{1}{2}}(z_2)\right], \tag{B.23}$$

and

$$\boldsymbol{Y}_{LM}^{L_1}=\sum_{M_1\mu}C_{L_1M_11\mu}^{LM}Y_{L_1M_1}\boldsymbol{e}_\mu. \tag{B.24}$$

For simplicity, one can write $\nabla_2\nabla_1 v$ into a more compact form

$$\nabla_2\nabla_1 v(\mu;\boldsymbol{r}_1,\boldsymbol{r}_2)=\mu^2\sum_{L}\sum_{L_1L_2}C_{L010}^{L_10}C_{L010}^{L_20}\mathscr{V}_L^{L_1L_2}(\mu;r_1,r_2)\boldsymbol{Y}_{LL_1}(\hat{\boldsymbol{r}}_1)\cdot\boldsymbol{Y}_{LL_2}(\hat{\boldsymbol{r}}_2), \tag{B.25}$$

with

$$\mathscr{V}_L^{L_1L_2}(\mu;r_1,r_2)=-R_{L_1L_2}(\mu;r_1,r_2)+D_{LL_1}(\mu;r_1,r_2)\delta(z_1-z_2), \tag{B.26}$$

or

$$\mathscr{V}_L^{L_1L_2}(\mu;r_1,r_2)=-R_{L_1L_2}(\mu;r_1,r_2)+\frac{1}{\mu^2r_1^2}\delta(r_1-r_2). \tag{B.27}$$

Remark 11 Expansion of Delta Function

The delta function $\delta(\boldsymbol{r}_1-\boldsymbol{r}_2)$ can be expanded in terms of spherical harmonics,

$$\delta(\boldsymbol{r}_1-\boldsymbol{r}_2)=\frac{\delta(r_1-r_2)}{r_1^2}\sum_{L=0}^{\infty}\boldsymbol{Y}_L(\hat{\boldsymbol{r}}_1)\cdot\boldsymbol{Y}_L(\hat{\boldsymbol{r}}_2). \tag{B.28}$$

Remark 12 Direct Product of Two Spherical Harmonics

A direct product of two spherical harmonics of the same arguments may be expanded as

$$Y_{l_1}^{m_1}(\Omega)Y_{l_2}^{m_2}(\Omega) = \sum_{L=|l_1-l_2|}^{l_1+l_2}\sum_{M=-L}^{L}(-)^M\frac{\hat{l}_1\hat{l}_2\hat{L}}{\sqrt{4\pi}}\begin{pmatrix} l_1 & l_2 & L \\ 0 & 0 & 0 \end{pmatrix}\begin{pmatrix} l_1 & l_2 & L \\ m_1 & m_2 & M \end{pmatrix}Y_L^{-M}(\Omega). \quad \text{(B.29)}$$

Remark 13 Wigner-Eckart Theorem

The Wigner-Eckart theorem states that in a representation according to the operators $\hat{J}^2$, $\hat{J}_z$, where the basis vectors are given by $|jm\rangle$, the matrix element $\langle jm|T_{kq}|j'm'\rangle$ of an irreducible tensor operator is given by the product of a so-called reduced matrix element $\langle j||T_k||j'\rangle$, which does not depend on m, m' and q, and a Clebsch-Gordan coefficient (or a Wigner 3-j symbol) (see Ref. (Varshalovich *et al.*, 1987)),

$$\begin{aligned}\langle jm|T_{kq}|j'm'\rangle &= (-)^{2k}\hat{j}^{-1}C^{jm}_{j'm'kq}\langle j||T_k||j'\rangle \\ &= (-)^{j-m}\begin{pmatrix} j & k & j' \\ -m & q & m' \end{pmatrix}\langle j||T_k||j'\rangle. \end{aligned} \quad \text{(B.30)}$$

The reduced matrix of the composite tensor

$$T_{KQ}(k_1k_2) = \sum_q C^{KQ}_{k_1qk_2Q-q}R_{k_1q}S_{k_2Q-q} \quad \text{(B.31)}$$

may be evaluated in terms of the reduced matrix elements of the R and S,

$$\langle J||T_K||J'\rangle = (-)^{K+J+J'}\hat{K}\sum_{J''}\begin{Bmatrix} J & J' & K \\ k_2 & k_1 & J'' \end{Bmatrix}\langle J||R_{k_1}||J''\rangle\langle J''||S_{k_2}||J'\rangle. \quad \text{(B.32)}$$

In a two-component system the tensor $R_{k_1}(1)$ acts only on the first part and $S_{k_2}(2)$ only on the second part. Then, the reduced matrix of the composite tensor

$$T_{KQ}(k_1k_2) = \sum_{q_1q_2} C^{KQ}_{k_1qk_2q_2}R_{k_1q_1}(1)S_{k_2q_2}(2) \quad \text{(B.33)}$$

may be evaluated in terms of the reduced matrix elements of the R and S,

$$\langle j_1j_2J||T_K(k_1k_2)||j_1'j_2'J'\rangle = \hat{J}\hat{K}\hat{J}'\begin{Bmatrix} J & J' & K \\ j_1 & j_1' & k_1 \\ j_2 & j_2' & k_2 \end{Bmatrix}\langle j_1||R_{k_1}||j_1'\rangle\langle j_2||S_{k_2}||j_2'\rangle. \quad \text{(B.34)}$$

Remark 14 Some Useful reduced matrix elements

The reduced matrix element of the spherical harmonic operator reads (Varshalovich *et al.*, 1987)

$$\langle a||Y_L||b\rangle = (-)^{j_b-L-\frac{1}{2}}\frac{\hat{j}_a\hat{j}_b\hat{L}}{\sqrt{4\pi}}\begin{pmatrix} j_a & j_b & L \\ \frac{1}{2} & -\frac{1}{2} & 0 \end{pmatrix} \quad \text{(B.35)}$$

provided $l_a + l_b + L$ is even, and zero otherwise. It obeys the symmetry property

$$\langle b||Y_L||a\rangle = (-)^{j_a - j_b}\langle a||Y_L||b\rangle. \tag{B.36}$$

The reduced matrix element of the vector spherical harmonic operator reads (Varshalovich *et al.*, 1987)

$$\langle a||\mathscr{T}_{JL}||b\rangle = (-)^{l_a}\frac{\sqrt{6}}{\sqrt{4\pi}}\hat{j}_a\hat{j}_b\hat{J}\hat{l}_a\hat{l}_b\hat{L}\begin{pmatrix} l_a & L & l_b \\ 0 & 0 & 0 \end{pmatrix}\begin{Bmatrix} j_a & j_b & J \\ l_a & l_b & L \\ \frac{1}{2} & \frac{1}{2} & 1 \end{Bmatrix}, \tag{B.37}$$

where

$$Y_{L\nu}\sigma_k = \sum_{JM}(-)^{L-1+M}\hat{J}\begin{pmatrix} L & 1 & J \\ \nu & k & -M \end{pmatrix}\mathscr{T}_{JM}, \tag{B.38}$$

or

$$\mathscr{T}_{JM} = \sum_{\nu k}(-)^{L-1+M}\hat{J}\begin{pmatrix} L & 1 & J \\ \nu & k & -M \end{pmatrix}Y_{L\nu}\sigma_k. \tag{B.39}$$

Using the following relations, when $c + d + e$ is even,

$$\sqrt{6}\hat{c}\hat{d}\hat{e}\begin{pmatrix} c & d & e \\ 0 & 0 & 0 \end{pmatrix}\begin{Bmatrix} a & b & c \\ d & e & c \\ \frac{1}{2} & \frac{1}{2} & 1 \end{Bmatrix} = \begin{pmatrix} a & b & c \\ \frac{1}{2} & \frac{1}{2} & -1 \end{pmatrix}, \tag{B.40}$$

$$\begin{pmatrix} a & b & c \\ \frac{1}{2} & \frac{1}{2} & -1 \end{pmatrix} = -\frac{1}{2}\begin{pmatrix} a & b & c \\ \frac{1}{2} & -\frac{1}{2} & 0 \end{pmatrix}\frac{\hat{b}^2 + (-)^{a+b+c}\hat{a}^2}{\sqrt{c(c+1)}}, \tag{B.41}$$

when $c + d + e$ is odd

$$\begin{pmatrix} c+1 & d & e \\ 0 & 0 & 0 \end{pmatrix}\begin{Bmatrix} a & b & c \\ d & e & c+1 \\ \frac{1}{2} & \frac{1}{2} & 1 \end{Bmatrix} = \frac{(-)^{b+e+\frac{1}{2}}[(d-a)\hat{a}^2 + (e-b)\hat{b}^2 + c + 1]}{\sqrt{6(c+1)(2c+3)}\hat{c}\hat{d}\hat{e}}\begin{pmatrix} a & b & c \\ \frac{1}{2} & -\frac{1}{2} & 0 \end{pmatrix}, \tag{B.42}$$

$$\begin{pmatrix} c-1 & d & e \\ 0 & 0 & 0 \end{pmatrix}\begin{Bmatrix} a & b & c \\ d & e & c-1 \\ \frac{1}{2} & \frac{1}{2} & 1 \end{Bmatrix} = \frac{(-)^{b+e+\frac{1}{2}}[(d-a)\hat{a}^2 + (e-b)\hat{b}^2 - c]}{\sqrt{6c(2c-1)}\hat{c}\hat{d}\hat{e}}\begin{pmatrix} a & b & c \\ \frac{1}{2} & -\frac{1}{2} & 0 \end{pmatrix}, \tag{B.43}$$

it can be simplified as

$$\langle a||\mathscr{T}_{JL}||b\rangle = (-)^{l_a}\frac{\hat{j}_a\hat{j}_b}{\sqrt{4\pi}}Z_{JL}(a,b)\begin{pmatrix} j_a & j_b & J \\ \frac{1}{2} & -\frac{1}{2} & 0 \end{pmatrix}, \qquad l_a + l_b + L \text{ is even}, \tag{B.44}$$

where

$$Z_{JL}(a,b) = \begin{cases} (-)^{j_b+l_b+\frac{1}{2}}\dfrac{(l_a - j_a)\hat{j}_a^2 + (l_b - j_b)\hat{j}_b^2 + L}{\sqrt{L}}, & \text{if } L = J+1, \\ -\dfrac{1}{2}\dfrac{\hat{J}}{[J(J+1)]^{\frac{1}{2}}}\left[\hat{j}_b^2 + (-)^{j_a+j_b+J}\hat{j}_a^2\right], & \text{if } L = J, \\ (-)^{j_b+l_b+\frac{1}{2}}\dfrac{(l_a - j_a)\hat{j}_a^2 + (l_b - j_b)\hat{j}_b^2 - L - 1}{\sqrt{L+1}}, & \text{if } L = J-1. \end{cases} \tag{B.45}$$

And it obeys the symmetry property

$$\langle b||\mathscr{T}_{JL}||a\rangle = (-)^{j_a+j_b+J+L}\langle a||\mathscr{T}_{JL}||b\rangle. \tag{B.46}$$

Remark 15 Dirac Matrices

A familiar representation of the Dirac matrices is

$$\gamma^0 = \begin{pmatrix} 1 & 0 \\ 0 & 1 \end{pmatrix}, \qquad \boldsymbol{\gamma} = \begin{pmatrix} 0 & \boldsymbol{\sigma} \\ -\boldsymbol{\sigma} & 0 \end{pmatrix}, \tag{B.47}$$

where

$$\sigma^1 = \begin{pmatrix} 0 & 1 \\ 1 & 0 \end{pmatrix}, \qquad \sigma^2 = \begin{pmatrix} 0 & -i \\ i & 0 \end{pmatrix}, \qquad \sigma^3 = \begin{pmatrix} 1 & 0 \\ 0 & -1 \end{pmatrix}. \tag{B.48}$$

Frequently appearing combinations are

$$\sigma^{\mu\nu} = \frac{i}{2}\left[\gamma^\mu, \gamma^\nu\right], \qquad \gamma^5 = i\gamma^0\gamma^1\gamma^2\gamma^3 = \gamma_5. \tag{B.49}$$

In this representation the components of $\sigma^{\mu\nu}$ are

$$\sigma^{0i} = i\begin{pmatrix} 0 & \sigma^i \\ \sigma^i & 0 \end{pmatrix}, \qquad \sigma^{ij} = \begin{pmatrix} \sigma^k & 0 \\ 0 & \sigma^k \end{pmatrix}, \tag{B.50}$$

with $i, j, k = 1, 2, 3$ in cyclic order, and

$$\gamma^5 = \gamma_5 = \begin{pmatrix} 0 & 1 \\ 1 & 0 \end{pmatrix}. \tag{B.51}$$

Remark 16 Some Useful Short-hand Notations

Some short-hand notations are often used in the derivations. Here we list them as follows,

$$\hat{j}^2 = 2j+1, \tag{B.52}$$

$$\alpha_{ll_1} = \begin{cases} -l & l_1 = l+1, \\ l+1 & l_1 = l-1. \end{cases} \tag{B.53}$$

$$\beta_{ll_1} = \begin{cases} -l & l_1 = l-1, \\ l+1 & l_1 = l+1. \end{cases} \tag{B.54}$$

$$\kappa_a = (l_a - j_a)(2j_a+1), \tag{B.55}$$

$$\kappa_{ab} = \kappa_a + \kappa_b. \tag{B.56}$$

Bibliography

Akimune, H., *et al.*, 1995, Phys. Rev. C **52**, 604

Alex Brown, B., 2000, Phys. Rev. Lett. **85**, 5296

Amsler, C., *et al.*, 2008, *Review of Particle Physics*, Phys. Lett. B **667**, 1

Anderson, B. D., *et al.*, 1985, Phys. Rev. C **31**, 1161

Anderson, J. D., and C. Wong, 1961, Phys. Rev. Lett. **7**, 250

Aste, A., and D. Trautmann, 2007, Eur. Phys. J. A **33**, 11

Athanassopoulos, C., *et al.*, 1998, Phys. Rev. Lett. **81**, 1774

Auerbach, L. B., *et al.*, 2001, Phys. Rev. C **64**, 065501

Auerbach, L. B., *et al.*, 2002, Phys. Rev. C **66**, 015501

Auerbach, N., 2009, Phys. Rev. C **79**, 035502

Auerbach, N., and B. A. Brown, 2002, Phys. Rev. C **65**, 024322

Auerbach, N., and A. Klein, 1983, Nucl. Phys. A **395**, 77

Auerbach, N., and A. Klein, 1984, Phys. Rev. C **30**, 1032

Auerbach, N., A. Klein, and N. Van Giai, 1981, Phys. Lett. B **106**, 347

Auerbach, N., N. Van Giai, and O. K. Vorov, 1997, Phys. Rev. C **56**, R2368

Bainum, D. E., *et al.*, 1980, Phys. Rev. Lett. **44**, 1751

Behrens, H., and W. Bühring, 1982, *Electron Radial Wave Functions and Nuclear Beta-decay* (Clarendon Press, Oxford)

Bender, M., J. Dobaczewski, J. Engel, and W. Nazarewicz, 2002, Phys. Rev. C **65**, 054322

Bodmann, B., *et al.*, 1994, Phys. Lett. B **332**, 251

Bohr, A., and B. R. Mottelson, 1969, *Nuclear Structure*, Vol. I (Benjamin Inc., New York)

Borzov, I., 2006, *Special Isseu on Nuclear Astrophysics*, Nucl. Phys. A **777**, 645

Bouyssy, A., J.-F. Mathiot, N. Van Giai, and S. Marcos, 1987, Phys. Rev. C **36**, 380

Brink, D. M., and G. R. Satchler, 1968, *Angular Momentum*, second edition ed. (Clarendon Press, Oxford)

Brockmann, R., and R. Machleidt, 1990, Phys. Rev. C **42**, 1965

Brockmann, R., and H. Toki, 1992, Phys. Rev. Lett. **68**, 3408

Cabibbo, N., 1963, Phys. Rev. Lett. **10**, 531

Caurier, E., K. Langanke, G. Martínez-Pinedo, and F. Nowacki, 1999, Nucl. Phys. A **653**, 439

Caurier, E., G. Martínez-Pinedo, F. Nowacki, A. Poves, and A. P. Zuker, 2005, Rev. Mod. Phys. **77**, 427

Centelles, M., X. Roca-Maza, X. Viñas, and M. Warda, 2009, Phys. Rev. Lett. **102**, 122502

Colò, G., N. Van Giai, P. F. Bortignon, and R. A. Broglia, 1994, Phys. Rev. C **50**, 1496

De Conti, C., A. P. Galeão, and F. Krmpotić, 1998, Phys. Lett. B **444**, 14

De Conti, C., A. P. Galeão, and F. Krmpotić, 2000, Phys. Lett. B **494**, 46

Doering, R. R., A. Galonsky, D. M. Patterson, and G. F. Bertsch, 1975, Phys. Rev. Lett. **35**, 1691

Engel, J., 1998, Phys. Rev. C **57**, 2004

Engel, J., M. Bender, J. Dobaczewski, W. Nazarewicz, and R. Surman, 1999, Phys. Rev. C **60**, 014302

Engelbrecht, C. A., and R. H. Lemmer, 1970, Phys. Rev. Lett. **24**, 607

Fracasso, S., and G. Colò, 2005, Phys. Rev. C **72**, 064310

Fracasso, S., and G. Colò, 2007, Phys. Rev. C **76**, 044307

Fuchs, C., H. Lenske, and H. H. Wolter, 1995, Phys. Rev. C **52**, 3043

Gaarde, C., 1985, in *Proceedings of the Niels Bohr Centennial Conference on Nuclear Structure, Copenhagen*, edited by R. Broglia *et al.* (North-Holland, Amsterdam) p. 449c

Ginocchio, J. N., 2005, Phys. Rep. **414**, 165

Hardy, J. C., and I. S. Towner, 2005, Phys. Rev. C **71**, 055501

Hardy, J. C., and I. S. Towner, 2009, Phys. Rev. C **79**, 055502

Haxton, W. C., 1987, Phys. Rev. D **36**, 2283

Hayes, A. C., 1999, Phys. Rep. **315**, 257

Horen, D. J., *et al.*, 1980, Phys. Lett. B **95**, 27

Horowitz, C. J., and J. Piekarewicz, 2001a, Phys. Rev. C **64**, 062802

Horowitz, C. J., and J. Piekarewicz, 2001b, Phys. Rev. Lett. **86**, 5647

Horowitz, C. J., and J. Piekarewicz, 2002, Phys. Rev. C **66**, 055803

Hu, J., H. Toki, W. Wen, and H. Shen, 2010a, Phys. Lett. B **687**, 271

Hu, J., H. Toki, W. Wen, and H. Shen, 2010b, Eur. Phys. J. A **43**, 323

de Huu, M., *et al.*, 2007, Phys. Lett. B **649**, 35

Ichimura, M., H. Sakai, and T. Wakasa, 2006, Prog. Part. Nucl. Phys. **56**, 446

Ikeda, K., S. Fujii, and J. I. Fujita, 1963, Phys. Lett. **3**, 271

Jachowicz, N., K. Heyde, J. Ryckebusch, and S. Rombouts, 2002, Phys. Rev. C **65**, 025501

Kobayashi, M., and T. Maskawa, 1973, Prog. Theor. Phys. **49**, 652

Kolbe, E., K. Langanke, G. Martínez-Pinedo, and P. Vogel, 2003, J. Phys. G **29**, 2569

Kolbe, E., K. Langanke, and P. Vogel, 2002, Phys. Rev. D **66**, 013007

Krakauer, D. A., *et al.*, 1992, Phys. Rev. C **45**, 2450

Krasznahorkay, A., *et al.*, 1999, Phys. Rev. Lett. **82**, 3216

Krmpotić, F., A. Samana, and A. Mariano, 2005, Phys. Rev. C **71**, 044319

Kuramoto, T., M. Fukugita, Y. Kohyama, and K. Kubodera, 1990, Nucl. Phys. A **512**, 711

Kurasawa, H., T. Suzuki, and N. Van Giai, 2003, Phys. Rev. Lett. **91**, 062501

Lalazissis, G. A., J. König, and P. Ring, 1997, Phys. Rev. C **55**, 540

Lalazissis, G. A., T. Nikšić, D. Vretenar, and P. Ring, 2005, Phys. Rev. C **71**, 024312

Langanke, K., and G. Martínez-Pinedo, 2003, Rev. Mod. Phys. **75**, 819

Lazauskas, R., and C. Volpe, 2007, Nucl. Phys. A **792**, 219

Liang, H., N. Van Giai, and J. Meng, 2008, Phys. Rev. Lett. **101**, 122502

Liang, H., N. Van Giai, and J. Meng, 2009, Phys. Rev. C **79**, 064316

Long, W. H., 2005, *Relativistic Hartree-Fock approach with density-dependent meson-nucleon couplings*, Ph.D. thesis (Peking University, China and Université Paris-Sud, France)

Long, W. H., P. Ring, N. Van Giai, and J. Meng, 2010, Phys. Rev. C **81**, 024308

Long, W. H., H. Sagawa, J. Meng, and N. Van Giai, 2008, Europhys. Lett. **82**, 12001

Long, W. H., H. Sagawa, N. Van Giai, and J. Meng, 2007, Phys. Rev. C **76**, 034314

Long, W. H., N. Van Giai, and J. Meng, 2006, Phys. Lett. B **640**, 150

Ma, Z.-Y., B.-Q. Chen, N. Van Giai, and T. Suzuki, 2004, Eur. Phys. J. A **20**, 429

Marciano, W. J., and A. Sirlin, 2006, Phys. Rev. Lett. **96**, 032002

Marketin, T., N. Paar, T. Nikšić, and D. Vretenar, 2009, Phys. Rev. C **79**, 054323

Maschuw, R., 1998, Prog. Part. Nucl. Phys. **40**, 183

Meng, J., and P. Ring, 1996, Phys. Rev. Lett. **77**, 3963

Meng, J., and P. Ring, 1998, Phys. Rev. Lett. **80**, 460

Meng, J., H. Toki, S. G. Zhou, S. Q. Zhang, W. H. Long, and L. S. Geng, 2006, Prog. Part. Nucl. Phys. **57**, 470

Naviliat-Cuncic, O., and N. Severijns, 2009, Phys. Rev. Lett. **102**, 142302

Nikšić, T., T. Marketin, D. Vretenar, N. Paar, and P. Ring, 2005, Phys. Rev. C **71**, 014308

Nikšić, T., D. Vretenar, P. Finelli, and P. Ring, 2002a, Phys. Rev. C **66**, 024306

Nikšić, T., D. Vretenar, and P. Ring, 2002b, Phys. Rev. C **66**, 064302

O'Connell, J. S., T. W. Donnelly, and J. D. Walecka, 1972, Phys. Rev. C **6**, 719

Osterfeld, F., 1992, Rev. Mod. Phys. **64**, 491

Paar, N., 2010, *private communication*

Paar, N., T. Nikšić, D. Vretenar, and P. Ring, 2004, Phys. Rev. C **69**, 054303

Paar, N., P. Ring, T. Nikšić, and D. Vretenar, 2003, Phys. Rev. C **67**, 034312

Paar, N., D. Vretenar, T. Marketin, and P. Ring, 2008, Phys. Rev. C **77**, 024608

Počanić, D., *et al.*, 2004, Phys. Rev. Lett. **93**, 181803

Radha, P. B., D. J. Dean, S. E. Koonin, K. Langanke, and P. Vogel, 1997, Phys. Rev. C **56**, 3079

Rapaport, J., *et al.*, 1983, Nucl. Phys. A **410**, 371

Reinhard, P.-G., 1989, Rep. Prog. Phys. **52**, 439

Ring, P., 1996, Prog. Part.Nucl. Phys. **37**, 193

Ring, P., Z.-Y. Ma, N. Van Giai, D. Vretenar, A. Wandelt, and L.-G. Cao, 2001, Nucl. Phys. A **694**, 249

Ring, P., and P. Schuck, 1980, *The Nuclear Many-Body Problem* (Springer-Varlag New York Inc.)

Sagawa, H., N. Van Giai, and T. Suzuki, 1996, Phys. Rev. C **53**, 2163

Sajjad Athar, M., S. Ahmad, and S. Singh, 2006, Nucl. Phys. A **764**, 551

Samana, A., F. Krmpotić, A. Mariano, and R. Zukanovich Funchal, 2006, Phys. Lett. B **642**, 100

Serot, B. D., and J. D. Walecka, 1986, *Advances in Nuclear Physics Vol. 16: The Relativistic Nuclear Many Body Problem* (Plenum Press, New York)

Sharma, M. M., G. A. Lalazissis, and P. Ring, 1993, Phys. Lett. B **317**, 9

Sugahara, Y., and H. Toki, 1994, Nucl. Phys. A **579**, 557

Sun, B. Y., W. H. Long, J. Meng, and U. Lombardo, 2008, Phys. Rev. C **78**, 065805

Tarpanov, D., H. Liang, N. Van Giai, and C. Stoyanov, 2008, Phys. Rev. C **77**, 054316

Thompson, D., 1990, J. Phys. G **16**, 1423

Thouless, D., 1961, Nucl. Phys. **22**, 78

Towner, I. S., and J. C. Hardy, 2008, Phys. Rev. C **77**, 025501

Van Giai, N., N. Auerbach, and A. Z. Mekjian, 1981, Phys. Rev. Lett. **46**, 1444

Van Giai, N., and H. Sagawa, 1981, Nucl. Phys. A **371**, 1

Varshalovich, D. A., A. N. Moskalev, and V. K. Khersonskii, 1987, *Quantum Theory of Angular Momentum* (World Scientific Pub. Co.,Teaneck, NJ)

Vogel, P., 2006, *Special Isseu on Nuclear Astrophysics*, Nucl. Phys. A **777**, 340

Volpe, C., 2004, J. Phys. G **30**, L1

Volpe, C., 2007, J. Phys. G **34**, R1

Volpe, C., N. Auerbach, G. Colò, T. Suzuki, and N. Van Giai, 2000, Phys. Rev. C **62**, 015501

Volpe, C., N. Auerbach, G. Colò, and N. Van Giai, 2002, Phys. Rev. C **65**, 044603

Vretenar, D., A. Afanasjev, G. Lalazissis, and P. Ring, 2005, Phys. Rep. **409**, 101

Vretenar, D., N. Paar, T. Nikšić, and P. Ring, 2003, Phys. Rev. Lett. **91**, 262502

Wakasa, T., *et al.*, 1997, Phys. Rev. C **55**, 2909

Walecka, J. D., 1974, Ann. Phys. **83**, 491

Walecka, J. D., 1975, *Muon Physics* (Academic Press, New York)

Woosley, S. E., D. H. Hartmann, R. D. Hoffman, and W. C. Haxton, 1990, Astrophys. J. **356**, 272

Yako, K., H. Sagawa, and H. Sakai, 2006, Phys. Rev. C **74**, 051303

Yako, K., *et al.*, 2005, Phys. Lett. B **615**, 193

Zhou, S.-G., J. Meng, and P. Ring, 2003, Phys. Rev. Lett. **91**, 262501

Zucchelli, P., 2002, Phys. Lett. B **532**, 166

Publication List

Peer-refereed publications

1. **Spin symmetry in Dirac negative energy spectrum in density-dependent relativistic Hartree-Fock theory**
   H.Z. Liang, W.H. Long, J. Meng, and N. Van Giai
   Eur. Phys. J. A **44**, 119 (2010).

2. **Avoid the tsunami of the Dirac Sea in the imaginary time step method**
   Y. Zhang, H.Z. Liang, and J. Meng
   Int. J. Mod. Phys. E **19**, 55 (2010).

3. **Solving the Dirac equation with nonlocal potential by imaginary time step method**
   Y. Zhang, H.Z. Liang, and J. Meng
   Chin. Phys. Lett. **26**, 092401 (2009).

4. **Isospin corrections for superallowed Fermi beta decay in self-consistent relativistic random-phase approximation approaches**
   H.Z. Liang, N. Van Giai, and J. Meng
   Phys. Rev. C **79**, 064316 (2009).

5. **Stability of Strutinsky shell correction energy in relativistic mean field theory**
   Y.F. Niu, H.Z. Liang, and J. Meng
   Chin. Phys. Lett. **26**, 032103 (2009).

6. **Spin-isospin resonances: a self-consistent covariant description**
   H.Z. Liang, N. Van Giai, and J. Meng
   Phys. Rev. Lett. **101**, 122502 (2008).

7. **Mean-field study of single-particle spectra evolution in $Z = 14$ and $N = 28$ chains**
   D. Tarpanov, H.Z. Liang, N. Van Giai, and Ch. Stoyanov
   Phys. Rev. C **77**, 054316 (2008).

Conference proceedings and others

1. **Spin-isospin resonances with relativistic RPA approaches**
   J. Meng, H.Z. Liang, and N. Van Giai
   NUCLEAR PHYSICS TRENDS (Proceedings of 7th Japan-China Joint Nuclear Physics Symposium, Tsukuba, Japan, 9-13 November 2009), American Institute of Physics, 2010, pages 29-35.

2. **Isospin symmetry-breaking corrections for superallowed beta decay in relativistic RPA approaches**
   H.Z. Liang, N. Van Giai, and J. Meng
   (Proceedings of the XVIII International School on Nuclear Physics, Neutron Physics and Applications, Varna, Bulgaria, 21-27 September 2009)
   J. Phys. Conf. Ser. **205**, 012028 (2010).

3. **Covariant density functional theory for nuclear structure and application in astrophysics**
   J. Meng, Z.P. Li, H.Z. Liang, Z.M. Niu, J. Peng, B. Qi, B. Sun, S.Y. Wang, J.M. Yao, and S.Q. Zhang
   The 10th International Conference on Nucleus-Nucleus Collisions (Proceedings of NN2009, Beijing, China, 16-21 August 2009)
   Nucl. Phys. A **834**, 436c (2010).

4. **Isospin corrections for superallowed beta-decay in self-consistent relativistic RPA approach**
   H.Z. Liang, N. Van Giai, and J. Meng
   NUCLEAR STRUCTURE AND DYNAMICS '09 (Proceedings of NSD09, Dubrovnik, Croatia, 4-8 May 2009), American Institute of Physics, 2009, pages 431-432.

5. **Imaginary time step method to solve the Dirac equation with nonlocal potential**
   Y. Zhang, H.Z. Liang, and J. Meng
   NUCLEAR STRUCTURE AND DYNAMICS '09 (Proceedings of NSD09, Dubrovnik, Croatia, 4-8 May 2009), American Institute of Physics, 2009, pages 279-282.

6. **First attempt to overcome the disaster of Dirac Sea in imaginary time step method**
   Y. Zhang, H.Z. Liang, and J. Meng
   (Proceedings of the 12th National Conference on Nuclear Structure, Chongqing, China, 9-16 May 2008)
   Chin. Phys. C **33(S1)**, 113 (2009).

7. **Pion- and rho-meson effects in relativistic Hartree-Fock and RPA**
   N. Van Giai, W.H. Long, H.Z. Liang, J. Meng, and H. Sagawa

Physics of Unstable Nuclei (Proceedings of ISPUN07, Hoi An, Vietnam, 3-7 July 2007), World Scientific, 2008, pages 416-423.

8. **RPA correlation and nuclear densities in relativistic mean field approach**
   N. Van Giai, H.Z. Liang, and J. Meng
   Romanian Reports in Physics **59**, 693 (2007).

Papers in preparation

1. **Relativistic symmetries in nuclei: a perturbative interpretation**
   H.Z. Liang, P.W. Zhao, Y. Zhang, J. Meng, and N. Van Giai
   submitted to *Phys. Rev. Lett.*

2. **Search for ring-like nuclei at extreme condition**
   W. Zhang, H.Z. Liang, S.Q. Zhang, and J. Meng
   submitted to *Chin. Phys. Lett.*

3. **Tensor effects in shell evolution at $Z, N = 8$, 20 and 28 using non-relativistic and relativistic mean field**
   M. Moreno-Torres, M. Grasso, H.Z. Liang, V. De Donno, M. Anguiano, and N. Van Giai
   submitted to *Phys. Rev. C*

Acknowledgments

This work would not have been possible without the valuable support and help that I have received from many people.

In particular, I wish to give my deepest gratitude to Prof. Nguyen Van Giai, Prof. Jie Meng, and Prof. Peter Schuck for their supervision of my work and for the continuous supports over the past five years. As much as I am indebted to them for all of the knowledge they conveyed to me, for the time they generously spent with me, and for the stimulating suggestions they gave to me. I also wish to express my sincerest respect for their hardworking spirits and serious attitude, which have always been inspiring me and encouraging me.

I am also most thankful for the great supports from the JCNP group in Beijing during the last six years. The shape and the results of my thesis have been greatly improved by the discussions with Zhipan Li, Prof. Wenhui Long, Yifei Niu, Zhongming Niu, Dr. Chunyan Song, Baoyuan Sun, Prof. Jiangming Yao, Dr. Wei Zhang, Ying Zhang, and Pengwei Zhao.

During my studies in France, I have found Institut de Physique Nucléaire to be a very stimulating place, with a friendly atmosphere. I really appreciate for the collaborations and discussions with Prof. Gianluca Colò, Jean-Paul Ebran, Anthea Fantina, Dr. Marcella Grasso, Dr. Elias Khan, Dr. Jérome Margueron, Dr. Elisabeth Massot, Dr. Daniel Pena Arteaga, Dr. Dimitar Tarpanov, Dr. Hoang Sy Than, Prof. Dario Vretenar. Especially, I am grateful to Prof. Nils Paar for kindly sharing his knowledge on neutrino-nucleus cross sections, and performing heavy numerical checks. Last but not least, I thank all my friends, who have made my five years at Orsay and Beijing very enjoyable.

My warmest thoughts go to my fiancee, Jun Wu, and to my family in Guangzhou, who support me whenever and wherever.